VNIVERSITAT DE VALÈNCIA

UNIVERSITAT DE VALÈNCIA

Departamento de Bioquímica y Biología Molecular

Programa de doctorado en Biotecnología

"FUNCTIONAL CHARACTERIZATION OF p24δ SUBFAMILY PROTEINS IN *A. thaliana*"

Tesis doctoral con Mención Internacional presentada por

Noelia Pastor Cantizano

Tesis dirigida por:

Dr. Fernando Aniento Company

Dra. María Jesús Marcote Zaragoza

Valencia, Octubre 2016

VNIVERSITAT DE VALÈNCIA

FERNANDO ANIENTO COMPANY, Catedrático del departamento de Bioquímica y Biología Molecular de la Universidad de Valencia y

MARIA JESÚS MARCOTE ZARAGOZA, Profesora titular del departamento de Bioquímica y Biología Molecular de la Universidad de Valencia,

CERTIFICAN:

Que la presente memoria titulada:

"**FUNCTIONAL CHARACTERIZATION OF p24δ SUBFAMILY PROTEINS IN *A. thaliana*"**

ha sido realizada por la Licenciada en Farmacia Noelia Pastor Cantizano bajo nuestra dirección, y que, habiendo revisado el trabajo, autorizamos su presentación para que sea calificada como tesis doctoral y obtener así el TITULO DE DOCTOR CON MENCIÓN INTERNACIONAL.

Y para que conste a los efectos oportunos, se expide la presente certificación en Burjassot, a 19 de octubre de 2016.

Fdo: Fernando Aniento Company Fdo: María Jesús Marcote Zaragoza

Esta Tesis Doctoral se ha realizado con la financiación de los siguientes proyectos:

1. "Tráfico intracelular de proteínas en células vegetales". Plan Nacional de I + D. Programa de Biología Fundamental (BFU2009-07039). I.P.: Dr. Fernando Aniento Company.

2. "Tráfico intracelular de proteínas en células vegetales". Plan Nacional de I + D. Programa de Biología Fundamental (BFU2009-07039). I.P.: Dr. Fernando Aniento Company.

3. "Tráfico intracelular de proteínas en células vegetales" GEVA-Generalitat Valenciana. I.P.: Fernando Aniento Company

El presente trabajo de investigación ha sido desarrollado durante el periodo des disfrute de una beca predoctoral FPU (Formación Profesorado Universitario) del Ministerio de Educación (AP2010-2326), durante los años 2009-2013, y una ayuda de la Universidad de Valencia para la realización de Estancias Breves en la "School of Life Sciences" de la Universidad China de Hong Kong.

AGRADECIMIENTOS

Y por fin llegó el momento de parar un segundo y echar la vista atrás para agradecer a todos los compañeros de viaje que he tenido durante estos años.

En primer lugar, me gustaría agradecer a mis directores Fernando y María Jesús su dedicación y su enorme paciencia, además de todo el cariño que me han dado estos años. Gracias también a mi querido Consejo Privado por todos esos buenos momentos dentro y fuera del lab y por todo el apoyo que me han dado incluso desde la distancia: Juan Carlos (obviamente la mano del Rey), gracias por ser mi maestro en el laboratorio; Gloria, te espero allá donde vaya para vivir más aventuras; y Joan, sigue intentando sacar una sonrisa a los demás en cualquier situación. A Fátima y César, a los que seguro que les va a ir muy bien en esto de la ciencia. A Pilar (ya te he dicho que McGyver a tu lado no sabe hacer nada) gracias no solo por haberme facilitado el trabajo sino también por todas esas charlas estos últimos meses. También quiero agradecer a toda la gente del departamento de Bioquímica su cariño durante todos estos años. Y ya puestos a quedarnos en el tercer piso, no me puedo olvidar de mi María, mi compañera de risas, llantos y cervezas, gracias por estar ahí en tantos momentos, sabes que nunca habría llegado al final sin ti. Y no puedo dejarme a Kelly, sin ella Hong Kong no habría sido lo mismo.

Una de las cosas que ha cambiado mientras hacía la tesis ha sido mi forma de disfrutar del deporte y eso se lo tengo que agradecer a que he tenido a los mejores monitores y amigos: Sebi, Marga y Pau. Y ahí conocí a dos personas que ahora mismo son muy importantes para mí. Babé, gracias por compartir conmigo tantísimos momentos, por ser capaz de hacer que lo de todo en un combat con un simple "¿preparada?" y por acudir siempre que necesito un abrazo. Sof, siempre serás mi mama pato que cuida de mi, gracias por tratarme siempre como tu hermana pequeña y estar a mi lado. Gracias también al resto de mi querida fila de atrás (Vane y Honga), a L-na, a mi Pili que ha sido mi gran apoyo estos últimos 10 meses y en pocas clases me ha dejado sola, a mis Chos (Ruth y Cristina) que aunque han sido la última incorporación en mi vida ya se han convertido en dos personitas muy importantes (Be junco my friend!), y aún montón de personas que más que me dejo!

Gracias también al resto de mis queridos "The Milk", a Javi, Jorge, Irene y sobre todo a Dani y Merch por esos picnics ilegales, por comer la tarta con las manos y apuntarse a cualquier plan descabellado (por introducir el término merchada en mi vida!). A mis golfos favoritos (Nacho, Cris, Mow, Mari, Carlos, Vane, César, Pablo y

Silvia) por todos esos grandes momentos rodeados comida y cerveza. A Damian, por hacer de su casa siempre nuestra casa también. A mis alumnas, Mari y Silvia, por enseñarme ellas a mí. Y no me puedo olvidar de mis estudiants post-aborigens (Inés, Eva, Nona y Ange) con los que empecé en la universidad y aún siguen a mi lado.

Pero si hay dos personas que han estado a mi lado casi desde el momento que puse un pie en la universidad han sido Jorge y Tam. Jorge, gracias por estar siempre a mi lado y aguantarme en tantos momentos, ninguna de mis etapas habría sido lo mismo sin ti, sé que estarás en las próximas también. A mi sis, por ser la niña mágica que un día el destino quiso poner en mi camino, aquel día no sabía lo afortunada que fui pero 11 años después te puedo decir que es un placer recorrer este camino a tu lado.

Gracias a la familia de Amadeo por tratarme como una más, sobre todo a mi "cuñao" Fran, a mi cuñada, Marisa y a mi suegra, Luisa, porque en el fondo y sin el fondo os quiero muchísimo. No me puedo olvidar de mi familia de Ceuta, especialmente a mi Tita Luchi, a la que quiero como si fuera mi segunda madre, y a los que me cuidan desde el cielo.

Dicen que la familia no se elige, pues a la mía la quiero muchísimo con sus defectos y sus virtudes. A mi hermana, Ana, por preocuparse tanto por mí. A mis niños, Alejandro y Adrián, espero que me perdonéis porque mis escapadas para veros no han sido todas las que me hubieran gustado. Sabéis que os quiero muchísimo. A mi hermano Rafa, porque siempre ha sido mi ejemplo a seguir, sin él hoy no estaría aquí y por ser además mi mejor amigo en todo momento. Y a mis padres, por todo el sacrificio que han hecho para que haya podido llegar hasta aquí, por todo su amor y por ser las personas con el corazón más grande y fuerte que conozco.

Y por último, a la persona que más ha sufrido esta tesis conmigo, la que ha estado en mis días buenos, en los malos y en mis noches de trabajo todos estos años. Amadeo, sí quiero compartir contigo lo que esté por venir, sí quiero estar a tu lado hasta que seamos abuelitos y echemos la vista atrás y veamos todo el camino que hemos recorrido juntos, sí quiero pasarme el resto de mis días junto a ti. Gracias por apoyarme siempre e impulsarme para que siga adelante. Te quiero.

A Rafa, a mis padres y

a Amadeo

TABLE OF CONTENTS

ABBREVIATIONS

***ACT2*: *Actin-2* gene**
***ACT7*: *Actin-7* gene**
AGD: ADP ribosylation factor GTPase activating protein domain
ATF6: Activating transcription factor 6
ARF: ADP ribosylation factor
BFA: Brefeldin A
BiP: Binding protein.
bp: Base pair
BSA: Bovine serum albumin
bZIP: basic leucine zipper
CC: coiled-coil domain
CCV: Clathrin-coated vesicle
cDNA: Complementary DNA
CLSM: Confocal laser scanning microscopy
CO-IP: co-immunoprecipitation
Col: Columbia ecotype
COP: Coat protein
CPS: Classical or conventional protein secretion
CRT: Calreticulin
CW: Cell wall
DNA: Deoxyribonucleic acid
dNTP: Deoxyribonucleotide triphosphate
DMSO : Dimethyl sulfoxide
DTT: dithiothreitol
EB: electroporation buffer
ECL: Enhanced chemiluminescence method
EDTA: Ethylenediaminetetraacetic acid
EE: Early endosome
EM: Electron microscopy
Endo H: Endoglycosidase H
EMP: Endomembrane protein
ER: Endoplasmic reticulum
ERD2: Endoplasmic reticulum-retention defective 2 receptor (K/HDEL receptor).
ERDA: Endoplasmic reticulum degradation system
ERDJ: Endoplasmic reticulum J domain proteins
ERAS: Endoplasmic reticulum arrival sites
ERES: Endoplasmic reticulum export sites
ERGIC: Endoplasmic reticulum-Golgi intermediate compartment
ERIS: Endoplasmic reticulum import sites
ERQC: Endoplasmic reticulum quality control
ERSE: Endoplasmic reticulum, stress-response element
EXPO: Exocyst-positive organelle
G: Golgi apparatus
GAP: GTPase activating protein
GAPDH: Glyceraldehyde-phosphate dehydrogenase
GEF: Guanine nucleotide exchange factor
GFP: Green fluorescent protein
GPI-AP: glycosylphosphatidylinositol-anchored proteins
GOLD: Golgi dynamics domain
HB: Homogenization buffer
HEK cells: Human embryo kidney cells
HRP: horseradish peroxidase
IRE: Inositol requiring enzyme
IP: Immunoprecipitation
IPs: Protease Inhibitor Cocktail Sigma®
KO: Knockout
LB: Luria-Bertani medium.
LE: Late endosomes
LSP: Leaderless secretory protein
MES: 2-(N-morpholino) ethanesulfonic acid
MIP: MAG" interacting protein

ABBREVIATIONS

MS: Murashige and Skoog medium used for *in vitro* cultivation of plants
MVB: Multivesicular body
ORF: open reading frame
PCD: Programmed cell death
PCR: Polymerase chain reaction
PD: pull-down
PDI: Protein disulfide isomerase
PEG: Polyethylene glycol
PERK: Protein kinase RNA-like ER kinase
PKA: Ser/Thr protein kinase A
PM: Plasma membrane
PSV: Protein storage vacuole
PVC: Prevacuolar compartment
RFP: Red fluorescent protein
RIDD: Regulated IRE1-dependent decay
RNA: Ribonucleic acid
RT: Room temperature
RT-qPCR: Reverse Transcription-quantitative PCR
RT-sqPCR: Reverse Transcription-semiquantitative PCR
S1P: site-1 protease
S2P: site-2 protease
SB: Sample buffer
SD: Standard deviation
SDS-PAGE: Sodium dodecyl sulfate – polyacrylamide gel electrophoresis
SE: Standard error
SNARE: Soluble N-ethylmaleimide-sensitive fusion protein attachment protein receptor
SP: Signal peptide
SS: Signal sequence
TEM: Transmission electron microscopy
t-ER: transitional ER
TGN: *trans*-Golgi network.
Tm: Melting temperature
Tm: Tunicamycin
TMD: transmembrane domain
TRAPPI: Transport protein particle I
UB: unspecific binding
UPR: Unfolded protein response
UPS: Unconventional protein secretion
VSS: Vacuolar sorting signal
VSR: Vacuolar sorting receptor
v/v: volume/volume
YFP: Yellow fluorescent protein
Wt: Wild type
w/v: weight/volume

ABSTRACTS

ABSTRACT

p24 proteins constitute a family of small (~ 24kDa) type-I transmembrane proteins which localize to the compartments of the early secretory pathway, including coated protein (COP) I- and COPII-coated vesicles, which mediate the bidirectional transport between the ER and the Golgi apparatus. Based on sequence homology, p24 proteins can be classified into four subfamilies: p24α, p24β, p24γ and p24δ. In contrast to animals and fungi, in plants there are only members of p24β and p24δ subfamilies. In particular, *Arabidopsis* contains 9 members of the p24δ subfamily which can be divided into two subclasses, δ-1 (p24δ3-p24δ6) and δ-2 (p24δ7-p24δ11), and 2 members of the p24β subfamily. Since p24 proteins cycle between the ER and the Golgi apparatus, they have been proposed to function as putative cargo receptors and to be involved in quality control during protein transport in the early secretory pathway, the organization of ER export sites or the biogenesis and maintenance of the Golgi apparatus. However, their functions in plants are essentially unknown.

The main aim of this work has been the functional characterization of p24 proteins of the p24δ subfamily in *Arabidopsis*. To this end, two different approaches have been followed.

On the one hand, quadruple knockout (KO) mutants of both p24δ-1 (p24δ3δ4δ5δ6 mutant) and p24δ-2 (p24δ7δ8δ9δ10 mutant) subclasses were obtained. The p24δ3δ4δ5δ6 and p24δ7δ8δ9δ10 mutant did not show

phenotypic alterations when they were grown under standard growth conditions, suggesting that p24 proteins from the delta subfamily are not necessary for growth under these conditions in Arabidopsis. The analysis of the levels of p24 proteins in both quadruple mutants showed a decrease in the levels of other p24 proteins, which may be due to a decrease in protein stability and not to a decrease in mRNA levels, suggesting that these p24 proteins may function together in heteromeric complexes. In addition, a possible alteration in the compartments of the early secretory pathway was investigated. It was found that loss of p24δ-1 or p24δ-2 proteins produce alterations mainly in the Golgi apparatus. These data suggest that p24 proteins of the delta subfamily are involved in the maintenance of the structure and organization of the compartments of the early secretory pathway in Arabidopsis. Moreover, the effect of the loss of p24δ proteins in the transport of the K/HDEL receptor ERD2 and a K/HDEL ligand, the chaperone BiP, was also investigated. It was found that loss of p24δ proteins induced the accumulation of the K/HDEL receptor ERD2a-YFP at the Golgi apparatus. This effect was reversed by co-expression of either p24δ5 (δ-1 subclass) or p24δ9 (δ-2 subclass) or of a K/HDEL ligand. In addition, loss of p24δ proteins induced secretion of BiP, probably due to an inhibition of COPI-dependent retrograde Golgi-to-ER transport of ERD2 and, in consequence, in the retrieval of K/HDEL ligands. Finally, it was found that both p24 quadruple mutants show a constitutive activation of the UPR pathway, which may act as a compensatory mechanism that helps the plant to cope with the transport defects in the absence of p24 proteins. Indeed,

an increase of the membrane association of several COPI and COPII subunits was observed in both quadruple mutants. In addition, loss of p24δ-1 and p24δ-2 proteins produced the up-regulation of SEC31A, a gene involved in the formation of COPII vesicles.

On the other hand, it was investigated whether Arabidopsis p24 proteins from the delta-1 subclass are glycosylated and if this glycosylation may have functional implications, in particular with respect to their role in sorting ERD2 within COPI vesicles for retrieval of K/HDEL ligands from the Golgi apparatus to the endoplasmic reticulum. It was found that a member of the p24δ-1 subclass, p24δ5, is N-glycosylated in its GOLD domain, in contrast to p24δ9, a member of the p24δ-2 subclass. The N-glycosylation of p24δ5 is not required for its steady-state localization at the endoplasmic reticulum, but it is important for its interaction with the K/HDEL receptor ERD2a and for retrograde transport of ERD2a and K/HDEL ligands from the Golgi apparatus to the endoplasmic reticulum.

RESUMEN

Las proteínas p24 constituyen una familia de pequeñas (~24kDa) proteínas transmembrana de tipo-1 que localizan en los compartimentos de la vía secretora temprana, incluyendo las vesículas recubiertas de proteínas COP (Coat protein) I y COPII, implicadas en el transporte bidireccional entre el retículo endoplasmático ("endoplasmic reticulum", ER) y el aparato de Golgi. En función de la homología de sus secuencias, las proteínas p24 pueden ser clasificadas en cuatro subfamilias: p24α, p24β, p24γ y p24δ. A diferencia de animales y levaduras, en plantas solo hay miembros de las subfamilias p24β y p24δ. En particular, *Arabidopsis* contiene 9 miembros de la subfamilia p24δ, los cuales se pueden dividir en dos subclases, δ-1 (p24δ3-p24δ6) y δ-2 (p24δ7-p24δ11), y 2 miembros de la subfamilia p24β. A partir de su transporte bidireccional entre el ER y el aparato de Golgi, se ha propuesto que las proteínas p24 funcionan como posibles receptores de cargo y que están implicadas en el control de calidad durante el transporte de proteínas en la vía secretora temprana, la organización de los sitios de salida del ER ("ER export sites", ERES) y la biogénesis y mantenimiento del aparato de Golgi.

El objetivo principal de la presente Tesis doctoral ha sido la caracterización funcional de las proteínas de la subfamilia p24δ en *Arabidopsis*. Para ello se han seguido dos aproximaciones diferentes.

Por un lado se han obtenido los mutantes cuádruples nulos de ambas subclases, p24δ-1 (mutante *p24δ3δ4δ5δ6*) y p24δ-2 (mutante

p24δ7δ8δ9δ10). Los mutantes *p24δ3δ4δ5δ6* y *p24δ7δ8δ9δ10* no mostraron alteraciones fenotípicas cuando fueron crecidos bajo condiciones estándar de crecimiento, lo que sugiere que las proteínas p24 de la subfamilia δ no son necesarias para el crecimiento bajo esas condiciones en *Arabidopsis*. El análisis de los niveles de proteínas en ambos cuádruples mutantes mostró una disminución en los niveles de otras proteínas p24, lo cual puede ser debido a una disminución de la estabilidad de dichas proteínas y no a una disminución de los niveles de mRNA, sugiriendo que esas proteínas p24 pueden funcionar formando complejos heteroméricos. Además, se investigó una posible alteración de los compartimentos de la vía secretora temprana. Se encontró que la pérdida de las proteínas p24δ-1 o p24δ-2 produce alteraciones principalmente en el aparato de Golgi. Esos datos sugieren que las proteínas p24 de la subfamilia δ están implicadas en el mantenimiento de la estructura y organización de los compartimentos de la vía secretora temprana en *Arabidopsis*. Además, se investigó el efecto de la pérdida de las proteínas p24δ en el transporte del receptor K/HDEL, ERD2, y de un ligando K/HDEL, la chaperona BiP. Se encontró que la pérdida de las proteínas p24 induce la acumulación del receptor ERD2a-YFP en el aparato de Golgi. Este efecto fue revertido mediante la co-expresión de p24δ5 (subclase δ-1) o de p24δ9 (subclase p24δ-2) o de un ligando K/HDEL. Además, la pérdida de proteínas p24δ induce la secreción de BiP, probablemente debido a una inhibición en el transporte retrógrado desde el aparto de Golgi hasta el ER de ERD2 mediado por vesículas COPI y, por tanto, en la recuperación de los ligandos K/HDEL. Finalmente se encontró que ambos mutantes cuádruples

presentan una activación constitutiva de la respuesta a proteínas desplegadas ("unfolded protein response", UPR), la cual puede actuar como mecanismo de compensación que ayuda a la planta a hacer frente a los defectos en el transporte en ausencia de las proteínas p24. De hecho, se observó un aumento de la asociación a membrana de varias subunidades COPI y COPII en ambos cuádruples mutantes. Además, la pérdida de proteínas p24δ-1 o p24δ-2 produjo un incremento en la expresión de *SEC31,* un gen implicado en la formación de vesículas COPII.

Por otro lado, se investigó si las proteínas p24 de la subclase δ-1 en *Arabidopsis* se encuentran glicosiladas y si está glicosilación puede tener implicaciones funcionales, en particular respecto a su papel en la inclusión de ERD2 dentro de vesículas COPI para la recuperación de ligandos K/HDEL desde el aparato de Golgi hasta el retículo endoplasmático. Se encontró que un miembro de la subclase p24δ-1, p24δ5, es *N*-glicosilado en su domino GOLD, a diferencia de p24δ9, un miembro de la subclase p24δ-2. La *N*-glicosilación de p24δ5 no es necesaria para su localización en el ER en el estado estacionario, pero es importante para su interacción con el receptor K/HDEL, ERD2a, y para el transporte retrógrado de ERD2a y ligandos K/HDEL desde el aparato de Golgi hasta el ER.

RESUM

Les proteïnes p24 constituïxen una família de xicotetes (~ 24kDa) proteïnes transmembrana de tipus-I que es localitzen en compartiments de la via secretora primerenca, incloent-hi vesícules recobertes de proteïnes COP (Coat Protein) I i COPII, que medien el transport bidireccional entre el reticle endoplasmàtic ("endoplasmatic reticulum", ER) i l'aparell de Golgi. Basant-se en l'homologia de seqüència, les proteïnes p24 poden ser classificades en quatre subfamílies: p24α, p24β, p24γ i p24δ. A diferència d'animals i fongs, en plantes hi ha només membres de les subfamílies p24β i p24δ. En particular, *Arabidopsis* conté 9 membres de la subfamília p24δ que poden ser dividits en dos subclasses, δ-1 (p24δ3-p24δ6) i δ-2 (p24δ7-p24δ11), i 2 membres de la subfamília p24β. A partir del seu transport bidireccional entre el ER i l'aparell de Golgi, s'ha proposat que funcionen com a possibles receptors de proteïnes *cargo* i que estan involucrades en el control de qualitat durant el transport de proteïnes en la via secretora primerenca, l'organització dels llocs d'eixida del ER o la biogènesi i manteniment de l'aparell de Golgi. No obstant això, les sues funcions en plantes són essencialment desconegudes.

El principal propòsit d'esta Tesis doctoral ha estat la caracterització funcional de les proteïnes p24 de la subfamília p24δ en *Arabidopsis*. Amb esta fi, han estat seguides dos aproximacions.

D'una banda, s'ha obtingut mutants quàdruples nuls de les subclasses p24δ-1 (mutant p24δ3δ4δ5δ6) i p24δ-2 (mutant p24δ7δ8δ9δ10). Els

mutants *p24δ3δ4δ5δ6* i *p24δ7δ8δ9δ10* no mostren alteracions fenotípiques quan són crescuts sota condicions de creixement estàndards, suggerint que les proteïnes p24 de la subfamília delta no són necessàries per al creixement en *Arabidopsis* sota eixes condicions. Les anàlisis dels nivells de proteïnes p24 en ambdós mutants quàdruples mostraren una disminució en els nivells d'altres p24, cosa que pot ser causada per una baixada en l'estabilitat de proteïnes i no a una baixada en els nivells de mRNA, suggerint que eixes proteïnes p24 poden funcionar formant complexos heteromèrics. A més, s'ha investigat una possible alteració en els compartiments de la via secretora primerenca. S'hi trobà que la pèrdua de proteïnes p24δ-1 or p24δ-2 produïx alteracions principalment en l'aparell de Golgi. Esta dada suggerix que les proteïnes p24 de la subfamília delta estan involucrades en el manteniment de l'estructura i organització de la via secretora primerenca en *Arabidopsis*. A més, s'ha investigat de la pèrdua de les proteïnes p24δ en el transport del receptor K/HDEL, ERD2, i un lligant K/HDEL, la xaperona BiP, ha estat també investigada. S'hi trobà que la pèrdua de proteïnes p24δ induïx l'acumulació del receptor K/HDEL, ERD2a-YFP, a l'aparell de Golgi. Este efecte va ser revertit per coexpressió de p24δ5 (subclasse δ-1), o de p24δ9 (subclasse δ-2) o del lligant K/HDEL. A més, la pèrdua de proteïnes p24δ de la subfamília delta induí la secreció de BiP, probablement a causa d'una inhibició del transport retrògrad des del ER fins a l'aparell de Golgi mediat per vesícules COPI i, en conseqüència, en la recuperació de lligant K/HDEL. Finalment, s'hi trobà que ambdós mutants quàdruples mostren una activació constitutiva de la resposta a proteïnes desplegades ("unfolded

protein response", UPR), que pot actuar com a mecanisme compensatori que ajuda la planta a fer front els defectes de transport en absència de proteïnes p24. En efecte, un increment de l'associació a membrana de diverses subunitats COPI i COPII va ser observat en ambdós quàdruples mutants. A més, la pèrdua de proteïnes p24δ-1 i p24δ-2 produí la regulació a l'alça de *SEC31A*, un gen involucrat en la formació de vesícules COPII.

D'altra banda, va ser investigat si les proteïnes p24 en *Arabidopsis* de la subclasse delta-1 són glicosilades i si esta glicosilació pot tindre implicacions funcionals, en particular respecte del seu paper en inclusió d'ERD2 dins de vesícules COPI per a recuperar lligants K/HDEL des de l'aparell de Golgi al reticle endoplasmàtic. S'hi trobà que un membre de la subclasse p24δ-1, p24δ5, és N-glicosilat en el seu domini GOLD, en contrast amb p24δ9, un membre de la subclasse p24δ-2. La N-glicosilació de p24δ5 no és requerida per a la seua localització en el ER en estat d'estacionari, però és important per a la seua interacció amb el receptor K/HDEL ERD2a i per al transport retrògrad de ERD2a i lligants K/HDEL des de l'aparell de Golgi cap al reticle endoplasmàtic.

INTRODUCTION

1. INTRACELLULAR MEMBRANE TRAFFIC

Eukaryotic cells show a complex endomembrane system composed by several membrane-bound compartments with a specific molecular composition and, therefore, functionally different. In plants, the major endomembrane compartments are the endoplasmic reticulum (ER), the Golgi apparatus, the *trans*-Golgi network (TGN), the prevacuolar compartment/multivesicular bodies (PVC/MVB) and the vacuoles (for more details, see section 2 of Introduction).

1.1. MEMBRANE TRAFFICKING PATHWAYS

The different compartments which are part of the endomembrane system are connected to exchange proteins, lipids and polysaccharides through small membrane-enclosed transport vesicles. Membrane trafficking allows the delivery of several thousands of proteins to their site of action and turnover. Thus, it is involved in cellular homeostasis, cell-cell communication, development, and physiological responses to changes in the environment (Bassham et al., 2008; Park and Jürgens, 2012; Pfeffer, 2013). This membrane trafficking system consist of highly organized directional routes of which two are the main "default" pathways, the biosynthetic or secretory pathway and the endocytic pathway (Bassham et al., 2008).

a) Biosynthetic or Secretory pathway: The secretory pathway starts when newly synthesized molecules are included into the ER to be

transported to different compartments or to be secreted. From the ER, molecular cargos are delivered to the PM or to the vacuole, mainly through the Golgi apparatus and the TGN (for more details, see section 2).

b) Endocytic pathway: Endocytosis is a process by which plant cells capture molecules from the apoplast or internalize plasma membrane proteins or receptor-ligand complexes via vesicles generated at the plasma membrane (PM) (Marsh and McMahon, 1999). Endocytic vesicles are released from the PM and move into the cell to the TGN (*trans*-Golgi Network)/EE (Early endosomes), where the endocytic cargos are sorted to follow different destinations: they can be recycled back to the PM or be delivered to the lytic vacuoles for degradation through the PVC/MVB (Valencia et al., 2016; Viotti et al., 2010).

c) "Retrograde" pathways: The retrograde pathways retrieve material back from later steps in either pathway for a variety of reasons. These retrograde pathways can serve to get back molecules which should remain in one compartment and have entered into vesicles in a nonspecific manner. In addition, molecules involved in vesicular transport must be recycled so that they can be re-used in a new round of vesicle formation.

d) Others: It has been shown the existence of different pathways which allow protein transport from the endomembrane system to peroxisomes and plastids (Titorenko and Mullen, 2006; Nanjo et al., 2006). It

has also been proposed that secretion may be redirected to the cell plate during cell division (Richter et al., 2009).

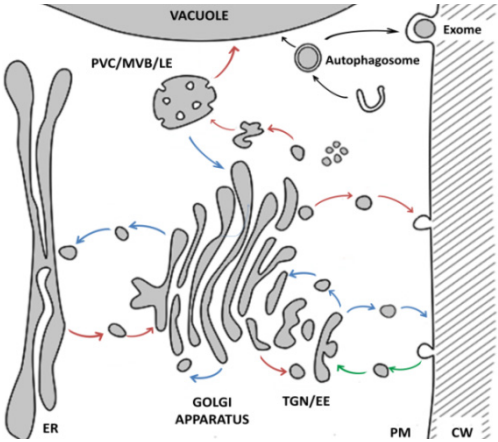

Figure 1. The endomembrane system of a plant cell (adapted from Vukašinović and Žárský, 2016). All compartments shown communicate with one another and the outside of the cell by means of transport vesicles. In the secretory pathway *(red arrows)*, protein molecules are transported from the ER to the PM or to the vacuole. In the endocytic pathway *(green arrows)*, molecules are endocytosed in endocytic vesicles derived from the PM and delivered to TGN/EE and then (via MBV/LE) to the vacuole. Many endocytosed molecules are retrieved from the TGN and returned to the cell surface for reuse; similarly, some molecules are retrieved from the MVB/LE and TGN and returned to the Golgi apparatus, and some are retrieved from the Golgi apparatus and returned to the ER. All of these retrieval pathways are shown with *blue arrows*. CW, cell wall; ER, endoplasmic reticulum; PVC/MVB/LE, prevacuolar compartment/multivesicular body/late endosome; PM, plasma membrane; TGN/EE, trans-Golgi network/early endosome.

1.2. VESICLE TRAFFICKING

In 2013, the Nobel Prize in Physiology or Medicine was awarded to James Rothman, Randy Schekman, and Thomas Südhorf “for their

discoveries of machinery regulating vesicle traffic" (Pfeffer, 2013). Thanks to their significative contribution together with other contributions, it is nowadays widely accepted that molecular transport through the compartments of the membrane trafficking system occurs via small coated vesicles. These vesicles bud off from a donor compartment and fuse with a target compartment, carrying cargo molecules, including membrane and soluble proteins, from one compartment to the next (Rothman and Wieland, 1996; Nickel et al., 1997; Paul and Frigerio, 2007; Klann et al., 2012).

1.2.1. Steps of the vesicular transport

The vesicular traffic between the different compartments of the plant endomembrane system occurs via similar mechanisms as in yeast and mammals. Each step of vesicle trafficking can be divided in three steps (Figure 2):

1.2.1.1. Budding

Transport vesicles bud from the donor compartment by the action of several ordered systems of coat proteins which are recruited through the activity of a specific GTPase (coat-GTPase). The coat-GTPase is recruited into the donor membrane through a GTP/GDP-exchange factor (GEF) localized to the coating site. This GEF triggers nucleotide exchange from GDP to GTP, such that the coat-GTPase assumes its active GTP-bound state. The active coat-GTPase recruits other subunits of the coat complex which polymerize on the membrane surface and deform it to form a free vesicle. During this process, cargo molecules are captured into the vesicle together with those

molecules that are necessary for transport or fusion with the target compartment, including soluble N-ethylmaleimide-sensitive factor attachment protein receptors (SNAREs), which catalyze the membrane fusion between the vesicle and the target compartment. Finally, a GTPase Activation Protein (GAP) triggers the hydrolysis of GTP to GDP of the coat-GTPase and the uncoating of the vesicle.

Plant cells contain four major types of vesicles: COP ("Coat Protein") I and COP II coated vesicles, which are involved in the transport in the early secretory pathway; clathrin coated vesicles (CCV) which have been proposed to be involved in the late secretory pathway and in endocytosis (Bassham et al., 2008); and retromer coated vesicles which are involved in post-Golgi trafficking, mainly recycling vacuolar sorting receptors from the PVC to the TGN (Niemes et al., 2010b).

1.2.1.2. Transport

Newly formed vesicles generated in the donor compartment have to be transported to the target compartment. This transport usually occurs along a cytoskeletal element via a motor-mediated process in which dynein and kinesin motors and other docking factors could be involved.

1.2.1.3. Fusion

Once the vesicles reach the target compartment, the membranes fuse and the cargo molecules are transferred into the target compartment. This requires well-defined specific mechanisms for recognition between the

membrane of the vesicle and the proper target membrane. The identification of the target compartment is mediated by different family proteins:

a) Rab family of small GTPases:

The Rab family of small GTPases are involved in vesicle formation, motility, tethering and docking, and also events preceding vesicle fusion through direct interaction or the selective recruitment of proteins onto membranes which catalyze theses processes. Therefore, Rab GTPases contribute to membrane identity and the accuracy of vesicle targeting (Pfeffer, 2001; Woollard and Moore, 2008). Through genomic analysis, Rab GTPases are divided into eight types (RabA-RabH) which are conserved among the majority of eukaryotes, and are thought to represent the "minimal" set of Rab GTPases (Bassham et al., 2008).

Rab GTPases undergo a regulated cycle between GDP-bound and GTP-bound forms. The GDP-bound form is usually localized in the cytosol associated with a RabGDI (GDP-displacement inhibitor) which masks the two prenyl-groups attached post-translationally to the C-terminus of the Rab GTPase. Rab GTPases are recruited onto the membrane by their interaction with RabGDI-displacement factors, which displace RabGDI and allow Rab attachment to the membrane through the prenyl-groups. Then, specific GEFs convert the protein to the GTP-bound form which can recruit a variety of effectors, including tethering factors, myosins, kinesins and regulators of SNARE protein assembly. Once the vesicle is fused with the target

membrane, GAPs stimulate the intrinsic GTPase activity of the Rab GTPase, and its inactive GDP-bound form is removed from the membrane by RabGDI (Woollard and Moore, 2008).

b) Tethering factors:

Tethering factors are single long rod-like proteins or protein complexes which mediate the first specific contact between the vesicle and the target membrane. They bridge newly formed vesicles with the target membrane through their interaction with Rab GTPases, SNAREs and even coat subunits, to ensure the appropriate docking and fusion. They can function also as GEFs or as effectors of activated RABs specific for each transport step. Two classes of tethers have been defined and characterized in eukaryotes: elongated coiled-coil tethers and multisubunit tethering complexes (Sztul and Lupashin, 2009; Brocker et al., 2010; Vukašinović and Žárský, 2016).

c) Soluble N-ethylmaleimide-sensitive fusion protein Attachment protein Receptors (SNAREs)

The SNARE family of proteins have a critical role in membrane fusion. SNAREs on a transport vesicle interact with the related SNAREs on the target membrane, forming a stable SNARE complex which provides energy for the membranes to fuse (Bombardier and Munson, 2015).

SNAREs can be divided into two types depending on their localization: v-SNAREs, as SNAREs on the vesicle, and t-SNAREs, as SNAREs on the target membrane. Once the vesicle is tethered to their target membrane prior to

fusion by Rab GTPases and tethering factors, a v-SNARE on the vesicle interacts with three t-SNAREs on the target membrane forming a parallel coiled-coil complex which drives membrane fusion (Kim and Brandizzi, 2012; Bombardier and Munson, 2015). The post-fusion assembled SNARE complex is very stable and needs to be mechanically disassembled.

In addition, according to their sequence of amino acids in the SNARE motif, SNAREs can be divided into four groups: Qa-, Qb-, Qc- and R-SNARES. The typical SNARE complex in mammals consists of a Qa- (syntaxin 1 like), Qb- (N-terminal half of SNAP25 like), and Qc- (C-terminal half of SNAP25 like) SNAREs on the target membrane, and R-SNAREs on the vesicle. The same combination seems to be conserved also in plants (Kim and Brandizzi, 2012). Specific SNAREs label unique target membranes, while others are incorporated into vesicles from only certain donor compartments. Therefore, different combinations of SNAREs can lead to additional levels of organization among the organelles (Bassham et al., 2008).

Therefore, during the fusion step, a Rab GTPase in its GTP-bound form which acts on both the vesicle and target membrane recruits tethering and docking factors that serve to attach the vesicle to the target membrane. Then, three t-SNAREs are bundled into a three SNARE-helix which serves as a binding site for the v-SNARE helix. Mutual twisting of the SNARE helices pulls the membrane into close proximity and drives fusion of the bilayers (Bassham et al., 2008).

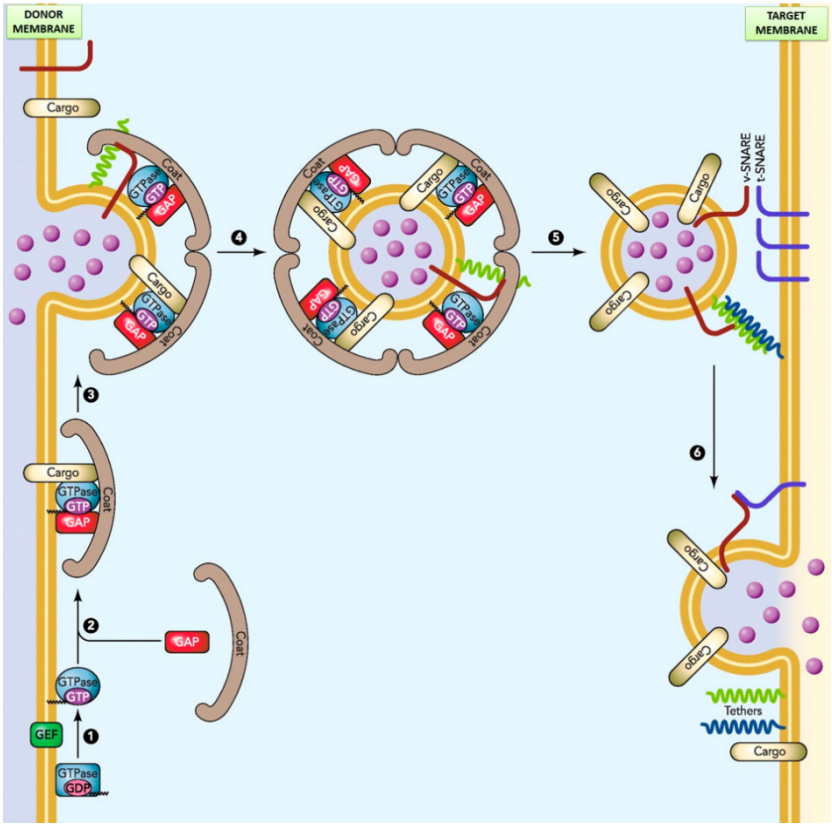

Figure 2. Steps of vesicular transport (adapted from Szul and Sztul, 2011). Protein traffic within the cell involves the packaging of cargo proteins into vesicles that bud from donor membranes, move to target membranes, and then tether and fuse with target membranes to release their cargo. The process involves activation of a GTPase (coat-GTPase) on a donor membranes by a GEF (step 1), recruitment of a coat and an ARF GAP (step 2), and cargo sorting/concentration (step 3) into a nascent bud. Coat polymerization is believed to deform the membrane, and following scission (step 4) the vesicle is pinched off from the donor membrane. After moving into the proximity of the target membranes, the coat dissociates (step 5), and the vesicles attaches to acceptor membrane via tethers and subsequently fuses through a SNARE-mediated mechanism (Step 6).

1.2.2. Principles of vesicular trafficking

The compartments which belong to the membrane trafficking system must maintain their unique composition of membrane and cargo proteins in spite of the constant flow of vesicles. To this end, there are two key principles in the vesicular transport:

1.2.2.1. Molecular sorting

Vesicular transport requires that each transport vesicle includes the appropriate molecules, including cargo molecules and the components required for the traffic of the vesicle, and exclude the ones which should remain in the donor compartment. There are three different ways to achieve the accurate selection of the desired molecules into the transport vesicles:

a) Sorting of cargo molecules into transport vesicles depends on the interaction between coat proteins involved in vesicle budding and the molecules that must be included in the vesicle. This interaction occurs through the recognition of particular motifs called sorting signals, localized in the cytoplasmic domain of the cargo molecules.

b) Resident proteins can be retained through their interaction with other components of the donor compartment, avoiding their inclusion in the newly formed vesicles.

c) Proteins that should remain at the donor compartment can be included in the vesicles by mistake or randomly and transported to the

target compartment. From this compartment, these proteins can be recovered through “recovery or rescue pathways”.

1.1.1.1. Vesicle targeting.

Transport vesicles must be transported towards the correct target compartment among all other possibilities and must be highly accurate in recognizing the correct target membrane with which to fuse. To this end, transport vesicles contain markers in their surface that identify them and target membranes display complementary receptors which recognize the vesicle markers. In particular, Rab GTPases, tethering proteins and N-ethylmaleimide-sensitive factor attachment protein receptors (SNAREs) are some of the proteins involved in the specific recognition between the vesicle and the target compartment (Pelham, 2001; Pfeffer, 2001; Sztul and Lupashin, 2009). These proteins exhibit restricted and specific subcellular localization (Uemura and Ueda, 2014).

2. THE SECRETORY PATHWAY

The secretory pathway is a complex system of membrane-bound compartments which are specialized in the synthesis, transport, modification and secretion of a wide range of proteins, complex carbohydrates and lipids. It provides the default exit route for secretory cargo proteins. In addition, the secretory pathway must respond to specific

cellular functional demands, which imply a highly dynamic trafficking. Therefore, this system is of vital importance in the life of a cell.

The secretory pathway includes the transport of newly synthesized proteins from the ER to the Golgi apparatus (early secretory pathway). Then, cargo molecules flow through the Golgi apparatus, from the *cis*- to *trans*-cisterna, to reach the TGN, where they are sorted into vesicles and transported to the PM (late secretory pathway) or to the vacuole through the PCV/MVB. It has also been proposed that secretion may be redirected to the cell plate during cell division (Richter et al., 2009).

At least for soluble cargo proteins, trafficking to the PM is a default pathway (Richter et al., 2007). This pathway is called "Classical or conventional protein secretion" (CPS) (Ding et al., 2012; Robinson et al., 2016). However, this term is also used to include the transport of soluble proteins to the vacuole through the Golgi apparatus and the TGN. In this conventional pathway, secreted proteins have in common three characteristics: they possess an N-terminal leader sequence, they show some kind of posttranslational modification and their transport is blocked by application of brefeldin A (BFA). In the case of vacuolar proteins, they should contain an additional sequence-specific sorting determinant (Robinson et al., 2016).

Protein transport through the secretory pathway is controlled by transport vesicles which carry cargo molecules from one organelle to the next. This transport can occur in the forward direction (anterograde

transport), from the ER to the PM, or in a reverse direction (retrograde transport) (Hanton et al., 2005):

a) Anterograde transport: Membrane traffic pathway in which a linear assembly of compartments facilitates cargo movement from the ER towards the cell surface through the Golgi apparatus or to the lytic vacuole via PVC and protein storage vacuole (Figure 3) (Brandizzi and Barlowe, 2013).

b) Retrograde transport: membrane traffic pathway in which a linear assembly of compartments facilitates cargo movement towards the ER (Figure 3) (Brandizzi and Barlowe, 2013).

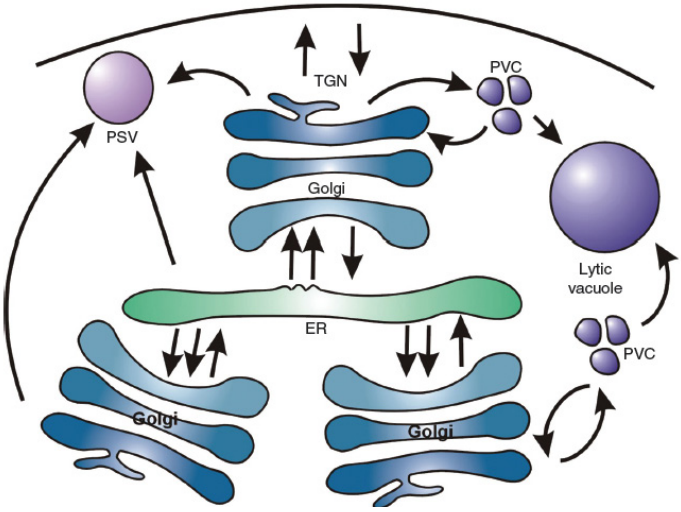

Figure 3. Overview of the secretory pathway in plants (Hanton et al., 2005). Schematic representation of organelles and their connecting protein transport routes in the plant-secretory pathway. ER, Endoplasmic reticulum; TGN, *trans*-Golgi network; PVC, prevacuolar compartment; PSV, protein storage vacuole.

The entire secretory pathway exists as an equilibrium between anterograde and retrograde transport. Retrograde transport is essential. It continually recycles proteins and lipids to maintain anterograde transport and the homeostasis of individual organelles. Disruption of retrograde transport inhibits anterograde transport, and thus, can result in dramatic changes in the biology of a cell (Hanton et al., 2005).

2.1. EARLY SECRETORY PATHWAY

The early secretory pathway includes the transport of newly synthesized proteins from the ER to the Golgi apparatus. Protein transport between ER and Golgi apparatus is bidirectional: anterograde transport (from the ER to the Golgi) is mediated by COPII-vesicles, while retrograde transport (from the Golgi to the ER) is mediated by COPI-vesicles (Figure 4) (Hawes et al., 2008; Marti el at., 2010; Brandizzi and Barlowe, 2013; Gao et al., 2014).

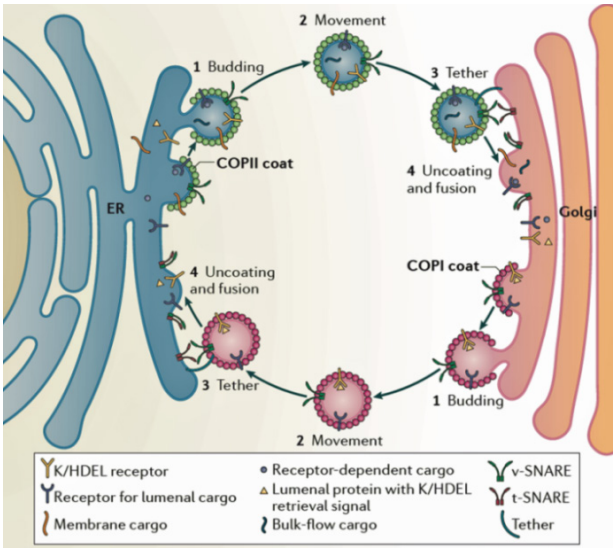

Figure 4. Bidirectional transport between the ER and the Golgi is mediated by COPI and COPII vesicles (Brandizzi and Barlowe, 2013). Bidirectional transport of secretory cargo between the ER and the Golgi requires budding, movement, tethering, as well as uncoating and fusion of COPII) and COPI vesicles with their respective compartments. These include bulk-flow, membrane cargo and receptor-dependent luminal cargo. COPII vesicles facilitate selective and bulk-flow cargo export towards the Golgi. One important function of COPI is to facilitate retrieval of escaped luminal proteins containing K/HDEL retrieval signals that are recognized by the K/HDEL receptor as well as other machinery required for optimal anterograde transport. Vesicle fusion is mediated by vesicular SNARE proteins (v-SNARE) a target-SNARES (t-SNAREs) upon anchoring of the vesicles to their target compartment via tethers.

2.1.1. The ER network

The early secretory pathway starts when secretory proteins and proteins destined for different compartments in the pathway, which contain an N-terminal signal peptide (SP) in their sequence or have analogous signals at other places within the protein, are translocated into the ER (Bassham et al., 2008; Ding et al., 2012; Robinson et al., 2016). The ER

extends from the nuclear envelope to the cortical regions of the cell pushed by the large central vacuole. It is characterized by a network of interconnected membrane tubules and sheets that form closed polygons. It is likely that some portions of the ER are in close contact with every organelle in the cell, performing various roles with each contact. In highly vacuolated cells, the ER is pushed to the cortex of the cell by the large central vacuole (Hanton et al., 2005; Bassham et al., 2008; Brandizzi and Barlowe, 2013).

The ER is responsible for initiating the synthesis, folding and quality control, as well as priming the glycosylation, of a large number of proteins. In the ER, proteins acquire their proper conformation and undergo initial post-translational modifications (Strating and Martens, 2009). In particular, *N*-glycosylation is initiated in the ER when a preperformed oligosaccharide ($Glc_3Man_9GlcNAC_2$) is transferred *en bloc* to the asparagine residue in an Asn-X-Ser/Thr motif (where X represents any amino acid residue except proline) of the nascent polypeptide chain during translation. The *N*-glycan is immediately modified and two molecules of glucose are removed in order to be recognized by the ER-resident lectin-like chaperone. Subsequently, the last glucose is removed to release these chaperones. If the protein is not properly folded, the *N*-glycan is reglycosylated (Ito et al., 2014; Caramelo and Parodi, 2008). Proteins which are not properly folded re-enter the folding cycle, but when folding fails those proteins are targeted to degradation by the ER-degradation system (ERAD). If the load of unfolded proteins increases, a signalling cascade, known as the unfolded protein

response (UPR) is activated. The UPR induces a number of events in order to decrease the amount of unfolded proteins (section 4 of Introduction).

2.1.2. ER export sites and ER-to-Golgi transport

Properly folded proteins and membrane cargos are transported from the ER to the Golgi through COPII-coat vesicles which are known to be recruited and bud from specialized subdomains of the ER, called ER export sites (ERES) (Brandizzi and Barlowe, 2013). Therefore, ERES are defined as the sites through which secretory proteins leave the ER and are characterized by the absence of ribosomes and the local accumulation of COPII proteins, so that COPII components are used as ERES markers (Langhans et al., 2012; Brandizzi and Barlowe, 2013). In addition to the COPII components, ERES also show large multidomain SEC16 proteins. SEC16 is required for ERES organization and has been proposed to function as a scaffold and regulator of COPII coat assembly at ERES (Budnik and Stephens, 2009; Miller and Barlowe, 2010; Brandizzi and Barlowe, 2013; Takagi et al., 2013).

In mammals, ERES are relatively stable and immobile structures. The domain of the ER containing ERES is sometimes termed “transitional ER” (t-ER) whose definition has been extended to include post-ER structures, such as the ER-Golgi Intermediate Compartment (ERGIC) (Hughes et al., 2009). Nowadays, it is more appropriate to consider the ERGIC as a distinct organelle to the ER which functions as an intermediate compartment of transport between the ER and the Golgi. It is involved in concentration of

anterograde biosynthetic cargo, in COPI-dependent sorting of retrograde cargo and possibly in post-ER protein quality control (Brandizzi and Barlowe, 2013). Two different models for the transport between the ER and the Golgi through the ERGIC have been proposed (Brandizzi and Barlowe, 2013; Ito et al., 2014):

a) Transport complex model: homotypic fusion of COPII vesicles forms the ERGIC which travels to the Golgi via long-range microtubule tracks to become the *cis*-Golgi by homotypic fusion or fusion with pre-existing *cis*-Golgi cisterna (Stephens and Pepperkok, 2001; Sztul and Lupashin, 2009).

b) Stable compartment model: COPII vesicles mediate the short-range microtubule-independent transport from the ERES to the ERGIC followed by long-range transport of anterograde cargo-rich domains from the ERGIC depending on microtubule tracks. Thus, ERGIC would be a static structure which facilitates a two-step transport process (Ben-Tekaya et al., 2005; Applenzeller-Herzong and Hauri, 2006).

However, the secretory system in plants lacks an intermediate compartment between the ER and the Golgi (such as the ERGIC in mammalian cells), so that COPII-coated carriers are thought to fuse with other COPII-coated carriers to form the first *cis*-cisterna or to attach to the rims of the *cis*-cisternae (Yang et al., 2005; Kang and Staehelin, 2008). This involves that the organization of the ER-Golgi interface varies greatly in different species. Moreover, the Golgi apparatus in plants is present as multiple stacks which are distributed throughout the cytosol and it shows

rapid motility (up to 4 µm per sec) and this requires the activity of actomyosin motors and close association with tubular ER strands, so that the distance between both organelles is very small (Figure 5) (Brandizzi and Barlowe, 2013).

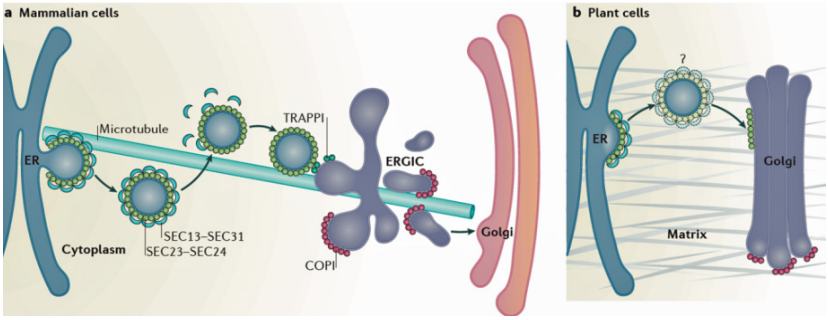

Figure 5. The ER-Golgi interface and ERES have a distinct organization in mammals and plants (Brandizzi and Barlowe, 2013) a) In mammalian cells, ER exit sites (ERES) are oriented towards a juxtaposed endoplasmic reticulum (ER)-Golgi intermediate compartment (ERGIC). Coat protein complex II (COPII)-coated vesicles originate within cup-shaped ER subdomains, which are associated with the plus end of microtubules. Upon fission of vesicles from the ERES, the SEC13-SEC31 cage is depolymerized, but the SEC23-SEC24 coat is partially retained. Vesicles reach the ERGIC in a microtubule-independent manner where they are tethered through the interaction between SEC23 and the TRAPPI (transport protein particle I) tethering complex. COPI mediates forward protein transport from the ERGIC towards the Golgi as well as recycling back to the ER membrane. B) In plant cells, ERES and Golgi are closely associated, possibly through a matrix (indicated in grey) that holds the ER and the Golgi together. The existence of COPII vesicles in plants is still debated. Unlike mammalian cells, plant cell ER-Golgi transport does not rely on the microtubule cytoskeleton.

These unique characteristics make difficult to identify a single model of transport between ERES and the Golgi in plant cells. The mobility of the early plant secretory pathway has suggested four possible mechanisms for protein transport from the ER to mobile Golgi stacks (Figure 6) (Ito et al., 2014):

a) "Kiss-and-run" or "stop-and-go" model: ERES are relatively stable, and the Golgi stacks travel from one ERES to another. In this model, it has been postulated that an active ERES produces a "stop signal" which causes the Golgi stack to pause. During this temporal association between the Golgi stack and the ERES, ER-to-Golgi transport takes place. After that, the Golgi stack resumes its movement (Nebenführ et al., 1999; Kang and Staehelin, 2008).

b) Secretory unit model: ERES are capable of movement over the ER and are in continuous association with Golgi stacks, so that both organelles move together. The ER-to-Golgi transport can occur also while the Golgi stacks are moving, not only during their pauses (daSilva et al., 2004; Stefano et al., 2006; Hanton et al., 2007; Takagi et al., 2013).

c) Hybrid model: Similarly to the secretory unit model, some of the ERES are continuously associated with the Golgi stacks. However, other ERES, which are not associated with the Golgi stacks, are smaller and move independently from the Golgi stacks. They get stable and active when they encounter the Golgi stacks (Ito et al., 2012).

d) Modified secretory unit model: The COPII and COPI vesicles are continuously formed during the Golgi movement. The anterograde COPII traffic is not restricted to temporary stationary Golgi stacks. In contrast, the temporal pauses of the Golgi stacks take place at the ER import sites (ERIS) and the fusion of COPI vesicles with the ERIS only occurs while the Golgi stacks are immobile. However, both types of vesicles accumulate between

the Golgi and the ER, and move together with the Golgi stacks (Lerich et al., 2012; Langhans et al., 2012).

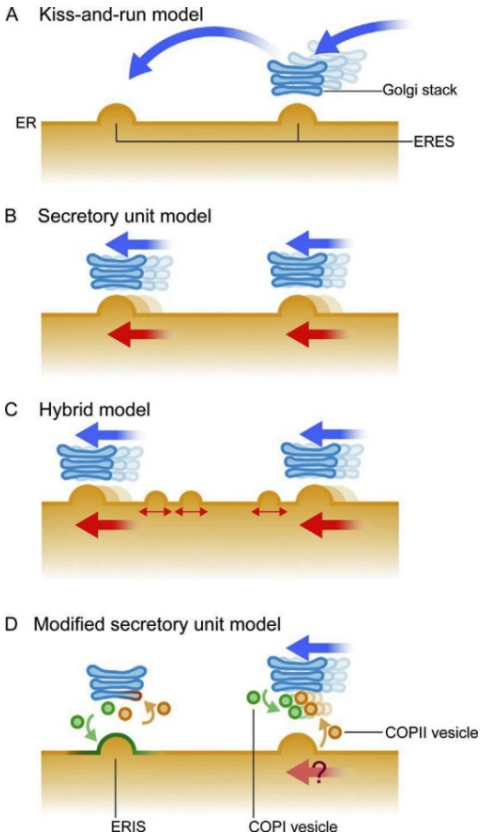

Figure 6. Models of ERES-Golgi organization in plant cells (Ito et al., 2014). Picture of the four models of protein transport between ERES and the Golgi stacks (see text for details).

In addition to these models, the major dispute is over the type of COPII-carriers involved in the ER-Golgi transport. Because vesicle-like structures have been rarely detected in electron microscopy analyses, the

possibility of membrane connections between the ER and the Golgi through interconnecting tubules, permanent or transitory, has been debated. Different models have been proposed to explain the ER export in plants (Figure 7) (Robinson et al., 2015; Chung et al., 2016).

a) **Vesicular-mediated ER export:** COPII coated vesicles bud from the ERES to the *cis*-Golgi carrying protein cargoes.
b) **Tubule-mediated ER export:** COPII mediates the formation of tubules that connect the ER and the Golgi apparatus which allow the direct transport of cargo proteins,
c) **Tubule-and vesicle-mediated ER export:** Vesicles and tubules mediate the ER export under specific conditions.

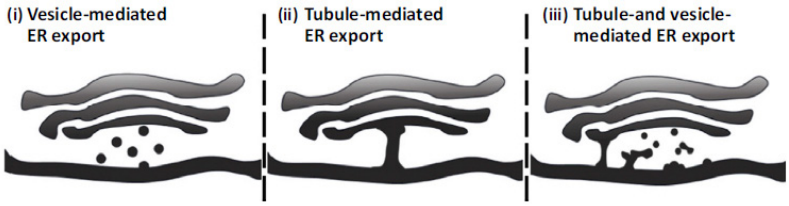

Figure 7. Working models of ER export in plants (Chung et al., 2016)

There are arguments based on experimental evidence for vesicular or tubular models which made unable to reach a consensus about the modality of membrane traffic between both organelles in plants (Robinson et al., 2015).

Nevertheless, it has been proposed that the close association between the ER and the Golgi stacks is due to the fact that both organelles are firmly

connected through a tethering matrix which might facilitate ER-Golgi COPII transport. Thus, cytoskeletal elements may not be needed to facilitate the bidirectional transport at the ER-Golgi interface. This might be true for highly vacuolated cells in which the Golgi was found to be mainly associated with the ER due to the presence of a central vacuole that occupies most of the cell volume. However, it does not seem to be the case for root meristems, where the Golgi stacks are not usually closely associated with the ER. Therefore, different plant cell types possibly use diverse ERES-Golgi spatial organization to accomplish ER export (Kang and Staehelin, 2008; Marti et al., 2010; Brandizzi and Barlowe, 2013).

Although COPII is essential for ER-to-Golgi transport, recent studies in yeast and animals have shown that depletion of some COPII component does not always inhibit cargo transport from the ER to the Golgi apparatus (Fatal et al., 2004; Mironov, 2014). However, there is no doubt that retrograde Golgi-to-ER transport is mediated by COPI-vesicles.

2.1.3. Golgi-to-ER transport

Golgi-to-ER transport is mediated by COPI vesicles which bud from the edges of Golgi cisternae. In plants, it has been proposed that ER export is a continuous process, but COPI vesicles are tethered by Dsl1 complex while the Golgi stack is moving, and fuse with the ER during temporary pauses of the Golgi. Thus, mobile Golgi stacks are accompanied by a domain of the ER containing COPI-tethering factors (Lerich et al., 2012).

Fusion between COPI vesicles and the ER membrane seems to occur at specialized ER subdomains named ERIS (ER import sites) or ERAS (ER arrival sites), which are close to the ERES. This spatial separation of exit and entry sites may facilitate the simultaneous arrival and departure of material (Lerich et al., 2012; Schöter et al., 2016).

2.1.4. The Golgi apparatus and intra-Golgi trafficking

The plant Golgi apparatus is a major sorting station and it is responsible for delivering cargo proteins to multiple destinations. Moreover, it functions as a polysaccharide factory and its activity is essential for the formation of the cell wall during cytokinesis and growth (Robinson et al., 2015). As described above, it consists of numerous individual stacks which are usually dispersed throughout the cytoplasm and can travel along actin filaments. Each Golgi stack has a polarized structure, from the *cis* side which receives cargo proteins from the ER, and the *trans* side which send cargo proteins to post-Golgi organelles. Along this axis, many glycosylation enzymes are arranged as a gradient, so that cargo proteins can be modified sequentially while crossing the Golgi stacks. Two major models have been proposed to explain how cargo molecules are transported through the stack of cisternae (Figure 8) (Ito et al., 2014).

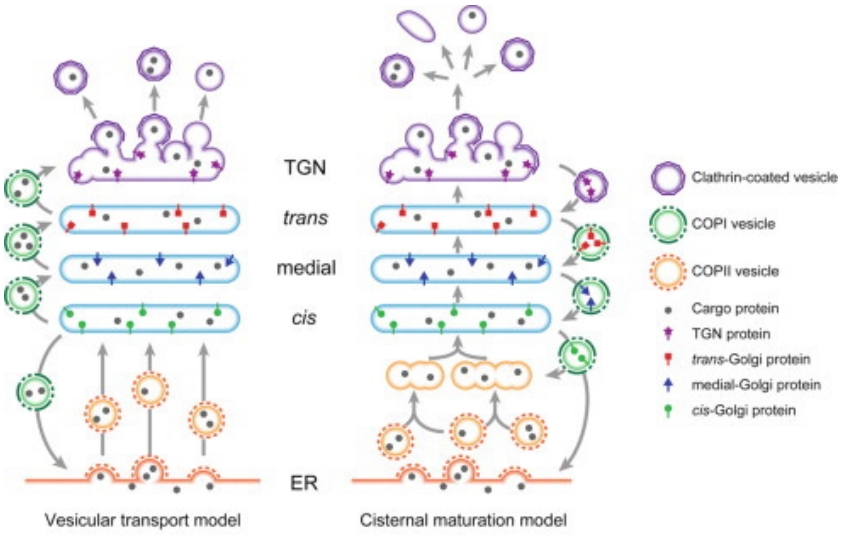

Figure 8. Two major models for intra-Golgi trafficking (Ito et al., 2014). A) The vesicular transport. B) The cisternal maturation model or cisternal progression model.

a) Vesicular transport model: The Golgi cisternae are stable compartments and each Golgi cisterna is viewed as a different suborganelle with a characteristic set of resident proteins. Thus, cargo proteins are transported from one cisterna to the other by anterograde or retrograde COPI vesicles, whereas the resident proteins are excluded from them and remain in the cisterna. Finally, cargo proteins reach the TGN.

b) Cisternal progression model: The Golgi cisternae themselves function as the cargo carriers. Each *cis*-cisterna is newly formed by the homotypic fusion of COPII vesicles, and functions as a transient compartment which progresses from the *cis* to the *trans* side to become the TGN. Thus, the nature of the cisternae gradually changes while they

progress along the secretory pathway. Retrograde COPI vesicles recycle Golgi proteins from later to earlier cisternae.

Regardless of whether COPI vesicles are involved in anterograde or retrograde intra-Golgi transport, it has been proposed the existence of two different populations of COPI-vesicle: COPIa-vesicles, which are derived from the *cis*-cisternae and could mediate Golgi-to-ER transport, and COPIb-vesicles, which derive from medial and *trans*-cisternae and could be involved in intra-Golgi transport (Hwang and Robinson, 2009).

2.2. LATE SECRETORY PATHWAY

2.2.1. The *trans*-Golgi Network (TGN)

Once the secretory proteins are transported through the Golgi stacks, they reach the *trans*-Golgi network, which is a tubule-vesicular compartment that is transiently associated with an individual Golgi stack and can move away independently (Viotti et al., 2010). The TGN is a major sorting station for exocytic cargo proteins except for some storage protein which are sorted at the ER or *cis*-Golgi. In addition, it also functions as an early endosome (EE) in plants, being the first compartment which receives endocytosed proteins. Thus, the TGN is at the convergence of the secretory and endocytic pathways. In spite of the distinct sorting functions performed by the TGN, there is no structural evidence for the existence of different TGN subdomains (Park and Jürgens, 2012). Finally, this compartment

appears to be formed from the *trans*-most cisternae of the Golgi stack, possibly by maturation. Its integrity seems to be maintained by anterograde traffic towards the PM and the vacuole as well as by retrograde traffic to the Golgi apparatus (Park and Jürgens, 2012).

2.2.2. Transport to the plasma membrane

The plasma membrane (PM) is the target membrane for secreted proteins and the components of the extracellular matrix are delivered to the apoplast where they can become incorporated or diffuse away (Bassham et al., 2008). Traffic of soluble proteins from the ER to the PM through the Golgi apparatus and the TGN occurs by default. The only requirement for soluble proteins is to contain an N-terminal signal peptide which allows their translocation across the ER membrane, as shown for several soluble enzymes as well as GFP (Park and Jürgens, 2012).

Membrane proteins destined to the PM may function as ion channels or membrane transporters, ligand receptors and signalling complexes, or even as physical contact points for both the intracellular cytoskeleton network or for the extracellular matrix (Bassham et al., 2008). Secretory trafficking of membrane proteins is less well characterized than that of secretory proteins. Membrane proteins with a single transmembrane domain appear to reach their destination along the secretory pathway according to the length of their hydrophobic region: proteins with a shorter membrane span are held back in the Golgi stack whereas those with a longer membrane span are trafficked to the PM (Brandizzi et al., 2002a). For

other membrane proteins such as those with multiple membrane spans or those with a hydrophobic tail anchor such as SNARE proteins that are inserted into the ER membrane, the situation might be different (Park and Jürgens, 2012).

Although secretory traffic to the PM seems to be the default pathway in interphase, in dividing cells, TGN-derived membrane vesicles that deliver the necessary material for building the PM and the cell wall are targeted to the plane of cell division. Thus, the default pathway changes from the PM to the cell plate during cell division (Richter et al., 2009; Park and Jürgens, 2012).

2.2.3. Vacuolar cargo trafficking pathway

In the conventional secretory pathway, newly synthesized soluble cargo proteins destined to the vacuoles contain an N- or a C-terminal vacuolar sorting sequence/signal (VSS), which binds to vacuolar sorting receptors (VSRs), to be delivered to the prevacuolar compartment (PVC) or Multivesicular Bodies (MVBs) and the vacuole. Therefore, PVC/MVBs can be considered the functional equivalents of late endosomes (LE) of animal cells (Park and Jürgens, 2012).

Sorting of vacuolar cargo has been long thought to occur at the TGN, but more recent observations suggest that this may occur at the ER (Niemes et al., 2010). It has been proposed that soluble cargo proteins are transported from the TGN to the MVB/PVC by clathrin-coated vesicles

(CCVs). Once in the MVBs/PVC, they are released from the VSRs due to its acidic pH. Whereas soluble cargo proteins are delivered to the vacuole via membrane fusion of the MVBs/PVC with the vacuole, the VSRs are recycled back to the TGN through the retromer (Park and Jürgens, 2012).

However, recently published data point to the existence of multiple transport routes for tonoplast proteins (Bottanelli et al., 2011; Viotti, 2014; Robinson and Pimpl, 2014). These observations include the possibility that post-TGN transport occurs independently of CCV and that the MVBs/PVC are derived from the TGN through maturation (Scheuring et al., 2011). In addition to post-TGN pathways, a Golgi-independent vacuolar transport pathway has also been proposed for some membrane proteins which involves the direct transport of vacuolar proteins from the ER to the vacuole (Viotti, 2014; Uemura and Ueda, 2014). These different pathways reflect the existence of different types of vacuoles which are diverse in shape, size, content, and function. These different functions include space filling to increase the volume of the cell, defense responses, and the functions of the two major types of vacuoles: the storage of proteins and sugars in protein-storage vacuoles, and the lytic function shared with other organisms in lytic vacuoles (Park and Jürgens, 2012; Uemura and Ueda, 2014).

2.3. UNCONVETIONAL PROTEIN SECRETION (UPS)

In addition to the “conventional secretion”, that is followed by proteins containing a signal peptide (see above), it has been identified the existence of non-classical protein secretion for proteins that lack a signal peptide,

called LSPs (leaderless secretory proteins). Therefore, unconventional protein secretion (UPS) is a collective term for mechanisms by which proteins that lack a leader peptide sequence, show no posttranslational modifications and are unaffected by BFA are released to the cell exterior (Robinson et al., 2015). Since many pathogen-related proteins released in response to pathogen attack or stress are LSPs, UPS seems to be involved in their secretion (Ding et al., 2012; Krause et al., 2013; Robinson et al., 2016).

Over 50% of the proteins belonging to the so-called plant secretome are LSPs (Ding et al., 2012; Drakakaki and Dandekar, 2013). However, there is a great variability in the numbers and types of LSP in the published data. In addition, the presence of LSPs in the plant secretome could merely reflect contamination with cytosolic proteins. Thus, it has been proposed that the decisive proof that a LSP is present in the apoplast requires immunological confirmation in situ (Robinson et al., 2016). There is only one verified case of UPS in plants with this stringent criteria and it is for Helja, a mannosidase-specific jacalin-related lectin in sunflower seedlings (Pinedo et al., 2012).

Four different types of UPS pathways have been proposed (Figure 9). One of them may occur through direct translocation of proteins across the PM, by a Golgi-bypass pathway. The other three secretion pathways are indirect, and involve the fusion of some kind of organelle carrier with the PM, including central vacuole, MVBs, and a double-membrane organelle termed EXPO (exocyst-positive organelle) (Ding et al., 2014).

EXPO is a novel double-membrane organelle recently identified in *Arabidopsis* which is characterized by the presence of EXO70E2, one of the subunits of the putative exocyst complex of *Arabidopsis* (Wang et al., 2010; Ding et al., 2012). The exocyst is an evolutionary conserved complex that consists of eight subunits and acts at specific domains of the PM that exhibit extensive fusion of exocytic vesicles in mammals and yeast (Wang et al., 2010; Ding et al., 2012). The exocyst complex in plants has been shown to participate in conventional exocytic events during normal cell wall growth, cell plate formation, compatible pollen responses in stigmatic papillae, in response to pathogen attacks and is also required for autophagosome formation (Robinson et al., 2016).

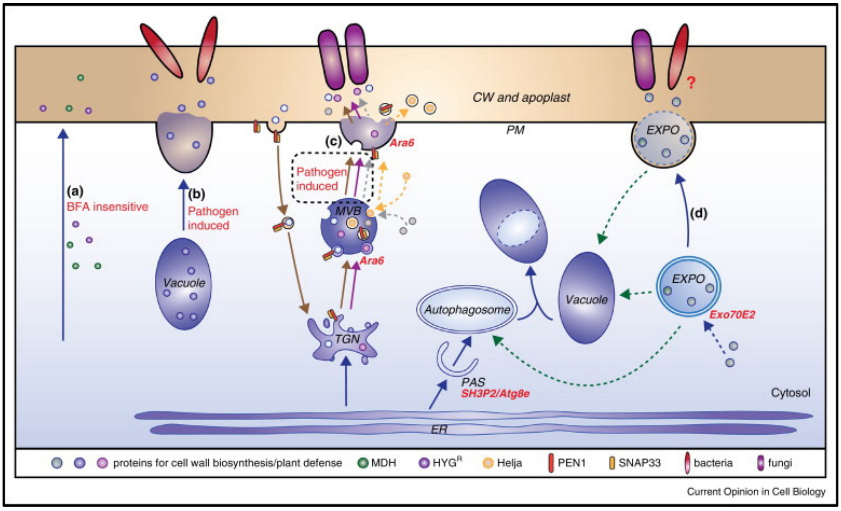

Figure 9. Working model of unconventional protein secretion (UPS) pathways and their potential functions in plant cell (Ding et al., 2014). A) Direct Golgi-bypass pathway. B) Indirect

vacuole mediated pathway. C) Indirect MVB mediated pathway. D) Indirect EXPO mediated pathway.

3. VESICLE TRAFFICKING MACHINERY AT THE ER-GOLGI INTERFACE

3.1. COPII VESICLES

3.1.1. Formation of COPII vesicles

Cargo sorting for exit from the ER is mediated by COPII coated vesicles. The COPII coat is composed of five proteins: Sar1, Sec23, Sec24, Sec13 and Sec31, which form the minimal machinery required to form vesicles *in* vitro.

COPII coat assembly is initiated by the activation of Sar1, a small GTPase, which is mediated by Sec12. Sec12 is a guanine-nucleotide exchange factor (GEF) localized to the ER membrane which recruits Sar1 through the exchange of GDP for GTP. When Sar1 is in its GTP-bound state, it exposes its N-terminal amphipathic helix, which is inserted in the ER membrane and induces initial membrane curvature. Next, two COPII coat complexes (Sec23/Sec24 and Sec13/Sec31) are recruited sequentially to form two layers. To this end, activated Sar1-GTP first interacts with Sec23, to recruit the Sec23/Sec24 complex and form the Sar1/Sec23/Sec24 “prebudding complex”. Sec23 is the GTPase activating protein (GAP) for Sar1, while Sec24 contains multiple independent domains that interact

directly with specific sorting signals on various cargo proteins. The "prebudding" Sar1/Sec23/Sec24 complex then recruits the heterotetramic complex Sec13/Sec31 via interaction between Sec23 and Sec31, which also contributes to the GTPase activity of Sec23. Thus, two different layers form the fully assembled coat: the "inner" membrane layer of Sar1/Sec23/Sec24, which contributes to cargo-binding function, and the "outer" membrane layer composed of Sec13/Sec31, which provide a scaffold that imposes curvature to the nascent vesicle as it buds from the ER. Although the majority of membrane bending force likely comes from Sec13/Sec31 complex, the Sar1 helix seems to drive scission.

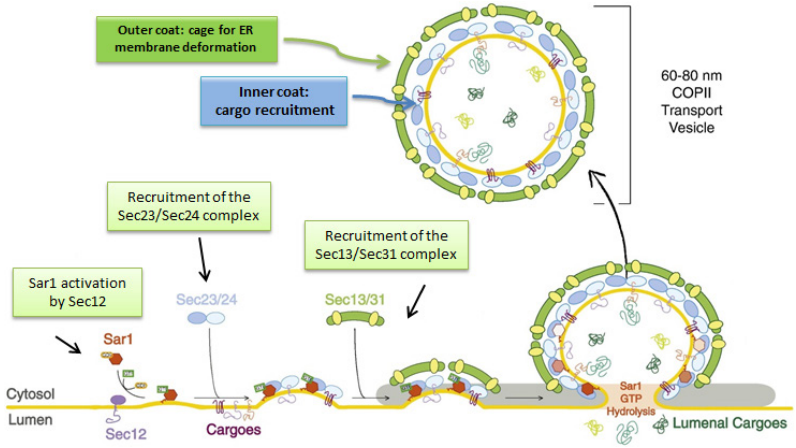

Figure 10. COPII assembly at the ER membrane (Adapted from D'Arcangelo et al., 2013). COPII coat formation at the ER is initiated by recruitment of Sar1 to the membrane in the GTP-bound state, enhanced by Sec12 GEF activity. Sar1-GTP recruits Sec23/Sec24 heterodimer through interaction with Sec23. At the ER, Sec24 recruits cargo into pre-budding complex. Sec13/Sec31 complex is recruited to the inner coat layer through interaction with Sec23. Sec13/Sec31 assembly into the coat drives membrane curvature, facilitating membrane deformation.

A subunit of the COPII coat complex, Sec23, is known to act as GAP for Sar1. In addition, the binding of Sec13/Sec31 increases Sec23-mediated GAP activity. Thus, GTP hydrolysis by Sar1 is maximal once the coat is completely assembled, so that, COPII vesicles are quickly uncoated after budding.

COPII components are highly conserved in eukaryotes. In particular, nineteen paralogs have been identified in *Arabidopsis*. There are five *sar1*, seven *sec23*, three *sec24*, two *sec13*, and two *sec31* isoforms in its genome, which largely outnumber those in other eukaryotes (Table 1). Recent studies have suggested the functional diversity of various COPII subunit paralogs in plants. For example, certain COPII subunit paralogs have shown either organ-specific or developmental stage-specific expression, which indicate the importance or certain isoforms in specific organs in plants. In addition, certain COPII subunit paralogs have been shown to change dramatically under stress. For instance, the expression of *sar1a* and *sec31a* is up-regulated during ER stress (Chung et al., 2016).

However, COPII vesicle-like structures are rarely found by electron microscopy in plants, especially in highly vacuolated cells, although there are a few reports (Robinson et al., 2007; Langhans et al., 2012; Donohoe et al., 2013). This is thought to be due to rapid consumption of the vesicles at the ER-Golgi interface (Brandizzi and Barlowe, 2013).

Table 1. *A.thaliana* COPII subunits have high diversities of isoforms.

Sar1	Sec23	Sec24	Sec13	Sec31
At1g09180 (a)	At4g01810 (a)	At3g07100 (a)	At2g30050 (a)	At1g18830 (a)
At1g56330 (b)	At1g05520 (b)	At3g44340 (b)	At3g01340 (b)	At3g63460 (b)
At4g02080 (c)	At2g21630 (c)	At4g32640 (c)		
At3g62560 (d)	At2g27460 (d)			
At1g02620 (e)	At3g23660 (e)			
	At4g14160 (f)			
	At5g43670 (g)			

() Assigned isoform name.

3.1.2. COPII interaction motifs

To some extent, cargo proteins can enter into vesicles in a nonspecific manner known as “bulk flow”, probably stemming from stochastic sampling of the ER membrane and lumen during vesicle formation. However, some cargos are dramatically enriched in vesicles (Barlowe and Miller, 2013).

Selective enrichment of transport vesicles occurs via specific sorting signals. In particular, Sec24 acts as the cargo binding adaptor for the COPII coat, with multiple binding sites for interaction with distinct sorting signals. Transmembrane cargo proteins contain in their cytosolic tail different sorting motifs that interact with Sec24 for their inclusion into COPII vesicles.

Some cargos, such as soluble proteins, do not interact directly with Sec24 but instead use cargo receptors which contain lumen-exposed domains that bind cargo proteins and cytoplasmic domains that interact

with Sec24 to couple cargo selection with COPII vesicle formation. p24 family proteins have been proposed to function as cargo receptors because they contain a luminal N-terminus that has been show to interact with different proteins, a single transmembrane segment and a small cytoplasmic tail which contains sorting signals that interact with the COPII coat (see below, section 5 of Introduction).

Different sorting signals have been identified on cargo proteins of COPII vesicles (ER export signals): a diacidic motif (DXD, DxE, EXE), a diaromatic motif (ϕϕ, FF) and a dibasic motif ([RX](X)[RX]). Finally, different motifs involved in sorting of the different SNAREs have been identified (Mossessova et al., 2003; Mancias and Goldberg, 2008). In mammals, Sec24 isoforms show different affinities for different export signals, which might lead to the selective accumulation of cargo in COPII vesicles (Mancias and Goldberg, 2008). In plants, different studies have shown differences between *Arabidopsis* SEC24 isoforms which may reflect specific cargo recognition (Ito et al., 2014).

3.1.3. Tethering, and fusion of COPII vesicles

The final stage of cargo delivery involves the recognition of the target membrane and the membrane fusion between the COPII vesicle and the *cis*-Golgi. In mammalian cells, the vesicle targeting stage depends on the RAB GTPase RAB1, and tethering factors, including the coiled-coil tethering factors p115, GM130 and GRASP65, as well as the TRAPPI tethering complex which consist in BET3, BET5, TRS20, TRS23, TRS31 and TRS33 subunits and

acts as GEF for RAB1 (Sztul and Lupashin, 2009; Brandizzi and Barlowe 2013). It has been proposed that TRAPP1 might bind COPII vesicles while they are forming since BET3 subunit directly interacts with TRAPPI and Sec23. Then, TRAPP1 activates Rab1 on the vesicles which recruits p115. Finally, p115 tethers COPII vesicles to the Golgi, presumably by interacting with GM130 and GRASP65 (Szul and Sztul, 2011).

In *Arabidopsis*, Rab1 homologs have been identified which belong to the Rab-D group and are divided into two subclasses, RabD1 and RabD2, according to their sequence. In particular, *Arabidopsis* has one RabD1 and three RabD2, and both subclasses are thought to be involved in ER-Golgi trafficking (Ito et al., 2014). On the other hand, a homolog of p115, GC6, has been also identified (Latinjhouwers et al., 2007). Finally, all six subunits of the TRAPPI complex have been also identified through genome analysis and large scale interactome databases (Vukašinović and Žárský, 2016)

The final step is the fusion of the COPII-vesicles with the *cis*-Golgi (section 1.2.1.3. Introduction). In mammals and probably plants, the typical SNARE complex consists of Qa-, Qb-, Qc- SNAREs on the target membrane, and a R-SNARE on the target membrane. In mammalian cells, the SNARE proteins syntaxin 5 (Qa), membrin (Qb), Bet1 (Qc) and Sec22B (R-SNARE) are thought to be responsible for COPII-vesicle fusion. In *Arabidopsis*, 21 SNARE proteins have been localized to the ER and the Golgi apparatus, which could be involved in different routes (Kim and Brandizzi, 2012). It has been proposed that AtSYP31 and AtSYP32 (Qa-SNAREs) are syntaxin 5 homologs;

AtMEMB11 and AtMEM12 (Qb-SNAREs) are membrin homologs; AtVAMP714 SNARE, belong to the R-SNARE group; AtBS14a and AtBS14b (Qc-SNAREs) are similar to Bet1 but they seem to be involved in the intra-Golgi trafficking. The identification of membranes in which individual SNAREs function at the ER-Golgi interface is extremely difficult because they are continuously cycling between these compartments.

3.2. COPI VESICLES

3.2.1. Formation of COPI vesicles

The retrograde transport from the Golgi to the ER is mediated by COPI vesicles. The COPI coat complex consists of a heptameric complex (α, β, β', γ, δ, ε and ζ) called coatomer, which is divided into two subcomplexes: the β/δ/γ/ζ F-complex, which has been proposed as inner layer core that binds cargo, and the α/β'/ε B-complex which has been proposed to function as the outer layer (Jackson, 2014). However, recent structural studies revealed that the seven subunits are highly connected to each other, which indicates that the COPI coat may not form a distinct two-layered structure like the COPII coat (Donova et al., 2015).

COPI assembly is initiated by the activation of the ARF1 GTPase. This activation involves GDP/GTP exchange and is mediated by a family of GEFs which contain a conserved Sec7 domain. ARF1 conformational change coupled with its activation produces the exposure of a myrisotylated, amphipathic N-terminal helix that is inserted into the Golgi membrane.

Next, membrane-anchored ARF1 recruits *en bloc* the coatomer complex through its interaction with the F-complex. In addition, COPI assembly has been shown to depend on both membrane and cargo (Jackson, 2014).

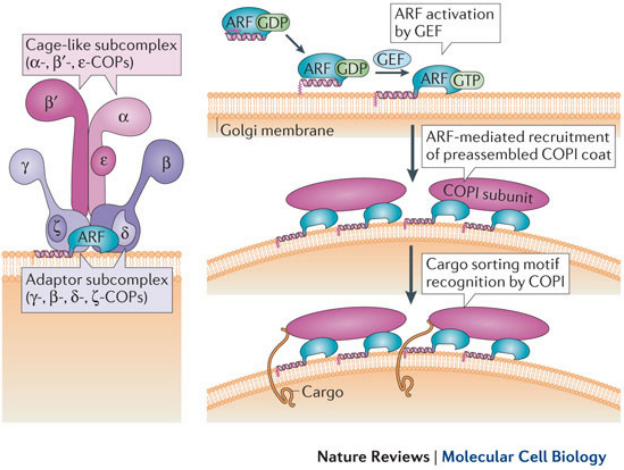

Figure 11. . COPI assembly at the Golgi membranes (Brandizzi and Barlowe, 2013). The COPI complex consist of a heptameric (α, β, β', γ, δ, ε and ζ) complex, also called coatomer, with two main subcomplexes: the γ-, δ-, ζ-, β-COP tetrameric complex (F-complex), which constitutes the inner layer core; and the α-, β'-, ε-COP trimeric complex (B-complex), which forms the outer layer of the COPI coat. One activated by ARF GEF containing a conserved SEC7 domain, myrisotylated membrane-anchored ARF GTPase recruit COPI to Golgi membranes.

COPI machinery is well conserved among eukaryotes, including plants. In humans, two isoforms of γ-COP and ζ-COP have been identified which showed different localization at the early secretory pathway, which suggest different budding sites for each population (Szul and Sztul, 2011). These alternative coatomer complexes may reflect distinct subpopulations of COPI vesicles that mediate different trafficking steps (Gao et al., 2014). In *Arabidopsis,* several isoforms of all the coatomer subunits, except for γ-COP

and ζ-COP subunits, have been identified (Table 2). The high number of isoforms suggests that plants are likely to contain more complex combinations of coatomer subunits for the formation of different subpopulations of COPI vesicles (Gao et al., 2014). In particular, electron tomography studies have already identified two structurally different types of COPI vesicles: COPIa vesicles that bud exclusively from the *cis*-cisternae, and are located at the ER-Golgi interface, and COPIb vesicles which bud from medial- and *trans*-Golgi cisternae (Donohoe et al., 2007; Hwang and Robinson, 2009; Gao et al., 2014). Thus, these different subpopulations of COPI vesicles might be formed by different coatomer isoforms.

Table 2. Plant COPI subunits have high diversities of isoforms[a] (Gao et al., 2014).

Organism	α-COP	β-COP	β′-COP	δ-COP	ε-COP	γ-COP	ζ-COP
Sc	Ret1	Sec26	Sec27	Ret2	Sec28	Sec21	Ret3
Hs	α	β	β′	δ	ε	γ1 γ2	ζ1 ζ2
At	At1g62020 At2g21390	At4g31480 At4g31490	At1g52360 At3g15980 At1g79990	At5g05010	At2g34840 At1g30630	At4g34450	At1g60970 At3g09800 At1g08520

[a] Abbreviation: At *Arabidopsis thaliana*; Hs, *Homo sapiens*; Sc *Saccharomyces cerevisiae*.

In order to fuse with the target membrane, coated vesicles need to be uncoated, which is mediated by the GAP activity of a separate protein, unlike in the COPII system. The GAP activity of mammalian ARF GAP1 is accelerated by binding with coatomer, but this effect is inhibited by a p24 protein which is suggested to act as a cargo receptor (section 3.2.2.). This may ensure that only the coatomer with cargo proteins can stay in the membrane long enough to polymerize. The *Arabidopsis* genome encodes 15

ARF GAP domain (AGD) proteins of which AGD7 has been shown to localize to the Golgi apparatus and to regulate ARF1 activity in ER-Golgi trafficking (Ito et al., 2014). Following hydrolysis by a GTPase activating protein (GAP), Arf1-GDP is displaced from the membrane for future rounds of recruitment.

3.2.2. COPI interaction motifs

Retrieval of ER and Golgi resident proteins via COPI vesicles requires different mechanisms such as transmembrane domain (TMD) length or amino acid sequence motif-based retention signals which may interact with COPI coat proteins directly or indirectly (Gao et al., 2014). The α, β', γ and δ subunits have been proposed to recognize sorting motifs on the cytosolic domain of membrane cargo and mediate its incorporation into COPI vesicles (Brandizzi and Barlowe, 2013). In particular, several studies indicate that the α-COP and β'-COP subunits are involved in cargo binding through their N-terminal WD repeat domain and the helix C-terminal to the longin domain of δ-COPI is required for efficient retrieval of HDEL proteins (Jackson, 2014; Arakel et al., 2016).

a) ER retention signals

The best characterized ER retention signal is the canonical dilysine motif (KKXX and KXKXX) which is essential for the ER retrieval of type I membrane proteins in mammals and plants. However, only p24 proteins have been shown to directly interact with COPI proteins in *Arabidopsis* (Gao et al, 2014). In particular, the cytosolic tail of p24 proteins of the delta

subfamily is able to interact with the coatomer and ARF1, which depends on both dilysine and diphenylalanine motifs (Contreras et al, 2004a). In plants, the canonical motif of soluble ER-resident proteins is the K/HDEL motif, which allows their binding to the retrieval receptor ERD2, which can interact with coatomer (Gao et al., 2014). Besides these canonical motifs, other variants have been reported, including a hydrophobic pentapeptide motif (ϕXX-K/R/D/E-ϕ-COOH, where ϕ are large hydrophobic residues), a divergent type of the dilysine motif (KK-COOH), and a N-terminal arginine-based motif (RXR) (Gao et al., 2014)

b) Golgi retention signals

The retention mechanisms of Golgi-localized membrane proteins usually are more diverse. However, a KXD/E motif has been recently identified as a novel COPI-interacting motif which seems to be responsible for the retention of integral membrane proteins, at least for the *Arabidopsis* endomembrane protein (EMP) family (Gao et al., 2012; Gao et al., 2014).

In mammalian cells, two different populations of COPI vesicles have been identified depending on their cargos. The ER-destined vesicles contained p24 family members while intra-Golgi vesicles carried mannosidase II (a Golgi resident protein) (Szul and Sztul, 2011). In *Arabidopsis*, two different population of COPI vesicles has been also described. Therefore, different sorting signals may be recognized by different coatomer isoforms for their sorting into a COPIa vesicle for ER retrieval or COPIb vesicles to Golgi retention (Gao et al., 2014).

3.2.3. Tethering and fusion of COPI vesicles

The final step of delivery of COPI vesicles involves a long-distance tether to bring the vesicle into proximity of the target membrane and SNARE proteins to drive membrane fusion and it is regulated by Rab GTPases (section 1.2.1. of Introduction). However, tethering COPI vesicles is significantly more complex because they bud from different cisternae of the Golgi and may fuse with many different compartments.

For the Golgi-to-ER COPI vesicles, tethering to the ER membrane seems to be mediated by the trimeric Dsl1 complex, which consists of Dsl1, Tip20 and Dsl3/Sec39 proteins in yeast. One of its three subunits, Dsl1 can bind two COPI subunits, α- and ε-COP, while Tip20 and Dsl3/Sec39 interact with the ER SNAREs Ufe1 (Qa-SNARE), Sec20 (Qb-SNARE) and Use1 (Qc-SNARE), which mediate fusion of COPI vesicles with the ER membrane (Szul and Sztul, 2011; Barlowe and Miller, 2013). Therefore, this complex may function as a bridge between the COPI coat and the ER SNAREs, and it has been proposed to coordinate tethering, uncoating, SNARE assembly, and membrane fusion. A Tip20 homolog was first identified in *Arabidopsis* and named MAG2/AtTIP20, which is associated with the ER membrane through its interaction with the SNAREs AtSec20 (Qb-SNARE) and AtSYP81 (Qa-SNARE). Three MAG2/AtTIP20 interactors, designed MAG2 INTERACTING PROTEINS (MIPs), have been identified in *Arabidopsis*. Therefore, an additional subunit of the Dsl1 complex was found to be part of the complex in *Arabidopsis* (Vukašinović and Žárský, 2016).

Finally, seven SNARES have been shown to localize to the ER in plant cells: Qa SNARE AtSYP82; Qb-SNARE AtSEC20; Qc-SNARE AtSYP71, AtSYP72, AtSYP73 and AtUSE1; and R-SNARE AtSEC2 and AtVAMP723 (Ito et al., 2014).

4. THE UNFOLDED PROTEIN RESPONSE (UPR) IN PLANTS

In the ER, newly synthesized proteins are properly folded and loaded for transfer to other organelles. Since misfolded proteins induce cellular toxicity effect, it is essential that only correctly folded proteins are exported to their final destination. To this end, the ER quality control (ERQC) machinery actively supervises protein assembly in the ER. The ERQC retains incomplete/mis-folded proteins for additional cycles of chaperone-assisted folding (Section 2.1.1. of Introduction) (Liu and Li, 2014). When misfolded proteins fail to achieve their native state, ERQC stop their futile folding cycle and deliver them into the ER-associated degradation (ERAD) pathway to their degradation. The ERAD involves ubiquitination, retrotranslocation, and cytosolic proteasome degradation (Lui and Li, 2014).

However, it is possible that adverse environmental or physiological conditions and pathogen infections increase the demands of protein folding which cannot be satisfied by the ERQC machinery, leading to an accumulation of potentially toxic mis-folded proteins, a situation designed as ER stress (Ruberti and Brandizzi, 2014; Wan and Jiang, 2016). To restore the ER homeostasis, plant cells activate intracellular signal transduction

pathways, collectively known as the unfolded protein response (UPR) (Walter and Ron, 2011).

The **unfolded protein response (UPR)** consists of a series of cytoprotective signalling pathways initiated by ER-resident stress sensors, who sense ER stress and regulate transcriptional or translational activities to alleviate ER stress and restore protein homeostasis in the ER (Deng et al., 2013; Ruberti and Brandizzi, 2014; Wan and Jiang, 2016). It involves the up-regulation of genes encoding ER chaperones and foldases to accelerate protein folding, up-regulation of components of the ERAD to accelerate the degradation of misfolding proteins, and the reduction of the secretory proteins synthesis to lighten misfolding protein loads (Wan and Jiang, 2016). Under extreme situations, these mechanisms of adaption and survival to ER stress may not be enough and fail, leading to autophagy or even programmed cell death (Hetz, 2012; Wan and Jiang, 2016).

Three major branches of UPR signalling pathways have been identified involving different ER-stress sensors (Figure 12):

1. **Activating transcription factor 6 (ATF6) homology pathway:** This pathway involves the releasing of a soluble and functional basic leucine zipper (bZIP) which up-regulates the synthesis of ER chaperones and foldases.
2. **Inositol requiring enzyme 1 (IRE1) pathway:** This pathway involves the unconventional splicing of *bZIP* mRNA which mainly increase the ERAD

components and a reaction called regulated IRE1-dependent decay (RIDD) where mRNAs are spliced randomly.

3. **Protein kinase RNA-like ER kinase (PERK) pathway:** This pathway involves the kinase autophosphorylation and the inactivation of a translation initiation factor, eIF2a, by PERK phosphorylation.

The IRE1 pathway is the only one well-conserved in all eukaryotes while the PERK pathway has been only identified in mammalian systems. In plants, two of the three major pathways have been identified, ATF6 homolog and IRE1 pathway (Walter and Ron, 2011; Deng et al., 2013; Wan and Jiang, 2016). Although both branches are involved in the salt and heat stress response, only AtIRE1-bZIP60 pathway play a role in virus infection (Zhang et al., 2015).

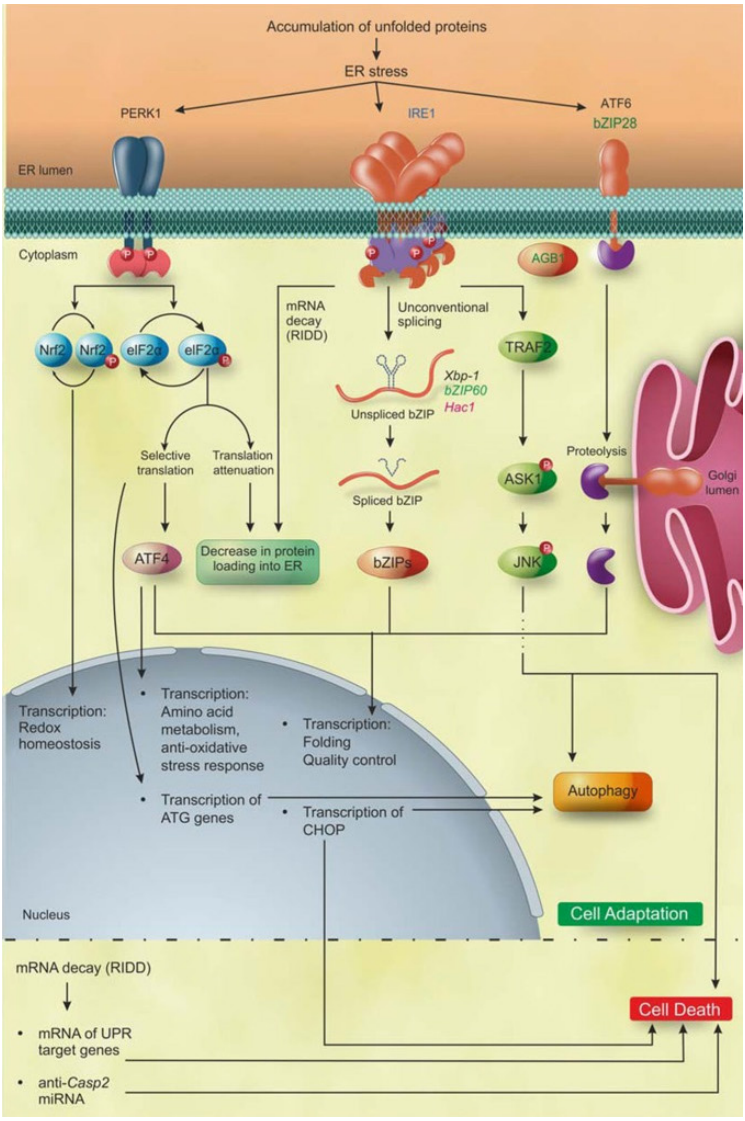

Figure 12. UPR pathways in eukaryotes (Ruberti and Brandizzi, 2014). Blue, eukaryotes; black, metazoan; green, plants; pink, yeast.

4.1. THE ATF6 HOMOLOG PATHWAY IN PLANTS

In mammalian, the ER-stress sensor ATF6 is a type II transmembrane protein with a single-pass transmembrane domain (TMD), whose N-terminus facing the cytosol contains a bZIP transcriptional factor domain and its C-terminus is ER luminal which interacts with the ER-resident chaperone called Binding Protein (BiP). In *Arabidopsis*, two homologs of ATF6 have been identified, AtZIP28 (Liu et al., 2007a) and bZIP17 (Liu et al., 2007b), which encode bZIP transcription factors and share similar functions and mechanisms to ATF6.

It is thought that bZIP28 sense the ER stress through its association with the ER chaperone, BiP. Under unstressed conditions, BiP interacts with the luminal domain of bZIP28 through its substrate binding domain retaining bZIP28 in the ER (Srivastava et al., 2013; 2014). Upon ER stress, the accumulation of misfolded proteins might force the release of bZIP28 from BiP which allows bZIP28 to exit the ER and be transported to the Golgi (Srivastava et al., 2014). In *Arabidopsis*, it has been detected a potential interaction between bZIP28 and Sar1 GTPase which is involved in the COPII vesicle formation (section 3.1.1. of Introduction). This interaction was enhanced upon ER stress (Srivastava 2012; 2014). This suggests that the transport of AtbZIP28 from the ER to the Golgi is mediated by COPII carriers.

Once in the Golgi apparatus, bZIP28 is cleaved by two subtilin-like serine proteases, site-1 protease (S1P) and site-2 protease (S2P) which remove the bZIP28 ER luminal domain and release the N-terminal bZIP

domain, respectively (Liu et al., 2007a). Thus, the N-terminal domain becomes a functional bZIP transcription factor that enters the nucleus to induce transcription of stress-related genes which share a consensus *cis*-element in their promoter called ER stress-response element (ERSE1) with assistance from the transcription factors NF-Y. AtbZIP28 activates mainly genes which encode ER-resident chaperones and foldases which increase the protein folding capacity (Liu and Howell, 2010).

AtbZIP17 and AtbZIP28 play usually identical functions and responses. However, some differences have been shown in the sensitivity to certain environmental stress such as salt stress which induces the activation of AtbZIP17 but not AtbZIP28 (Liu et al., 2007b).

4.2. THE IRE1 PATHWAY IN PLANTS

The ER-stress sensor IRE1 is a type I ER membrane which contains an ER luminal-facing N-terminus and a cytosolic C-terminus with two different enzymatic functions: an endoribonuclease which catalyzes mRNA splicing, and a Ser/Thr protein kinase that is involved in its autophosphorylation, which leads to the activation of the endoribonuclease domain (Koizumi et al., 2001; Wan and Jiang, 2016). In *Arabidopsis*, two genes have been identified as genes encoding IRE1 proteins, *AtIRE1a* and *AtIRE1b* (Koizumi et al., 2001).

It has been proposed that IRE1 normally exits as an inactive monomer and sense the ER stress also through its interaction with BiP. Unlike

AtbZIP28, the release of IRE1 from BiP upon ER stress might expose the ER luminal domain for the direct binding of unfolded proteins. Thus, unfolded proteins might serve as activating ligands to trigger IRE1 dimerization (Walter and Ron, 2011; Hetz, 2012; Wan and Jiang, 2016). The activation of IRE1 has been shown to trigger two disparate signalling pathways: a canonical pathway which involved the splicing of a specific mRNA, and an alternative pathway which randomly cleaves mRNAs (Wan and Jiang, 2016)

4.2.1. IRE1-bZIP60 mRNA splicing pathway

Ire1 endonuclease domain catalyzes the non-conventional cytoplasmic splicing of *bZIP60* mRNA. Upon activation under stress conditions, the kinase domain catalyzes autophosphorylation to form dimers, which are critical for bZIP60 splicing, and produces Ire1 oligomerization, increasing the efficiency of splicing (Wan and Jiang, 2016). In *Arabidopsis*, the target of the IRE1-bZIP splicing pathway is *AtbZIP60* mRNA (Iwata and Koizumi 2005; Iwata et al., 2008; Nagashima et al., 2011; Deng et al., 2011). Unspliced *AtbZIP60* mRNA folds in an antiparallel manner forming “kissing” hairpin loops. The IRE1 oligomers cut the mRNA in both loops which remove a 23 nucleotides segment of mRNA (Deng et al., 2011). This removes the transmembrane domain of the unspliced bZIP60 and produces a frameshift which leads to the activation of another open reading frame (ORF) (Deng et al., 2011).

The translational product of spliced At*bZIP60* is a soluble transcriptional factor which up-regulate genes involved in protein folding, transport, and degradation (Deng et al., 2011; Iwata et al., 2008). To this

end, spliced AtbZIP60 directly binds the *cis*-element called plant UPR element III (pUPRE-III), and also regulates promoters containing the consensus region ERSE-I and UPRE-I (Ruberti and Brandizzi, 2014). In addition, spliced AtbZIP60 seems to up-regulate the nuclear transcription factor NAC103 which in turn up-regulates the UPR downstream genes (Ruberti and Brandizzi, 2014).

Although AtIre1a and AtIre1b seem to be functionally redundant, AtIre1b may play a major role in the *AtbZIP60* splicing under mild, short-term ER stress (Zhang et al., 2015; Wan and Jiang, 2016).

4.2.2. IRE1-RIDD pathway

Another IRE1 signalling pathway is called regulated IRE1-dependent decay (RIDD) and involves the degradation of diverse mRNAs (Mishiba et al., 2013). It was reported that under intense ER stress, IRE1 promotes the degradation of a considerable amount of mRNAs that encode secretory pathway proteins which is independent of bZIP60 splicing (Mishiba et al., 2013; Wan and Jiang, 2016). It has been proposed that RIDD contributes to reduce the amount of proteins entering the ER during ER stress. In mammals, this pathway may increase the intensity of the ER stress through the degradation of mRNA encoding UPR target genes leading to the cell death. However, it seems that plant IRE1 might not function as an apoptosis executor (Chen and Brandizzi, 2013b).

4.3. UPR AND AUTOPHAGY

Autophagy is a conserved process in which large portions of cytoplasmic and organelle components are degraded to be recycled. It involves the formation of double-membrane vesicles called autophagosomes which deliver their contents to the vacuole in plants. Due to his studies about the mechanisms underlying this process, Yoshinori Ohsumi has been awarded this year with the Nobel Prize of Physiology or Medicine (van Noorden and Ledford, 2016).

During ER stress, autophagy is activated in yeast, mammals and plants to clear unfolding protein from the ER alleviating stress (Liu et al., 2012; Ruberti and Brandizzi, 2014; Wan and Jiang, 2016). In *Arabidopsis*, it has been reported that AtIre1b activates autophagy independently from the bZIP60 splicing (Liu et al., 2012).

4.4. UPR AND PROGRAMMED CELL DEATH (PCD)

If the ER stress persists or under severe conditions, the UPR switches from a pro-survival process to a pro-apoptotic process, inducing the programmed cell death (PCD). In mammals, it has been proposed that all UPR branches are involved in the PCD (Deng et al., 2013). Plants have a specific type of PCD which involves the degradation of the cell contents by vacuolization until the vacuole lyses. However, the mechanisms implicated in ER-stress-induced PCD are unknown but recent studies suggest that several proteases with caspase-like cleavage activity are involved in this process (Deng et al., 2013; Wan and Jiang, 2016).

5. p24 PROTEINS

p24 proteins constitute a family of small (~24 kDa) type-I transmembrane proteins which were initially identified as abundant components of the compartments of the early secretory pathway (Wada et al., 1991; Singer-Krüger., 1993), including COPI- and COPII-coated vesicles (Stamnes et al., 1995; Schimmöller et al., 1995; Belden and Barlowe, 1996), which mediate the bidirectional transport between the ER and the Golgi apparatus (Section 2.1. of Introduction). p24 proteins cycle between both compartments, and thus, they play important roles in transport along the early secretory pathway.

5.1. PHYLOGENY AND NOMENCLATURE

Members of the p24 family have been identified in yeast, plants and animals. Based on sequence homology, they can be divided into four subfamilies, named α, β, γ and δ. Several nomenclatures have been used for p24 proteins. Dominguez et al. (1998) proposed a systematic nomenclature which involves the use of a Greek letter corresponding to the subfamily followed by a number (starting with the first-discovered member) (Figure 13) (Dominguez et al., 1998; Strating and Martens, 2009; Pastor-Cantizano et al., 2016). This nomenclature has been used in this work to facilitate their identification within the family, except for *Drosophila* and yeast where the original name is still used.

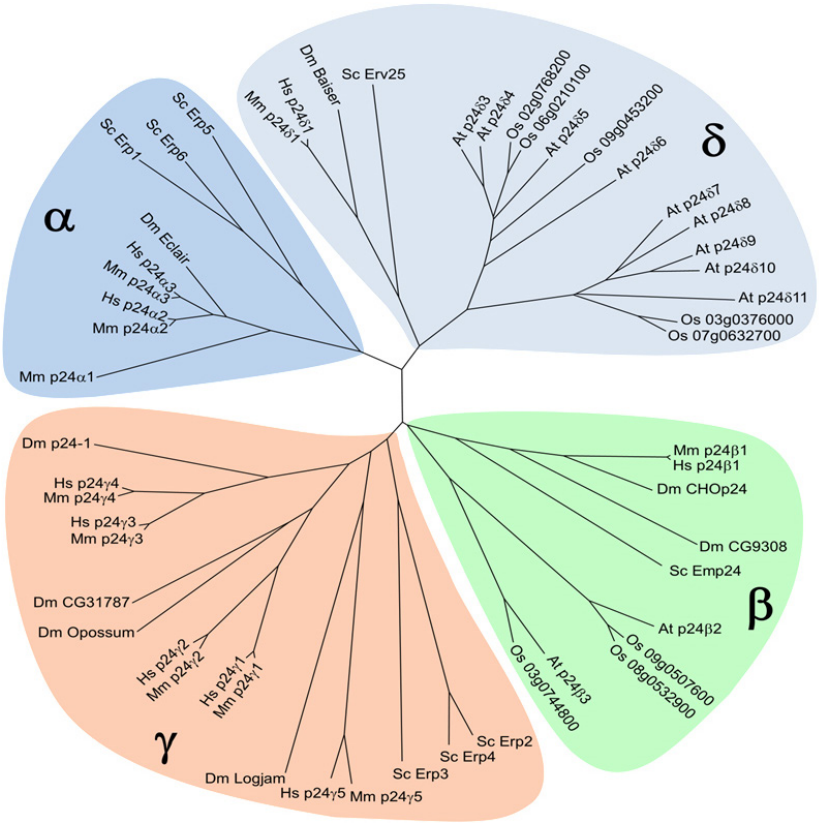

Figure 13.Unrooted tree of the p24 protein family. A multiple alignment of the p24 proteins sequence was constructed using T-Coffee, and the tree was generated from this alignment using the Molecular Evolutionary Genetics Analysis software (MEGA, version 6.06) with the Neighbour-Joining method. The four p24 subfamilies (α, β, γ and δ) are highlighted by colour background shading. Hs, *Homo sapiens*; Mm, *Mus musculus*; Sc *Saccharomyces cerevisiae*; Dm, *Drosophila melanogaster*; At, *Arabidopsis thaliana*; Os, *Oryza sativa*.

The number of p24 proteins in each family varies among species. Yeast and animals contain at least one member of each subfamily, while plants seem to have only members of the p24β and p24δ subfamilies (Carney and

Bowen, 2004). Phylogenetic analysis of p24 proteins in vertebrates showed that the p24α and p24δ subfamilies have a common origin, as it is the case for p24β and p24γ subfamilies. In vertebrates and *Drosophila*, the p24α and p24γ subfamilies have expanded independently, whereas the p24β and p24δ families have only a single member (Strating et al., 2009). In particular, proteins of p24γ subfamily show the largest variability in their amino acid sequences (Theiler et al., 2014). In plants, the p24δ subfamily seems to have greatly expanded independently from the animals and fungi. In particular, *Arabidopsis* contains 9 members of the p24δ subfamily, which can be divided into two subclasses, p24δ-1 (p24δ3-p24δ6) and p24δ-2 (p24δ7-p24δ11) and 2 members of the p24β subfamily, called p24β2 and p24β3 (Figure 14) (Chen et al., 2012; Montesinos et al., 2012).

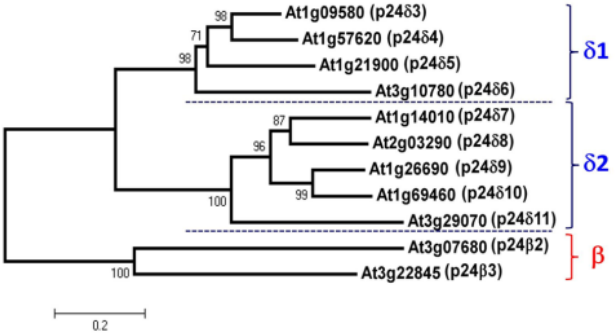

Figure 14. Phylogenetic tree containing the p24δ and p24β subfamilies of p24 proteins in *Arabidopsis* (Montesinos et al., 2012). A multiple alignment of the p24 proteins was constructed using ClustalW and the tree was generated from this alignment using the Molecular Evolutionary Genetics Analysis software (MEGA, version 5.03) with the Neighbour-Joining method. The number beside the branches represents bootstrap percentage bases on 1000 replications. The names assigned to these proteins, following the nomenclature proposed by Dominguez et al. (1998) are shown next to the AGI code.

5.2. PROTEIN DOMAIN STRUCTURE

All p24 proteins share a similar structure: a large N-terminal region, which includes a Golgi dynamics (GOLD) domain, that contains a putative disulphide bound, a linker region and a coiled-coil domain; a single transmembrane domain; and a short (13-20 residues) cytosolic C-terminal tail (Figure 15).

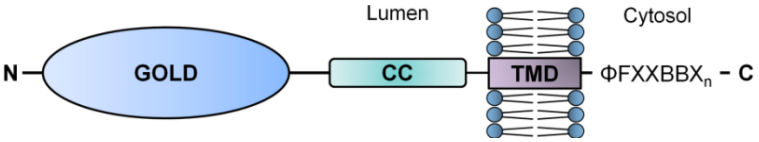

Figure 15. Domain organization of p24 proteins. The structure of p24 proteins includes two luminal domains, the Golgi dynamics (GOLD) domain and a coiled-coil (CC) domain, separated by a linker region, a single transmembrane (TM) domain and a short cytoplasmic C-terminal tail which contains signals for binding COPI and COPII subunits in the form of a ϕFXXBBXn motif, where ϕ is a bulky hydrophobic residue (F/Y/L/I), B is a basic residue and n is ≥2.

a) The GOLD domain: The GOLD domain is a β-strain-rich globular domain which is also present in several proteins related to Golgi dynamics and secretion and has been suggested to be involved in cargo recognition and protein-protein interactions (Anantharaman and Aravind, 2002; Carney and Bowen, 2004; Nagae et al., 2016).

b) The coiled-coil (CC) domain: The CC domain has been shown to be involved in the interaction between p24 proteins and their oligomerization (Ciufo and Boyd, 2000; Emery et al., 2000; Montesinos et al., 2012). However, it has been recently reported that the CC domain is also important for recognition and transport of GPI-anchored proteins (Theiler et al., 2014).

c) The transmembrane (TM) domain: The TM domain seems to interact specifically with one single sphingomyelin species and it has been proposed to modulate the equilibrium between monomeric and oligomeric states of p24 proteins (Contreras et al., 2012).

d) The cytosolic tail: The cytosolic tail of p24 proteins contains signals for binding COPI and COPII subunits. All of them have a conserved phenylalanine residue, which is often part of a diaromatic motif. Moreover, many of them also contain a dibasic (dilysine) motif, in the form of a ϕFXXBB(X)n, where ϕ is a bulky hydrophobic residue, B is a basic residue, X can be any amino acid, and n≥2 (Figure 14 and 15). The dilysine motif present in members of the α and δ subfamilies is directly involved in COPI binding (Belden and Barlowe, 2001b; Contreras et al., 2004a; Gao et al., 2014), while the ϕF motif present in all p24 proteins has been shown to bind COPII subunits (Dominguez et al., 1998; Belden and Barlowe, 2001b; Contreras et al., 2004b; Aniento et al., 2006). In addition, this motif seems to be also involved in binding COPI subunits (Belden and Barlowe, 2001b; Contreras et al., 2004b; Aniento et al., 2006).

Members of the same subfamily show significant differences among different organisms (Figure 16) (for a review, see Pastor-Cantizano et al., 2016). In particular, all members of the p24δ subfamily in plants have a dilysine motif in the -3,-4 position (relative to the C-terminus) and a diaromatic motif in the -7,-8 position, like members of the p24α subfamily in animals. In *Arabidopsis*, this dilysine motif has been shown to bind ARF1 and

COPI subunits, while the diaromatic motif has been shown to bind COPII subunits but also to cooperate with the dilysine motif in COPI binding. Therefore, proteins of the p24δ subfamily in plants bind COPI with much higher affinity than COPII (Contreras et al., 2004a, b).

p24α					*															
Hs_p24α2	-	K	S	F	F	E	A	K	K	L	V									
Dm_Eclair	-	K	S	F	F	E	A	K	K	L	V									
Sc_Erp1	-	G	K	F	F	V	K	Q	K	I	L									
p24δ					*															
Hs_p24δ1	-	R	R	F	F	K	A	K	K	L	I	E								
Dm_Baiser	-	R	R	Y	F	K	A	K	K	L	I	E								
Sc_Erv25	-	K	N	Y	F	K	T	K	H	I	I									
At_p24d5	-	K	R	Y	F	H	K	K	K	L	I									
At_p24d9	-	K	T	F	F	E	K	K	K	L	I									
p24β					*															
Hs_p24β1	-	K	R	F	F	E	V	R	R	V	V									
Dm_CG9308	-	K	H	F	F	E	V	K	R	V	V									
Sc_Emp24	-	R	R	F	F	E	V	T	S	L	V									
At_p24β2	-	R	R	L	F	E	R	K	L	G	M	S	R	V						
At_p24β3	-	R	K	L	F	S	K	S	V	A	Y	N	R	V						
p24γ					*															
Hs_p24γ3	-	K	S	F	F	S	D	K	R	T	T	T	T	R	V	G	S			
Dm_Longjam	-	R	K	L	F	E	V	K	S	S	S	K	S	R	I					
Sc_Erp2	-	Q	F	L	F	T	G	R	Q	K	N	Y	V							

Figure 16. Amino acid sequence of the cytosolic tail of p24 proteins from different subfamilies. Abbreviation: Hs, *Homo sapiens*; Dm, *Drosophila melanogaster*; Sc, *Saccharomyces cerevisiae*; At, *Arabidopsis thaliana*. One representative of each subfamily is shown, except for *Arabidopsis*. Classical dilysine residues are shown in red, other basic residues are shown in green and ϕF motifs are shown in blue. The asterisk indicates the position of the conserved phenylalanine residue present in all p24 proteins.

5.3. OLIGOMERIZATION

p24 proteins are able to interact with each other through their coiled-coil domains (Ciufo and Boyd, 2000; Emery et al., 2000; Montesinos et al.,

2012; Liaunardy-Jopeace and Gay, 2014) to form different types of heteromeric complexes which are important for their stability, trafficking and localization.

In yeast, immunoprecipitation and gel-filtration experiments have suggested that p24 proteins form a heterotetrameric complex, containing members of the four p24 subfamilies, named the yeast p24 complex (Marzioch et al., 1999). It has been recently reported that this complex should contain Emp24 (p24β), Erv25 (p24δ) and different combinations of p24α and p24γ isoforms (Hirata et al., 2013). However, in gel-filtration experiments it was also found that p24 proteins can also elute at a molecular mass which is consistent with p24 dimers and even p24 monomers (Marzioch et al., 1999). Indeed, in the absence of Erp1 (p24α) or Erp2 (p24γ), Emp24 (p24β) and Erv25 (p24δ) were present mostly as dimers, indicating that these two proteins can form a stable complex (Marzioch et al., 1999).

In mammalian cells, the same type of experiments has been performed to identify the composition of p24 complexes. Immunoprecipitation or pull-down experiments with p24γ3 and p24δ1 also suggested that p24 proteins also form heterotetramers including members of the four p24 subfamilies (Füllekrug et al., 1999; Fujita et al., 2011). However, gel-filtration experiments in HeLa cells suggested that p24 proteins exist mostly as monomers and dimers of different composition depending on their subcellular localization (Jenne et al., 2002).

These data are consistent with a model where p24 proteins exist in a dynamic equilibrium between complexes and individual proteins (Figure 17). Therefore, the postulated heterotetramer could be a dimer of dimers, as proposed by Ciufo and Boyd (2000). Dimers composed of p24β and p24δ proteins have been extensively characterized in yeast and animals (Belden and Barlowe, 1996; Belden and Barlowe, 2001b; Gommel et al., 1999; Emery et al., 2000). It both cases, it was postulated that the dilysine motif present in the p24δ member is responsible for their retrograde Golgi-to-ER transport (Gommel et al., 1999; Belden and Barlowe, 2001b). However, the contribution of the α/γ subunit to the function of the putative complex is not clear. In yeast, it has been proposed that p24α and p24γ subunits are required for the function of the p24 complex (Hirata et al., 2013). In mammals, different p24γ proteins have been recently proposed to form different hetero-oligomeric complexes which appeared to determine the cargo specificity (Theiler et al., 2014).

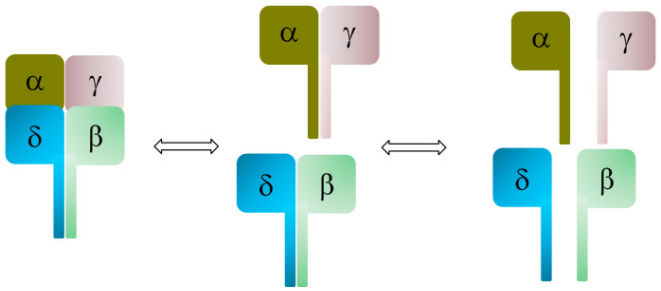

Figure 17. Proposed model for a dynamic equilibrium between monomeric, dimeric and heterotetrameric forms of p24 family members.

The interactions between the p24 proteins are required for their stability, since deletion or knock down of a single member of the p24 family produces a decrease in the protein levels of other p24 proteins, suggesting that p24 proteins form hetero-oligomeric complexes (for a revision, see Pastor-Cantizano et al., 2016). In yeast, strains deleted for one member of each subfamily showed reduced levels of members of the others subfamilies Marzioch et al., 1999). In mammals, it has been extensively investigated the stability of these complexes. In particular, knocking down of p24δ1 (Denzel et al., 2000; Vetrivel et al., 2007; Takida et al., 2008; Zhang and Volchuk, 2010; Fujita et al., 2011; Theiler et al., 2014), p24γ2 (Koegler et al., 2010) and p24β1 (Jerome-Majewska et al., 2010) caused reduced levels of other p24 proteins.

Since plants contain only members of the p24δ and p24β subfamilies, any complex should be formed with only members of these two subfamilies. It has been shown that mutants lacking p24δ5 or p24δ4 (p24δ-1 subclass) had reduced levels of p24δ9 (p24δ-2 subclass), p24β2 and p24β3. Similarly, mutants in which p24β2 or p24β3 was knocked down (since T-DNA insertion mutants are not available in mutant collections), showed reduced levels of p24δ5 and p24δ9. Interestingly, a mutant lacking p24δ10 (p24δ-2 subclass) showed increased levels of other p24δ-2 protein, p24δ9, and no decrease in the levels of p24δ5 (δ1 subclass) or p24β proteins, indicating that increased levels of p24δ9 may compensate for the lack of p24δ10. Altogether these results suggest an interdependence in the protein levels of p24δ proteins from both subclasses and the two members of the p24β subfamily. In

addition, co-immunoprecipitation and pull-down experiments also suggested the existence of a direct interaction between p24δ5, p24δ9, p24β2 and p24β3 (Montesinos et al., 2012; 2013).

5.4. p24 TRAFFICKING AND LOCALIZATION

p24 proteins have been shown to localize to the compartments of the early secretory pathway (Stamnes et al., 1995; Belden and Barlowe, 1996; Blum et al., 1996; Sohn et al., 1996; Nickel et al., 1997; Rojo et al., 1997; Dominguez et al., 1998; Füllekrug et al, 1999; Gommel et al., 1999; Emery et al., 2000; Rojo et al., 2000). In addition, they are also major constituents of both COPI-vesicles (Stamnes et al., 1995; Sohn et al., 1996; Gommel et al., 1999) and COPII-vesicles (Schimmöller et el., 1995; Belden and Barlowe, 1996). Subsets of p24 proteins have been also found to localize to membranes outside the ER-Golgi interface, including peroxisomes (Marelli et al., 2004), secretory granules (Hosaka et al., 2007) and even to the plasma membrane (Chen et al., 2006; Blum and Lepier, 2008; Langhans et al., 2008).

The steady-state localization and recycling of p24 proteins in the early secretory pathway is mainly dependent on their interaction with COPI and COPII subunits, through dilysine and diaromatic motifs in their C-terminal tail (Dominguez et al., 1998; Contreras et al., 2004a, b) and the interaction with other p24 proteins (Emery et al., 2000; Blum and Lepier, 2008). In animal cells, members of p24β, p24δ and p24γ subfamilies mainly localize to the Golgi or the ERGIC. In contrast, p24α2 proteins localize primarily to the ER (Schuiki and Volchuk, 2012). In *Arabidopsis*, p24δ proteins have been

shown to localize mainly to the ER, with a partial Golgi localization, while p24β proteins localized mainly to the Golgi apparatus (Montesinos et al., 2012; 2013).

In *Arabidopsis*, the cytosolic tail of p24δ5, which contains a dilysine and diaromatic motifs at -3,-4 and -7,-8 positions (relative to the C-terminus), was found to be necessary and sufficient for its trafficking in the early secretory pathway (Montesinos et al., 2012). In contrast, the coiled-coil domain of p24δ5 was shown to be required for its interaction with p24β2 as well as for its post-Golgi trafficking to the PVC and the vacuole (Montesinos et al., 2012).

5.5. TISSUE-SPECIFIC AND REGULATED EXPRESSION

In general, most members of p24 family are ubiquitously expressed, although some members have tissue-specific expression and regulated expression, suggesting that some p24 proteins have a housekeeping function, while others may have more specialized functions, such as the transport of a specific set of cargo proteins.

In *Xenopus*, some p24 proteins have been found to be cell-type-specific and selectively expressed during background colour adaptation (Rötter et al., 2002). In *Drosophila*, some p24 genes have developmental, tissue-specific, or sex-specific expression and tissue- and sex-limited functions (Boltz et al., 2007). Moreover, the expression of some Drosophila p24 genes is mediated by CrabA/Creb3-like family of bZIP transcription factors which

have been proposed to be the direct and major regulators of the secretory capacity (Fox et al., 2010). Regarding that, several p24 proteins have been found to be highly expressed in secretory cell types such as exocrine, endocrine, and neural cells in mouse (Hosaka et al., 2007; Zhang and Volchuk, 2010; Wang et al., 2012). In addition, the tissue-specific expression pattern of p24 genes has been investigated in mouse and it was found that only p24α1 and p24γ5 show restricted expression patterns (Strating et al., 2009). In humans, only the expression of p24δ1 has been studied in detail (Vetrivel et al., 2008; Liu et al., 2011; Xie et al., 2014). In *Arabidopsis*, there are only data from public microarray databases. According with them, only p24δ6 and p24δ11 have flower-specific expression, while other five p24 genes show high/medium levels of expression in different organs (Zimmermann et al., 2004).

Finally, some p24 proteins have been shown to be up-regulated in response to ER stress in *Arabidopsis* (p24β2) (Kamauchi et al., 2005) and in mammals (p24γ4) (Hartley et al., 2010), suggesting that they may be induced as a part of the unfolded protein response to ER stress (Schuiki and Volchuk, 2012).

5.6. FUNCTIONS OF P24 PROTEINS

p24 proteins can interact with COPI and COPII subunits through their cytosolic tail, and cycle between the ER and the Golgi apparatus. Due to these properties, numerous functions have been proposed for 24 proteins:

5.6.1. COPI and COPII vesicle formation

Although p24 proteins are not essential for COPI function, they play an important role by facilitating the formation of COPI-coated vesicles (Aguilera-Romero et al., 2008). In this respect, a large number of reports indicate that p24 proteins are involved in the formation of COPI vesicles from Golgi membranes (for reviews, see Popoff et al., 2011; Jackson, 2014; Pastor-Cantizano et al., 2016).

Based on these reports, a model for the participation of p24 proteins in COPI vesicle formation has been proposed (Figure 18) (Pastor-Cantizano et al., 2016). Dimers of p24 proteins (probably p24β/p24δ dimers) can directly interact with ARF1-GDP for the recruitment of ARF1 to Golgi membranes. Once in the membrane, ARF1 is activated by GDP/GTP exchange which produces its dissociation from p24 proteins. Then, ARF1-GTP interacts with coatomer which can also interact with p24 proteins (either through the γ-subunit of the F-complex or to the B-complex). At this stage, p24α and p24γ proteins can be also recruited forming a tetramer with p24β/p24δ dimers. Interaction with p24 proteins leads to coatomer polymerization and the formation of COPI vesicles. p24 proteins can also interact with the K/HDEL receptor ERD2, which can also interact with coatomer and has also been proposed to be involved in a variety of interactions which contribute to COPI vesicle formation. Moreover, p24 proteins also control coat depolymerization inhibiting GTP hydrolysis in ARF1 which is required for uncoating. This may prevent immature uncoating and allow cargo selection.

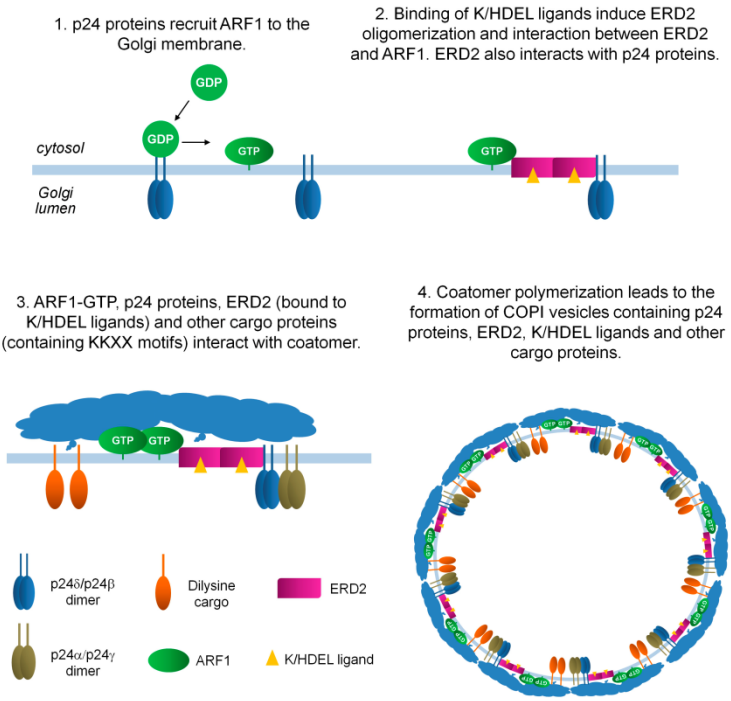

Figure 18. p24 proteins and COPI vesicle formation. p24 proteins are involved in a number of events important for COPI vesicle formation, including the recruitment of ARF1 to the Golgi membrane (1), the interaction with the K/HDEL receptor ERD2 (2) and the interaction with coatomer, which also binds to ARF1, ERD2 and other dilysine cargo (3). These array of interactions facilitates coatomer polymerization and the formation of COPI vesicles (4).

p24 proteins are also enriched in COPII vesicles and can interact with Sec23 and Sec24 subunits (Schimmöller et al., 1995; Belden and Barlowe, 1996; Dominguez et al., 1998; Miller et al., 2003; Contreras et al., 2004b). Although p24 proteins are not essential for the formation of COPII vesicles, it has been proposed that p24 proteins influence this process through the alteration of the physical properties of the ER membrane due to their

abundance and asymmetric distribution (Copic et al., 2012). In addition, it has been reported that asymmetrically localized proteins like p24 proteins require the scaffolding function of the cargo adaptor Lst1p (a Sec24 homolog) to form large COPII vesicles (D'Arcangelo et al., 2015).

5.6.2. Maintenance of the structure and organization of the early secretory pathway

Several reports have suggested that p24 proteins may play a role in the structure and organization of the compartments of the early secretory pathway. In particular, p24 proteins have been proposed to be involved in the formation of ER export sites (ERES), the structure of the ER and the ERGIC and the biogenesis and maintenance of the Golgi apparatus. In addition, it has been suggested that p24 proteins may be important for recycling of components required for ER-Golgi transport or in ER function. The first proposal of a possible structural role for p24 proteins was its possible involvement in the formation of ER exit sites (ERES) (Lavoie et al., 1999).

In mammals, overexpression of p24δ1 and p24β1 led to Golgi fragmentation and the appearance of smaller Golgi fragments (Rojo et al., 2000; Blum et al., 1999; Gong et al., 2011). Silencing of p24β1, p24γ2 and p24α2 led to Golgi fragmentation as well (Luo et al., 2007; Koegler et al., 2010; Mitrovic et al., 2008). In addition, silencing of p24α2 also produced a reduction in the number of ERGIC clusters as well as the destabilization of the ERGIC (Mitrovic et al., 2008). In contrast, inactivation of one allele of

p24δ1 was shown to induce the dilation of the Golgi cisternae, which was more prominent at the rim (Denzel et al., 2000). In *Arabidopsis*, single knockout mutants did not show any obvious ultrastructural alterations, perhaps because of functional redundancy with other p24 family members (Montesinos et al., 2012).

5.6.3. Cargo protein receptor

p24 proteins have long been proposed to function as cargo receptors for protein transport in the early secretory pathway. Most putative p24 cargos described so far are lipid-linked proteins or membrane proteins, in contrast to many classical cargo receptors (for a revision, see Pastor-Cantizano et al., 2016).

a) GPI-anchored proteins: Early studies in yeast already suggested that p24 proteins may be involved in the transport of glycosylphosphatidylinositol (GDPI)-anchored proteins (GPI-APs) (Schimmöller et al., 1995; Belden and Barlowe, 1996; Marzioch et al., 1999; Muñiz et al., 2000). It has been proposed that the yeast p24 complex may function as an adaptor connecting remodeled GPI-APs with the COPII coat to facilitate their incorporation into COPII vesicles, instead of participating in sorting of GPI-APs (Castillon et al., 2011; Manzano-Lopez et al., 2015). Moreover, the p24 complex may be also involved in retrograde Golgi-to-ER transport of unremodeled GPI-APs (Castillon et al., 2011).

In mammals, p24 have also been proposed to participate in efficient ER-to-Golgi transport of GPI-APs (Takida et al., 2008; Bonnon et al., 2010).

However, in contrast to the situation in yeast, p24 proteins seem to be required for concentration of remodeled GPI-APs at ERES and their packaging into COPII vesicles (Fujita et al., 2011). The interaction between GPI-APs and p24 proteins has been shown to be pH-dependent and takes place at the neutral pH of the ER but not at the mildly acidic pH of the Golgi apparatus (Fujita et al., 2011).

b) K/HDEL-receptor ERD2: p24 proteins of the p24δ subfamily have been shown to be involved in retrograde transport of K/HDEL ligands through interaction between p24δ proteins and the K/HDEL receptor ERD2 in mammals and plants (Majoul et al., 2001; Montesinos et al., 2014). In *Arabidopsis*, two p24δ proteins, p24δ5 and p24δ9, were shown to interact with two different K/HDEL receptors, ERD2a and ERD2b, an interaction that required the GOLD domain of p24δ5 and was pH-dependent. In particular, this interaction was optimal at acidic pH but very low at neutral pH, consistent with the interaction taking place at Golgi apparatus and the dissociation of p24 proteins from ERD2 at the ER lumen (Montesinos et al., 2014).

c) Other putative cargos: various other putative cargo proteins have been described for p24 proteins, including Wnt glycoproteins, which are lipid-modified secreted signalling proteins that are involved in controlling animal development (Port et al., 2011; Buechling et al., 2011; Lie et al., 2015). Other putative cargos are: G-protein-coupled receptors (Luo et al.,

2007; 2011); Toll-like receptors (Liaunardy-Jopeace and Gay, 2014); and GLL3, a putative myrosinase-associated protein in plants (Jancowski et al., 2014).

5.6.4. ER quality control

Several reports have been proposed that p24 proteins prevent exiting from the ER of misfolded and aberrant proteins, suggesting a role of p24 proteins in the ER quality control of certain secretory proteins (Wen and Greenwald, 1999; Springer et al., 2000; Belden and Barlowe, 2001a; Vetrivel et al., 2007).

5.6.5. p24 proteins in physiology and pathology

Due to the implication of p24 proteins in a variety of specific functions in animals, they have been proposed to be involved in different physiological processes and diseases, including:

- Early embryotic mouse development and morphogenesis of the mouse embryo and placenta (Denzel et al., 2000; Jerome-Majewska et al., 2010).
- Normal insulin biosynthesis and subsequent secretion in pancreatic β-cells, with a putative role in diabetes (Zhang and Volchuk, 2010; Wang et al., 2012).
- Trafficking and metabolism of amyloid-β precursor and pathogenesis of Alzheimer's disease (Chen et al., 2006; Vetrivel et al., 2007, 2008; Hasegawa et al., 2010; Liu et al., 2015).

6. K/HDEL RECEPTOR ERD2

ERD2 proteins are a family of proteins which are highly conserved across species and consist of seven-transmembrane domains with the N-terminal region localized to the lumen of the organelles and the C-terminus to the cytosol. They recognize a conserved C-terminal tetrapeptide sequence (mainly KDEL or HDEL) on luminal ER proteins in the *cis*-Golgi that have escaped from the ER, and cycle them back into the ER (Munro and Pelham, 1987; Lewis et al., 1990; Semenza et al., 1990; Lewis and Pelham, 1992; Townsley et al., 1993; Wilson et al., 1993). Indeed, the first family member was identified through a genetic screen for ER-retention defective yeast mutants which failed to retain a HDEL-tagged protein (Capitani and Sallese, 2009).

Only one ERD2 protein has been found in yeast, while three different KDEL receptors have been identified in the human genome (KDEL receptor 1, KDEL receptor 2 and KDEL receptor 3) (Capitani and Sallese, 2009). In *Arabidopsis*, seven ERD2-like proteins have been identified in its genome which can be divided in two classes, two belonging to class I (ERD2a and ERD2b) and the other five, which are more distantly related, belonging to class II. The same number of ERD2-like proteins has been identified in *Nicotiana benthamiana*, which are also divided in two classes.

6.1. ERD2 TRAFFICKING AND LOCALIZATION

In animal cells, the KDEL receptor was found mainly in the *cis*-Golgi and the ERGIC at steady-state (Lewis and Pelham, 1992). In plants, fluorescently tagged ERD2 proteins have been also shown to localize either to the Golgi apparatus, with a lower level of labelling in the ER (Boevink et al., 1998; Brandizzi et al., 2002a) or to be equally distributed to the ER and the Golgi (Xu et al., 2012). This steady-state distribution is thought to be the result of its bidirectional transport between the ER and the Golgi apparatus which is mediated by COPII- (ER-to-Golgi transport) and COPI- (Golgi-to-ER transport) coated vesicles.

In mammalian cells, direct interaction between ERD2 and COPII subunits has not yet been reported, although ERD2 has been shown to co-localize partially with Sec13 punctate structures, which represented COPII vesicles (Majoul et al., 2001).

Respect to COPI-mediated Golgi-to-ER trafficking, the mammalian KDEL receptor has been shown to interact with ARF1 (ADP-ribosylation factor 1) GTPase, ARF GTPase-activating protein 1 (ARF-GAP1), the β-subunit of the coatomer, and p24 proteins (Aoe et al., 1997, 1998; Majoul et al., 2001). The interaction between ERD2 and coatomer involves a KKXSXXX motif in the cytosolic tail of ERD2 which has been shown to be active when Ser-209 is phosphorylated by Ser/Thr protein kinase A (PKA) (Cabrera et al., 2003; Capitani and Sallese, 2009). Moreover, it has been reported that upon overexpression of KDEL ligands, the KDEL receptor is redistributed to the ER

(Lewis and Pelham, 1992). It has been proposed that this take places because ligand binding induces ERD2 oligomerization, facilitating their inclusion in COPI vesicles (Aoe et al., 1998).

In plants, *N. benthamiana* ERD2a/b have been shown to form homo- or hetero-oligomeric complexes and to interact with ARF1 and its potential GAPs (Xu and Liu, 2012). In addition, it has been reported that ERD2a can interact with coatomer and p24δ proteins in a pH-dependent manner being optimal at acidic pH, but very low at neutral pH, consistent with this interaction taking place at the Golgi apparatus (Montesinos et al., 2014). However, there is no evidence of ERD2 phosphorylation, although *Arabidopsis* ERD2 proteins contain a serine residue in their cytosolic tail which is located upstream of the lysine residues.

6.2. FUNCTION OF ERD2 PROTEINS

The best characterized function of ERD2 proteins is the recognition of a KDEL/HDEL motif at the C-terminus of soluble ER-resident proteins for their retrograde transport from the Golgi apparatus to the ER via COPI vesicles.

In animal cells, the three isoforms of the KDEL receptor are expressed to different extents in all human tissues. Each of the KDEL receptor isoforms has been shown to bind preferentially to a specific set of KDEL-like sequences. In particular, KDEL receptor 1 preferentially binds the KDEL motif, KDEL receptor 3 prefers the HDEL motif, and the KDEL receptor 2 preferentially recognises variants of the HDEL. Thus, each KDEL receptor can

bind a sub-population of KDEL ligands (Capitani and Sallese, 2009). In addition, these interactions showed a strong dependency on pH, suggesting that the association of the KDEL-ligands with the KDEL receptor occurs in the Golgi and the dissociation takes place in the ER (Capitani and Sallese, 2009).

In plants, *N. benthamiana* ERD2a and ERD2b have been shown to act as ER-luminal receptors for retrieval of K/HDEL-containing proteins, although ERD2b was found to bind preferably KDEL motif (Xu and Liu, 2012). In *Arabidopsis*, ERD2b has been proposed to be a specific HDEL receptor for calreticulin 3 (CRT3), but not for CRT1, CRT2 or BiP (Li et al., 2009).

Other functions have been proposed for K/HDEL receptor, including recycling of other components required for anterograde transport and regulation of the ER quality control (Capitani and Sallese, 2009; Yamamoto et al., 2001).

OBJECTIVES

p24 proteins constitute a family of proteins which localize to the compartments of the early secretory pathway, including COPI- and COP II-coated vesicles which mediate the bidirectional transport between the ER and the Golgi apparatus. Therefore, they have been proposed to function as putative cargo receptor and to be involved in quality control during protein transport, the organization of ER export sites or the biogenesis and maintenance of the Golgi apparatus. However, their functions in plants are essentially unknown. Plants contain only members of the p24δ and p24β subfamilies. In particular, *Arabidopsis* contains 9 members of the p24δ subfamily which can be divided into two subclasses, p24δ-1 (p24δ3-p2δ6) and p24δ-2 (p24δ7-p24δ11) and 2 members of the p24β subfamily. The main objective of this work has been the functional characterization of p24 proteins of the p24δ subfamily in *Arabidopsis*.

Specific objectives:

1. To obtain loss-of-function quadruple mutants of p24 genes of p24δ-1 and p24δ-2 subclasses and to study their morphological and functional characteristics by genetic and biochemical approaches.

2. To investigate whether Arabidopsis p24 proteins from the delta-1 subclass are glycosylated and whether this glycosylation may have functional implications, in particular with respect to their role in sorting ERD2 within COPI vesicles for retrieval of K/HDEL ligands from the Golgi apparatus to the endoplasmic reticulum.

MATERIALS AND METHODS

1. BIOLOGICAL MATERIAL

1.1. MICROORGANISMS

1.1.1. Growth of *Escherichia coli*

E. coli DH5α strain (Invitrogen) was incubated at 37ºC and 200 rpm in liquid LB (Luria-Bertani) (Bertani, 1951) medium or solid LB medium [1 % (w/v) tryptone, 0.5 % (w/v) yeast extract and 1% (w/v) NaCl, pH 7; for solid medium 1.5 % (w/v) bacteriological agar (Pronadisa) was added]. Media for selection of transformants were supplemented with antibiotic (100 µg/mL kanamycin or 100 µ/mL ampicillin).

1.1.2. Growth of *Agrobacterium tumefaciens*

A. tumefaciens C58 MP90 strain (Koncz & Schell, 1986) was incubated at 28ºC and 200 rpm in liquid or solid LB medium plus 25 µg/mL gentamicin and 100 µg/mL kanamycin, to ensure the presence of the Ti plasmid and T-DNA sequence of interest (when using T-DNA vectors with the kanamycin resistence gene), respectively, to select and grow transformants.

1.2. PLANTS

1.2.1. *Arabidopsis thaliana*

1.2.1.1. Insertion mutants

Table 3 shows the *Arabidopsis* insertion mutants used in this work.

Table 3. *Arabidopsis* insertion mutants used in this work.

GENE (Gene identifier)	Mutant (ID number)	Ecotype	Origin[a]
p24δ3 **(At1g09580)**	GK_029E10	Col-0	GABI-KAT project (Kleinboelting et al., 2012)
p24δ4 **(At1g57620)**	SAIL_664_A06	Col-0	SAIL collection (Sessions et al., 2002)
p24δ5 **(At1g21900)**	SALK_016402C	Col-0)	SALK collection (Alonso et al., 2003)
p24δ6 **(At3g10780)**	GK_823G03	Col-0	GABI-Kat project (Kleinboelting et al., 2012)
p24δ7 **(At1g14010)**	GK_503A10	Col-0	GABI-KAT project (Kleinboelting et al., 2012)
p24δ8 **(At2g03290)**	SM_3_36686	Col-0	John Innes Centre (Tissiera et al., 1999).
p24δ9 **(At1g26690)**	WiscDSLoxHs161_04H	Col-0	WiscDSLox collection (Wood et al., 2007)
p24δ10 **(At1g69460)**	SALK_144586	Col-0	SALK collection (Alonso et al., 2003)

[a] All seeds were provided by NASC (Nottingham *Arabidopsis* Stock Centre)

1.2.1.2. Growth conditions in soil

Seeds were suspended in 1 mL distilled H_2O and kept in darkness for 2 days at 4ºC to synchronize germination. Then, they were sown in plastic pots containing a mixture of compost:perlite:vermiculite (2:1:1). Two sizes of plastic pots were used, pots of 6 cm diameter (one plant per pot) to perform phenotypic analysis or to obtain protoplasts, or pots of 15 cm diameter (25 plants per pot) to transform the plants. After sowing, pots were covered with plastic film the first five days to maintain high humidity during germination and to prevent contamination of seeds from other plants nearby.

Plants were grown in the greenhouse or chambers under controlled conditions of temperature, 21ºC, and 16h/8h photoperiod with 16 hours of white, cold and fluorescent light (150 µE m^{-2} s^{-2}, Sylvania Standard F58W/133-T8), watering them manually by immersion in distilled water twice a week.

1.2.1.3. Growth conditions in Petri dishes

Arabidopsis was cultured *in vitro* in culture chambers in Murashige and Skoog (MS) medium with agar, which contains 2.2 g/L MS salts (Duchefa), 10 g/L sucrose, 0.1 g/L 2-(N-Morpholino) ethanesulfonic acid (MES), pH 5.9 and 0.6% (horizontal oriented plates) or 1% (vertical oriented plates) phytoagar.

Seeds were sterilized by immersion for 3 minutes in 70% (v/v) ethanol and 0.05% (v/v) Triton X-100, and for one minute in 96% (v/v) ethanol. Then,

seeds were left until they got dry over sterile Whatman™ paper at the laminar flow hood. After sowing them, plates were put for 2 days at 4ºC and kept in darkness to synchronize germination and then they were moved into the growth chamber.

To select homozygous lines by segregation analysis, the seeds of the different insertion mutants were plated in Petri dishes containing selection medium (MS with sulfadiazine).

1.2.1.4. Growth conditions in liquid medium

To obtain protein extracts from *A.thaliana* roots of wild-type and different mutants, 10 mg of seeds were collected. Seeds were sterilized by immersion for 1.5 minutes in 70% (v/v) ethanol and for 7 minutes in 40% (v/v) $NaClO_4$ and 0.02% (v/v) Triton X-100 and then washed 6-8 times with sterile Milli-Q water in a laminar flow hood. Finally, seeds were suspended in 1 mL distilled H_2O and kept in darkness for 2 days at 4ºC to synchronize germination. After 2 days, seeds were put in 250 mL flasks with 120 ml MS liquid and cultured *in vitro* in controlled growth chambers at 25ºC, 16h/8h photoperiod and 115 rpm shaking for 20 days.

1.2.1.5. Crosses of different transgenic lines

The technique to cross different *Arabidopsis* plants consist in rubbing gently the convex surface of the anthers from the male parent against the stigmatic surface of an exposed carpel on the female parent.

For the different crosses between single, double and triple mutants, selection of F1 and F2 progeny was performed by PCR (section 4.2.3. Materials and methods) using genomic DNA as a temple and specific primers of the different p24 genes and their corresponding insertions (Tables 8 and 9).

1.2.1.6. Isolation of *Arabidopsis* protoplasts

To obtain mesophyll protoplasts from *Arabidopsis* plants, the Tape-*Arabidopsis* Sandwich method was used as described previously (Wu et al., 2009). In this protocol, two kinds of tape (Autoclave tape adhered to the upper epidermis and 3 M magic tape to the lower epidermis) were used to make a "sandwich".

4-week rosette leaves were adhered to the autoclave tape which the adaxial surface down during manipulation. Then, the 3 M magic tape was adhered to the abaxial surface of the leaves. Tearing off the 3 M magic tape allowed easy removal of the lower epidermal layer and exposed mesophyll cells to cell wall digesting enzymes. The autoclave tapes containing the leaves were incubated in an enzyme solution [1.5% Cellulase R10 (Yakult Pharmaceutical, Japan), 0.4% Macerozyme R10 (Yakult Pharmaceutical, Japan), 0.4 M mannitol, 20 mM KCl, 20 mM MES, 10 mM $CaCl_2$, 5 mM β-mercaptoethanol and 0.1% Bovine serum albumin (BSA), brought to pH 5.7 with KOH] for 2 h at room temperature (RT) with gentle shaking.

After digestion, the suspension was filtered through a 100-µm nylon mesh and briefly washed of the cell debris to release further protoplasts from the tissue remnants with W5 medium which contains 154 mM NaCl, 125 mM $CaCl_2$, 5 mM KCl and 2 mM MES and pH 5.7. The protoplast suspensions were then centrifuged in Falcon tubes (50 mL) for 5 min at 800 rpm and 4ºC. Protoplasts were washed twice with W5 medium and the protoplast pellets were used to PEG transformation.

1.2.2. *Nicotiana tabacum* cv. Petit Havana SRI

1.2.2.1. Growth conditions

N. tabacum cv. Petit Havana SRI was cultured *in vitro* in controlled growth chambers at 25ºC and 16/8h photoperiod, in MS tobacco medium with agar. This medium contains 4.4 g/L MS salts (Duchefa), 20 g/L sucrose, 0.4 g/L MES, pH 5.7 and 0.8 % phytoagar.

Seeds were sterilized by immersion for 1.5 minutes in 70% (v/v) ethanol and for 7 minutes in 40% $NaClO_4$ and 0.02% (v/v) Triton X-100, followed by 6-8 washes with sterile Milli-Q water in a laminar flow hood.

1.2.2.2. Isolation of *N. tabacum* protoplasts

Preparation of tobacco mesophyll protoplasts was done using a digestion mix containing 0.2% Macerozyme R10 and 0.4% Cellulase R10 (Yakult Pharmaceutical, Japan) in TEX buffer [B5 salts, 500 mg/L MES, 750 mg/L $CaCl_2$, 250 mg/L NH_4NO_3 and O.4 M sucrose (13.7%), brought to pH 5.7

with KOH]. Stocks with 10-fold concentrated enzymes were prepared by dissolving the lyophilized powders in TEX buffer for 2-3 h, followed by centrifugation at 5000 g for 15 min and filter sterilization (0.2 µm) of the clear supernatant. Aliquots (5 mL) of filtered supernatant were kept at -80ºC for routine use. The digestion mix was always prepared freshly by adding 45 mL of TEX buffer to these stocks.

To obtain protoplasts, leaves from 8-week-old plants were perforated using a needle bed. Then, the leaves were overlaid on top of the digestion mix and incubated overnight in darkness at 25ºC. After digestion, the suspension was filtered through a 100-µm nylon mesh and briefly washed of the cell debris with electroporation buffer (EB) [0.4 M sucrose, 2.4 g/L HEPES, 6 g/L KCL and 600 mg/L $CaCl_2$, brought to pH 7.2 with KOH] to release further protoplasts from the tissue remnants. The protoplast suspensions were then centrifuged in Falcon tubes (50 mL) for 15 min at 800 rpm at RT in a swing-out rotor to prevent resuspension in the floating protoplast band. The pellet with dead cells and the underlying medium were removed and discarded using a peristaltic pump and a sterile Pasteur pipette until the band of floating (living) protoplasts reached the bottom. After resuspending the cells in 40 mL of EB buffer and one further centrifugation at 800 rpm for 10 min, the pellet and the underlying medium were removed again. This procedure was repeated twice reducing the volume of EB buffer (Foresti et al., 2006; Bubeck et al., 2008). Protoplasts were resuspended in the corresponding EB buffer volume for

electroporation transformation or washed twice with W5 medium to precipitate them and use them for PEG transformation.

2. TRANSFORMATION PROCEDURES

2.1. TRANSFORMATION OF *E.coli*

MAX Efficiency® DH5α™ competent cells from Invitrogen™ (Ref. 18258012) were used. Heat shock transformation was performed according to the manufacturer's protocol.

2.2. TRANSFORMATION OF *A. tumefaciens*

Competent cells were prepared growing *A. tumefaciens* in liquid LB plus gentamicin (25 µg/mL) until an OD_{600} of 0.5-1.0 was reached. Then, the cells were collected and resuspended in 20 mM $CaCl_2$, as described previously (Weigel and Glazebrook, 2002). *A. tumefaciens* transformation was performed using the freeze-thaw method. Competent cells were incubated with 1 µg plasmid DNA for 5 minutes at 0ºC. Then, they were transferred to liquid nitrogen for 5 minutes and after, they were incubated for another 5 minutes at 37ºC. Finally, 1 mL of LB was added and the cells were incubated 2-4 hours at 28ºC and 200 rpm. The cells were plated in solid LB medium with antibiotic (gentamicin and kanamycin) and incubated for 2 days at 28ºC until colonies appeared.

Colony PCR was performed to identify *A. tumefaciens* colonies containing the plasmid of interest. A transformant colony was taken with a yellow tip and was spread vigorously inside a sterile PCR tube for 30 seconds to run a hot start PCR reaction as described in section 4.2.3. Materials and methods. Then, the yellow tip was introduced in a culture tube containing 2 ml of LB medium with antibiotic and it was incubated 1-2 days at 28ºC and 200 rpm to obtain a culture and store it at 4ºC for further use.

2.3. *Arabidopsis* TRANSFORMATION BY FLORAL DIP METHOD

For the generation of transgenic plants expressing different ER and Golgi markers, wild-type (ecotype Columbia, Col-0), *p24δ3δ4δ5δ6* and *p24δ7δ8δ9δ10* plants were used. The transformations were performed following the protocol described by Clough and Bent, 1998. Approximately, 25 seeds of wild-type, *p24δ3δ4δ5δ6* or *p24δ7δ8δ9δ10* were sown and cultured for 5 to 6 weeks in pots, as described in section 1.2.1.2 Materials and methods. The first inflorescence shoots were removed as soon as they emerged, to promote secondary inflorescences development.

Three days before transformation, a culture of 10 mL LB medium (containing the corresponding antibiotics) inoculated with an *Agrobacterium* strain carrying the construction of interest was incubated as described in section 1.1.2. Then, 600 mL of LB medium containing the corresponding antibiotics was inoculated with the 10 mL of the preculture and incubated overnight under same conditions. Finally, the culture was collected by centrifugation (6000 rpm, 15 minutes) and the bacteria pellet was

resuspended in 600 mL of infiltration medium [5% (w/v) sucrose and 0.05% (v/v) Silwet L-77] with a final OD_{600} of 0.8.

The pots containing the plants were inverted and all the plants were immersed in the suspension of *Agrobacterium* in infiltration medium for 1 min with gentle shaking. Then, the pots were placed horizontally on trays which were covered with plastic film and a sheet of paper to avoid excess of light and were placed into the growth chamber. After 24 hours, the covers were removed and the pots with the transformed plants were placed as usual, letting plants to grow until the end of their reproductive cycle, when the seeds were harvested.

To select primary transformants, T1 seeds were sown on Petri dishes with MS medium supplemented with the corresponding antibiotic according to the antibiotic resistence gene of the construct (Table 4). After 7-10 days from sowing, transformants could be clearly distinguished by their green colour and developed roots. Selected plants were transferred into soil for growth under conditions described in section 1.2.1.2 Materials and methods. Secondary transformants from T2 seeds that showed a 3:1 (resistant:senstitive) ratio when grown in MS plus antibiotic plates were selected and at least 6 seedlings resistant to the corresponding antibiotic were transferred to soil. Finally, T2 transformants with seed that showed 100% resistance to the corresponding antibiotic were selected as homozygous plants.

Selection of transformants could be performed also by fluorescence detection in roots of 4-days-old seedlings grown in MS plates, through a fluorescence microscope (Olympus SZX9).

The different constructs used for *A*rabidopsis transformation are summarized in Table 4.

Table 4. Secretory compartment marker constructs used for *Arabidopsis* transformation.

(X)FP-protein	Antibiotic resistance	Origin
mCherry-HDEL	Kanamycin	Denecke et al., 1992
ST-YFP	Hygromycin	Dr. David Robinson
ERD2a-YFP	Kanamycin	Brandizzi et al., 2002a

2.4. SEGREGATION ANALYSIS OF TRANSGENIC LINES

To estimate the number of *loci* in which T-DNA has been inserted in the different primary transformants of *A.thaliana*, 40 seeds from individual T1 plants were sown after sterilization and grown in MS solid medium supplemented with the corresponding antibiotic, as described in section 1.2.1.3 of Materials and methods. The counting of green and white seedlings, resistant or sensitive to the antibiotic, respectively, was performed 7-10 days after sowing. T2 homozygous and heterozygous plants were identified by analysing the T3 generation with the same technique.

To analyse segregation data of the corresponding antibiotic resistance in the progeny of the different T1 plants, the null hypothesis (H0) were that the data were compatible with a 3:1 segregation (resistant:sensitive), which

corresponds with an unique insertion of the T-DNA in a locus or with a 15:1 segregation, which corresponds to the insertion of the T-DNA in two *loci*. The alternative hypothesis (H1) was that H0 was not true, setting as categories resistant and sensitive plants to the corresponding antibiotic.

To analyse segregation data of the corresponding antibiotic resistance in the progeny of the selected T2 transgenic plants with an unique insertion, the null hypothesis (H0) were that the data were compatible with 40:0 segregation (resistant:sensitive), which corresponds with an homozygous line or with a 3:1 segregation, which corresponds with an heterozygous line. The alternative hypothesis (H1) was that H0 was not true, setting as categories resistant and sensitive plants to the corresponding antibiotic

The Chi-square (χ^2) statistical test was used to determine how well our sets of segregation data fit this particular hypothesis (H0). The formula is:

$$\boldsymbol{\chi^2 = \sum_{i=1}^{k} \frac{[(Oi - Ei) - 0.5]^2}{Ei}}$$

k = number of categories (2); *Oi* = number of plants observed in a category; *Ei* = number of plants expected in a category; the degree of freedom (*i* = *k*-1) is 1.

The calculated χ^2 value was then compared with computed critical values. In this case, for 2 different categories and one degree of freedom, a value of χ^2 equal or less than 3.841 should indicate that the null hypothesis (H0) was accepted.

2.5. TRANSIENT GENE EXPRESSION OF PROTOPLASTS BY PEG TRANSFORMATION METHOD

For transient expression by PEG transformation method, the protocol described by Yoo et al. (2007) was followed. Protoplasts isolated from *Arabidopsis* rosette leaves (of wild-type, *p24δ3δ4δ5δ6* or *p24δ7δ8δ9δ10*) (section 1.2.1.6) or tobacco mesophyll protoplasts (section 1.2.2.2.) were washed with 40 mL of W5 medium and collected by centrifugation at 800 rpm and 4ºC for 5 minutes.

For transformation, protoplasts were resuspended in 1 mL of W5 medium and incubated 30 minutes on ice. An aliquot of the protoplast suspension was taken and used to calculate the concentration of protoplasts (protoplasts/mL). Then, protoplasts were collected by centrifugation (at 800 rpm and 4ºC and for 5 min) and resuspended in MMG solution (0.4 M mannitol; 15 mM $MgCl_2$; 4 mM MES) to $2\text{-}5\cdot10^5$ cells/mL. 200 µl of protoplasts suspension was mixed with 50 µl of DNA(s) and 250 µL of PEG solution (0.1 M PEG 4000; 0.2 M mannitol; 80 mM $CaCl_2$) was added. After 5 minutes of incubation, 3 mL of W5 was added. Protoplasts were collected as described previously and washed twice with W5. Finally, transformed protoplasts were resuspended in 1 or 1.5 mL of W5 for confocal analysis or for secretion assays, respectively, and incubated for 16 hours at 25ºC and darkness. Protoplasts were then analysed by confocal laser scanning microscopy, as described in section 6.1., or used to perform secretion assays, as described in section 5.5.

2.6. TRANSIENT GENE EXPRESSION OF PROTOPLASTS BY ELECTROPORATION TRANSFORMATION

Tobacco mesophyll protoplasts obtained as described in section 1.2.2.2. of Materials and methods were transfected as described previously (Bubeck et al., 2008). Briefly, protoplasts were resuspended in electroporation buffer (EB, see section 1.2.2.2.) at a concentration of 5 x 10^6 protoplasts/mL. 500 µL of the protoplast mix was transferred into a disposable 1-mL plastic cuvette and mixed with 1-50 µg of plasmid DNA or mixtures of plasmids which were previously dissolved in 100 µl of EB. The protoplasts were electroporated with stainless steel electrodes at a distance of 3.5 mm using a complete exponential discharge of a 100 µF capacitor charged at 160 V. Protoplasts were left in the cuvettes for 30 minutes. Then, they were removed from the cuvettes and transferred to 5-cm Petri dishes with 2 mL of TEX buffer. Transformed protoplasts were incubated for 20 h at 25ºC in a dark chamber.

2.7. PLASMIDS USED IN TRANSIENT GENE EXPRESSION

Table 5 shows all the plasmids encoding proteins of interest used in transient gene expression.

Table 5. Plasmids used in transient gene expression in this work.

(X)FP protein	Origin
BP80-GFP	daSilva et al., 2005
ERD2a-YFP	Brandizzi et al., 2002a
GFP-HDEL	Nebenführ et al., 2000
ManI-GFP	Nebenführ et al., 1999
ManI-RFP	Nebenführ et al., 1999
RFP-KDEL	De Caroli et al., 2011
RFP-p24δ5	Montesinos et al., 2012
RFP-p24δ5N86Q	Obtained in this work
RFP-p24δ5ΔGOLD	Montesinos et al., 2012
RFP-p24δ9	Montesinos et al., 2013
Sec-GFP	DiSansebastiano et al., 1998; Leucci et al., 2007
ST-YFP	Brandizzi et al., 2002b

3. TREATMENTS

3.1. TUNICAMYCIN TREATMENT

3.1.1. Germination under tunicamycin treatment

To examine the tolerant ability of plants in coping with different intensities of ER stress, seeds were directly germinated on MS solid medium supplemented with 25, 50, 75 or 100 ng/ml Tunicamycin (Tm), as described previously by Chen and Brandizzi (2013a). Seeds were grown as described in section 1.2.1.3 of Materials and methods. 10 days after sowing, comparison of phenotype between wild-type plants and mutants was performed.

3.1.2. Short-term treatment

To investigate whether UPR genes were up-regulated in *p24δ3δ4δ5δ6* and *p24δ7δ8δ9δ10* mutants, short-term ER stress treatment with Tm was performed as described previously by Chen and Brandizzi (2013a). To this end, seeds from wild-type, *p24δ3δ4δ5δ6* and *p24δ7δ8δ9δ10* plants were sown in MS solid medium and grown vertically for 10 days. Then, 10-day-old seedlings were gently transferred to Petri dishes containing MS liquid supplemented with 5 µg/mL Tm. Seedlings were incubated 0h, 2h or 4 hours. Finally, seedlings were collected and snap frozen in liquid nitrogen. Samples were stored at -80ºC until use.

3.1.3. Protoplast treatment

To verify whether p24 proteins are glycosylated, *A.thaliana* protoplasts from wild-type plants (obtained as described in section 1.2.1.5. of Materials and methods) or tobacco mesophyll protoplasts expressing RFP-p24δ5, RFP-p24δ5N86Q or RFP-p24δ9 (obtained as described in section 1.2.2.2. and 2.6 of Materials and methods) were incubated with Tm. To this end, *Arabidopsis* protoplasts were resuspended in 2 mL of W5 medium and transferred to 5-cm Petri dishes. Then, 100 µg/mL Tm or DMSO was added to the medium. For tobacco mesophyll protoplasts, 100 µg/mL Tm or DMSO (dimethylsulfoxide) was added to the 5-cm Petri dished containing TEX buffer upon electroporation. Protoplasts were incubated for 16 h in darkness at 25ºC. Finally, protoplasts were collected and sedimented with

W5 medium to extract their membrane proteins as described in sections 5.1 or 5.2. of Materials and methods.

3.2. TREATMENT WITH INHIBITORS OF PROTEIN DEGRADATION

To investigate the degradation pathway involved in the degradation of the p24δ9 mutant, wild-type or *p24δ9* seeds were grown in MS liquid for 19 days as described in section 1.2.1.3. of Materials and methods. Then, 19-day-old seedlings were gently transferred to a beaker containing 40 mL of MS liquid only or supplemented with 50 µM E-64 or 100 µM MG-132. Seedlings were incubated for 16 h in darkness at 25ºC and 115 rpm shaking. Finally, seedling roots were cut and snap frozen in liquid nitrogen. Roots were stored at -80ºC until use.

4. ISOLATION AND ANALYSIS OF NUCLEIC ACIDS

4.1. ISOLATION OF NUCLEIC ACIDS

4.1.1. Isolation of plasmid DNA

For small-scale preparations of plasmid DNA, an alkaline lysis method described by Sambrook (Sambrook et al., 1989) was used beginning with 1 mL culture grown overnight in LB supplemented with the corresponding antibiotic.

Middle-scale preparations of plasmid DNA were performed beginning with 100 mL cultures grown overnight in LB with antibiotic, and following

the manufacturer's instructions for extraction and purification of plasmid DNA indicated in Quiagen® Plasmid Midi Kit (Qiagen columns tip-100, Ref. 12143).

For large-scale preparations of plasmid DNA, two different methods were used. For one of them, the Qiagen® Plasmid Maxi Kit (Ref. 12163) was used following the manufacturer's instructions. This method was used mainly to obtain plasmid DNA for PEG transformation. Alternatively, it was also used a protocol which allows to obtain a high concentration of plasmid DNA (Peter Pimpl, Silke Sturm –Heidelberg Germany-, personal communication) that works very well in the electroporation transformations. Briefly, bacteria containing the plasmid of interest were grown in 500 mL of LB medium supplemented with the corresponding antibiotic for 21-24 h. After collecting bacteria by centrifugation, the following solutions were sequentially added at 0ºC: 8 ml of TE 50/1 (50 mM Tris-HCl, 1 mM EDTA, pH 8.0); 2.5 mL of 10 mg/mL lysozyme; 2 mL 0.5 M EDTA pH 8.0; and 100 µl of 20 mg/mL Ribonuclease A with 150 µL 10% Triton X-100 in 1 mL of TE 50/1. The samples were mixed by inversion and incubated 5 minutes between each step, except the last one, that lasted 45 minutes. After another centrifugation to remove traces of bacteria, the supernatant was mixed with equilibrated phenol pH 8.0 with 0.1% 8-hydroxyquinoline, shaking vigorously for one minute. The upper phase was recovered and chloroform was added in a 1:1 proportion, shaking one minute again. The aqueous phase was recovered and mixed with 1 mL 5 M $NaClO_4$ and 8 mL of isopropyl alcohol (10% and 80% of the total volume,

respectively). After centrifugation, the DNA pellet was resuspended in TE (10 mM Tris-HCL, 0.1 mM EDTA, pH 8.0) and stored at 4ºC.

4.1.2. Isolation of genomic DNA from *Arabidopsis*

To isolate *A thaliana* genomic DNA, 100 mg of rosette leaves of 3-4-week-old plants, before the main shoot elongated, were collected and snap frozen in liquid nitrogen. The genomic DNA was obtained following a protocol described previously (Edwards et al., 1991).

4.1.3. Isolation of total RNA from *Arabidopsis*

To obtain *Arabidopsis* total RNA, the Rneasy® Plant Mini Kit (Qiagen, Ref. 74904) system, which is specific for plants, was used. 75 mg of the indicated tissue was collected and snap frozen in liquid nitrogen. Samples were homogenized by grinding them in liquid nitrogen with a pestle. Total RNA extraction was performed following the instructions of the manufacturer. All samples were treated with DNase (Qiagen, Ref 79254).

RNA quantification was performed in a spectrophotometer (Ultrospec 2000, Pharmacia Biotech) and total RNA was stored at -80ºC for further use.

4.2. MANIPULATION AND ANALYSIS OF NUCLEIC ACIDS

4.2.1. Recombinant plasmid production

The coding sequence of red fluorescent protein (RFP)-p24δ5N86Q was commercially synthesized *de novo* (Geneart AG) based on the sequence of RFP and that of the *Arabidopsis* p24δ5 protein (At1g21900) whose Asn

residue in position 86 was changed to Gln. To this end, the codon AAT which codes for Asn was mutated to CAA which codes for Gln. The sequence of the fluorophore is behind the coding sequences of the p24 signal sequence (SS) and before the 5' extreme end of the mature p24 coding sequence. The coding sequence of RFP-p24δ5N86Q were cloned into the pBP30 vector (carrying the CaMV 35S promoter, Nebenführ et al., 1999) through *Bgl*II/*Not*I.

4.2.2. Agarose gel electrophoresis

DNA fragments were visualized in 1-2% agarose gels (depending on the size of the fragments to be analysed) in TBE buffer (89 mM Tris, 89 mM boric acid, 2 mM EDTA, pH 8.0), stained with 10 µg/mL Real Safe® (Durviz, S.L.), and separated by electrophoresis with a constant voltage between 100-150 V, immersed in TBE. Samples were diluted in 6X Loading buffer [50% (v/v) glycerol, 0.05% (w/v) bromophenol blue, 100 mM EDTA]. DNA bands were visualized by lighting up the gel with ultraviolet light, using the UVITEC system (Cambridge). This system allows also to photograph the gel.

4.2.3. Amplification by polymerase chain reaction (PCR)

Amplification reactions were performed in the cycler GeneAmp PCR system 2400 (Perkin Elmer), following the instructions contained in the kit from WVR Red Taq DNA Polymerase Master Mix (Ref 5200300-1250).

For genotyping by PCR, samples consisted of 2 µl from genomic DNA isolated as described in section 4.1.2., 2 µl of each primer at 10 µM (Table

S1), 19 µl sterile Milli-Q water and 25 µl of WVR Red Taq DNA Polymerase Master Mix, which contains dNTPs (dATP, dCTP, dGTP and dTTP at 0.4 mM), 0.2 units/µl VWR Taq polymerase in Tris-HCl pH 8.5, $(NH_4)_2SO_4$, 3 mM $MgCl_2$ and 0.2% Tween ® 20. Total volume was 50 µl.

Genotypic analysis by PCR consisted in running a first denaturation step of 2 minutes at 95ºC, followed by 36 cycles. Each cycle was divided in three sections: 30 seconds at 95ºC (denaturation), 30 seconds at the respective annealing temperature of specific primers (usually 55ºC) and 1 to 3 minutes according to the size of the fragment at 72ºC (elongation). Finally, a final period of 7 min at 72 ºC was added to assure the elongation of all fragments.

The primers used in this work for PCR and RT-sqPCR are listed in the Table A1 (see Appendix 1).

4.2.4. Synthesis of cDNA by retrotranscription

This procedure allows obtaining complementary (cDNA) from RNA by the action of a reverse transcriptase which is a viral enzyme that synthesizes DNA using RNA as a template. To obtain cDNA, the Maxima® First Strand cDNA Synthesis Kit for RT-qPCR (Fermentas, Ref. #K1641) was used. The starting point was 3 µg of total RNA, to which 2 µl of Maxima enzyme mix, 4 µl of 5X Reaction mix and free ribonuclease water to a total volume of 20 µl were added. PCR tubes were incubated for 25 minutes at 25ºC, then 30 minutes at 50ºC and finally, the reverse transcriptase was inactivated

incubating the PCR tubes for 5 minutes at 85ºC. The cDNA obtained was stored at -20ºC until its use.

4.2.5. Semiquantitative PCR (RT-sqPCR)

For semiquantitative expression PCR (RT-sqPCR) analysis, amplification reactions were performed in the cycler GeneAmp PCR system 2400 (Perkin Elmer), following the instructions contained in the kit from Roche PCR Master.

In this case, samples consist of 3 µl (initially) of cDNA from the retrotranscription reaction and 2 µl of each primer at 10 µM (Table S1) diluted in the H_2O provided by the kit, up to 25 µl. To avoid non-specific amplification, a "hot start" protocol was used. It consisted in running a first denaturation period of 2 minutes at 95ºC, after which 25 µl of PCR Master [which contains dNTPs at 0.4 mM, 25 U of DNA polymerase thermophilic eubacterium *Thermus aquaticus* BM (Taq polymerase) in 20 mM Tris-HCl, 100 mM KCl, 3 mM $MgCl_2$ and 0.01% (v/v) Brij 35 at pH 8.3] pre-heated at 50ºC (total volume of 50 µL) was added.

The amplification cycles were divided into 15 initial cycles which consisted in three sections as described in section 4.2.3. To these initial cycles, a variable number of cycles were added depending on the level of mRNA expression of the analyzed gene in the tissue. 10 µL aliquots of the PCR products were taken at a consecutive number of cycles (to check the linear range) and incubated 7 min at 72ºC, for further analysis. The

temperature was kept at 4ºC till the samples were removed from the thermal cycler.

The primers used in this work for PCR and RT-sqPCR are listed in the Table A1 (see Appendix 1).

4.2.6. Quantitative PCR (RT-qPCR)

To quantify the expression levels of mRNA from the genes of interest, quantitative PCR (qPCR) was performed using the SYBR® Primex Ex Taq (Tli RnaseH Plus) (Takara) according to the manufacturer's protocol. Each reaction was performed in triplicate with 100 ng of the first-strand cDNA, 0.4 µl of each primer (forward and reverse) of the gene of interest whose optimal concentration was previously analyzed (as recommended by the manufacturer's protocol), 0.4 µl of ROX Reference Dye and 10 µl of SYBR® Premix Ex Taq™ (2x) diluted in water, up to 20 µl. Each reaction mix was deposited in a well of a MicroAmp® Fast Optical 96-Well Reaction Plate (Applied Biosystems, Ref 4346907). The analysis by RT-qPCR was done by the StepOne® Plus System (Applied Biosystems), which detects the emitted fluorescence of the SYBR® GREEN I inserted between the double strand of the DNA. The amplification method consisted in 30 seconds at 95ºC, followed by 40 cycles of 5 seconds at 95ºC, 30 seconds at a specific primer temperature (usually 60ºC). The specificity of the PCR amplification was confirmed wit a heat dissociation curve (from 60ºC to 95ºC). The relative mRNA abundance was calculated using the comparative Ct method according to Pfaffl (2004).

The primers used for RT-qPCR in this work are listed in the Table A2 (see Appendix 2).

5. ISOLATION AND ANALYSIS OF PROTEINS

5.1. TOTAL PROTEIN EXTRACTION OF *Arabidopsis* ROOTS

To obtain protein extracts from cytosolic and membrane fractions, roots of 20-day-old seedlings grown in MS liquid medium (section 1.2.1.4. Materials and methods) were cut with a razor blade on ice, dried well and frozen in liquid nitrogen until use. Next, they were homogenized in homogenization buffer (HB) (0.3 M sucrose; 1 mM EDTA; 1 mM dithiothreitol DTT; 20 mM HEPES pH 7.5; 20 mM KCl; pH 7.5) supplemented with 1mM DTT and 0.1% Protease Inhibitor Cocktail Sigma® (IPs) using a mortar and a pestle, maintaining always the mortar on ice. The homogenate was centrifuged for 10 minutes at 2000 rpm and 4ºC. The supernatant was centrifuged again for 10 minutes at 4500 rpm and 4ºC. The final supernatant was considered as the post-nuclear supernatant (PNS). PNSs from different samples were adjusted to the same protein total concentration by adding HB.

Cytosol and membrane fractions were obtained by centrifugation of the PNS fraction for 1h at 45000 rpm. The supernatant was considered as the cytosolic fraction. Membrane pellets were extracted using a lysis buffer which contains 50 mM Tris-HCl pH 7.5, 150 mM NaCl, 0.5 mM DTT, 0.5%

Triton X-100 and supplemented with 0.1% of IPs. Protein extracts were obtained after centrifugation for 5 min at 13000 rpm. Cytosolic fractions or protein extracts from membrane fractions were used for SDS-PAGE followed by Western blot analysis.

5.2. TOTAL PROTEIN EXTRACTION OF *Arabidopsis* PROTOPLASTS

Protoplasts obtained as described in section 1.2.1.6. and incubated in presence or absence of Tm (section 3.1.3) were collected in W5 medium by centrifugation for 5 minutes at 800 rpm and 4ºC. Pellet was homogenized in 1 mL of HB with 10% IPs and protoplasts were disrupted by sonication (6x5 s). Protoplast extracts were separated from unbroken protoplasts by centrifugation (10 min at 2500 rpm and 4ºC). Membranes were pelleted by centrifugation of the supernatant for 10 minutes at 470000 *g* and 4ºC. Membrane pellets were extracted in lysis buffer supplement with 0.1% IPs, leaving them on ice for 30 minutes. Finally, the resultant supernatants after a centrifugation of 5 minutes at 13000 rpm and 4ºC were the total membrane protein extract, which were used for SDS-PAGE and Western blot analysis.

5.3. TOTAL PROTEIN EXTRACTION OF *N. tabaccum* PROTOPLASTS

Protein extracts from tobacco protoplasts obtained and transfected as described in sections 1.2.2.2. and 2.6 of Materials and methods, respectively, were obtained as described previously (Montesinos et al., 2014). Briefly, transfected protoplasts were collected by centrifugation and

washed twice with W5 medium. Pellets were resuspended 1:1 (v/v) in HB supplemented with 01% IPs and cells were disrupted by sonication (6x5 s). Homogenates were centrifuged and the post-nuclear supernatant (PNS) was collected. Membrane proteins from PNSs were extracted by adding 0.5% Triton X-100, leaving them on ice for 30 minutes. PNS was diluted with co-immunoprecipitation buffer (CO-IP buffer) (10 mM Tris-HCl pH 7.5, 150 mM NaCl and 0.5 mM EDTA). After a centrifugation of 5 minutes at 13000 rpm and 4ºC, PNSs were used for pull-down experiments.

5.4. PULL-DOWN EXPERIMENTS

Pull-downs experiments from tobacco protoplasts expressing RFP-tagged proteins or co-expressing ERD2a-YFP with RFP-tagged were performed using RFP-Trap or GFP-Trap magnetic beads (Chromotek®), following the recommendations of the manufacturer, as described previously (Montesinos et al., 2013).

5.5. DEGLYCOSYLATION ASSAYS

Deglycosylation assays were performed using Endo H enzyme (BioLabs®, Ref. P0702S) according to the manufacturer's protocol. Briefly, pull-downs obtained from tobacco protoplasts expressing RPF-tagged proteins were incubated with 1 µl of 10x Glycoprotein Denaturating Buffer (5% SDS, 0.4 M DTT) and 9 µl of sterile Milli-Q H_2O at 100ºC for 10 min. Then, 2 µl of 10X G5 Reaction Buffer (0.5 M Sodium Citrate, pH 5.5) and 5 µl of Endo H were added in treated samples. Samples were diluted in water, up

to 20 µl. Finally, they were incubated at 37ºC for 2 h, and were used for SDS-PAGE followed by Western blot analysis.

5.6. SECRETION ASSAYS

Secretion assays were performed as described previously (Crofts et al., 1999). Briefly, protoplast from tobacco leaves were obtained as described in section 1.2.2.2. of Materials and methods and transient transformed as described in section 2.5. of Materials and methods. Transfected protoplasts were centrifuged for 5 minutes at 800 rpm to pellet them. Medium was collected and centrifuged for 10 minutes at 100000 rpm and 4ºC to remove traces of protoplasts. Culture medium was concentrated 5x by methanol/chloroform precipitation of proteins. Protoplasts were homogenized in HB supplemented with 0.1% IPs with the same volume of the original suspension, as described in section 5.3. Equal volumes of protoplasts and medium were analyzed by SDS-PAGE and Western blotting. Secretion of GFP-HDEL, Sec-GFP or BiP was analyzed by Western blot with antibodies against GFP (to detect GFP-HDEL and Sec-GFP) or BiP and calculated as the percentage of the amount of these markers in the medium (extracellular) with respect to their amount in the protoplasts (intracellular), as described previously (Philipson et al., 2001).

5.7. ISOLATION OF APOPLASTIC FLUID FROM LEAF TISSUE

For the isolation of apoplastic fluid from leaf tissue, it was followed the vacuum infiltration-centrifugation technique, as described previously

(Joosten, 2012). To this end, 1g of leaves from plants grown 4 weeks in soil were cut and transferred to Falcon tubes (50 mL). Leaves were submerged in Infiltration Buffer (25 mM MES, 150 mM NaCl and pH 6.2). Then, leaves were subjected to vacuum infiltration for 15 minutes. Infiltrated leaves were washed with water and dried well before to be transferred into a syringe place into a Falcon tube (50 mL). Falcon tubes with the leaves were centrifuged for 10 minutes at 2300 rpm and 4ºC. Apoplastic fluid was collected from the falcon tubes and used for SDS-PAGE and Western blot analysis.

Finally, leaves were homogenized in 2 mL of HB supplemented with 0.1% IPs using a mortar and a pestle, maintaining always the mortar on ice. The homogenates were centrifuged for 10 minutes at 2500 rpm and 4ºC. The final supernatant was used for SDS-PAGE and Western blot analysis.

5.8. DETERMINATION OF PROTEIN CONCENTRATION

To quantify the protein concentration in a sample, the Bio-Rad® Protein Assay kit was used. It is based on the method described by Bradford (1976), which allows to correlate the variation of absorbance at 595 nm from an acidic solution of Coomasie Brilliant Blue G-250 with the quantity of proteins in a sample (optimum range of 0.2-2 mg/mL of protein), using different concentrations of BSA as a standard.

5.9. SDS-POLYACRYLAMIDE GEL ELECTROPHORESIS (SDS-PAGE)

Proteins from different samples were separated through electrophoresis in vertical gels of SDS-polyacrylamide, following the protocol described by Laemmli (1970), at constant voltage (100 V). Previously, samples were mixed 1:1 with 2X Sample buffer (SB), which contains 125 mM Tris-HCl, 20% glycerol, 4% SDS, 25 µg/mL Bromophenol blue and 50 µl/mL of 14 M β-mercaptoethanol, pH 6.8. Then, samples were incubated for 5 minutes at 95ºC.

The acrylamide/bisacrylamide gels consisted in two different parts:

- Running gel: 8-14% polyacrylamide [30% acrylamide/bis (29:1), Bio-Rad], 0.39 mM Tris-HCl pH 8.8, 0.1% SDS, 0.1% APS (ammonium persulfate, Bio-Rad), 1/1000-1/2500 TEMED (N, N, N', N'-tetramethilethilendiamine, Bio-Rad).
- Stacking gel: 5% polyacrylamide, 0.13% Tris-HCl pH 6.8, 1% APS, 1/1000 TEMED.

The electrophoresis was performed with the Electrophoresis buffer, which contains 192 mM glycine, 25 mM Trizma® base, 01% SDS, pH 8.3. After SDS-PAGE, proteins were transferred to a nitrocellulose membrane to perform Western blot analysis.

5.10. PROTEIN DETECTION: WESTERN BLOT ANALYSIS

Proteins separated by SDS-PAGE were transferred to a nitrocellulose membrane of 0.45 µm (Bio-Rad) following the Burnette protocol (Burnette, 1981) through a humid transfer system (Bio-Rad) with constant voltage

(100V) for 1 h, all immersed in Transfer buffer (25 mM Trizma® base; 192 mM glycine; 20% MeOH; pH 8.5). The efficiency of the transference and the proper loading of the different samples were tested in the membranes staining them with Ponceau S 0.5% solution (SIGMA).

Western blot analysis is based on the indirect detection of proteins placed in a nitrocellulose membrane, using specific antibodies. To this end, membranes were blocked with blotto-Tween (powdered milk in 3-5% PBS; 0.01% Tween 20) for 16 h at 4ºC or 1 h at RT with gentle shaking (see-saw rocker SSL4, Stuart), which was maintained during all the process. After blocking, membranes were incubated with the pertinent primary antibody (Table 6) diluted in PBS-BSA [PBS (8 mM Na_2HPO_4, 1.7 mM KH_2PO_4, 137 mM NaCl, 2.7 mM KCl), 2 mg/mL BSA, 0.02% sodium azide] for 1h at RT. Next, 5 incubations of 5 minutes with TBS-Tween [0.01% Tween® 20in TBS [24 mM Tris-HCl, 150 mM NaCl, pH 7.5)] were performed to wash out the excess of antibody. The incubation with the secondary antibody (Table 7) which is conjugated to horseradish peroxidase (HRP) was performed for 1 h at RT. After the incubation, the excess of secondary antibody was washed out as the primary antibody.

Developing was performed by the Enhanced chemiluminescence method (ECL). This method is based on the chemiluminiscence reaction of luminol. The enzyme HRP, which is linked to secondary antibodies, catalyses the oxidation of luminol when there is hydrogen peroxide in alkaline conditions, generating a product that emits luminescence (Whitehead et al.,

1979). Developing was performed following the instructions of the manufacturer (Western blotting detection reagents, Thermo Scientific), using the automatic system Molecular Imager® ChemiDoc™ XRS+ Imaging system (Bio-Rad), with variable exposure times. The intensity of the bands obtained from Western-blots in the linear range of detection was quantified using the Quantity One software (Bio-Rad Laboratories).

Nitrocellulose membranes can be reused for another Western blot analysis after stripping the antibodies. To this end, membranes were incubated with 0.5 M glycine pH 2.5 for 15 minutes at RT with constant shaking. Then, they were washed five times, twice with distilled water and three times with TBS-Tween. Finally, membranes were blocked again with blotto-Tween.

Table 6. Primary antibodies used in this work.

Target	Host	Dilution	Reference
p24δ5-Nt	Rabbit	1/500	Montesinos et al.,2012
p24δ9-Nt	Rabbit	1/500	Montesinos et al., 2013
p24β2-Ct	Rabbit	1/500	Montesinos et al., 2012
p24β3-Nt	Rabbit	1/500	Montesinos et al., 2013
Sec21	Rabbit	1/2000	Dr. David G. Robinson
Sec23	Rabbit	1/1000	Dr. David G. Robinson
Sec13	Rat	1/1000	Dr. David G. Robinson
BiP	Rabbit	1/1000	Dr. David G. Robinson
H^+-ATPase	Rabbit	1/500	Dra. Karen Schumacher
Syc21	Rabbit		Dr. David G. Robinson
GAPDH	Rabbit	1/500	Santa Cruz Biotechnologies
RFP	Rabbit	1/200	Clontech
GFP	Rabbit	1/200	Life technologies

Table 7. Secondary antibodies used in this work.

Target	Host	Dilution	Reference
IgG Rabbit	Donkey	1/7500	GE Healthcare
IgG Rat	Goat	1/7500	Thermo Scientific

6. *IN SITU* DETECTION AND VISUALIZATION OF PROTEINS

6.1. CONFOCAL MICROSCOPY

Confocal fluorescent images from protoplasts or 4.5-day-old seedlings were collected using an Olympus FV1000 confocal microscope with 60x water lens. Fluorescence signals for GFP (488 nm/496-518 nm), YFP (514 nm/529-550 nm) and RFP/cherry (543 nm/593-636 nm) were detected. Sequential scanning was used to avoid any interference between fluorescence channels. Post-acquisition image processing was performed using the FV10-ASW 4.2 Viewer and ImageJ (v.1.45).

6.2. ELECTRON MICROSCOPY (EM)

For electron microscopy, seedlings were grown on MS medium containing 1% agar, and the seedlings were harvested after 4 days. Two different technics were used for the fixation.

6.2.1. Chemical fixation

For the chemical fixation, cotyledons and roots were fixed with 2.5% glutaraldehyde, and postfixed in 1% osmium. Samples were dehydrated in an ethanol series and infiltrated with L-White resin. Ultrathin sections (70 nm) were cut on Microtome Leica UC6, stained with uranyl acetate and lead citrate and observed with a JEM-1010 (JEOL) transmission electron microscope.

6.2.2. High-pressure freezing

High-pressure freezing was performed as described previously (Tse et al., 2004; Gao et al., 2012). Briefly, root types were cut and immediately frozen in a high-pressure freezer (EM PACT2; Leica), followed by subsequent freeze substitution in dry acetone containing 0.1% uranyl acetate at -85ºC in an AFS freeze substitution unit (Leica). Infiltration with Lowicryl HM20, embedding, and uv polymerization were performed stepwise at -35ºC. Transmission EM examination was performed with a Hitachi H-7650 transmission electron microscope with a charge-couple device camera (Hitachi High-Technologies).

RESULTS AND DISCUSSION

CHAPTER I: FUNTIONAL CHARACTERIZATION OF QUADRUPLE KNOCKOUT MUTANTS, *p24δ3δ4δ5δ6* AND *p24δ7δ8δ9δ10*, OF THE p24δ SUBFAMILY

1.1. EXPRESSION ANALYSIS OF p24 FAMILY GENES IN *Arabidopsis*

Most previous expression studies have examined only a limited number of p24 proteins or a limited number of tissues (Denzel et al., 2000; Kuiper et al. 2000, Rötter et al., 2002; Hosaka et al., 2007; Vetrivel et al., 2008; Xie et al., 2014). Only two studies have examined the expression of all p24 family members in whole organisms, one in *Drosophila* (Boltz et al., 2007) and the other one in mouse (Strating et al., 2009). These studies show that most p24 proteins are ubiquitously expressed, although a few of them are expressed in a tissue-specific manner and show regulated expression.

In *Arabidopsis*, five out of the eleven *p24* genes (*p24δ4*, *p24δ5*, *p24δ9*, *p24β2* and *p24β3*) have high/medium levels of expression in different organs, according to public microarray databases. In contrast, *p24δ6* and *p24δ11* have floral tissue-specific expression (Zimmermann et al., 2004). To verify the microarray data, the mRNA expression levels of all *p24* genes were analyzed by Reverse Transcription-semiquantitative PCR (RT-sqPCR).

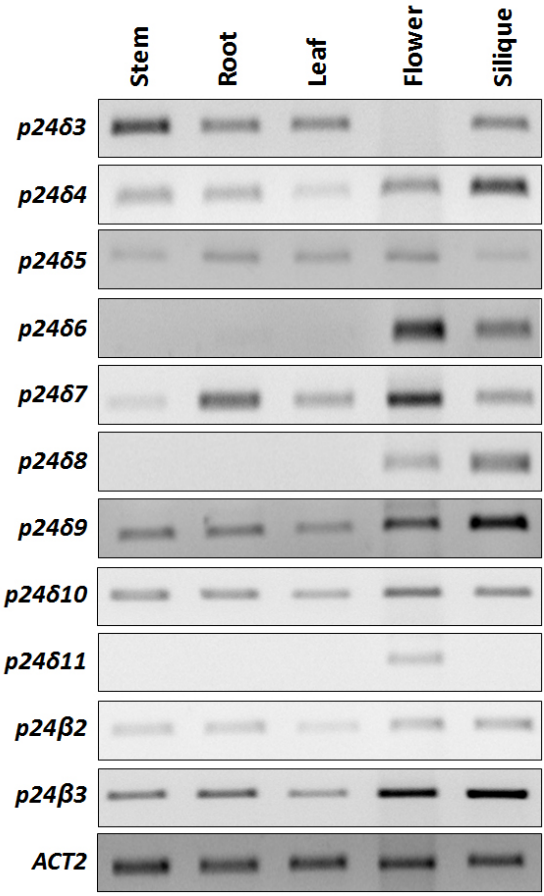

Figure 19. Expression of the p24 family genes in *Arabidopsis* organs. Different organs from wild-type plants grown 45 days in soil were used. Total RNA was obtained from stem (between the first and the second internode), root, rosette leaves, flowers (at stage 13) and siliques (at stage 17). In the PCRs, gene specific primers were used (Table A1). *Actin-2* (*ACT2*) was used as a control for gene expression in the different *Arabidopsis* organs. The PCRs were performed as described in section 4.2.3 of Materials and methods and PCR samples were collected at cycle 26 for *ACT2,* at cycle 28 for *p24δ10, p24β2* and *p24β3*, at cycle 30 for *p24δ9,* at cycle 32 for *p24δ3*, *p24δ5*, *p24δ6*, *p24δ7* and *p24δ8*; and at cycle 34 for *p24δ4* and *p24δ11*.

As shown in Figure 19, it was found that *p24δ4*, *p24δ5*, *p24δ7*, *p24δ9*, *p24δ10*, *p24β2* and *p24β3* genes are widely expressed. *p24δ3* mRNA expression was observed in all organs examined except in flowers. In contrast, expression of *p24δ6* and *p24δ8* was only detected in flowers and siliques and *p24δ11* expression was only observed in flowers, whereas no expression was found in the other organs examined. Therefore, most p24 genes are widely expressed in *Arabidopsis* which indicates that these genes may play a housekeeping function. However, the restricted expression patterns of three genes of the p24δ subfamily, p24δ6, p24δ8 and p24δ11, may reflect specialized functions for the p24 proteins coded by these genes in floral tissues.

1.2. IDENTIFICATION OF SINGLE KNOCKOUT MUTANTS OF THE p24δ SUBFAMILY

To study the role of the p24 proteins of the δ subfamily, a reverse genetic approach was chosen. Previously, knockout T-DNA insertion mutants of *p24δ4*, *p24δ5*, *p24δ9*, *p24δ10* and *p24δ11* were identified in our laboratory from different mutant collections (Montesinos et al., 2012, 2013 and Semenzin, 2014). Several T-DNA insertion mutants of *p24δ3*, *p24δ6*, *p24δ7* and *p2δ8* were found in the Arabidopsis SALK collection (http://signal.salk.edu/cgi-bin/tdnaexpress). Seeds were purchased to identify knockout mutants of these *p24* genes.

1.2.1. Identification of a *p24δ3* knockout mutant

It was found one T-DNA insertion mutant of the *p24δ3* gene (At1g09580) that corresponded to the number GK_029E10 and it was called *p24δ3E10.* DNA insertion sequence adjacent to the T-DNA obtained from GABI-Kat project (Kleinboelting et al., 2012) indicates that the insertion of the T-DNA is located in the second exon (Figure 20).

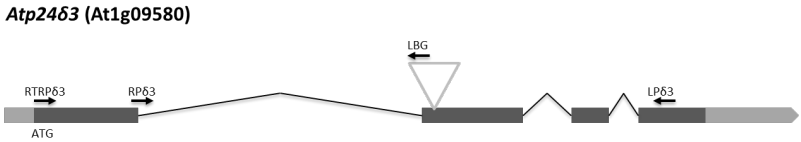

Figure 20. Localization of the T-DNA insertion in the p24δ3E10 mutant (GK_020E10). Diagram of the *p24δ3* gene and localization of the T-DNA insertion (triangle). Black boxes represent coding regions and grey boxes represent 5'-UTR and 3'-UTR regions. The primers used to identify the homozygous mutant plants for the T-DNA insertion are shown.

Seeds from 10 different individual plants of the *p24δ3E10* mutant (*p24δ3E10.01* to *p24δ3E10.10*) were provided by NASC (Nottingham Arabidopsis Stock Centre). Each individual plant was considered as a different line. The identification of homozygous plants for the insertion of the T-DNA was performed by sulfadiazine resistance segregation analysis of the different lines (Appendix 3, Table A3.) as described in section 2.4. of Materials and methods. Four lines, *p24δ3E10.04, p24δ3E10.5*, *p24δ3E10.6* and *p24δ3E10.7*, were identified as possible homozygous lines. One plant of each homozygous line was selected for further studies. The confirmation of the homozygous plants for the T-DNA insertion was performed by PCR (Appendix 3, Figure A3.1)

The homozygous plants were used to verify the absence of *p24δ3* mRNA. RT-sqPCR analysis showed that they lacked the full length transcript of *p24δ3* (Figure 21). As the insertion is in the middle of the gene no functional transcript is expected to be synthesized and thus, *p24δ3E10.04, p24δ3E10.5*, *p24δ3E10.6* and *p24δ3E10.7* can be considered knockout (KO) mutants of *p24δ3* gene. *p24δ3E10.04* plant was selected for further experiments and those seeds were used in this work as *p24δ3* seeds.

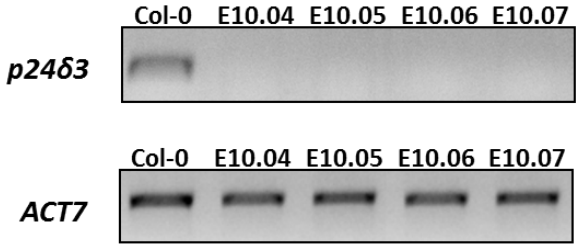

Figure 21. RT-sqPCR analysis to show the absence of full-length *p24δ3* mRNA in the *p24δ3E10* mutants. Total RNA from 7-day-old seedlings of *p24δ3E10.04, p24δ3E10.05, p24δ3E10.06*, *p24δ3E10.07* and wild-type (Col-0) were used for the RT-PCR. In the PCRs, specific primers of *p24δ3*, RPδ3 and LPδ3, were used (Figure 20). *Actin-7* (*ACT7*) was used as a control. The PCRs were performed as described in section 4.2.3. of Materials and methods and PCR samples were collected at cycle 22 for *ACT7* and at cycle 36 for *p24δ3*. It was observed that in wild-type plants, a cDNA fragment of 570 bp was amplified. In contrast, no fragment was amplified in *p24δ3E10.04, p24δ3E10.05, p24δ3E10.06* and *p24δ3E10.07* lines.

1.2.2. Identification of a *p24δ6* knockout mutant

It was found one T-DNA insertion mutant of the *p24δ6* gene (At3g10780) that corresponded to the number GK_823G03 and it was called *p24δ6*. The DNA insertion sequence adjacent to the T-DNA obtained from GABI-Kat project (Kleinboelting et al., 2012) indicates that the insertion of the T-DNA is located in the third exon (Figure 22).

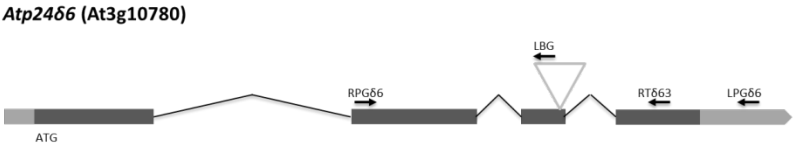

Figure 22. Localization of the T-DNA insertion in the *p24δ6* mutant (GK_823G03). Diagram of the *p24δ6* gene and localization of the T-DNA insertion (triangle). Black boxes represent coding regions and grey boxes represent 5'-UTR and 3'-UTR regions. The primers used to identify the homozygous mutant plants for the T-DNA insertion in the GK_823G03 mutant are shown.

Seeds from 12 different individual plants of the *p24δ6* mutant were provided by NASC (Nottingham Arabidopsis Stock Centre) which were enumerated from *p24δ6.38* to *p24δ6.49*. Each individual plant was considered as a different line. The sulfadiazine resistance segregation analysis of the different lines was performed to identify homozygous plants for the T-DNA insertion (Appendix A4, Table A4) as described in section 2.4. Materials and methods. Two different lines, *p24δ6.45* and *p24δ6.48*, were identified as possible homozygous lines of which *p24δ6.48* was selected for further studies. The confirmation of homozygous plants for the T-DNA insertion was performed by PCR (Appendix 4, Figure A4.1.). Seeds from the homozygous plants were pooled and were used in this work as *p24δ6* seeds.

RT-sqPCR analysis showed that *p24δ6* lacked the full length transcript of *p24δ6* (Figure 23). As the insertion is in the middle of the gene no functional transcript is expected to be synthesized and *p24δ6* can be considered a knockout (KO) mutant of *p24δ6*.

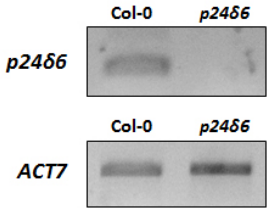

Figure 23. RT-sqPCR analysis to show the absence of full-length *p24δ6* mRNA in the *p24δ6* mutant Total RNA from *p24δ6* and wild-type (Col-0) 7-day-old seedlings were used for the RT-PCR. In the PCRs, *p24δ6* specific primers, RPGδ6 and RTδ63, were used (Figure 22). *Actin-7* (*ACT7*) was used as a control. The PCRs were performed as described in section 4.2.3. of Materials and methods and PCR samples were collected at cycle 22 for *ACT7* and at cycle 36 for *p24δ6.* It was observed that in wild-type plants, a cDNA fragment of 370 bp was amplified. In contrast, no fragment was amplified in *p24δ6* mutant.

1.2.3. Identification of a *p24δ7* knockout mutant

It was found one T-DNA insertion mutant of *p24δ7* gene (At1g14010) which corresponded to the number GK_503A10 that was called *p24δ7*. The DNA insertion sequence adjacent to the T-DNA obtained from GABI-Kat project (Kleinboelting et al., 2012) indicates that there are two different insertion sites for the T-DNA. One of them is located into the second intron of the *p24δ7* gene (Figure 24). The other one is located into the last exon of the At5g22130 gene, which codes a mannosyltransferase.

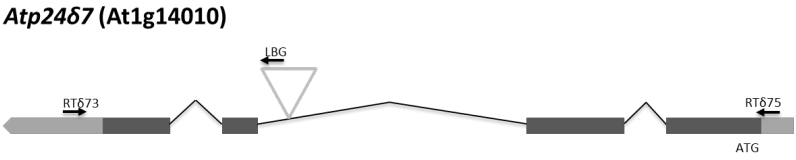

Figure 24. Localization of the T-DNA insertion in the *p24δ7* mutant (GK_503A10). Diagram of the *p24δ7* gene and localization of the T-DNA insertion (triangle). Black boxes represent coding regions and grey boxes represent 5'-UTR and 3'-UTR regions. The primers used to identify the homozygous mutant plants are shown.

Seeds from 5 different individual plants of the *p24δ7* T-DNA insertion mutant (*p24δ7*-1 to *p24δ7*-5) were provided by NASC (Nottingham Arabidopsis Stock Centre). Each individual plant was considered as a different line. First, the sulfadiazine resistance segregation of the lines was analyzed (Appendix 5, Table A5) as described in section 2.4. of Materials and methods.

Then, the identification of plants with a T-DNA insertion in the *p24δ7* and/or *At5g22130* genes was performed by PCR (Appendix 5, Figure A5.1. and A5.2.). Lines that contained a T-DNA insertion in *At5g22130* were discarded and three homozygous plants for the insertion of the T-DNA in *p24δ7* were selected (*p24δ7-1.1, p24δ7-1.2 and p24δ7-5.1*) to verify the absence of *p24δ7* mRNA.

RT-sqPCR analysis showed that all of them lacked the full length transcript of *p24δ7* (Figure 25). Seeds from the homozygous plants were pooled and were used in this work as *p24δ7* seeds. As the insertion is in the middle of the gene no functional transcript is expected to be synthesized and *p24δ7* can be considered a knockout (KO) mutant of *p24δ7* that was named p*24δ7*.

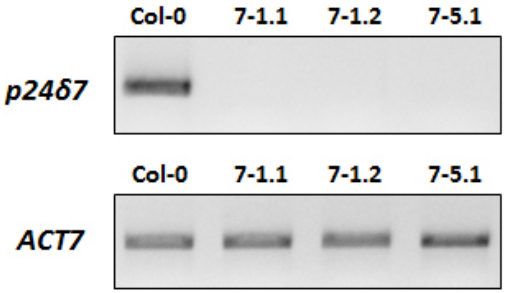

Figure 25. RT-sqPCR analysis to show the absence of full-length *p24δ7* mRNA in the *p24δ7-1.1*, *p24δ7-1.2* and *p24δ7-5.1* mutants. Total RNA from 7-day-old seedlings of *p24δ7-1.1, p24δ7-1.2*, *p24δ7-5.1* and wild-type plants (Col-0) were used for the PCR. In the PCRs, specific primers of *p24δ7*, RTδ75 and RTδ73, were used (Figure 24). *Actin-7* (*ACT7*) was used as a control. PCR samples were collected at cycle 22 for *ACT7* and at cycle 36 for *p24δ7*. It was observed that in wild-type plants, a cDNA fragment of 0.7 Kb was amplified. In contrast, no fragment was amplified in p24δ7-1.1, p24δ7-1.2 and p24δ7-5.1 plants.

1.2.4. Identification of a *p24δ8* knockout mutant

For the *p24δ8* gene (At2g03290), three mutants from the JIC SM collection (Tissier et al, 1999) were found which correspond to the numbers SM_3_36681, SM_3_36682 and SM_3_36686 and they were called *p24δ8.81*, *p24δ8.82* and *p24δ8.86,* respectively. SM transposon lines carry a single defective Spm (dSpm) transposon element as a stable insertion in the genome. The original DNA transformant lines contained an active Spm transposase which has been segregated out of the lines (Tissier et al., 1999). The flanking genomic DNAs obtained from the John Innes Centre indicate that the insertion of the transposon element of the three mutants is located at the same point within the third intron (Figure 26).

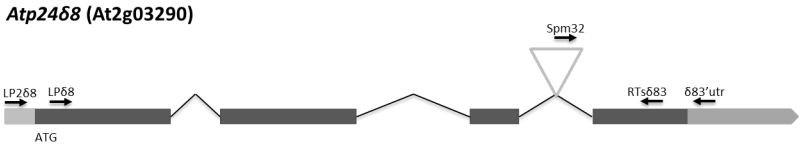

Figure 26. Localization of the SM transposon insertion in the SM_3_3668 mutants. Diagram of the *p24δ8* gene and localization of the dSpm transposon (triangle) in the SM_3_36681, SM_3_36682 and SM_3_36686 mutants. Black boxes represent the coding regions and grey boxes represent the 5'-UTR and 3'-UTR regions. The primers used to identify the homozygous mutant plants for the T-DNA insertion are shown.

Seeds of the *p24δ8.81*, *p24δ8.82* and *p24δ8.86* mutants were provided by NASC (Nottingham Arabidopsis Stock Centre). PCR analysis was performed to identify plants homozygous for the insertion of the transposon element (Appendix 6, Figure A6.1.).

The *p24δ8.81-4*, *p24δ8.82-2* and *p24δ8.86-1* homozygous plants were chosen to verify the absence of *p24δ8* mRNA. RT-sqPCR analysis showed that they lacked the full length transcript of *p24δ8* (Figure 27). As the insertion is at the end of the gene no functional transcript is expected to be synthesized. Seeds from the homozygous plants were pooled and called *p24δ8* which can be considered a knockout (KO) mutant of p24δ8.

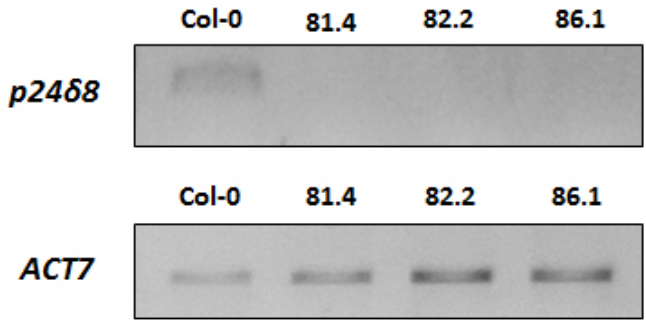

Figure 27. RT-sqPCR analysis to show the absence of full-length *p24δ8* mRNA in the *p24δ8.81-4*, *p24δ8.82-2* and *p24δ8.86-1* mutants. Total RNA from *p24δ8.81-4*, *p24δ8.82-2* and *p24δ8.86-1* and wild-type (Col-0) 7 day-old seedlings were used for the RT-PCR. In the PCRS, *p24δ8* specific primers, LPδ8 and δ83'utr, were used (Figure 26). *Actin-7* (*ACT7*) was used as a control. The PCRs were performed as described in section 4.2.3. of Materials and methods and PCR samples were collected at cycle 22 for *ACT7* and at cycle 36 for *p24δ8*. It was observed that in wild-type plants, a cDNA fragment of 0.6 Kb was amplified. In contrast, no fragment was amplified in *p24δ8.81-4*, *p24δ8.82-2* and *p24δ8.86-1* plants.

1.2.5. *p24δ9* mutant is a loss-of-function mutant of *p24δ9*

6 T-DNA insertion mutants of *p24δ9* (At1g26690) can be found in the Arabidopsis SALK collection (http://signal.salk.edu/cgi-bin/tdnaexpress). They were all previously characterized in our laboratory (data not shown). Only WiscDSLoxHs161_04H seems to have affected the expression of *p24δ9* (Semenzin, 2014). This mutant was called *p24δ9* mutant. The sequence analysis showed that the T-DNA is inserted one nucleotide before the stop codon of *p24δ9* and the T-DNA insertion sequence added before the stop codon is in frame with the sequence of *p24δ9* for 105 nucleotides before one stop codon is found (Semenzin, 2014). It was also shown that the mRNA

of *p24δ9* in the *p24δ9* mutant contained indeed an extra-sequence at the 3'end. This extra-sequence will make the protein 35 amino acids longer at the carboxi-terminal end. Moreover, the protein levels of p24δ9 in the *p24δ9* mutant were analysed by Western Blot analysis with Nt-p24δ9 antibodies (Montesinos et al., 2013) and it was found that the levels of p24δ9 were undetectable when compared with the wild-type (Col-0) (Semenzin, 2014).

As described in the introduction, the C-terminal cytoplasmic tail of all *Arabidopsis* p24 delta proteins contains several motifs that are responsible for their intracellular trafficking and localization. It has a canonical dilysine (KK) motif in the -3,-4 position (with respect to the C-terminus) which binds COPI subunits and mediates Golgi-to-ER retrograde transport (Contreras et al., 2004a; Langhans et al., 2008). It also has a diaromatic (FF) motif in the -7,-8 position which has been shown to bind COPII subunits and thus may function as an ER export signal (Dominguez et al., 1998; Contreras et al., 2004b; Aniento et al., 2006). Therefore, *Arabidopsis* p24 proteins of δ subfamily contain signals for binding both COPII and COPI subunits and thus for anterograde and retrograde transport in the early secretory pathway (Contreras et al., 2004b). At steady-state, p24δ5 and p24δ9 localized at the ER (Montesinos et al., 2013). The dilysine motif was found to be necessary and sufficient for ER localization of p24δ5 (Langhans et al., 2008). In contrast, p24δ5 mutants lacking the dilysine motif, when they are transiently expressed in tobacco protoplasts, do not localize to the ER but instead are transported along the secretory pathway

to the prevacuolar compartment (PVC) and the vacuole (Langhans et al., 2008). Therefore, the extra-sequence at the C-terminus of p24δ9 protein in the *p24δ9* mutant might mask the dilysine motif. As a consequence, p24δ9 might be transported to the vacuole where it would be degraded and this could explain why no p24δ9 protein is detected In the mutant.

To study this possibility or whether, by contrast, p24δ9 protein degradation in the *p24δ9* mutant is mediated by the proteasome pathway, the mechanisms involved in its degradation were analysed. *p24δ9* seedlings were incubated with 50 µM E-64, an inhibitor of cysteine proteinases, or 100 µM MG-132, a proteasome inhibitor (section 3.2. of Materials and methods). After 24 hours of incubation, protein extracts were obtained from membranes of wild-type or *p24δ9* roots (see sections 5.1. of Materials and methods). Western blot analysis shows that the Nt-p24δ9 antibody (Montesinos et al., 2013) detected a band around 27 kDa in the *p24δ9* mutant in presence of MG-132. This band was not detected in the wild-type or in the *p24δ9* mutant in the presence of E-64 or in absence of inhibitors (Figure 28). This 27 kDa band should correspond to p24δ9 protein with the extra-sequence. These results suggest that the p24δ9 protein synthesized in the *p24δ9* mutant may be degraded by the proteasome system, but not by cysteine proteases upon transport to post-Golgi compartments (PVC, vacuole). As the p24δ9 protein is degraded in the *p24δ9* mutant, it can be considered a loss-of-function mutant of *p24δ9*.

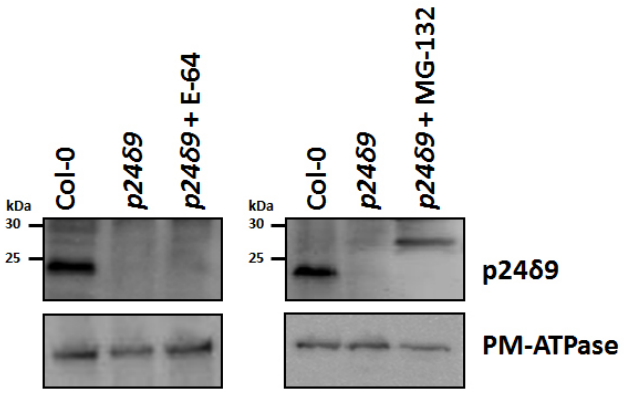

Figure 28. Proteasome inhibition increases p24δ9 protein levels in *p24δ9* mutant. *p24δ9* and wild-type (Col-0) seedlings grown for 19 days in MS were incubated with 50 µM E-64 (left panel) or 100 µM MG-132 (right panel) (section 3.2. of Materials and methods). After 24 hours, protein extracts were obtained from membranes of wild-type or *p24δ9* mutant roots, as described in the section 5.1 of Materials and methods. 30 µg of protein extracts were analysed by Western blotting with an antibody against the p24δ9 N-terminus (upper panel). Western blotting with an antibody against the plasma membrane (PM)-ATPase was used as a loading control (lower panel). The position of MW protein markers is indicated on the left.

1.3. GENERATION OF p24δ3δ4δ5δ6 AND p24δ7δ8δ9δ10 MUTANTS

As described in the introduction, *Arabidopsis* contains 9 members of the p24δ subfamily which have been proposed to belong to two different subclasses. The p24δ-1 subclass comprises p24δ3-p24δ6 and the p24δ-2 subclass comprises p24δ7-p24δ11 (Chen et al., 2012; Montesinos et al., 2012) (Figure 29).

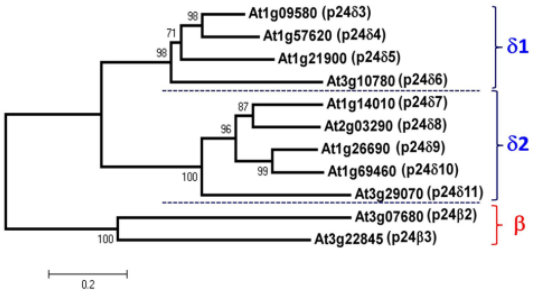

Figure 29. Phylogenetic tree of the p24 protein family in *Arabidopsis*. The names assigned to the Arabidopsis p24 proteins are shown next to the AGI code (Montesinos et al., 2012).

Previous studies indicated that p24 family members in *Arabidopsis* may be functionally redundant (Montesinos et al., 2012). In order to investigate possible functional differences between both subclasses, quadruple mutants of both subclasses were obtained.

1.3.1. Generation of a *p24δ3δ4δ5δ6* (δ-1 subclass) mutant

As described above, single KO mutants of all the genes of the p24δ-1 subclass have been identified. To obtain the quadruple KO mutant, double KO mutants were first generated by crossing KO single mutants. All the single mutants used to obtain the quadruple *p24δ3δ4δ5δ6* mutant are summarized in Table 8. Then, triple mutants were generated by crossing double mutants sharing one allele. Finally, the *p24δ3δ4δ5δ6* quadruple mutant was generated by crossing *p24δ3δ4δ5* with *p24δ4δ5δ6*. Genotype analysis of the progenies was performed by PCR in order to obtain the homozygous lines of the multiple mutant (Appendix 7).

Table 8. KO p24δ-1 mutants and PCR primers used for their identification.

GENE (Gene identifier)	Mutant (ID number)	Genotyping primers [()]		sqRT-PCR primers[c ()]
		T-DNA insertion[a]	Wild-type allele[b]	
p24δ3 **(At1g09580)**	GK_029E10 (This thesis)	LBG/RPδ3 (~ 0.7 Kb)	LPδ3/RPδ3 (1141 bp)	LPδ3/RTRPδ3 (570 bp)
p24δ4 **(At1g57620)**	SAIL_664_A06 (Montesinos et al, 2012)	LB3/δ43 (~ 1.3 Kb)	δ45/δ43c (1165 bp)	δ45/δ43c (657 bp)
p24δ5 **(At1g21900)**	SALK_016402C (Montesinos et al, 2012)	LBb1/RP241 (~ 0.6 Kb)	LP24M11/RP241 (613 bp)	LP24M11/RP241 (273 bp)
p24δ6 **(At3g10780)**	GK_823G03 (This thesis)	LBG/RPGδ6 (~ 0.4 KB)	LPGδ6/RPGδ6 (1089 bp)	RPGδ6/RTδ63 (379 bp)

[()] Expected Mw of the amplified fragment.

[a] Primers used for the identification of the corresponding insertions.

[b] Primers used for the identification of the wild-type alleles.

[c] Primers used for the verification of the absence of mRNA.

RT-sqPCR analysis showed that the quadruple *p24δ3δ4δ5δ6* mutant lacked the full length transcript of *p24δ3*, *p24δ4*, *p24δ5* and *p24δ6*, (Figure 30). Therefore, *p24δ3δ4δ5δ6* can be considered a quadruple KO mutant of *p24δ-1* subclass.

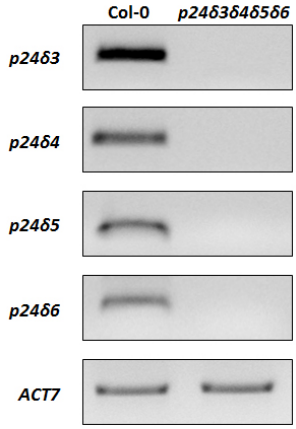

Figure 30. RT-sqPCR analysis of *p24δ3δ4δ5δ6* mutant to show the absence of full-length *p24δ3*, *p24δ4, p24δ5* and *p24δ6* mRNA. Total RNA from the quadruple T-DNA insertion mutant *p24δ3δ4δ5δ6* and wild-type (Col-0) 7-days-old seedlings were used for the RT-PCR. In the PCRs, specific primers for *p24δ3, p24δ4, p24δ5* and *p24δ6* were used (Table 8). *Actin-7* (*ACT7*) was used as a control. The PCRs were performed as described in section 4.2.3. of Materials and methods and PCR samples were collected at cycle 22 for *ACT7* and at cycle 36 for *p24δ3*, *p24δ4*, *p24δ5* and *p24δ6* genes. Col-0, wild-type plant (ecotype Columbia). It was observed that in wild-type seedlings, the expected molecular weight cDNA fragments were amplified. In contrast, no fragments were amplified in the mutant.

1.3.2. Generation of a *p24δ7δ8δ9δ10* (δ-2 subclass) mutant

p24δ-2 subclass comprises p24δ7-p24δ11. As described above, the single KO mutants of the 5 genes of the p24δ-2 subclass have been identified. To obtain a quadruple KO mutant of this subclass, the 4 most related genes were chosen (*p24δ7-p24δ10*), excluding the floral-specific *p24δ11* gene (Figure 19). Double KO mutants were first obtained by crossing KO single mutants. All the single mutants used to obtain the quadruple *p24δ7δ8δ9δ10* mutant are summarized in Table 9. Then, triple mutants were generated by crossing double mutants sharing one allele. Finally, the

p24δ7δ8δ9δ10 quadruple mutant was generated by crossing *p24δ7δ9δ10* with *p24δ8δ9δ10.* Genotype analysis of the progenies was performed by PCR in order to obtain the homozygous lines of the multiple mutants (Appendix 8).

Table 9. KO p24δ-2 mutants and the primers used for its identification.

GENE (Gene identifier)	Mutant (ID number)	Genotyping primers ()		sqRT-PCR primers[c] ()
		T-DNA insertion[a]	Wild-type allele[b]	
p24δ7 **(At1g14010)**	GK_503A10 (This thesis)	LBG/RTδ73 (~ 1 Kb)	RTδ75/RTδ73 (1463 bp)	RTδ75/RTδ73 (696 bp)
p24δ8 **(At2g03290)**	SM_3_36686 (This thesis)	Spm32/RTsδ83 (~ 1.3 Kb)	LPδ8/δ83'utr (999 bp)	LPδ8/δ83'utr (627 bp)
p24δ9 **(At1g26690)**	WiscDSLoxHs161_04H (This thesis)	L4/RPwδ9 (~ 0.8 Kb)	LPwδ9/RPwδ9 (1200 bp)	δ95/qPCRδ93 (601 bp)
p24δ10 **(At1g69460)**	SALK_144586 (Montesinos et al., 2013)	LBb1/RPδ10 (~ 0.8 KB)	LPδ10/RPδ10 (1163 bp)	δ105/δ103 (499 bp)

() Expected Mw of the amplified fragment.

[a] Primers used for the identification of the corresponding insertions.

[b] Primers used for the identification of the wild-type alleles.

[c] Primers used for the verification of the absence of mRNA.

To check the absence of *p24δ7*, *p24δ9* and *p24δ10* mRNA in the *p24δ7δ8δ9δ10* mutant, RT-sqPCR was performed with total RNA extracted from wild-type and *p24δ7δ8δ9δ10* seedlings. However, to verify the absence of *p24δ8* mRNA, RT-sqPCR was performed with total RNA extracted from wild-type and *p24δ7δ8δ9δ10* inflorescences as the *p24δ8* gene shows a specific expression in floral tissues (Figure 19). RT-sqPCR analysis showed

that the quadruple *p24δ7δ8δ9δ10* mutant lacked the full-length transcript of *p24δ7*, *p24δ8*, *p24δ9* and *p24δ10* (Figure 31). Therefore, *p24δ7δ8δ9δ10* can be considered a quadruple KO mutant of *p24δ-2* subclass.

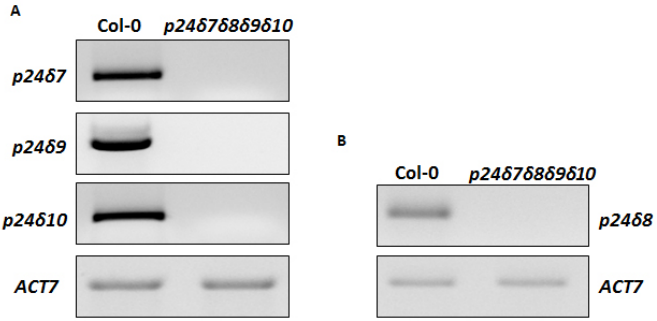

Figure 31. RT-sqPCR analysis of *p24δ7δ8δ9δ10* mutant to shown the absence of full-length *p24δ7*, *p24δ8*, *p24δ9* and *p24δ10* mRNA. A) Total RNA from 7 day-old seedlings of the quadruple mutant *p24δ7δ8δ9δ10* and wild-type (Col-0) was used for the RT-PCR. In the PCRs, specific primers for *p24δ7*, *p24δ9,* and *p24δ10* genes were used (Table 9). B) Total RNA from inflorescences of *p24δ7δ8δ9δ10* and wild-type (Col-0) plants grown 45 days was used for the RT-sqPCR. In the PCRs, specific primers for *p24δ8* were used (Table 9). *Actin-7* (*ACT7*) was used as a control. The PCRs were performed as described in section 4.2.3. of Materials and methods and PCR samples were collected at cycle 22 for *ACT7* and at cycle 36 for *p24δ7*, *p24δ8*, *p24δ9* and *p24δ10* genes. It was observed that in wild-type seedlings and inflorescences, the expected molecular weight cDNA fragments were amplified. In contrast, no fragments were amplified in the mutant.

1.4. *p24δ3δ4δ5δ6* AND *p24δ7δ8δ9δ10* MUTANTS DID NOT SHOW PHENOTYPIC ALTERATIONS

Neither the single KO mutants nor the double and triple mutants showed phenotypic differences with wild-type plants under standard growth conditions. No phenotypic differences were observed either in the *p24δ3δ4δ5δ6* mutant or in the *p24δ7δ8δ9δ10* mutant when compared with

wild-type plants (Figure 32). Therefore, p24 proteins of the δ-1 subclass or the p24δ7-10 of the δ-2 subclass do not seem to be necessary for growth under standard conditions in *Arabidopsis*. This is consistent with results obtained in yeast. The yeast p24Δ8 strain, that lacks all the eight members of the yeast p24 family, grows identically to wild-type, although it shows delayed transport of GPI-anchored proteins (Springer et al., 2000).

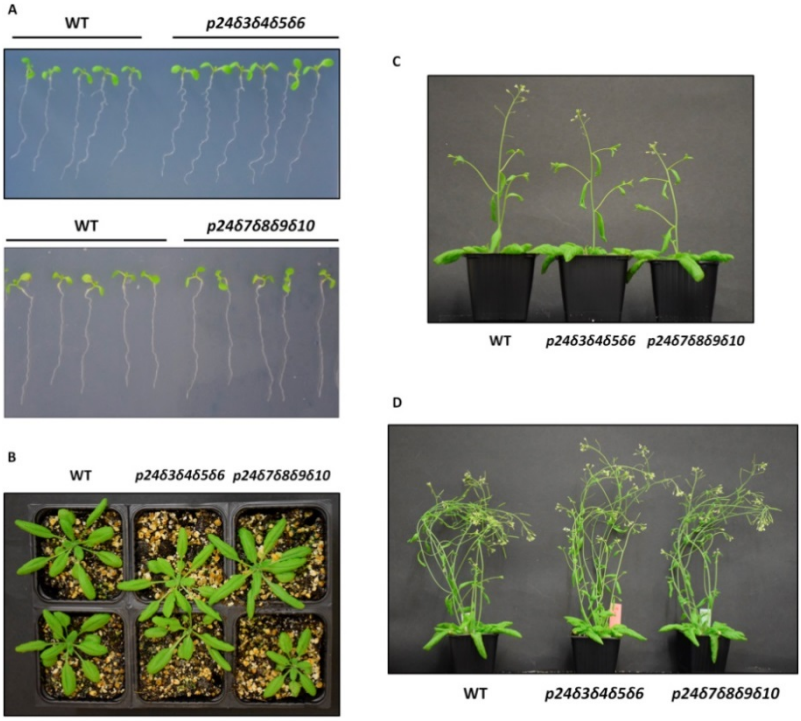

Figure 32. *p24δ3δ4δ5δ6* and *p24δ7δ8δ9δ10* mutants did not show a different phenotype compared to wild-type. A) Wild-type (Col-0), *p24δ3δ4δ5δ6* and *p24δ7δ8δ9δ10* mutant seedlings grown on MS agar plates for 7 days. B-D) 3-week-old (B), 4-week-old (C) and 6-week-old (D) plants of wild-type and *p24δ3δ4δ5δ6* and *p24δ7δ8δ9δ10* mutants.

1.5. p24 PROTEIN LEVELS ARE INTERDEPENDENT

In a large number of previous studies where a single member of the p24 family had been deleted or knocked down, a reduction in the protein levels of other p24 proteins was observed. It was shown that depletion of one p24 family member affects the stability of other members of the p24 family which probably reflects the fact that these p24 proteins interact with each other in hetero-oligomeric complexes (Belden and Barlowe, 1996; Marzioch et al., 1999; Denzel et al., 2000; Vetrivel et al., 2007; Takida et al., 2008; Koegler et al., 2010; Jerome-Majewska et al., 2010; Zhang and Volchuk, 2010; Fujita et al., 2011; Theiler et al., 2014).

In *Arabidopsis*, previous studies done in our group showed that silencing of p24β2 or p24β3 caused reduced levels of p24δ5 and p24δ9. In addition, *p24δ5* or *p24δ4* (p24δ-1 subclass) mutants had similar levels of p24δ4 or p24δ5, respectively, but both had reduced levels of p24δ9 (p24δ-2 subclass), p24β2, and p24β3 (Montesinos et al., 2012; 2013). On the other hand, the *p24δ10* (p24δ-2 subclass) mutant showed increased protein levels of the closely related p24δ9 (p24δ-2 subclass) and no decrease in the levels of p24δ5 (p24δ-1 subclass) or p24β proteins, suggesting that p24δ9 may compensate the absence of p24δ10 and maintain the stability of the remaining p24 family members (Montesinos et al., 2013). These studies have been now extended by using a *p24δ9* mutant, a *p24δ9δ10* double mutant and two quadruple mutants affecting the members of the p24δ-1 and p24δ-2 subclass.

Proteins extracts from roots of wild-type (Col-0) and the *p24δ9* and *p24δ9δ10* mutants were obtained as described in section 5.1. of Materials and methods and the protein levels of p24δ5, p24β2 and p24β3 were analyzed by Western blotting with the corresponding antibodies. Both *p24δ9* and *p24δ9δ10* mutants lacked p24δ9 protein, as shown by Western blotting with antibodies against the N-terminus of p24δ9 (Figure 33). The *p24δ9* mutant showed similar protein levels of p24δ5, p24β2 and p24β3, which agrees with the results obtained with the *p24δ10* mutant. In contrast, in the absence of both proteins (p24δ9 and p24δ10) in the *p24δ9δ10* double mutant, the protein levels of other p24 proteins (p24δ5, p24β2 and p24β3) were severely reduced (Figure 33). These results suggest that p24δ9 or p24δ10 may compensate for the lack of p24δ10 or p24δ9, respectively, and at least one of them, either p24δ9 or p24δ10, has to be present to maintain the expression levels of the other p24 proteins in *Arabidopsis*. In summary, the protein levels of p24δ9 (p24δ-2 subclass) and p24β2 and p24β3 of p24β subfamily are dependent on p24δ4 or p24δ5 (p24δ-1 subclass). In addition, the protein levels of p24δ5, p24β2 and p24β3 are dependent on the protein levels of p24δ9 and p24δ10 when both proteins are depleted.

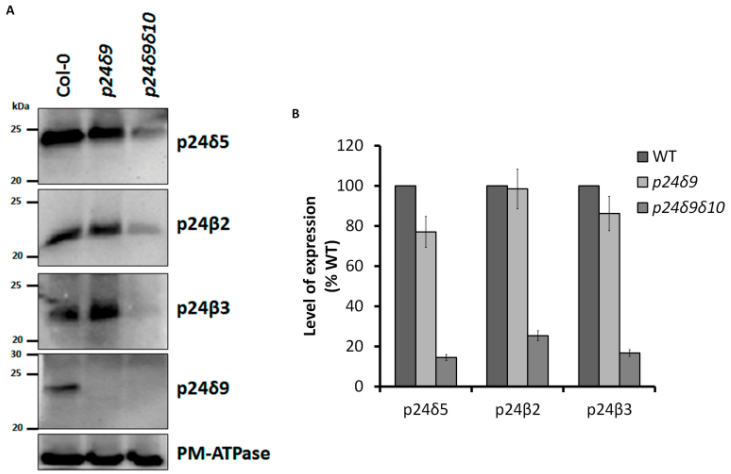

Figure 33. Levels of p24 proteins in *p24δ9* and *p24δ9δ10* mutants. A) Western blot analysis with antibodies against the N-terminus of p24δ5, p24δ9, or p24β3, or the C-terminus of p24β2 in membranes from the wild-type (Col-0) or the indicated KO mutants. Molecular weight markers are indicated on the left. A 25 µg aliquot of protein was loaded in each lane. Western blotting with an antibody against the plasma membrane (PM)-ATPase was used as a loading control. B) Quantification of the levels of each of the proteins in each mutant calculated as a percentage of the levels present in wild-type (Col-0) membranes. Error bars represent SE of the mean.

Next, to investigate how the deletion of four p24δ-1 subclass members or four p24δ-2 subclass members affects the levels of other p24 proteins, protein extracts from roots of wild-type and the *p24δ3δ4δ5δ6* and *p24δ7δ8δ9δ10* mutants were obtained and analyzed by Western blotting with the available antibodies for p24 proteins in *Arabidopsis* (p24δ5, p24δ9, p24β2 and p24β3) (Table 6 of Materials and methods). As expected, the *p24δ3δ4δ5δ6* mutant lacked p24δ5, but also had drastically reduced levels of p24δ9, p24β2 and p24β3 compared with the wild-type (Figure 34). Indeed, these proteins were almost undetectable in this mutant. As

expected, the *p24δ7δ8δ9δ10* mutant lacked p24δ9, but had also reduced levels of p24δ5 and p24β2, and greatly reduced levels of p24β3. Indeed, p24β3 was almost undetectable in this mutant, as in the *p24δ3δ4δ5δ6* mutant. In contrast to the *p24δ3δ4δ5δ6* mutant, however, p24δ5 and p24β2 showed detectable levels (~25% of wild-type) (Figure 34, B).

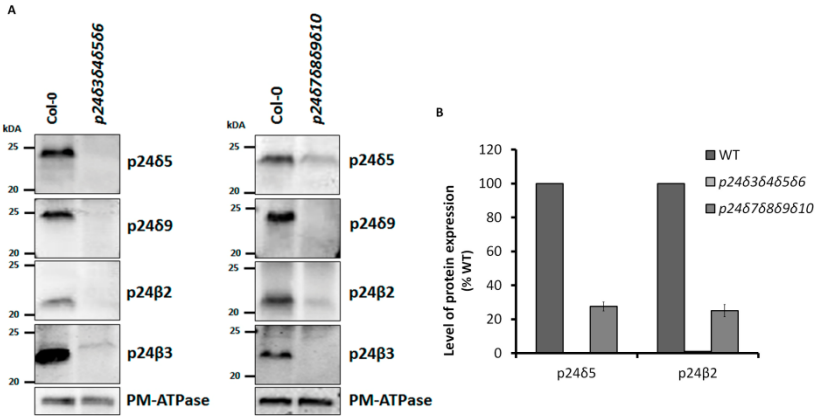

Figure 34. Protein Expression of p24 family in *p24δ3δ4δ5δ6* and *p24δ7δ8δ9δ10* mutants. A) Western blot analysis with antibodies against the N-terminus of p24δ5, p24δ9, or p24β3, or the C-terminus of p24β2 in membranes from the wild-type (Col-0) or the quadruple mutants. Molecular weight markers are indicated on the left. A 25 µg aliquot of protein was loaded in each lane. Western blotting with an antibody against the plasma membrane (PM)-ATPase was used as a loading control. B) Quantification of the levels of p24δ5 and p24β2 in each mutant calculated as a percentage of the levels present in wild-type (Col-0) membranes (mean±SD from three independent experiments).

To check if the decrease in p24 proteins levels found in both mutants correlated with a decrease in mRNA levels, the levels of the different p24 mRNA were analysed by RT-quantitative PCR (RT-qPCR). As shown in Figure 35, no reduction of the *p24* mRNA levels was observed in both quadruple mutants in any of the *p24* genes. These results are consistent with studies in

the animal field which showed that in single p24 mutants, the protein levels of several p24 family members were diminished, without a concomitant change in their mRNA levels (Denzel et al., 2000; Jerome-Majewska et al., 2010). Only one previous report in *Drosophila* showed that knockdown of a single p24 protein caused both reduction and up-regulation of several p24 transcripts (Buechling et al., 2011). Interestingly, an increase in the *p24δ6* mRNA levels was detected in the *p24δ7δ8δ9δ10* mutant.

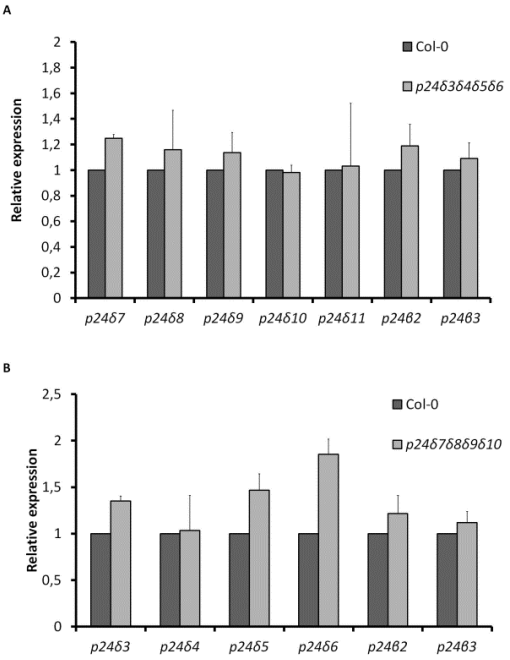

Figure 35. RT-qPCR analysis of *p24* genes expression in *p24δ3δ4δ5δ6* and *p24δ7δ8δ9δ10* mutants. Total RNAs were extracted from 4-day-old seedlings and inflorescences of 40-day-old plants. The mRNA was analysed by RT-qPCR with specific primers for the corresponding genes and normalized to *UBIQ10* gene expression (Appendix 2, Table A2). Results are from at least three biological samples. mRNA levels are expressed as relative expression levels and represent fold changes of mutant/wild-type. Values represent mean ± SD of at least three biological samples.

Altogether, these results strongly suggest that the protein levels of the two members of the p24β subfamily are dependent on the protein levels of p24δ proteins from the two subclasses and their stability depend on the presence of p24δ-1 or p24δ-2 proteins. In addition, protein levels of one p24δ-2 protein, p24δ9, were strongly dependent on p24δ-1 proteins. This interdependence between different members of the p24 family indicates that these proteins may function together in heteromeric complexes, as previously described (Montesinos et al., 2013). In particular, it has been proposed that hetero-oligomeric complexes between proteins from the p24β and p24δ subfamilies may cycle between the ER and the Golgi apparatus. Although the stoichiometry and composition of these complexes remains to be established, it has been proposed that "anterograde" (ER-to-Golgi) complexes should include p24β2, which has been shown to facilitate transport of p24δ5 (δ-1 subclass) and p24δ9 (δ-2 subclass) to the Golgi complex. p24β3 may bind to complexes containing p24β2/p24δ5 or p24β2/p24δ9 for its transport to the Golgi apparatus. In contrast, "retrograde" (Golgi-to-ER) complexes should contain p24δ proteins (for sorting into COPI vesicles), probably including members from both subclasses. Co-expression experiments also suggested that p24β3 may be recycled to the ER in complexes containing both p24δ5 and p24δ9 (Montesinos et al., 2012; 2013). This would be consistent with the observation that p24β3 is almost undetectable in both p24 quadruple mutants, which suggests that its stability requires p24δ proteins from both subclasses.

On the other hand, it is possible that the low amounts of p24δ5 (and perhaps of other p24δ-1 proteins) and p24β2 which are still present in the *p24δ7δ8δ9δ10* mutant can provide some p24 function. Indeed, p24δ5 and p24β2 have been shown to form stable complexes which can cycle between the ER and the Golgi apparatus (Montesinos et al., 2012; 2013). This could justify the milder alterations found in this mutant compared to the *p24δ3δ4δ5δ6* mutant (described in the following sections). It cannot be ruled out that p24δ11, the p24δ-2 protein that still remains in the *p24δ7δ8δ9δ10* mutant, may also contribute to this difference, although it has a floral tissue specific expression. To check for this possibility, silencing of *p24δ11* in the *p24δ7δ8δ9δ10* mutant is currently in progress.

1.6. STRUCTURE OF THE COMPARTMENTS OF THE EARLY SECRETORY PATHWAY IN *p24δ3δ4δ5δ6* AND *p24δ7δ8δ9δ10* MUTANTS

Several reports have suggested that p24 proteins may be involved in the structure and organization of the compartments of the early secretory pathway, including the formation of ER exit sites, the structure of the ER and the ERGIC and the biogenesis and maintenance of the Golgi apparatus (for a review, see Pastor-Cantizano et al., 2016). In particular, silencing of different p24 proteins was shown to induce structural changes in the Golgi apparatus. Indeed, the inactivation of one allele of p23 (p24δ1) in mice produced the dilation of the Golgi cisternae which was more prominent at the rim of the Golgi cisternae (Denzel et al., 2000). In contrast, silencing of p25 (p24α2), p28 (p24γ2) or p24A (p24β1) led to Golgi fragmentation (Mitrovic et al.,

2008; Koegler et al., 2010; Luo et al., 2007). In order to investigate possible alterations of the compartments of the early secretory pathway in both quadruple mutants, different strategies were performed.

1.6.1. Localization of organelle marker proteins in the *p24δ3δ4δ5δ6* and *p24δ7δ8δ9δ10* mutants

As a first approach, marker proteins of different organelles were transiently expressed in protoplasts obtained from *p24δ3δ4δ5δ6* and *p24δ7δ8δ9δ10* plants, as described previously (Yoo et al., 2007) (section 1.2.1.6. and 2.5. of Materials and methods), and the steady-state location of these markers was analyzed by confocal laser scanning microscopy (CLSM).

To analyze a possible alteration of the ER structure, protoplasts obtained from *p24δ3δ4δ5δ6* and *p24δ7δ8δ9δ10* plants were transiently transformed with constructs of two very similar ER markers, GFP-HDEL (Nebenführ et al., 2000) and RFP-KDEL (De Caroli et al., 2011). Both markers contain the K/HDEL signal which results in retention of soluble proteins within the ER in plant cells. Loss of p24 proteins of the δ-1 or δ-2 subclass did not seem to affect the ER structure since no obvious alteration was observed in the staining pattern of both ER markers (Figure 36).

Transient expression of GFP-BP80, a marker of the prevacuolar compartment (PVC), produced a typical punctate pattern, both in protoplasts from wild-type plants and in protoplasts from the *p24δ3δ4δ5δ6* and *p24δ7δ8δ9δ10* mutants (Figure 36), suggesting that the structure of this organelle was not modified in the mutants.

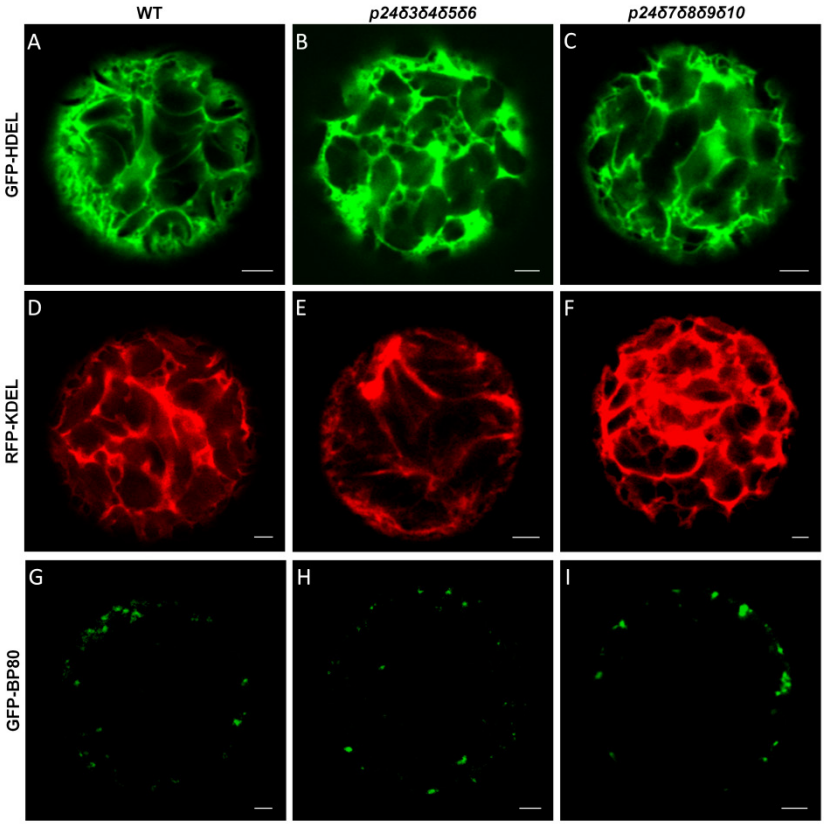

Figure 36. Localization of ER (RFP-KDEL and GFP-HDEL) and PVC (GFP-BP80) markers in *p24δ3δ4δ5δ6* and *p24δ7δ8δ9δ10* protoplasts. Transient gene expression in *Arabidopsis* protoplasts obtained from wild-type (Col-0), *p24δ3δ4δ5δ6* or *p24δ7δ8δ9δ10* plants grown 4 weeks in soil. A-F) Both GFP-HDEL and RFP-KDEL localized exclusively to the ER. G-I) BP80-GFP showed a punctate localization which is characteristic of the PVC. Therefore, neither *p24δ3δ4δ5δ6* nor *p24δ7δ8δ9δ10* protoplasts showed a different localization for GFP-HDEL, RFP-KDEL or BP80-GFP markers with respect to wild-type protoplast. WT, wild-type (col-0). Scale bars = 5 μm.

To investigate a possible alteration of the Golgi apparatus, protoplasts from *p24δ3δ4δ5δ6* and *p24δ7δ8δ9δ10* mutants were transiently transformed with constructs of two different Golgi markers: Mannosidase I

fused to GFP or RFP (ManI-GFP/RFP) (Nebenführ et al., 1999), which localize to the *cis* side of the Golgi apparatus, and sialyltransferase-YFP (ST-YFP) (Brandizzi et al., 2002b), which localizes to the *medial/trans* cisternae. Transient expression of ManI-GFP/RFP and ST-YFP showed the typical punctate pattern characteristic of normal Golgi stacks in protoplasts obtained from wild-type plants (Figure 37). However, in protoplasts obtained from the *p24δ3δ4δ5δ6* mutant, ManI-GFP/RFP and ST-YFP often localized to clusters of punctate structures, which suggest an alteration in the organization of the Golgi apparatus in this mutant. These clusters were also observed in protoplasts from the *p24δ7δ8δ9δ10* mutant, although with a lower frequency (Figure 37).

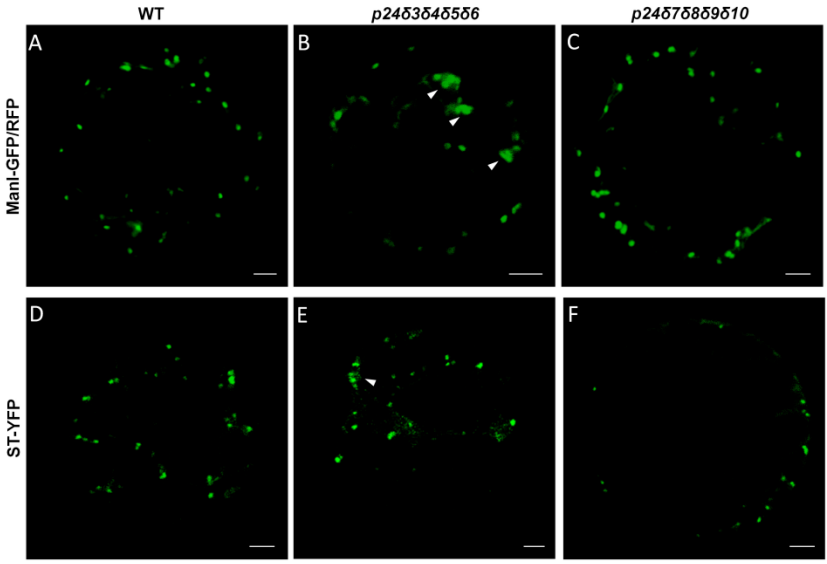

Figure 37. Localization of Golgi markers, ManI-GFP and ST-YFP. Transient gene expression in *Arabidopsis* protoplasts obtained from wild-type (Col-0), *p24δ3δ4δ5δ6* or *p24δ7δ8δ9δ10* plants grown 4 weeks in soil. ManI-GFP or ManI-RFP (data not shown) (A-C) and ST-YFP (D-F) showed its typical punctate pattern corresponding to the Golgi apparatus in both mutants. However, several transformed protoplasts from *p24δ3δ4δ5δ6* or *p24δ7δ8δ9δ10* mutants showed small clusters of punctate structures (arrowheads). Scale bars = 5 µm.

To confirm these results, transgenic plants expressing ER and Golgi markers were also generated. To this end, *p24δ3δ4δ5δ6* and *p24δ7δ8δ9δ10* plants were transformed with constructs of two different markers: a soluble ER marker, mCherry-HDEL (Denecke et al., 1992), and a membrane Golgi marker, ST-YFP (Brandizzi et al., 2002), as described in section 2.3. of Materials and methods. As it is shown in Figure 38, mCherry-HDEL showed its typical ER pattern in both mutants, very similar to that observed in wild-type plants. ST-YFP showed the typical punctate pattern characteristic of normal Golgi stacks in wild-type and *p24δ7δ8δ9δ10* plants. In contrast, in the *p24δ3δ4δ5δ6* mutant, ST-YFP partially localized to clusters of punctate structures and to the ER network (Figure 38, panels E and G-I). This result is consistent with the results obtained from this marker in transient expression experiments, and is consistent with an alteration of the Golgi apparatus.

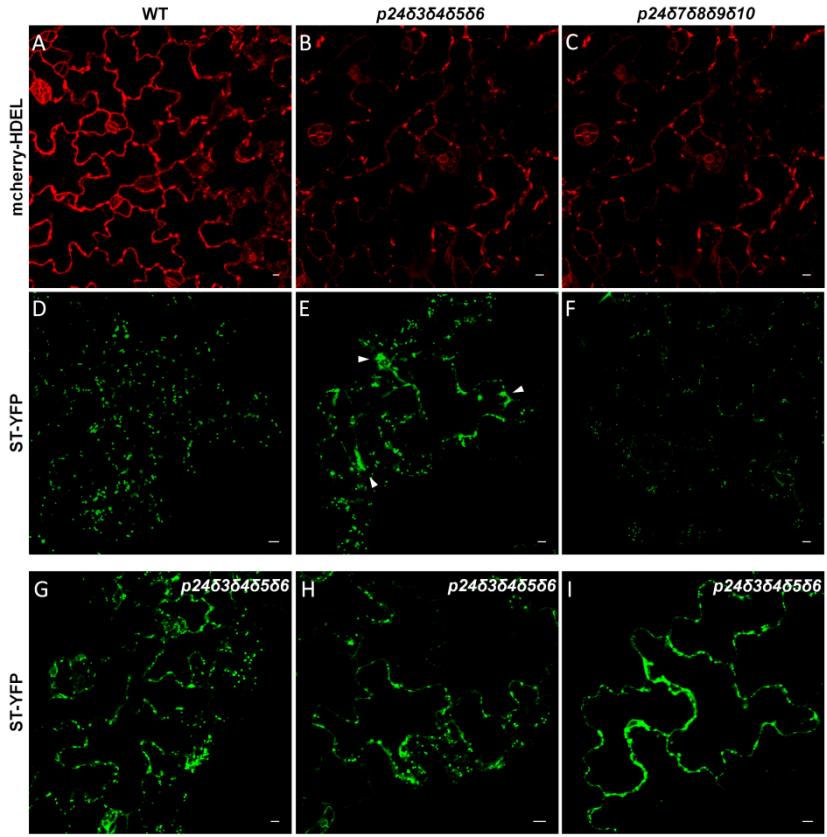

Figure 38. Localization of the ER marker mCherry-HDEL and the Golgi marker ST-YFP in *p24δ3δ4δ5δ6* and *p24δ7δ8δ9δ10* transgenic plants. CLSM of epidermal cells of 4-DAG cotyledons. For *p24δ3δ4δ5δ6* transgenic lines, two independent homozygous lines were obtained for each marker by segregation analysis (section 2.4. Materials and methods). For *p24δ7δ8δ9δ10* transgenic lines, T1 seedling was selected by observing the roots of 4-days-old seedlings at a fluorescence microscope (section 2.3 of Materials and methods), and choosing those plants which showed red or green fluorescence. A-C) mCherry-HDEL mainly localized to the ER network wild-type, *p24δ3δ4δ5δ6* and *p24δ7δ8δ9δ10* plants. D-I) ST-YFP showed the typical Golgi pattern in wild-type and *p24δ7δ8δ9δ10* plants. However, ST-YFP partially localized to clusters of punctate structures (arrowheads) and to the ER network (E, G-I). Scale bars = 5 μm

1.6.2. Ultrastructural analysis of *p24δ3δ4δ5δ6* and *p24δ7δ8δ9δ10* mutants

To gain further insight into the traffic defects observed in the *p24δ3δ4δ5δ6* and *p24δ7δ8δ9δ10* mutants at the ultrastructural level, transmission electron microscopy (TEM) analysis was performed using seedlings processed by chemical fixation or high-pressure freezing/freeze substitution. As shown in Figure 39, *p24δ3δ4δ5δ6* and *p24δ7δ8δ9δ10* mutants showed a clear alteration in the Golgi apparatus, which was more prominent in the *p24δ3δ4δ5δ6* mutant than in the *p24δ7δ8δ9δ10* mutant. In the *p24δ3δ4δ5δ6* mutant, the Golgi apparatus showed dilated areas throughout the whole cisternae which were usually more prominent at the rim of the Golgi cisternae (Figure 39, C-D). In some cases, discontinuous cisternae were also observed (Figure 39, C). When high-pressure fixation was performed in the *p24δ3δ4δ5δ6* mutant (Figure 40), the number of vacuoles surrounding the Golgi apparatus appeared to be increased and the ER network was more marked (Figure 40, C-D) than in wild-type plants (Figure 40, A-B). These results are consistent with previous results which were obtained from the silencing of different p24 proteins (Denzel et al., 2000; Mitrovic et al., 2008; Koegler et al., 2010; Luo et al., 2007) and are also consistent with the results observed in protoplasts and transgenic plants. Therefore, the morphological changes in the Golgi apparatus observed in both mutants suggest that p24 proteins are involved in the maintenance of the structure and organization of the compartments of the early secretory pathway in *Arabidopsis*.

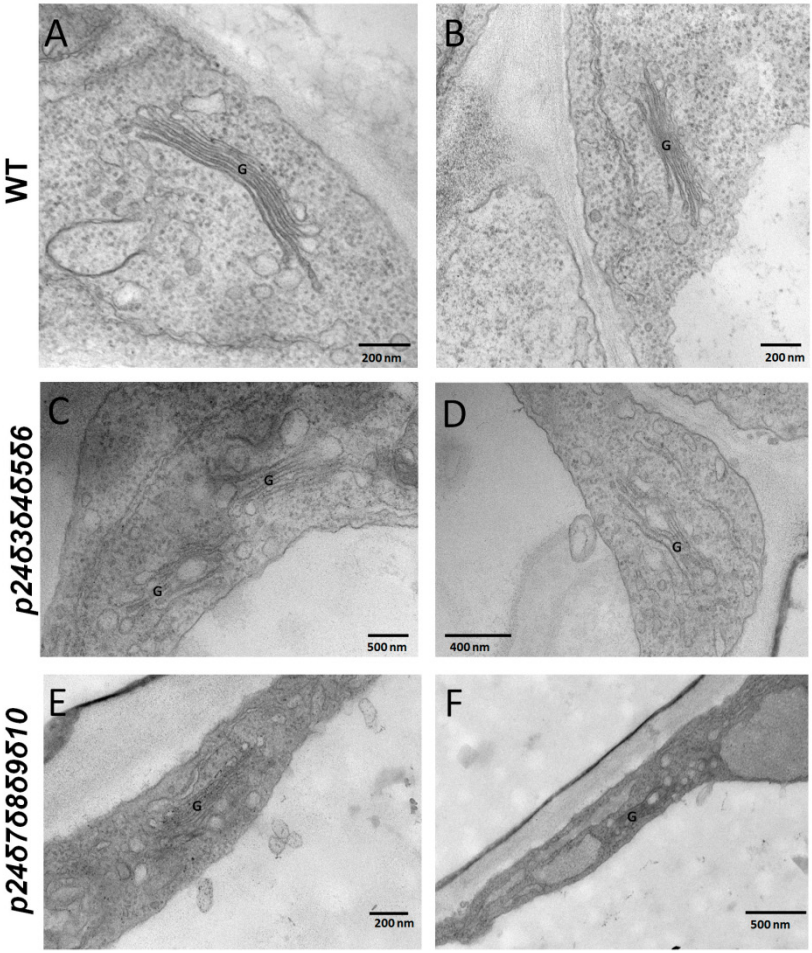

Figure 39. Alteration of Golgi morphology in the *p24δ3δ4δ5δ6* and *p24δ7δ8δ9δ10* mutant. Chemically fixed cotyledon cells from 4 day-old seedlings of wild-type (A-B), *p24δ3δ4δ5δ6* mutant (C-D), and *p24δ7δ8δ9δ10* mutant (E-F). G, Golgi apparatus.

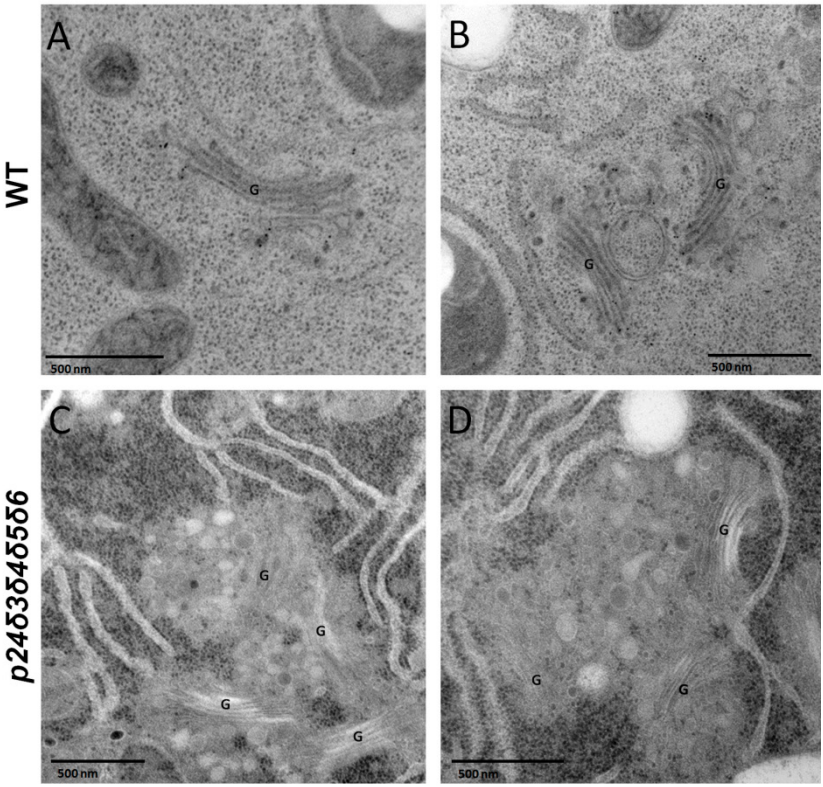

Figure 40. Alteration of Golgi morphology in cell roots from the *p24δ3δ4δ5δ6* mutant. High-pressure fixed root cells from 4 day-old seedlings of wild-type (A-B) and *p24δ3δ4δ5δ6* mutant (C-D). G, Golgi apparatus.

1.7. ERD2a-YFP ACCUMULATES IN GOLGI-DERIVED GLOBULAR STRUCTURES IN *p24δ3δ4δ5δ6* AND *p24δ7δ8δ9δ10* MUTANTS

p24 proteins have long been proposed to function as cargo receptors facilitating the transport of specific cargoes between the ER and the Golgi apparatus (for a review, see Pastor-Cantizano et al., 2016). In particular,

proteins of the p24 delta subfamily have been shown to be involved in the retrograde transport of K/HDEL ligands bound to the K/HDEL receptor ERD2 via a direct interaction between p24δ proteins and ERD2 (Majoul et al., 2001; Montesinos et al., 2014). Experiments in animal cells showed that the interaction between p23 (p24δ1) and ERD2 takes place at the Golgi apparatus. Once the KDEL ligand reaches the ER, p23 and ERD2 no longer interact (Majoul et al., 2001). In *Arabidopsis*, p24δ5 and p24δ9 proteins were shown to interact with two different K/HDEL receptors, ERD2a and ERD2b. This interaction required the GOLD domain in p24δ5 and was pH-dependent, being maximal at acidic pH but very low at neutral pH, consistent with the interaction taking place at the Golgi apparatus (Montesinos et al., 2014). Therefore, since p24δ proteins have been shown to play a role in Golgi-to-ER transport of ERD2, it was investigated whether loss of p24 delta proteins affect the steady-state distribution of ERD2 in *Arabidopsis*.

To this end, ERD2a-YFP (Brandizzi et al., 2002a) was transiently expressed in protoplasts obtained from *p24δ3δ4δ5δ6* and *p24δ7δ8δ9δ10* plants. As shown in Figure 41, ERD2a-YFP showed its typical punctate pattern characteristic of the Golgi apparatus in protoplasts obtained from wild-type plants. In contrast, in protoplasts obtained from the *p24δ3δ4δ5δ6* mutant, ERD2a-YFP localized to big globular structures. A similar pattern was also found in the *p24δ7δ8δ9δ10* mutant, although with a much lower frequency (~20% of protoplasts) (Table 10). This severe mislocalization was not a general effect on Golgi proteins, since the pattern of other Golgi

markers, ManI-GFP and ST-YFP, did not show such a drastic alteration as ERD2a-YFP in the same mutants (Figure 37, section 1.6.1 of Results and discussion). Fluorescently-tagged ERD2 proteins in plants have been shown to localize either to the Golgi apparatus, with a lesser level of labelling in the ER (Boevink et al., 1998; Brandizzi et al., 2002a; Li et al., 2009) or be equally distributed to the ER and Golgi (Xu et al., 2012). To rule out that this mislocalization was a consequence of ERD2a-YFP overexpression, the amount of DNA was reduced to the minimum that produced a significant percentage of transformed protoplasts, and the same result was obtained. In addition, in protoplasts with very high levels of ERD2a-YFP, ERD2a-YFP was localized to the ER and not in these globular structures (Appendix 9). This is consistent with previous results obtained from overexpression of human ERD2-like receptors in mammalian cells (Capitani and Sallese, 2009). These results suggest that loss of p24 proteins from the δ-subfamily specifically affects the steady-state localization of ERD2a-YFP.

Table 10. Quantification of the percentage of protoplasts showing ERD2a-YFP mislocalization in *p24δ3δ4δ5δ6* and *p24δ7δ8δ9δ10* mutants.

Mutant	Nº protoplasts	ERD2a-YFP typical pattern	ERD2a-YFP mislocali-zation	% of mislocalization
WT	25	25	0	0
p24δ3δ4δ5δ6	42	0	42	100
p24δ7δ8δ9δ10	74	59	15	20

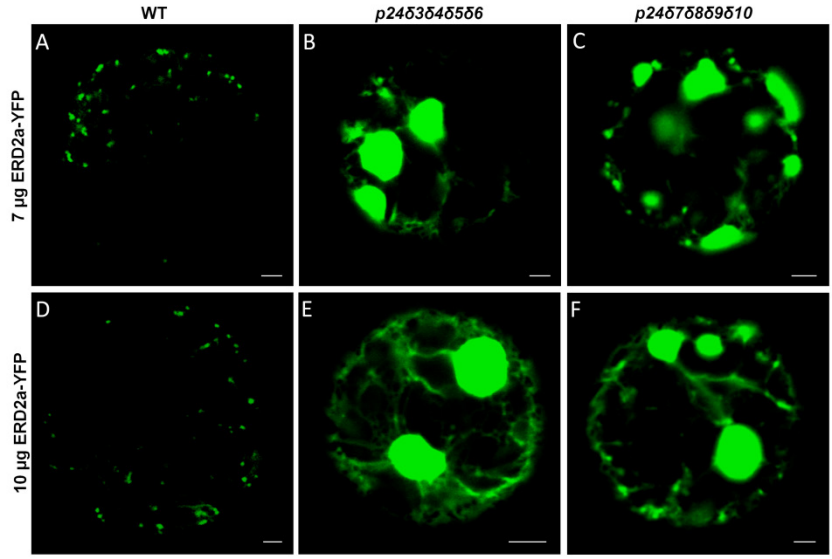

Figure 41. *p24δ3δ4δ5δ6* and *p24δ7δ8δ9δ10* mutants show abnormal distribution of ERD2a-YFP. Transient gene expression in *Arabidopsis* protoplasts obtained from wild-type (Col-0), *p24δ3δ4δ5δ6* or *p24δ7δ8δ9δ10* plants grown 4 weeks in soil. ERD2a-YFP was mislocalized in *p24δ3δ4δ5δ6* or *p24δ7δ8δ9δ10* protoplasts using 7 or 10 µg of DNA. WT, wild-type (col-0). Scale bars = 5 µm.

To try to identify the structures where ERD2a-YFP accumulates in *p24δ3δ4δ5δ6* and *p24δ7δ8δ9δ10* mutants, ERD2a-YFP was transiently co-expressed with the Golgi marker ManI-RFP. As shown in Figure 42, ERD2a-YFP partially co-localized with ManI-RFP in punctate structures in protoplasts obtained from wild-type plants. In protoplasts from *p24δ3δ4δ5δ6* and *p24δ7δ8δ9δ10* mutants, ManI-GFP localized to clusters of punctate structures similar to those shown previously (Figure 37, section 1.6.1 of Results and discussion), while ERD2a-YFP accumulated in big

globular structures which partially co-localized with ManI-RFP, suggesting that ERD2a-YFP might accumulate in Golgi derived structures.

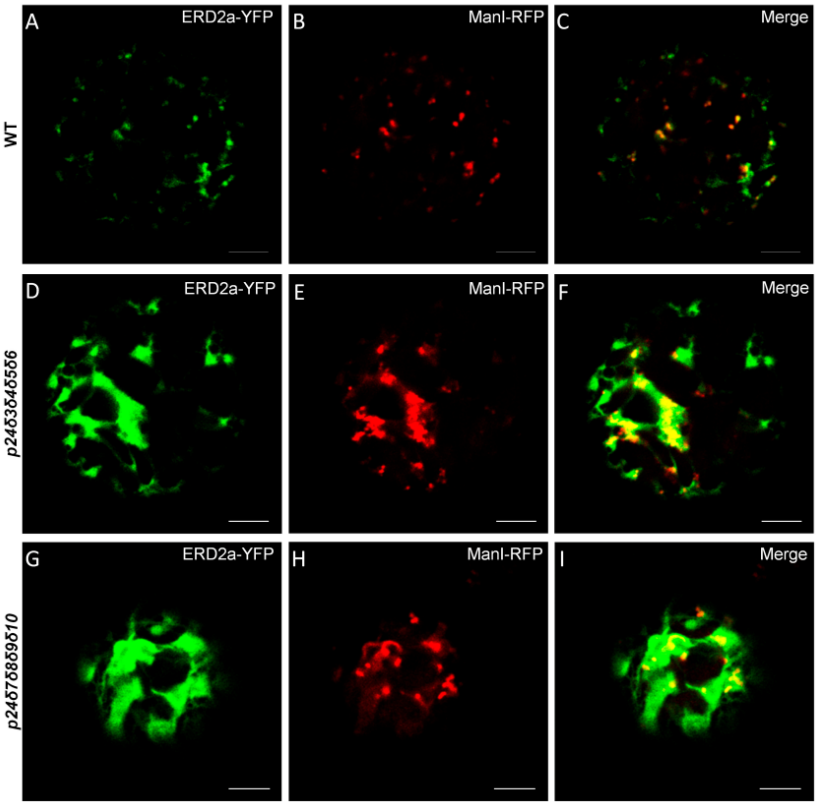

Figure 42. ERD2a-YFP partially colocalized with ManI-RFP in *p24δ3δ4δ5δ6* and *p24δ7δ8δ9δ10* protoplasts. Transient gene expression in *Arabidopsis* protoplasts obtained from wild-type (Col-0), *p24δ3δ4δ5δ6* or *p24δ7δ8δ9δ10* plants grown 4 weeks in soil. A-C) In wild-type protoplasts both ERD2a-YFP and ManI-RFP showed a punctate pattern characteristic of the Golgi apparatus and partially co-localized. D-I) ERD2a-YFP partially co-localized with ManI-RFP in *p24δ3δ4δ5δ6* (D-F) or *p24δ7δ8δ9δ10* (G-I) protoplasts and it took place mainly in the clusters of punctate structures of ManI-RFP.

To confirm that the mislocalization of ERD2a-YFP was caused by the loss of p24 proteins from the δ subfamily, ERD2a-YFP was transiently co-expressed with RFP-p24δ5 or RFP-p24δ9 in protoplasts from the *p24δ3δ4δ5δ6* or *p24δ7δ8δ9δ10* mutants, respectively. As shown in Figure 43, ERD2a-YFP localized both to punctate Golgi structures but also to the ER network in protoplasts obtained from wild-type plants. This is consistent with previous results obtained in tobacco protoplasts or in tobacco leaf epidermal cells. In those experiments, expression of RFP-p24δ5 or RFP-p24δ9 induced a partial re-localization of ERD2a-YFP from the Golgi to the ER network (Montesinos et al., 2014). In the *p24δ3δ4δ5δ6* mutant, transient expression of RFP-p24δ5 changed the localization of ERD2a-YFP, which was no longer mislocalized to the big globular structures that were observed in the absence of RFP-p24δ5 (Figure 43). In this mutant, ERD2a-YFP localized both to standard punctate structures characteristic of the Golgi apparatus and partially to the ER network, as in protoplasts obtained from wild-type plants. These results suggest that the function of p24δ5 is enough to restore the normal trafficking of ERD2a. Similar results were obtained when RFP-p24δ9 was transiently expressed in the *p24δ7δ8δ9δ10* mutant.

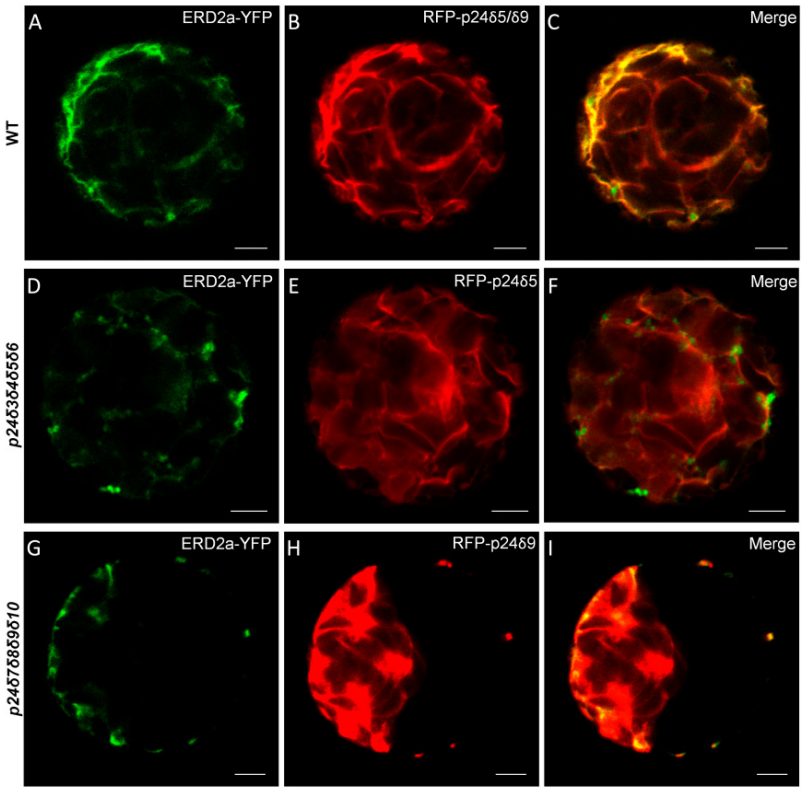

Figure 43. RFP-p24δ5 or RFP-p24δ9 expression inhibits ERD2a-YFP mislocalization observed in *p24δ3δ4δ5δ6* and *p24δ7δ8δ9δ10* protoplasts. Transient gene expression in *Arabidopsis* protoplasts obtained from wild-type (Col-0), *p24δ3δ4δ5δ6* or *p24δ7δ8δ9δ10* plants grown 4 weeks in soil. A-C) RFP-p24δ5 or RFP-p24δ9 caused a partial relocalization of ERD2a-YFP to the ER in wild-type protoplasts. RFP-p24δ5 (D-F) or RFP-p24δ9 (G-I) co-expressed with ERD2a-YFP in *p24δ3δ4δ5δ6* or *p24δ7δ8δ9δ10* protoplasts, respectively, induced the localization of ERD2a-YFP mainly to the Golgi apparatus. Scale bars = 5 µm.

Previous studies in animals indicated that overexpression of HDEL ligands induced a redistribution of the human KDEL receptor from the Golgi complex to the ER (Lewis and Pelham, 1992). It has been proposed that

ligand binding induce oligomerization of ERD2 and thus favors its inclusion in COPI-coated vesicles for their Golgi-to-ER transport (Majoul et al., 2001). In *Arabidopsis*, it has been previously shown that overexpression of an HDEL-ligand, cherry-HDEL, also produces a partial redistribution of both ERD2a and ERD2b to the ER in tobacco leaf epidermal cells (Montesinos et al., 2014). Therefore, it was investigated whether a KDEL-ligand also induces the redistribution of ERD2a in *p24δ3δ4δ5δ6* and *p24δ7δ8δ9δ10* mutants.

To this end, ERD2a-YFP was co-expressed with RFP-KDEL in protoplasts obtained from *p24δ3δ4δ5δ6* and *p24δ7δ8δ9δ10* plants. As shown in Figure 44, ERD2a-YFP was partially redistributed to ER upon transient expression of RFP-KDEL in both mutants, which is consistent with the effect of RFP-KDEL expression in protoplasts from wild-type plants. In addition, ERD2a-YFP was also observed in punctate Golgi structures. Therefore, ERD2a-YFP localization in protoplasts from *p24δ3δ4δ5δ6* and *p24δ7δ8δ9δ10* mutants was the same as in protoplasts from wild-type upon RFP-KDEL or RFP-p24δ5/δ9 expression. Altogether, these results indicate that loss of p24 proteins of the delta subfamily induces the ERD2a-YFP accumulation at the Golgi apparatus probably due to a inhibition of its retrograde Golgi-to-ER transport mediated by COPI-vesicles. Co-expression of a K/HDEL ligand may facilitate ERD2a-YFP oligomerization and its inclusion in COPI vesicles for its retrograde Golgi-to-ER transport even in the absence of p24 proteins.

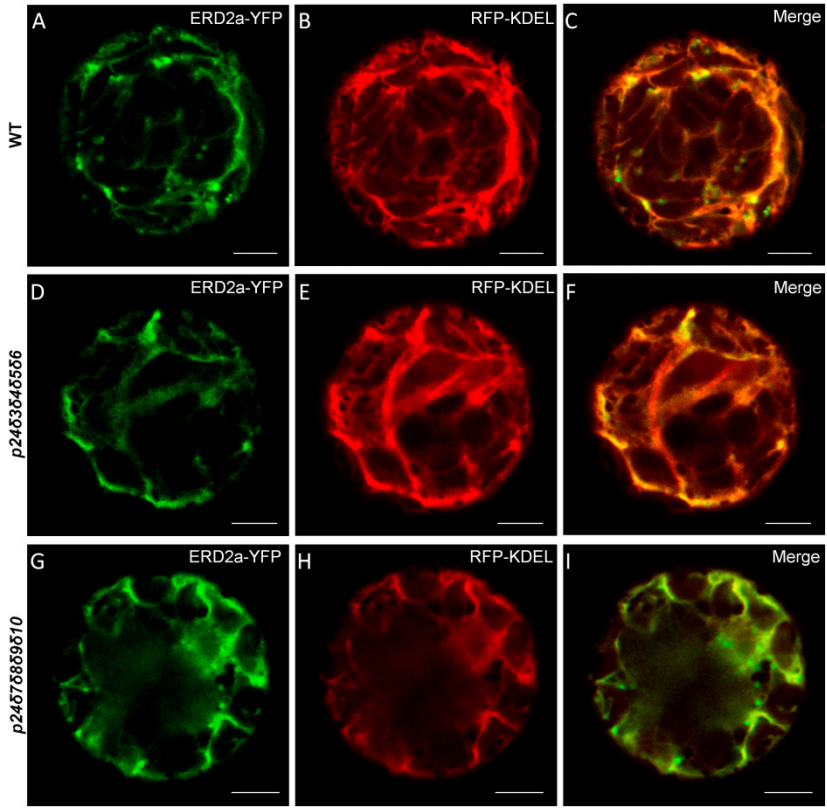

Figure 44. RFP-KDEL partially relocalized ERD2a-YFP to the ER in *p24δ3δ4δ5δ6* and *p24δ7δ8δ9δ10* protoplasts. Transient gene expression in *Arabidopsis* protoplasts obtained from wild-type (Col-0), *p24δ3δ4δ5δ6* or *p24δ7δ8δ9δ10* plants grown 4 weeks in soil. Co-expression of ERD2a-YFP with RFP-KDEL caused a partial relocalization of ERD2-YFP to the ER, although ERD2a-YFP also showed a punctate Golgi localization in wild-type (A-C), *p24δ3δ4δ5δ6* (D-F) or *p24δ7δ8δ9δ10* (G-I) protoplasts. Scale bars = 5 μm.

Finally, to investigate whether ERD2a was also mislocalized in planta, *p24δ3δ4δ5δ6* and *p24δ7δ8δ9δ10* plants were transformed with a construct of ERD2a-YFP (Brandizzi et al., 2002a), as described in section 2.3 of

Materials of methods. As shown in Figure 45, ERD2a-YFP showed the typical punctate pattern which is characteristic of normal Golgi stacks in wild-type plants. However, in *p24δ3δ4δ5δ6* and *p24δ7δ8δ9δ10* mutants ERD2a-YFP partially localized to clusters of punctate structures and the ER network. This alteration was more marked in *p24δ3δ4δ5δ6* plants than in *p24δ7δ8δ9δ10* seedlings. These results are consistent with those obtained from ST-YFP expression in plants (Figure 38, section 1.6.1 of Results and discussion). However, the alteration observed in the ERD2a-YFP overexpression in planta is not as severe as that observed in protoplasts (Figure 41). This difference might be due to the existence of mechanisms which may compensate the transport defects in both p24 mutant plants.

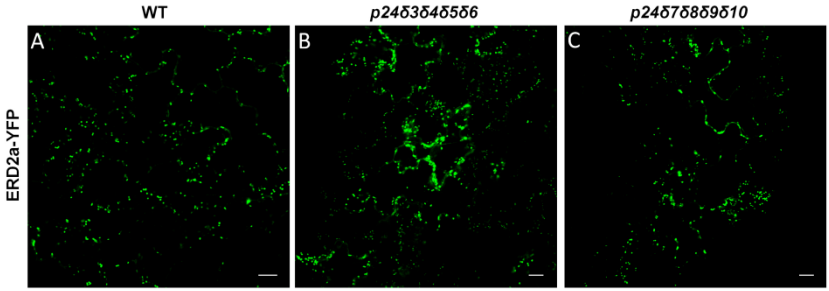

Figure 45. ERD2a-YFP was localized in clusters of punctate structures in *p24δ3δ4δ5δ6* and *p24δ7δ8δ9δ10* mutants. CLSM of epidermal cells of 4-DAG cotyledons. T1 seedlings were selected by observing the roots of 4-days-old seedlings at a fluorescence microscope and choosing those plants which showed red fluorescence. A) ERD2a-YFP showed the typical Golgi pattern in wild-type plants. B-C) However, ERD2a-YFP partially localized to clusters of punctate structures and to the ER network in *p24δ3δ4δ5δ6* (B) and *p24δ7δ8δ9δ10* (C) plants. Scale bars = 10 µm

1.8. BIP SECRETION IN *p24δ3δ4δ5δ6* AND *p24δ7δ8δ9δ10* MUTANTS

p24 proteins are key molecular players in the formation of COPI vesicles from Golgi membranes (for a review see Popoff et al., 2011; Jackson, 2014; Pastor-Cantizano et al., 2016). In *Arabidopsis*, p24δ5 and p24δ9 have been shown to interact with ARF1-GDP and coatomer and this interaction involves both the dilysine motif in the -3, -4 position and the diphenylalanine motif in the -7, -8 position, acting cooperatively. This suggests that all *Arabidopsis* p24 proteins of the p24δ subfamily contain a cytosolic tail with a high affinity for COPI and could be involved in the formation of COPI vesicles and thus in retrograde transport from the Golgi to the ER (Contreras et al., 2004a; Montesinos et al., 2012; 2014).

In yeast, most mutants that block retrograde Golgi-to-ER transport show an increased secretion level of ER resident proteins containing an HDEL signal into the media, because the ERD2 receptor fails to retrieve the ER resident proteins back from the Golgi apparatus (Semenza et al., 1990). This is the case of the chaperone BiP, which is efficiently retrieved from the Golgi through its interaction with the KDEL/HDEL-receptor ERD2 by COPI vesicles. Therefore, alterations in this transport may produce a partial secretion of BIP. To investigate whether retrograde Golgi-to-ER trafficking of ERD2 (and thus of K/HDEL ligands) was altered in both quadruple mutants, the levels of BiP in the apoplastic fluid of leaves from wild-type plants and the *p24δ3δ4δ5δ6* and *p24δ7δ8δ9δ10* mutants was analyzed.

Apoplastic fluid was obtained as described in section 5.7. of Materials and methods and was analyzed by Western blotting using an antibody against BiP. As shown in Figure 46, wild-type and mutants contained similar amounts of intracellular BiP, as determined by Western blot analysis of total leave extracts. Wild-type plants did not secrete detectable levels of BiP into the apoplastic fluid; in contrast, *p24δ3δ4δ5δ6* and *p24δ7δ8δ9δ10* mutants secreted significant amounts of BiP. Moreover, BiP secretion was higher in the *p24δ3δ4δ5δ6* mutant than in the *p24δ7δ8δ9δ10* mutant.

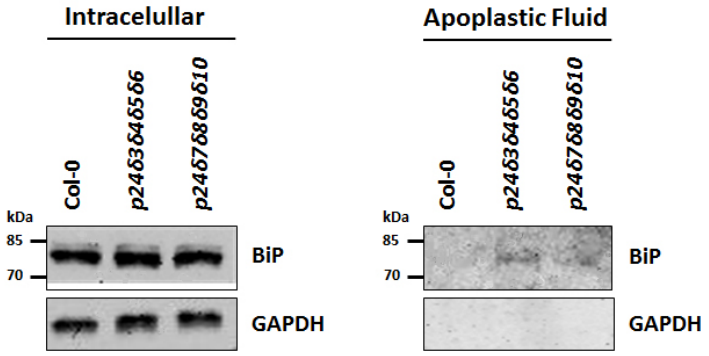

Figure 46. Secretion of BiP in the *p24δ3δ4δ5δ6* and *p24δ7δ8δ9δ10* mutants. Apoplastic fluid was obtained from rosette leaves of wild-type (Col-0) and *p24δ3δ4δ5δ6* and *p24δ7δ8δ9δ10* plants grown 30 days in soil as described in section 5.7. of Materials and methods. As a control, total proteins were obtained from the same leaves used to obtain the apoplastic fluid. Total proteins from leaves and apoplastic fluid were analyzed by SDS-PAGE and Western blotting with antibody against BiP. The western blot analysis of glyceraldehyde-phosphate dehydrogenase (GAPDH), a cytosolic protein, was used as a control.

In yeast, deletion mutants of some p24 proteins also showed an increased secretion of Kar2p/BiP (Elrod-Erickson and Kaiser, 1996; Marzioch et al., 1999; Belden and Barlowe, 2001a). It has been shown that in addition

to a defect in retrograde transport, the activation of the unfolded protein response (UPR) in yeast mutants may also contribute to Kar2p/BiP secretion (Belden and Barlowe, 2001a). As UPR is activated in *p24δ3δ4δ5* and *p24δ7δ8δ9δ10* mutants (see next section), it cannot be ruled out that this activation may contribute to the increase in the levels of secreted BiP, although both mutants contained similar amounts of intracellular BiP as wild-type (Figure 46). On the other hand, UPR only increased expression of BiP3 (see below), whose expression is ~150-fold lower than that of BiP1 and BiP2 (Zimmermann et al., 2004), and thus it would not be detectable by Western blot analysis. In any case, it has been demonstrated that retrograde traffic is indeed affected in a yeast mutant with a deletion in one p24 gene and IRE1 gene (the UPR effector in yeast) and besides UPR may compensate for the loss of p24 function in retrograde transport from Golgi to the ER (Aguilera-Romero et al., 2008).

Previous studies done in the lab showed that p24δ5 and p24δ9 interact with ERD2, which may contribute to sorting of ERD2 within COPI vesicles and retrieval of K/HDEL ligands (Montesinos et al., 2014). Moreover, ERD2a-YFP seems to accumulate in Golgi derived structures in *p24δ3δ4δ5δ6* and *p24δ7δ8δ9δ10* mutants (section 1.7 of Results and discussion). These results together with the increase of BiP secretion in *p24δ3δ4δ5δ6* and *p24δ7δ8δ9δ10* mutants suggest a possible decrease in the retrograde traffic of ERD2 and, in consequence, in the retrieval of BiP in the quadruple mutants.

1.9. UPR ACTIVATION IN *p24δ3δ4δ5δ6* AND *p24δ7δ8δ9δ10* MUTANTS

In yeast, deletion of p24 proteins activates the unfolded protein response (UPR), which may compensate the transport defects caused by the loss of p24 function (Belden and Barlowe, 2001a; Aguilera-Romero et al., 2008). This UPR activation may be related with the fact that, in yeast, a mutant strain lacking all eight p24 members does not show severe transport phenotypes or morphological alterations in the endomembrane system (Sprinter et al., 2000). Indeed, the concomitant loss of some of the *p24* genes with *IRE1*, an UPR activator, produces a slow growth and more severe transport defects than the deletion of the *p24* genes alone (Belden and Barlowe, 2001a).

To investigate whether the UPR pathway was activated in both quadruple mutants, variations in the mRNA levels of *BIP3* and *BIP1/2* (Hsp70 proteins)*, ERDJ3A* and *ERDJ3B* (J domain proteins), *PDI6* (Protein Disulfide Isomerase 6), and *CRT1* (Calreticulin 1), which are well-established UPR molecular markers, were analyzed by quantitative RT-PCR (RT-qPCR) (Chen and Brandizzi, 2013a). In Arabidopsis, BiP is encoded by three genes (*BiP1-*3). While *BiP1* and *BiP2* transcript levels are constitutively quite high, *BiP3* is usually expressed at lower levels but is induced to a much larger extent under stress conditions and has been shown to be one of the main transcriptional targets of active bZIP60 transcription factor (Iwata and Koizumi, 2005; Iwata et al., 2008; Noh et al., 2002). Similar to *BiP* expression,

AtERDJ3A expression is highly up-regulated after UPR activation; in contrast, expression of *AtERDJ3B* shows only a modest induction (Yamamoto et al., 2008). Finally, the expression of *PDI6* and *CRT1* are significantly up-regulated by UPR (Lu and Christopher, 2008; Kamauchi et al., 2005). Furthermore, as UPR activation induces the unconventional splicing of *AtbZIP60* mRNA by AtIRE1 in *Arabidopsis* (Iwata and Koizumi, 2005; Iwata et al., 2008; Deng et al., 2011; Nagashima et al., 2011), the levels of spliced *AtbZIP60* mRNA were also analyzed. Total RNA was obtained from wild-type (Col-0), *p24δ3δ4δ5δ6* and *p24δ7δ8δ9δ10* seedlings to analyse the mRNA levels of these UPR markers in the quadruple mutants and the RT-qPCR was performed as described in section 4.2.6. of Materials and methods.

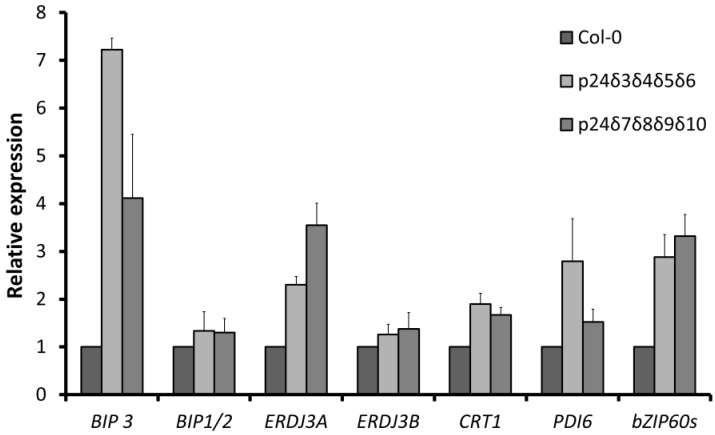

Figure 47. Expression of UPR genes and alternative spliced *bZIP60* (*bZIP60s*) mRNA analysis by RT-qPCR in *p24δ3δ4δ5δ6* and *p24δ7δ8δ9δ10* mutants. Total RNA was extracted 10-day-old seedlings. The mRNA was analysed by RT-qPCR with specific primers obtained from Chen and Brandizzi (2013a) and Lai et al. (2014) and normalized to *UBIQ10* gene expression (Appendix 2, Table A2). Results are from at least three biological samples. mRNA levels are expressed as relative expression levels and represent fold changes of mutant/wild-type. Values represent mean ± SD of at least three biological samples. Wild-type (Col-0).

As shown in Figure 47, an increase of *BiP3*, *ERDJ3A*, *CRT1*, and *PDI6* mRNA levels was observed in both *p24δ3δ4δ5δ6* and *p24δ7δ8δ9δ10* mutants. The *p24δ3δ4δ5δ6* mutant showed a higher increase of *BiP3* expression (7.2-fold) than *p24δ7δ8δ9δ10* mutant (4.1-fold). As expected, no high increase was observed in *BIP1/2* and *ERDJ3B* levels when compared to *BiP3* and *ERDJ3A* mRNA levels, respectively. These data indicate that both mutants exhibit up-regulation of UPR genes in the absence of an exogenous ER stress. Interestingly, both mutants also showed high mRNA levels of spliced *bZIP60* mRNA. These results strongly suggest that UPR pathway is constitutively activated in *p24δ3δ4δ5δ6* and *p24δ7δ8δ9δ10* mutants, and the IRE1-bZIP60s branch is involved.

Next, the activation of UPR in the presence of an ER-stress inducer was studied in the *p24δ3δ4δ5δ6* and *p24δ7δ8δ9δ10* mutants. The levels of *BIP3*, *ERDJ3A* and *ERDJ3B* mRNA in both mutants were analyzed in the presence of the ER-stress inducer tunicamycin (Tm) by RT-qPCR. Seedlings from wild-type (Col-0), *p24δ3δ4δ5δ6* and *p24δ7δ8δ9δ10* were incubated with 5 µg/ml Tm for 0h, 2h or 4h. After 2 h of incubation, wild-type and *p24δ3δ4δ5δ6* and *p24δ7δ8δ9δ10* seedlings showed similar levels of *BIP3*, *ERDJ3A* and *ERDJ3B* transcripts. Surprisingly, after 4h of incubation, the expression levels of UPR genes were significantly higher in both mutants compared to wild-type. This suggests that a greater UPR activation may be required for overcoming the additional endogenous ER-stress in the mutants (Figure 48).

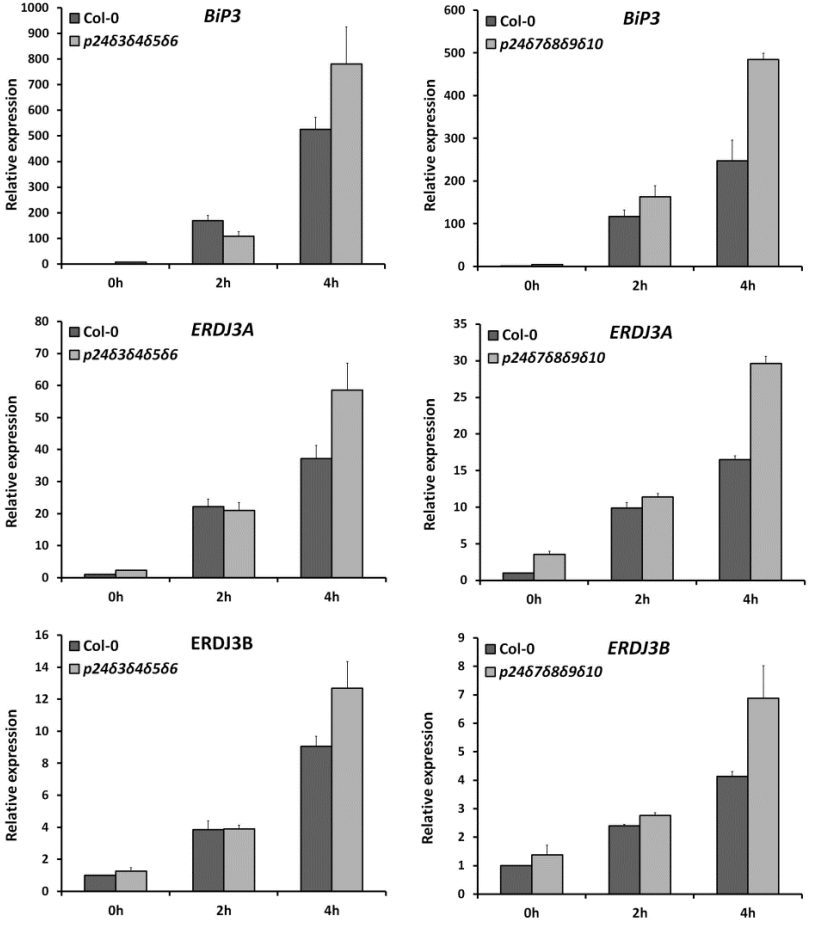

Figure 48. Expression analysis of UPR genes by RT-qPCR analysis in *p24δ3δ4δ5δ6* and *p24δ7δ8δ9δ10* mutants after ER stress induction. Total RNA was extracted from 10 day-old seedlings incubated for 0h, 2h or 4h with 5 µg/ml Tm. The mRNA was analysed by RT-qPCR with specific primers obtained from Chen and Brandizzi (2013a) and normalized to *UBIQ10* gene expression (Appendix 2, Table A2). Results are from three technical samples. Left panels correspond to *p24δ3δ4δ5δ6* relative expression and right panels correspond to *p24δ7δ8δ9δ10* relative expression. mRNA levels are expressed as relative expression levels and represent fold changes of mutant or wild-type/wild-type without treatment. Values represent mean ± SD of the three technical samples. Wild-type (Col-0).

To investigate whether this higher UPR activation implies a different sensitivity to ER-stress conditions, seeds from wild-type, *p24δ3δ4δ5δ6* and *p24δ7δ8δ9δ10* were directly germinated on MS medium containing 25 ng/ml, 50 ng/ml, 75 ng/ml or 100 ng/ml Tm, as described previously by Chen and Brandizzi (2013a). It was observed that *p24δ3δ4δ5δ6* and *p24δ7δ8δ9δ10* mutants grew similar to wild-type plants in all conditions (Figure 49 and Appendix 10). To check for slight growth defects, fresh weight of the mutants compared to wild type will be analysed in the future. Nevertheless, these results suggest that the greater UPR activation observed in both mutants does not confer either a resistant or an over-sensitive phenotype to *p24δ3δ4δ5δ6* and *p24δ7δ8δ9δ10* mutants.

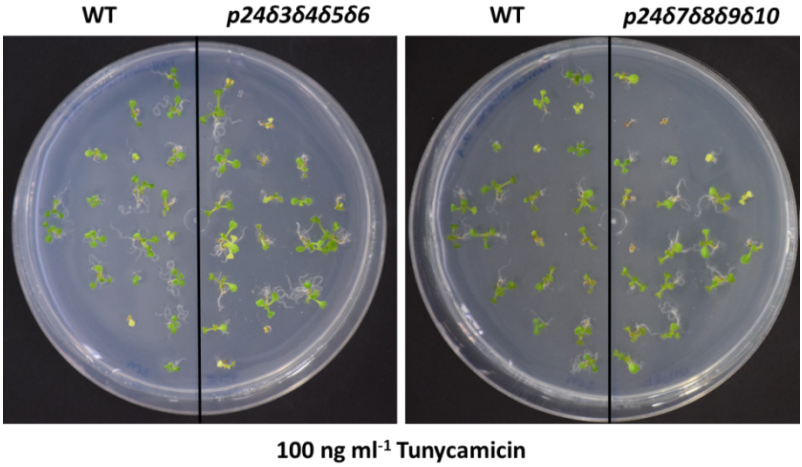

Figure 49. Germination of *p24δ3δ4δ5δ6* and *p24δ7δ8δ9δ10* seeds under ER stress conditions. Wild-type, *p24δ3δ4δ5δ6* and *p24δ7δ8δ9δ10* were germinated on MS medium containing 100 ng/ml Tm for 10 days. Wild-type (Col-0).

In yeast, UPR activation may help to alleviate the transport defect caused by the loss of p24 function (Aguilera-Romero et al., 2008). In *Drosophila*, loss of p24 function also activates an ER stress response, but it seems to be activated by NF-κB proteins instead of by splicing of *Xbp1* (homolog to *AtbZIP60*) (Boltz and Carney, 2008). In mammals, the knock-down of p24β1 in mouse or knock-down of p24δ1 in rat cells does not activate the splicing of *Xbp1* (Jerome-Majewska et al., 2010; Zhang and Volchuk, 2010). Our results suggest that, in *Arabidopsis*, the loss of p24δ proteins activates at least the IRE1-bZIP60s branch of the UPR pathway and it may act as compensatory mechanism that helps the plant to cope with the traffic defects. In the future, it would be interesting to study whether the ATF6 branch of the UPR pathway is also involved in the UPR activation in *p24δ3δ4δ5δ6* and *p24δ7δ8δ9δ10* mutants.

1.10. ANALYSIS OF COPI AND COPII SUBUNITS IN *p24δ3δ4δ5δ6* AND *p24δ7δ8δ9δ10* MUTANTS

1.10.1. Membrane association of COPI and COPII proteins

In yeast, the UPR causes the up-regulation of genes coding COPII components, like *SEC13*, *SEC16* and *SEC24*, and coatomer subunits, like *SEC26* (β-COP) and *SEC27* (β'-COP) (Travers et al., 2000), suggesting an increase of vesicular transport under ER stress conditions. To investigate the possibility that the COPII- and COPI- mediated transport was altered in both quadruple mutants, the levels of different COPI and COPII subunits were analyzed in cytosolic and membrane fractions from roots of wild-type and

p24 quadruple mutants by Western blotting using antibodies against Sec13, Sec23 and Sec21 (γ-COP). As shown in Figure 50, no differences were observed between the levels of these proteins in the cytosol. However, it was observed a significant increase in the amount of these proteins in membrane fractions from both mutants relative to wild-type, which was more prominent in the *p24δ3δ4δ5δ6* mutant than in *p24δ7δ8δ9δ10*. The significance of this increased membrane association of COPI and COPII proteins in both p24 quadruple mutants is not clear, although it might indicate an increase in vesicle formation, which would be consistent with the higher number of vesicles found in those mutants in TEM analysis (Figure 40, section 1.6.2. of Results and discussion). There is a previous report showing increased protein trafficking and increased membrane association of coat proteins following knockdown of the Golgi matrix proteins GRASP55/65. However, depletion of these proteins also had a negative impact on protein sorting (Xiang et al., 2013). It is thus possible that the increase in membrane association of COPI and COPII proteins in the absence of p24 proteins does not correlate with a correct sorting of cargo proteins into COPI or COPII vesicles.

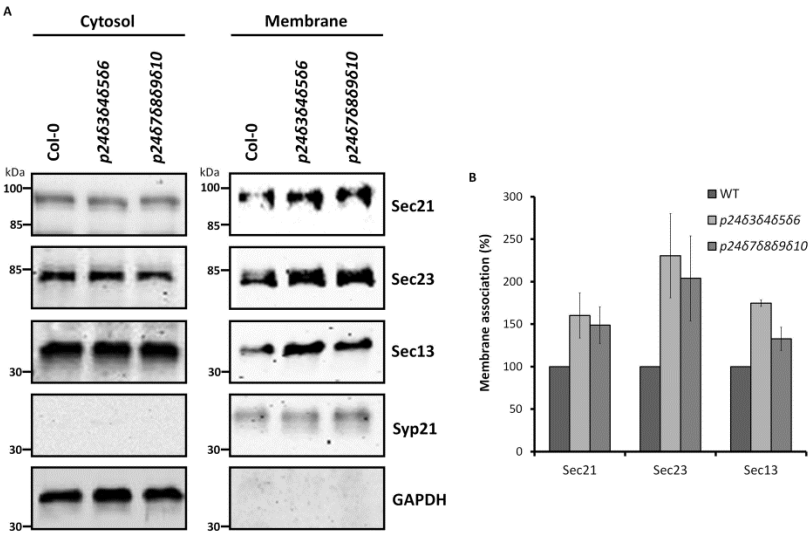

Figure 50. Membrane association of COPI and COPII subunits in *p24δ3δ4δ5δ6* and *p24δ7δ8δ9δ10*. A) Proteins from cytosol and membranes were obtained from roots of wild-type, *p24δ3δ4δ5δ6* and *p24δ7δ8δ9δ10* 20-day-old seedlings grown in MS liquid medium as described in section 5.1 of Materials and methods. Protein extracts were analyzed by SDS-PAGE and Western blotting using antibodies against Sec21 (γ-COP), Sec23 and Sec13. The Western blot analysis of glyceraldehyde-phosphate dehydrogenase (GAPDH), a cytosolic protein, and Syp21, a membrane protein, were used as controls. Wild-type (Col-0). B) Quantification from three independent experiments as the ones shown in panel (A), with duplicated samples. Membrane association was calculated as a percentage of the membrane association of wild-type. Values represent mean ± SD of at least three biological samples.

1.10.2. COPII *SEC31A* gene expression is up-regulated

Since, as described above, UPR has been shown to cause the up-regulation of genes coding COPII and COPI components in yeast (Travers et al., 2000), the transcription levels of COPI and COPII genes were also analyzed in *p24δ* mutants. COPI consists of a hetameric complex and, in *Arabidopsis,* there are 14 genes that code for COPI subunits. All the COPI

transcripts were analyzed by RT-sqPCR using specific primers for their coding sequences (Appendix 1, Table A1). In addition, the mRNA levels of *γ-COP* (*Sec21*) were also analyzed by RT-qPCR since it showed an increased membrane association in both mutants (Figure 50). As shown in Figures 51 and A11 (Appendix 11), no significant up-regulation was detected in the expression of any of the COPI genes analyzed. On the other hand, there are 24 genes which code for COPII components in *Arabidopsis*. Interestingly, it has been shown that the *SEC31A* but not *SEC31B* is up-regulated under ER stress conditions (Zimmermann et al., 2004; Nagashima et al., 2011; Song et al., 2015). *SEC31A* and *SEC31B* are differently expressed in *Arabidopsis* organs, being *SEC31B* expression about ten times higher than *SEC31A* expression. Considering that Sec31 is the partner of Sec13, whose membrane association was increased in the *p24δ3δ4δ5δ6* mutant (Figure 50), the expression levels of *SEC31A* and *SEC31B* were analyzed in both quadruple mutants. RT-qPCR analysis indicated that the expression of *SEC31A* is approximately 6-fold higher in *p24δ3δ4δ5δ6* and *p24δ7δ8δ9δ10* mutants than in wild-type (Figure 51). In contrast, *SEC31B* expression was not up-regulated in either the *p24δ3δ4δ5δ6* mutant or the *p24δ7δ8δ9δ10* mutant. Altogether, these results indicate that loss of *p24δ* produces the up-regulation of a COPII subunit but not of COPI subunits. Studies done in our group have showed that deletion of *α-COP* genes (*α2-COP*) produces the up-regulation of *SEC31A*, suggesting that the increase in *SEC31A* expression might be part of a general response to alterations of the secretory pathway (Gimeno-Ferrer et al, accepted manuscript). The induction of *SEC31A* might

enable efficient packaging of specific cargo proteins into anterograde vesicles or simply increase the overall capacity of anterograde transport to compensate the traffic defects in the mutants caused by the loss of p24δ proteins.

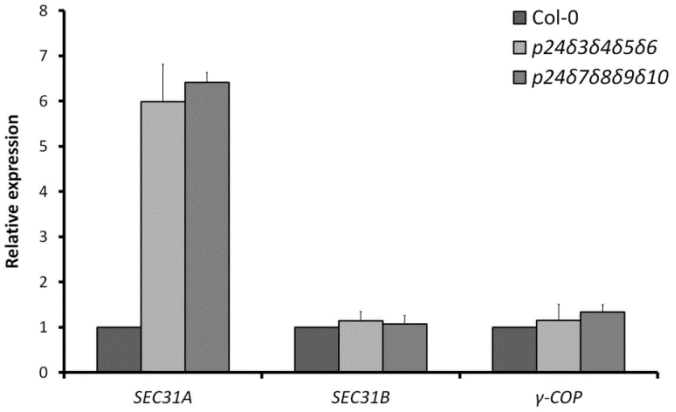

Figure 51. RT-qPCR analysis of *SEC31A*, *SEC31B* and *γ-COP* in *p24δ3δ4δ5δ6* and *p24δ7δ8δ9δ10* mutants. Total RNAs were extracted from 10-day-old seedlings. The mRNA was analysed by RT-qPCR with specific primers and normalized to *UBQ10* gene expression (Appendix 2, Table A2). Results are from at least three biological samples. mRNA levels are expressed as relative expression levels and represent fold changes of mutant/wild-type. Values represent mean ± SD of the three biological samples. Wild-type (Col-0).

CHAPTER II: *N*-LINKED GLYCOSYLATION OF p24δ5 (δ-1 SUBCLASS) AND RETROGRADE GOLGI-TO-ER TRANSPORT OF K/HDEL LIGANS IN *ARABIDOPSIS.*

When newly synthesized glycoproteins enter the lumen of the endoplasmic reticulum, an oligosaccharyl transferase associated to the translocon catalyzes the transfer of an oligosaccharide precursor to specific asparagine residues which are part of a consensus site for *N*-glycosylation (Asn-X-Ser/Thr, where X can be any amino acid except proline). The subsequent action of glycosyltransferases and glycosidases in the ER and the Golgi apparatus modify the *N*-linked glycans of glycoproteins. Plant *N*-linked glycans can be classified in high-mannose-type and complex-type (Strasser, 2016). The enzyme Endoglycosidase H (Endo H) cleaves high-mannose and some hybrid *N*-linked glycosylation modifications, but not complex oligosaccharides from *N*-linked glycoproteins (Maley et al. 1989). While glycosylated proteins entering the *cis*-Golgi are sensitive to Endo H treatment, the acquisition of complex oligosaccharides only occurs in the *medial*- and *trans*-Golgi, rendering proteins Endo H resistant. Protein glycosylation may contribute to their folding, stability, transport or interaction with other molecules, and therefore it is important for their function (Moremen et al. 2012; Hebert et al. 2014; Strasser, 2016).

Several reports have shown differential glycosylation of p24 family members. p24α2, p24γ3 and p24δ1 have shown to be glycosylated in

different studies (Dominguez et al., 1998; Füllekrug et al., 1999; Zhang and Volchuck, 2010; Liu et al., 2015), in contrast to p24β1, p24γ4 and p24γ2 (Füllekrug et al., 1999; Koegler et al., 2010; Zhang and Volchuck, 2010). In particular, p24α2 has been shown to be glycosylated, although it was found to be Endo H sensitive in HeLa cells (Füllekrug et al. 1999), suggesting that it does not reach the *medial*- and *trans*-Golgi, but Endo H resistant in rat liver (Dominguez et al. 1998; Lavoie et al. 1999) and human embryo kidney (HEK) cells (Liu et al. 2015). p24γ3 has also been shown to be glycosylated in HeLa cells, in contrast to p24γ4 and p24γ2, which do not contain any *N*-glycosylation site (Füllekrug et al. 1999; Koegler et al., 2010). This is an example of differential glycosylation between p24 proteins from the same subfamily. In the case of p24δ1, there are conflicting results about its glycosylation; it was found to be glycosylated in chondrocytes (Osiecka-Iwan et al. 2014) but not in HeLa and Rat INS-1 cells (Füllekrug et al. 1999; Zhang and Volchuck, 2010). However, none of these reports investigated further whether glycosylation of p24 proteins may have functional implications. In yeast, a novel p24δ isoform, Rtr6, is the only p24 protein which has been found to be *N*-glycosylated, and this glycosylation was proposed to be important to modulate cargo specificity (Hirata et al. 2013).

2.1. *ARABIDOPSIS* p24δ-1 PROTEINS HARBOR ONE CONSERVED *N*-GLYCOSYLATION SITE IN THE GOLD DOMAIN.

Sequence analysis of p24δ proteins using the NetNGlyc server (http://www.cbs.dtu.dk/services/NetNGlyc/) has predicted that *Arabidopsis* p24 proteins from the δ-1 subclass (including p24δ3-p24δ6) contain in their

GOLD domain a consensus sequence for N-linked glycosylation (Asn-X-Ser/Thr), precisely located at the same position when their sequences are aligned using ClustalW or T-Coffee, which is not present in the proteins of the δ-2 subclass (p24δ7-p24δ11) (Figure 52).

Figure 52. Alignment of the Arabidopsis p24 proteins from the delta subfamily. Arabidopsis p24 proteins from the δ-1 subclass (p24δ3-δ6) contain a potential *N*-linked glycosylation site (shown in red) in the same position which is not present in p24 proteins from the δ-2 subclass (p24δ7-δ11). Multiple alignment of the p24 proteins from the delta subfamily was constructed using T-Coffee. Classical dilysine residues are shown in green, ϕF motifs are shown in navy blue, the predicted signal peptides are shown in blue and the predicted transmembrane region is underlined.

2.2. p24δ5 IS *N*-GLYCOSYLATED *IN VIVO*

With the aim to investigate the glycosylation of p24 proteins of the delta subfamily *in vivo*, p24δ5 and p24δ9 were selected as representatives of *Arabidopsis* p24 proteins from the p24δ-1 and p24δ-2 subclasses, respectively, since antibodies against these two proteins had been generated previously (Montesinos et al., 2012; 2013). Sequence analysis of p24δ5, a member of the δ-1 subclass, predicts a potential *N*-glycosylation site at residue Asn86; in contrast, p24δ9, a member of the δ-2, does not contain any *N*-glycosylation consensus site.

To investigate putative glycosylation of endogenous p24 proteins, the relative molecular migration of both proteins was analyzed in the absence or presence of Tunicamycin (Tm), a chemical inhibitor of protein *N*-linked glycosylation (Ericson et al., 1977). *Arabidopsis* protoplasts obtained from wild-type plants (Col-0) were incubated with or without 100 µg/ml Tm for 16 h. Protein extracts were obtained as described in section 5.2. of Materials and methods and analyzed by SDS-PAGE and Western blotting with antibodies against the N- terminus of p24δ5 or p24δ9 (Montesinos et al., 2012; Montesinos et al., 2013). As shown in Figure 53, p24δ5 migrated faster upon Tm treatment (~ 2.5 kDa), consistent with a single site of *N*-glycosylation. In contrast, a shift in the mobility of p24δ9 was not detected upon Tm treatment. These results indicate that endogenous p24δ5 contains a single *N*-glycosylation site which is glycosylated *in vivo*, in contrast to p24δ9, which is not glycosylated.

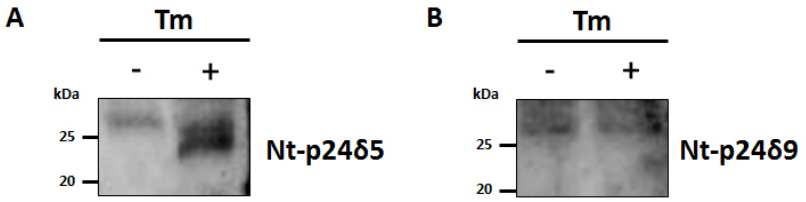

Figure 53. *N*-glycosylation of endogenous p24δ5 *in vivo*. Arabidopsis protoplasts obtained from wild-type plants (Col-0) were incubated in presence or absence of 100 µg/ml Tm. Membrane protein extracts were analyzed by SDS-PAGE and Western blotting using antibodies against Nt-p24δ5 (A) and Nt-p24δ9 (B). A 25 µg aliquot of protein was loaded in each lane. For details see section 5.2. of Materials and methods.

2.3. RFP-p24δ5 IS ALSO *N*-GLYCOSYLATED.

To analyze the impact of *N*-glycosylation in the trafficking of p24δ5, transient expression experiments in tobacco mesophyll protoplasts of its RFP-tagged version, RFP-p24δ5 (Langhans et al., 2008), or a mutant version where the Asn residue in position 86 was muted to Gln, RFP-p24δ5N86Q, were performed.

First, the electrophoretic mobility of the RFP-p24δ5N86Q mutant was compared with that of the wild-type version. Protein extracts were obtained from protoplasts expressing RFP-p24δ5 or the RFP-p24δ5N86Q mutant and used for pull-down experiments using a RFP-trap, as described previously (Montesinos et al., 2012; 2013; 2014). Pull-downs were analyzed by SDS-PAGE and Western blotting using antibodies against RFP. As shown in Figure 54, the RFP-p24δ5N86Q mutant migrated faster than wild-type RFP-p24δ5,

suggesting that RFP-p24δ5 is also *N*-glycosylated in Asn86, as endogenous p24δ5.

Next, protoplasts expressing RFP-p24δ5, RFP-p24δ5N86Q or RFP-p24δ9 were incubated in the absence or presence of 100 µg/ml Tm for 16 h. Protein extracts were processed and analyzed as described above. As shown in Figure 54, RFP-p24δ5 migrated faster upon Tm treatment, to a position identical to that of RFP-p24δ5N86Q. In contrast, a shift in the mobility of RFP-p24δ9 was not detected. To further confirm these results, pull-downs from protoplasts expressing RFP-p24δ5, RFP-p24δ5N86Q or RFP-p24δ9 were obtained as described above and treated in the absence or presence of Endoglycosidase H (Endo H). Endo H is an enzyme which cleaves high-mannose and some hybrid *N*-linked glycosylation modifications. Upon Endo H treatment, RFP-p24δ5 was detected as a double band. The upper band migrated to the same position as that of RFP-p24δ5 from untreated protoplasts, suggesting that it corresponds to the glycosylated form of RFP-p24δ5. The lower band migrated to an identical position to that of RFP-p24δ5N86Q, indicating that it corresponds to the non-glycosylated form of RFP-p24δ5. No difference in the mobility of RFP-p24δ9 was detected after Endo H treatment.

Altogether these results strongly suggest that RFP-p24δ5 is *N*-glycosylated and that glycosylation of Asn86 is responsible of the change in electrophoretic mobility of RFP-p24δ5. Moreover, the mobility of RFP-p24δ5N86Q was not changed upon Tm or Endo H treatment, indicating that

RFP-p24δ5 does not contain any other *N*-glycosylation site. In contrast, no shift in the mobility of RFP-p24δ9 was detected upon Tm or Endo H treatment, confirming the absence of *N*-glycosylation of RFP-p24δ9.

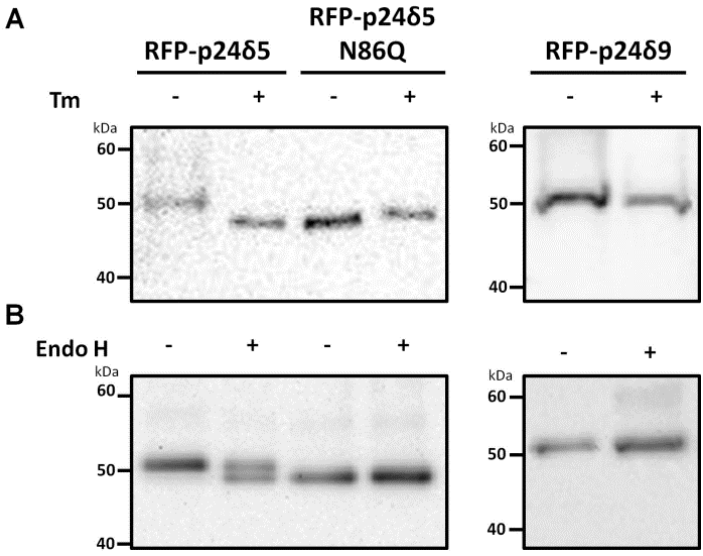

Figure 54. RFP-p24δ5, but not RFP-p24δ9, is *N*-glycosylated *in vivo*. A) RFP-p24δ5, RFP-p24δ5N86Q and RFP-p24δ9 were transiently expressed in tobacco mesophyll protoplast incubated in absence or presence of 100 µg/ml Tm for 16h. RFP-p24δ5, RFP-p24δ5N86Q or RFP-p24δ9 were pull-down using RFP-trap and analyzed by SDS-PAGE and Western blotting using an antibody against RFP. B) Protein extracts from tobacco mesophyll protoplast expressing RFP-p24δ5, RFP-p24δ5N86Q or RFP-p24δ9 were pull-down using RFP-trap and treated with or without Endo H. The difference in molecular weight was analyzed by SDS-PAGE and Western blotting using an antibody against RFP.

2.4. A RFP-p24δ5N86Q MUTANT LOCALIZES TO THE ER AT STEADY-STATE

Next, to investigate whether *N*-glycosylation of p24δ5 is important for its steady-state localization, the RFP-p24δ5N86Q mutant, which cannot be glycosylated, was transiently expressed in tobacco mesophyll protoplasts. The steady-state location of RFP-p24δ5N86Q was analyzed by confocal laser scanning microscopy. As shown in Figure 55, this mutant mostly localized to the ER network, as wild-type RFP-p24δ5 (Langhans et al., 2008). This suggests that the ER localization of p24δ5 at steady-state is not dependent on its *N*-linked glycosylation.

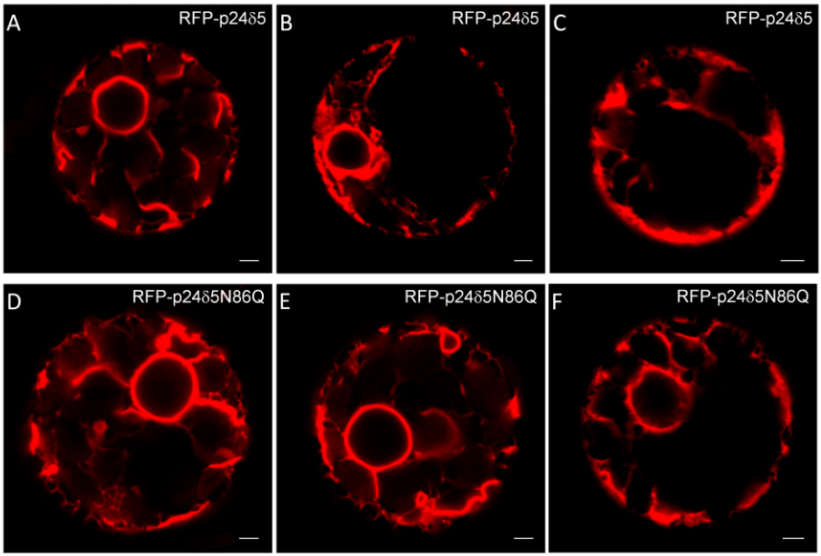

Figure 55. RFP-p24δ5N86Q localizes to the ER at steady-state. (A-F) Transient gene expression in tobacco mesophyll protoplast. RFP-p24δ5N86Q (D-F) shows the typical ER pattern as RFP-p24δ5 (A-C). Scale bars=5 µm.

2.5. p24δ5 *N*-GLYCOSYLATION IS IMPORTANT FOR ITS INTERACTION WITH THE K/HDEL RECEPTOR ERD2

It has been previously shown that p24δ5 interacts with the K/HDEL receptor ERD2a at slightly acidic pH but not at neutral pH, consistent with this interaction taking place at the Golgi apparatus but not at the ER (Montesinos et al., 2014). The interaction between p24δ5 and ERD2 was shown to require the presence of the luminal GOLD domain in p24δ5 (Montesinos et al., 2014). Since the *N*-glycosylation site is located within the GOLD domain, it was investigated whether the interaction between both proteins is dependent on p24δ5 glycosylation of Asn86. To this end, pull-down experiments were performed using protein extracts from tobacco mesophyll protoplasts after transient co-expression of RFP-p24δ5 or RFP-p24δ5N86Q and ERD2a-YFP (Brandizzi et al., 2002a) and GFP- or RFP-trap, as described previously (Montesinos et al., 2014; section 5.4. of Materials and methods). As shown in Figure 56, RFP-p24δ5 interacted with ERD2a-YFP, while a deletion mutant of RFP-p24δ5 lacking the GOLD domain showed a strongly reduced ability to interact with ERD2a-YFP, as shown previously (Montesinos et al., 2014). Using the same type of experiments, it has been now found that the interaction between the RFP-p24δ5N86Q mutant and ERD2a-YFP was reduced by about a 50% when compared with that of wild-type RFP-p24δ5 (Figures 56 and 57). This suggests that p24δ5 glycosylation is important for its interaction with the K/HDEL receptor ERD2.

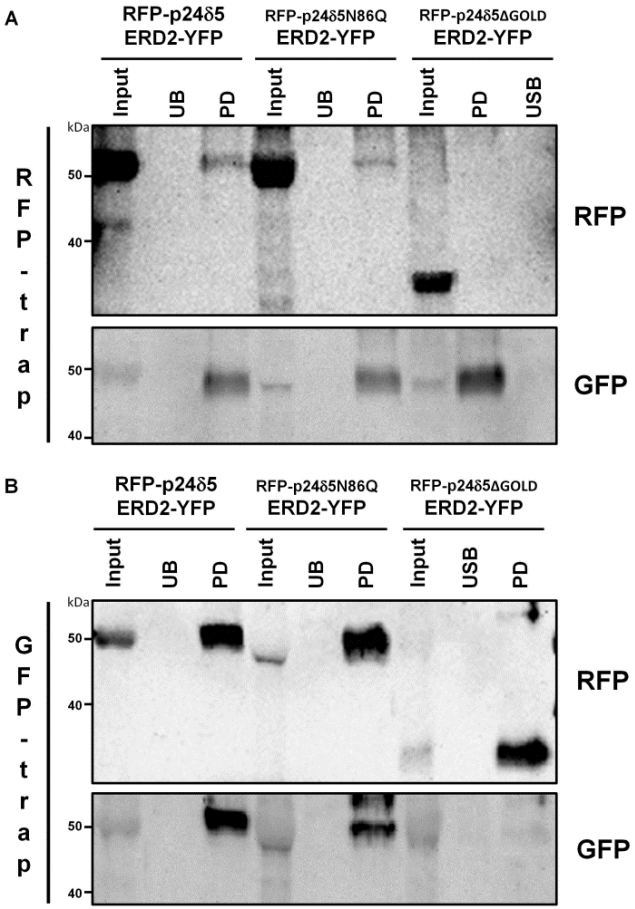

Figure 56. p24δ5 *N*-glycosylation is important for its interaction with the K/HDEL receptor ERD2. A) Pull-down of RFP-p24δ5 or mutant versions from PNS of protoplasts expressing these proteins and ERD2a-YFP, using a RFP-trap at pH 6.0. B) Pull-down of ERD2a-YFP from PNS of protoplasts expressing ERD2a-YFP and RFP-p24δ5 or mutant versions, using a GFP-trap at pH 6.0. Bound proteins were analyzed by SDS-PAGE and Western blotting with antibodies against RFP (to detect RFP-p24δ5 or mutant versions) or GFP (to detect ERD2a-YFP). Input: 5% of the PNS used for the pull-down assay. UB: unspecific binding (using blocked magnetic particles). PD: pull-down.

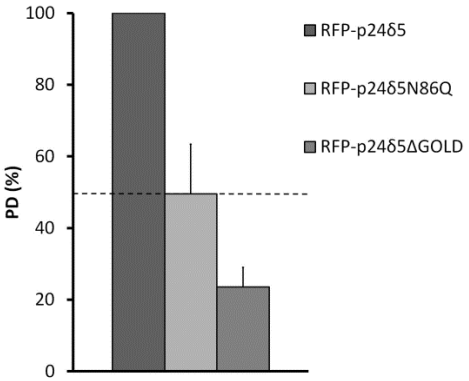

Figure 57. Quantification of the biochemical interactions in pull-down experiments. In experiments using the RFP-trap (Figure 56, A), the amount of GFP-labelled interacting protein (PD, pull-down) was normalized to the amount of RFP-labelled protein bound to the beads, although the latter was consistently similar in the different points of the same experiments (as it was the case with the inputs). The opposite was done when using the GFP-trap (Figure 56, B). When the interaction was monitored both using the RFP-trap and GFP-trap, the average between both values was obtained. Error bars represent SD of the mean from at least three independent experiments.

2.6. p24δ5 *N*-GLYCOSYLATION IS REQUIRED FOR SHIFTING THE STEADY-STATE DISTRIBUTION OF THE K/HDEL RECEPTOR ERD2 FROM THE GOLGI TO THE ER

Previous studies have shown that p24δ5 partially shifts the steady-state distribution of the K/HDEL receptor ERD2 from the Golgi to the ER, an effect that required the GOLD domain in p24δ5 (Montesinos et al., 2014). Now, it was investigated whether this effect was dependent on the glycosylation of p24δ5. To this end, ERD2a-YFP was transiently co-expressed with RFP-p24δ5 or the RFP-p24δ5N86Q mutant in tobacco mesophyll

protoplast and the steady-state localization of ERD2a-YFP was analyzed by confocal laser scanning microscopy (Figure 58). In the absence of RFP-p24δ5, the steady-state localization of ERD2a-YFP was mainly the Golgi apparatus (74%), with only a partial ER and Golgi localization (26%) (Figure 58 and 59). However, in the presence of RFP-p24δ5, there was a significant relocalization of ERD2a-YFP from the Golgi apparatus to the endoplasmic reticulum (Figure 58), as described previously (Montesinos et al., 2014). As quantified in Figure 59, the percentage of protoplasts where ERD2a-YFP localized to Golgi stacks decreased to a 22% when co-expressed with RFP-p24δ5. In the remaining protoplasts, ERD2a-YFP localized both to ER and Golgi (54%) (main pattern, Figure 58), or ER only (24%). In clear contrast, co-expression of ERD2a-YFP with the RFP-p24δ5N86Q mutant did not produce a significant change in the localization of ERD2a-YFP (Figure 58). Its localization was mainly the Golgi apparatus (62%) and while a 33% of protoplasts showed a ER and Golgi localization (Figure 59 and Appendix 12). This suggests that p24δ5 glycosylation is required for shifting the steady-state distribution of the K/HDEL receptor ERD2 from the Golgi to the ER.

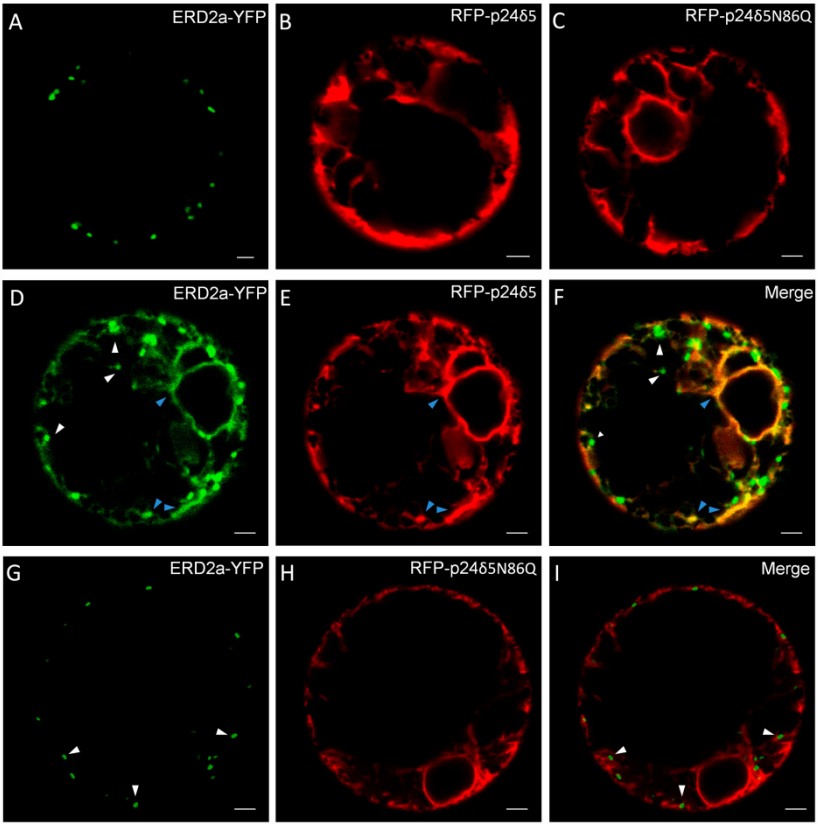

Figure 58. p24δ5 *N*-glycosylation is required for shifting the steady-state distribution of the K/HDEL receptor ERD2 from the Golgi to the ER. Transient gene expression in tobacco mesophyll protoplast. A) ERD2a-YFP mainly localized to punctate Golgi structures. B-C) RFP-p24δ5 (B) and RFP-p24δ5N86Q (C) localized exclusively to the ER. D-F) RFP-p24δ5 caused a partial relocalization of ERD2a-YFP (D) to the ER (blue arrowheads), although ERD2a-YFP also showed a punctate localization (white arrowheads) (ER and Golgi localization) (merged image in F). G-I) RFP-p24δ5N86Q had no effect on the localization of ERD2a-YFP (G), which localized exclusively to punctate Golgi structures (white arrowheads) (merge image in I). Images included in the panels show the most representative pattern found for each condition according to the quantification shown in Figure 57. Scale bars = 5 µm.

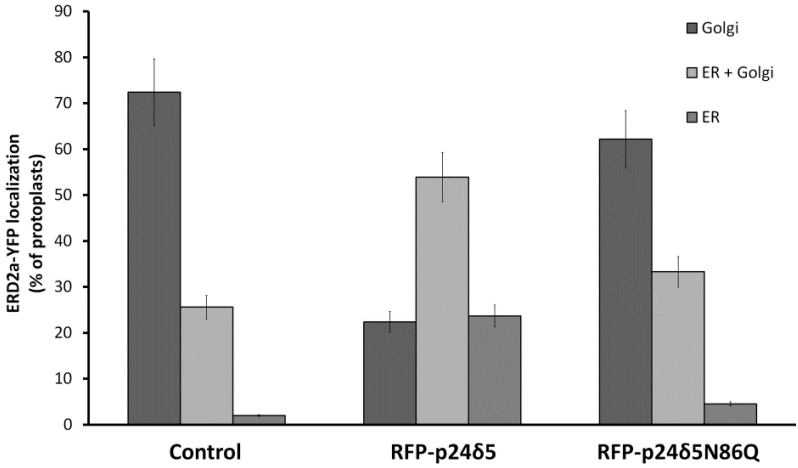

Figure 59. Quantification of the localization of ERD2a-YFP when it is expressed alone and co-expressed with RFP-p24δ5 or RFP-p24δ5N86Q. A significant number of protoplasts (from at least three independent experiments), showing comparable expression levels of ERD2a-YFP and RFP-p24δ5 or RFP-p24δ5N86Q, were analyzed per condition, using identical laser output levels and imaging conditions. Number of protoplasts analyzed per condition: ERD2a-YFP (39); ERD2a-YFP + RFP-p24δ5 (76); ERD2a-YFP + RFP-p24δ5N86Q (111). The localization of ERD2a-YFP was assigned as Golgi, ER and Golgi or ER (see Figure 56 and Appendix 12) and calculated as a percentage. Error bars represent SE of the mean.

2.7. p24δ5 *N*-GLYCOSYLATION IS REQUIRED FOR ITS INHIBITORY EFFECT ON SECRETION OF K/HDEL LIGANDS

It has previously been shown that by facilitating the retrograde transport of ERD2 (bound to K/HDEL ligands) from the Golgi apparatus to the endoplasmic reticulum, p24δ5 inhibits the secretion of K/HDEL ligands, an effect which was dependent on the GOLD domain in p24δ5 (Montesinos et al., 2014). Therefore, it was investigated whether this function of p24δ5 was dependent on its *N*-linked glycosylation. To this end, secretion assays

were performed in tobacco mesophyll protoplasts upon transient co-expression of a HDEL ligand, GFP-HDEL and RFP-p24δ5 or the RFP-p24δ5N86Q mutant, as described previously (Montesinos et al., 2014 and section 5.6. of Materials and methods). GFP-HDEL mostly localizes to the ER at steady-state, but it can be partially secreted upon overexpression, like other HDEL ligands (Phillipson et al., 2001). Therefore, the secretion of this marker was monitored by analyzing its presence in the culture medium by SDS-PAGE and Western blotting using GFP-antibodies (Figure 60). In addition, overexpression of GFP-HDEL also causes a partial secretion of the chaperone BiP, an endogenous HDEL ligand whose secretion was also monitored as described for GFP-HDEL using a antibody against BiP. A secretory reporter, Sec-GFP, which lacks a K/HDEL signal and is mostly secreted into the medium, was used as a control (Di Sansebastiano et al., 1998; Leucci et al., 2007).

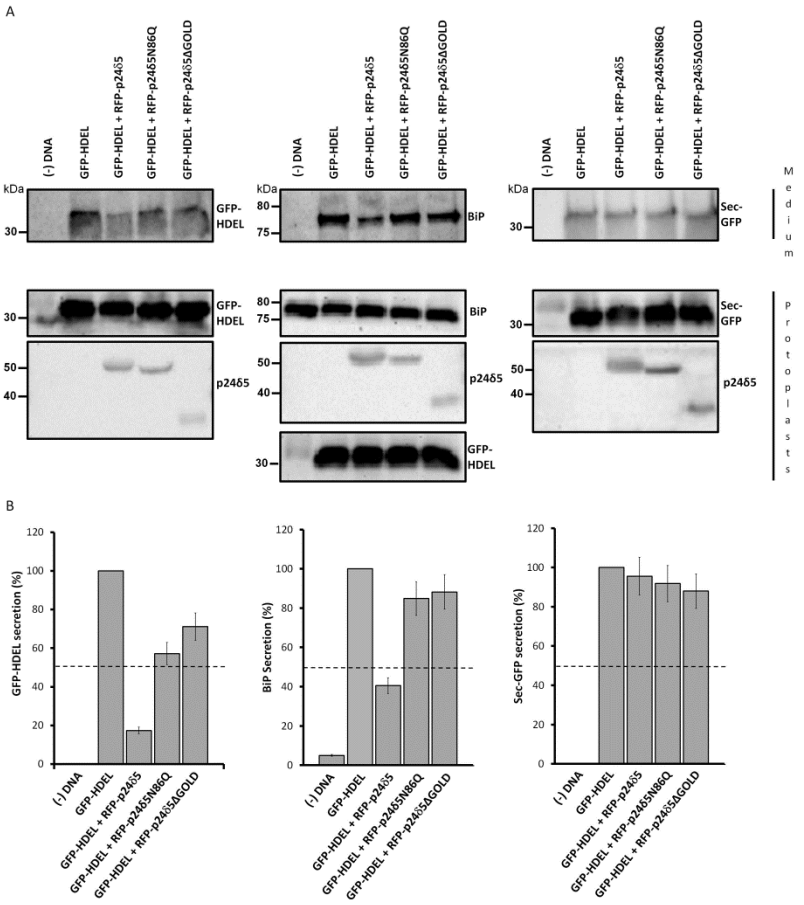

Figure 60. Secretion assays. A) Tobacco mesophyll protoplasts were transformed with the indicated constructs and incubated for 20 h. Total proteins from protoplasts and culture medium (concentrated 5x by methanol/chloroform precipitation), were analyzed by SDS-PAGE and Western blotting with antibodies against GFP (to detect GFP-HDEL or Sec-GFP), RFP (to detect RFP-p24δ5 and mutant versions) or BiP. Notice the difference in molecular weight between wild-type RFP-p24δ5 and mutant versions. B) Quantification from at least three independent experiments as the ones shown in panel A, with duplicated samples. Secretion of GFP-HDEL, Sec-GFP or BiP under different conditions of co-expression was calculated as a percentage of the secretion of these markers when expressed alone.

As shown in Figure 60, co-expression of RFP-p24δ5 caused a significant inhibition of GFP-HDEL and BiP secretion, an effect which required the GOLD domain in p24δ5, as described previously (Montesinos et al., 2014). In contrast, this effect was not observed when the RFP-p24δ5N86Q mutant was used, suggesting that *N*-linked glycosylation of p24δ5 is essential for its function to inhibit secretion of HDEL ligands. As expected, neither RFP-p24δ5 nor its mutant versions had a significant effect on overall secretion, as shown by monitoring Sec-GFP secretion.

2.8. *N*-LINKED GLYCOSYLATION OF THE p24 FAMILY PROTEIN p24δ5 IS IMPORTANT FOR RETROGRADE GOLGI-TO-ER TRANSPORT OF K/HDEL LIGANDS IN *ARABIDOPSIS*

There are many reports which indicate that p24 proteins are key players in the formation of COPI vesicles involved in retrograde Golgi-to-ER transport (section 5.6.1 of Introduction). p24 proteins can also interact with the K/HDEL receptor ERD2, facilitating its sorting within COPI vesicles (Majoul et al. 1998; Majoul et al. 2001; Montesinos et al. 2014). ERD2 itself has been proposed to participate actively in COPI vesicle formation (section 6 of Introduction). Binding of K/HDEL ligands, which takes place at the slightly acidic pH of the *cis*-Golgi (Wilson et al. 1993; Scheel and Pelham, 1996), induces ERD2 oligomerization (Majoul et al. 20001) and facilitates its interaction with ARF1 and ARF-GAP (which is also part of the machinery involved in COPI vesicle formation) or between ARF1 and ARF-GAP (Aoe et al. 1997; Majoul et al. 2001). ERD2 can also interact with coatomer, thus contributing to the formation of COPI vesicles (Majoul et al. 2001). In

Arabidopsis, it has been shown previously that a member of the p24δ subfamily, p24δ5, interacts with both ARF1 and coatomer via a dilysine and a diaromatic motif in their C-terminal tail which are present in all members of the Arabidopsis p24δ subfamily (Contreras et al. 2004a). In addition, it has been shown recently that Arabidopsis p24δ5 and p24δ9 interact with two different K/HDEL receptors, ERD2a and ERD2b (Montesinos et al. 2014). In the case of p24δ5, the interaction required its luminal GOLD domain and was optimal at acidic pH, consistent with this interaction taking place at the Golgi apparatus, as is the case for the interaction between ERD2 and K/HDEL ligands. Acidic pH also favors the interaction of p24δ5 with both ARF1 and coatomer (Montesinos et al. 2014). Therefore, pH-dependent interactions seem to be essential for the bidirectional transport of ERD2 and K/HDEL ligands between ER and Golgi.

In this work, it has been further investigated the molecular basis of the effect of p24 proteins in efficient retrieval of K/HDEL ligands from the Golgi back to the ER, and the putative role in this process of N-linked glycosylation of Arabidopsis p24 proteins has been analyzed. It has been found that p24δ5 (p24δ-1 subclass) is *N*-glycosylated in its GOLD domain (which is important for its interaction with ERD2), in contrast to p24δ9 (p24δ-2 subclass). Endo H sensitivity indicates that p24δ5 is not modified by glycosylation enzymes of the *medial*- and *trans*-Golgi to acquire complex oligosaccharides. This would be consistent with its predominant localization at the *cis*-side of the Golgi apparatus which has been previously shown by immunogold labeling with p24δ5 antibodies (Montesinos et al. 2012). It has been previously shown

that p24δ9, which is not glycosylated, can also bind to ERD2a. This would be consistent with the fact that a mutant version of p24δ5 lacking Asn 86, which is not glycosylated, still bound to ERD2, although with much lower efficiency (50 %). However, it is not clear whether p24δ9 (and perhaps other members of the p24δ-2 subclass) can also contribute to sorting of ERD2 within COPI vesicles without the need of N-linked glycosylation.

There is a previous report showing differential glycosylation of p24 proteins from the same subfamily. In particular, p24γ3 was shown to be glycosylated, in contrast to p24γ4 (Füllekrug et al. 1999). The p24γ subfamily appears to be the most divergent within the p24 family, and it has been proposed that different p24γ proteins may be involved in cargo specificity; although there is no evidence that differential glycosylation may influence cargo binding. Plants do not contain p24 proteins from the γ- and α-subfamilies, but only p24 proteins from the δ- and β-subfamilies. In plants, the p24δ subfamily seems to have greatly expanded from the fungi/animals (Strating et al. 2009), but it is not clear whether this may reflect functional differences. However, glycosylation of p24δ5 (and perhaps of other p24 proteins from the δ-1 subclass) may increase its ability to interact with ERD2 and therefore to facilitate its sorting within COPI vesicles and thus retrieval of K/HDEL ligands in vivo.

It has been found that *N*-linked glycosylation of p24δ5 does not change its steady-state ER localization, which has been shown to depend on a dilysine and a diaromatic motif in its cytosolic tail which is involved in binding ARF1 and coatomer subunits (Contreras et al. 2004a; Montesinos et

al. 2014). ER export of p24δ5 is COPII dependent and depends on a diaromatic motif in its cytosolic tail (Contreras et al. 2004b). Therefore, *N*-glycosylation of p24δ5 at its luminal side is not expected to interfere with its cycling between ER and Golgi mediated by COPI and COPII vesicles. The same would apply to the oligomerization of p24 proteins, which involves their coiled-coil domain, as shown previously (Montesinos et al. 2012). Actually, it has been shown recently that a p24δ5 deletion mutant lacking the coiled-coil domain was still able to bind efficiently ERD2a, in contrast with a deletion mutant lacking the GOLD domain (Montesinos et al. 2014). However, glycosylation of p24δ5 may be important for its interaction with the K/HDEL receptor ERD2a at the Golgi apparatus. There are many reports showing that glycosylation may affect protein-protein and receptor-ligand interactions (Yang et al., 1993; Kaushal et al., 1994; Huang and Tai, 1998; Wang et al., 2001; Zhang et al., 2001; Ho et al., 1999; Pang et al., 1999; Kamitani, 2001; van der Hoorn et al., 2005; Häweker et al., 2010). In a recent manuscript, it was shown that *N*-glycosylation of the vacuolar sorting receptor AtVSR1 affects the binding affinity of AtVSR1 to cargo proteins and therefore vacuolar protein sorting, without affecting its targeting to the prevacuolar compartment (Shen et al. 2014). Here it has been shown that *N*-glycosylation of p24δ5 may increase its binding affinity towards the K/HDEL receptor ERD2 thus facilitating its sorting within COPI vesicles and thus retrieval of ER resident K/HDEL ligands.

CONCLUSIONS

1. Most p24 genes are widely expressed in *Arabidopsis,* which indicates that these genes may play housekeeping functions. However, the restricted expression patterns of three genes of the p24δ subfamily, *p24δ6*, *p24δ8* and *p24δ11*, may reflect that they have specialized functions in floral tissues.

2. Quadruple mutants affecting p24 genes from the δ-1 and δ-2 subclasses have been generated. These mutants did not show phenotypic alterations when they were grown under standard growth conditions, suggesting that p24 proteins from the delta subfamily are not necessary for growth under these conditions in *Arabidopsis*.

3. The protein levels of p24 family members are interdependent. In the p24δ-1 and p24δ-2 quadruple mutants, a decrease in other p24 protein levels has also been found, which may be due to a decrease in the protein stability and not to a decrease in the mRNA levels. These results suggest that these p24 proteins may function together in heteromeric complexes. In particular, the protein levels of the two members of the p24β subfamily are both dependent on the proteins levels of p24δ-1 and p24δ-2 proteins. In addition, p24β3 seems to require p24 proteins from both subclasses for its stability. Besides, p24δ-1 proteins seem to play a more important role in the stability of other p24 proteins than p24δ-2 proteins.

4. Loss of p24δ-1 or p24δ-2 proteins produces alterations in the Golgi apparatus, which consist of dilated areas in the cisternae and an increased in the number of vesicles surrounding the Golgi apparatus. These data

suggest that p24 proteins of the delta subfamily are involved in the maintenance of the structure and organization of the compartments of the early secretory pathway in *Arabidopsis*.

5. Loss of p24 proteins of the delta subfamily induced the accumulation of the K/HDEL receptor ERD2a-YFP at the Golgi apparatus. This effect was reversed by co-expression of either p24δ5 (δ-1 subclass) or p24δ9 (δ-2 subclass) or a K/HDEL ligand. In addition, loss of p24 proteins from the delta subfamily induced secretion of the chaperone BiP (an HDEL-ligand), probably due to an inhibition of COPI-dependent retrograde Golgi-to-ER transport of ERD2 and, in consequence, in the retrieval of K/HDEL ligands.

6. Both p24 quadruple mutants showed a constitutive activation of the UPR pathway, which may act as a compensatory mechanism that helps the plant to cope with the transport defects in the absence of p24 proteins. Indeed, an increase of the membrane association of several COPI and COPII subunits was observed in both quadruple mutants. In addition, loss of p24δ-1 and p24δ-2 proteins produced the up-regulation of *SEC31A*, a gene involved in the formation of COPII vesicles.

7. A member of the p24δ-1 subclass, p24δ5, is *N*-glycosylated in its GOLD domain, in contrast to p24δ9, a member of the p24δ-2 subclass. The *N*-glycosylation of p24δ5 is not required for its steady-state localization at the ER, but it is important for its interaction with the K/HDEL receptor ERD2a and for retrograde transport of ERD2a and K/HDEL ligands from the Golgi apparatus to the endoplasmic reticulum.

REFERENCES

Aguilera-Romero, A., Kaminska, J., Spang, A., Riezman, H., and Muñiz, M. (2008). The yeast p24 complex is required for the formation of COPI retrograde transport vesicles from the Golgi apparatus. *The Journal of Cell Biology, 180*(4), 713-720.

Alonso, J. M., Stepanova, A. N., Leisse, T. J., Kim, C. J., Chen, H., Shinn, P., Stevenson, D.K., Zimmerman, J., Barajas, P., Cheuk, R., Gadrinab, C., Heller, C., Jeske, A., Koesema, E., Meyers, C.C., Parker, H., Prednis, L., Ansari, Y., Choy, N., Deen, H., Geralt, M., Hazari, N., Hom, E., Karnes, M., Mulholland, C., Ndubaku, R., Schmidt, I., Guzman, P., Aguilar-Henonin, L., Schmid, M., Weigel, D., Carter, D.E., Marchand, T., Risseeuw, E., Brogden, D., Zeko, A., Crosby, W.L., Berry, C.C. and Ecker, J. R. (2003). Genome-wide insertional mutagenesis of arabidopsis thaliana. *Science, 301*(5633), 653-657.

Anantharaman, V., and Aravind, L. (2002). The GOLD domain, a novel protein module involved in golgi function and secretion.*Genome Biology, 3*(5), research0023.7.

Aniento, F., Matsuoka, K., and Robinson, D. G. (2006). ER-to-golgi transport: The COPII-pathway. In D. G. Robinson (Ed.), *The plant endoplasmic reticulum* (pp. 99-124) Springer Berlin Heidelberg.

Aoe, T., Cukierman, E., Lee, A., Cassel, D., Peters, P. J., and Hsu, V. W. (1997). The KDEL receptor, ERD2, regulates intracellular traffic by recruiting a GTPase-activating protein for ARF1. *The EMBO Journal, 16*(24), 7305-7316.

Aoe, T., Lee, A. J., Donselaar, E. v., Peters, P. J., and Hsu, V. W. (1998). Modulation of intracellular transport by transported proteins: Insight from regulation of COPI-mediated transport. *Proceedings of the National Academy of Sciences, 95*(4), 1624-1629.

Appenzeller-Herzog, C., and Hauri, H. (2006). The ER-golgi intermediate compartment (ERGIC): In search of its identity and function. *Journal of Cell Science, 119*(11), 2173-2183.

Arakel, E. C., Richter, K. P., Clancy, A., and Schwappach, B. (2016). δ-COP contains a helix C-terminal to its longin domain key to COPI dynamics and function. *Proceedings of the National Academy of Sciences of the United States of America,113*(25), 6916-6921.

Barlowe, C. K., and Miller, E. A. (2013). Secretory protein biogenesis and traffic in the early secretory pathway. *Genetics, 193*(2), 383-410.

REFERENCES

Bassham, D. C., Brandizzi, F., Otegui, M. S., and Sanderfoot, A. A. (2008). The secretory system of arabidopsis. *The Arabidopsis Book / American Society of Plant Biologists, 6.*

Belden, W. J., and Barlowe, C. (1996). Erv25p, a component of COPII-coated vesicles, forms a complex with Emp24p that is required for efficient endoplasmic reticulum to golgi transport. *Journal of Biological Chemistry, 271*(43), 26939-26946.

Belden, W. J., and Barlowe, C. (2001a). Deletion of yeast p24 genes activates the unfolded protein response. *Molecular Biology of the Cell, 12*(4), 957-969.

Belden, W. J., and Barlowe, C. (2001b). Distinct roles for the cytoplasmic tail sequences of Emp24p and Erv25p in transport between the endoplasmic reticulum and golgi complex. *Journal of Biological Chemistry, 276*(46), 43040-43048.

Ben-Tekaya, H., Miura, K., Pepperkok, R., and Hauri, H. (2005). Live imaging of bidirectional traffic from the ERGIC. *Journal of Cell Science, 118*(2), 357-367.

Bertani, G. (1960). Sensitivities of different bacteriophage species to ionizing radiations1. Journal of Bacteriology, 79(3), 387-393.

Blum, R., Pfeiffer, F., Feick, P., Nastainczyk, W., Kohler, B., Schafer, K. H., and Schulz, I. (1999). Intracellular localization and in vivo trafficking of p24A and p23. *Journal of Cell Science, 112*(4), 537.

Blum, R., Feick, P., Puype, M., Vandekerckhove, J., Klengel, R., Nastainczyk, W., and Schulz, I. (1996). Tmp21 and p24A, two type I proteins enriched in pancreatic microsomal membranes, are members of a protein family involved in vesicular trafficking. *Journal of Biological Chemistry, 271*(29), 17183-17189.

Blum, R., and Lepier, A. (2008). The luminal domain of p23 (Tmp21) plays a critical role in p23 cell surface trafficking. *Traffic,9*(9), 1530-1550.

Boevink, P., Oparka, K., Cruz, S. S., Martin, B., Betteridge, A., and Hawes, C. (1998). Stacks on tracks: The plant golgi apparatus traffics on an actin/ER network. *The Plant Journal, 15*(3), 441-447.

Boltz, K. A., and Carney, G. E. (2008). Loss of p24 function in drosophila melanogaster causes a stress response and increased levels of NF-κB-regulated gene products. *BMC Genomics, 9*, 212.

Boltz, K. A., Ellis, L. L., and Carney, G. E. (2007). Drosophila melanogaster p24 genes have developmental, tissue-specific, and sex-specific expression patterns and functions. *Developmental Dynamics, 236*(2), 544-555.

Bombardier, J. P., and Munson, M. (2015). Three steps forward, two steps back: Mechanistic insights into the assembly and disassembly of the SNARE complex. *Current Opinion in Chemical Biology, 29*, 66-71.

Bonnon, C., Wendeler, M. W., Paccaud, J., and Hauri, H. (2010). Selective export of human GPI-anchored proteins from the endoplasmic reticulum. *Journal of Cell Science, 123*(Pt 10), 1705-1715.

Bottanelli, F., Foresti, O., Hanton, S., and Denecke, J. (2011). Vacuolar transport in tobacco leaf epidermis cells involves a single route for soluble cargo and multiple routes for membrane cargo. *The Plant Cell, 23*(8), 3007-3025.

Bradford, M. M. (1976). A rapid and sensitive method for the quantitation of microgram quantities of protein utilizing the principle of protein-dye binding. *Analytical Biochemistry, 72*(1), 248-254.

Brandizzi, F., and Barlowe, C. (2013). Organization of the ER-golgi interface for membrane traffic control. *Nature Reviews. Molecular Cell Biology, 14*(6), 382.

Brandizzi, F., Frangne, N., Marc-Martin, S., Hawes, C., Neuhaus, J., and Paris, N. (2002a). The destination for single-pass membrane proteins is influenced markedly by the length of the hydrophobic domain. *The Plant Cell, 14*(5), 1077-1092.

Brandizzi, F., Snapp, E. L., Roberts, A. G., Lippincott-Schwartz, J., and Hawes, C. (2002b). Membrane protein transport between the endoplasmic reticulum and the golgi in tobacco leaves is energy dependent but cytoskeleton independent. *The Plant Cell, 14*(6), 1293-1309.

Bröcker, C., Kuhlee, A., Gatsogiannis, C., Balderhaar, H.J.K., Hönscher, C., Engelbrecht-Vandré, S., Ungermann, C. and Raunser, S. (2012). Molecular architecture of the multisubunit homotypic fusion and vacuole protein sorting (HOPS) tethering complex. *Proceedings of the National Academy of Sciences of the United States of America,*109(6), pp. 1991-1996.

Bröcker, C., Engelbrecht-Vandré, S., and Ungermann, C. (2010). Multisubunit tethering complexes and their role in membrane fusion. *Current Biology, 20*(21), R952.

REFERENCES

Bubeck, J., Scheuring, D., Hummel, E., Langhans, M., Viotti, C., Foresti, O., Denecke, J., Banfield, D.K. and Robinson, D. G. (2008). The syntaxins SYP31 and SYP81 control ER–Golgi trafficking in the plant secretory pathway. *Traffic, 9*(10), 1629-1652.

Budnik, A., and Stephens, D. J. (2009). ER exit sites – localization and control of COPII vesicle formation. *FEBS Letters, 583*(23), 3796-3803.

Buechling, T., Chaudhary, V., Spirohn, K., Weiss, M., and Boutros, M. (2011). p24 proteins are required for secretion of wnt ligands. *EMBO Reports, 12*(12), 1265-1272.

Burnette, W. N. (1981). "Western blotting": Electrophoretic transfer of proteins from sodium dodecyl sulfate-polyacrylamide gels to unmodified nitrocellulose and radiographic detection with antibody and radioiodinated protein A. *Analytical Biochemistry, 112*(2), 195-203.

Cabrera, M., Muñiz, M., Hidalgo, J., Vega, L., Martín, M. E., and Velasco, A. (2003). The retrieval function of the KDEL receptor requires PKA phosphorylation of its C-terminus. *Molecular Biology of the Cell, 14*(10), 4114-4125.

Capitani, M., and Sallese, M. (2009). The KDEL receptor: New functions for an old protein. *FEBS Letters, 583*(23), 3863-3871.

Caramelo, J. J., and Parodi, A. J. (2008). Getting in and out from calnexin/calreticulin cycles. *The Journal of Biological Chemistry, 283*(16), 10221-10225.

Carney, G. E., and Bowen, N. J. (2004). *p24 proteins, intracellular trafficking, and behavior: Drosophila melanogaster provides insights and opportunities*. France: Elsevier SAS.

Castillon, G. A., Aguilera-Romero, A., Manzano-Lopez, J., Epstein, S., Kajiwara, K., Funato, K., Watanabe, R., Riezman, H., and Muñiz, M. (2011). The yeast p24 complex regulates GPI-anchored protein transport and quality control by monitoring anchor remodeling. *Molecular Biology of the Cell, 22*(16), 2924-2936.

Chen, F., Hasegawa, H., Schmitt-Ulms, G., Kawarai, T., Bohm, C., Katayama, T., GU, Y., Sanjo, N., Glista, M., Rogaeva, E., Wakutani, Y., Pardossi-Piquard, R., Ruan, X., Tandon, A., Checler, F., Marambaud, P., Hansen, K., Westaway, D., St George-Hyslop, P., and Fraser, P. (2006). TMP21 is a presenilin complex component that modulates γ-secretase but not ε-secretase activity. *Nature, 440*(7088), 1208-1212.

Chen, J., Qi, X., and Zheng, H. (2012). Subclass-specific localization and trafficking of arabidopsis p24 proteins in the ER–Golgi interface. *Traffic, 13*(3), 400-415.

Chen, Y., and Brandizzi, F. (2013a). Analysis of unfolded protein response in arabidopsis. *Methods in Molecular Biology (Clifton, N.J.), 1043*, 73.

Chen, Y., and Brandizzi, F. (2013b). IRE1: ER stress sensor and cell fate executor. *Trends in Cell Biology, 23*(11), 547-555.

Chung, K. P., Zeng, Y., and Jiang, L. (2016). COPII paralogs in plants: Functional redundancy or diversity? *Trends in Plant Science, 21*(9), 758-769.

Ciufo, L. F., and Boyd, A. (2000). Identification of a lumenal sequence specifying the assembly of Emp24p into p24 complexes in the yeast secretory pathway. *Journal of Biological Chemistry, 275*(12), 8382-8388.

Clough, S. J., and Bent, A. F. (1998). Floral dip: A simplified method forAgrobacterium-mediated transformation of Arabidopsis thaliana. *The Plant Journal, 16*(6), 735-743.

Contreras, F., Ernst, A. M., Haberkant, P., Björkholm, P., Lindahl, E., Gönen, B., Tischer, C., Elofsson, A., von Heijne, G., Thiele, C., Pepperkok, R., Wieland, F. and Brügger, B. (2012). Molecular recognition of a single sphingolipid species by a protein/'s transmembrane domain. *Nature, 481*(7382), 525-529.

Contreras, I., Ortiz-Zapater, E., and Aniento, F. (2004a). Sorting signals in the cytosolic tail of membrane proteins involved in the interaction with plant ARF1 and coatomer. *The Plant Journal, 38*(4), 685-698.

Contreras, I., Yang, Y., Robinson, D. G., and Aniento, F. (2004b). Sorting signals in the cytosolic tail of plant p24 proteins involved in the interaction with the COPII coat. *Plant and Cell Physiology, 45*(12), 1779-1786.

Čopič, A., Latham, C. F., Horlbeck, M. A., D'Arcangelo, J. G., and Miller, E. A. (2012). ER cargo properties specify A requirement for COPII coat rigidity mediated by Sec13p. *Science, 335*(6074), 1359-1362.

Crofts, A. J., Leborgne-Castel, N., Hillmer, S., Robinson, D. G., Phillipson, B., Carlsson, L. E., Ashford, D.A. and Denecke, J. (1999). Saturation of the endoplasmic reticulum retention machinery reveals anterograde bulk flow. *The Plant Cell, 11*(11), 2233-2248.

D'Arcangelo, J. G., Crissman, J., Pagant, S., Copic, A., Latham, C. F., Snapp, E. L., and Miller, E. A. (2015). Traffic of p24 proteins and COPII coat composition mutually influence membrane scaffolding. *Current Biology : CB, 25*(10), 1296-1305.

REFERENCES

D'Arcangelo, J., Stahmer, K. R., and Miller, E. A. (2013). Vesicle-mediated export from the ER: COPII coat function and regulation.*Biochimia Et Biophysica Acta, 1833*, 2464-2472.

daSilva, L. L. P., Snapp, E. L., Denecke, J., Lippincott-Schwartz, J., Hawes, C., and Brandizzi, F. (2004). Endoplasmic reticulum export sites and golgi bodies behave as single mobile secretory units in plant cells. *The Plant Cell, 16*(7), 1753-1771.

daSilva, L. L. P., Taylor, J. P., Hadlington, J. L., Hanton, S. L., Snowden, C. J., Fox, S. J., Foresti, O., Brandizzi, F., and . Denecke, J. (2005). Receptor salvage from the prevacuolar compartment is essential for efficient vacuolar protein targeting. *The Plant Cell, 17*(1), 132-148.

De Caroli, M., Lenucci, M. S., Di Sansebastiano, G., Dalessandro, G., De Lorenzo, G., and Piro, G. (2011). Protein trafficking to the cell wall occurs through mechanisms distinguishable from default sorting in tobacco. *The Plant Journal, 65*(2), 295-308.

Denecke, J., De Rycke, R., and Botterman, J. (1992). Plant and mammalian sorting signals for protein retention in the endoplasmic reticulum contain a conserved epitope. *The EMBO Journal, 11*(6), 2345-2355.

Deng, Y., Humbert, S., Liu, J., Srivastava, R., Rothstein, S. J., and Howell, S. H. (2011). Heat induces the splicing by IRE1 of a mRNA encoding a transcription factor involved in the unfolded protein response in arabidopsis. *Proceedings of the National Academy of Sciences, 108*(17), 7247-7252.

Deng, Y., Srivastava, R., and Howell, S. H. (2013). Endoplasmic reticulum (ER) stress response and its physiological roles in plants. *International Journal of Molecular Sciences, 14*(4), 8188-8212.

Denzel, A., Otto, F., Girod, A., Pepperkok, R., Watson, R., Rosewell, I., Bergeron, J.J.M., Solarie, R.C.E. and Owen, M. J. (2000). The p24 family member p23 is required for early embryonic development. *Current Biology, 10*(1), 55-58. doi:10.1016/S0960-9822(99)00266-3

Di Sansebastiano, G., Paris, N., Marc-Martin, S., and Neuhaus, J. (1998). Specific accumulation of GFP in a non-acidic vacuolar compartment via a C-terminal propeptide-mediated sorting pathway. *The Plant Journal, 15*(4), 449-457.

Ding, Y., Robinson, D. G., and Jiang, L. (2014). Unconventional protein secretion (UPS) pathways in plants. *Current Opinion in Cell Biology, 29*, 107-115.

Ding, Y., Wang, J., Chun Lai, J. H., Ling Chan, V. H., Wang, X., Cai, Y., TAN, X., BAO, Y., XIA, J., ROBINSON, D.G. and Jiang, L. (2014). Exo70E2 is essential for exocyst subunit recruitment and EXPO formation in both plants and animals. *Molecular Biology of the Cell, 25*(3), 412-426.

Ding, Y., Wang, J., Wang, J., Stierhof, Y., Robinson, D. G., and Jiang, L. (2012). Unconventional protein secretion. *Trends in Plant Science, 17*(10), 606-615.

Dominguez, M., Dejgaard, K., Füllekrug, J., Dahan, S., Fazel, A., Paccaud, J., Thomas, D.Y., Bergeron, J.J.M. and Nilsson, T. (1998). gp25L/emp24/p24 protein family members of the cis-golgi network bind both COP I and II coatomer. *The Journal of Cell Biology, 140*(4), 751-765.

Donohoe, B. S., Kang, B., and Staehelin, L. A. (2007). Identification and characterization of COPIa- and COPIb-type vesicle classes associated with plant and algal golgi. *Proceedings of the National Academy of Sciences of the United States of America, 104*(1), 163-168.

Donohoe, B. S., Kang, B., Gerl, M. J., Gergely, Z. R., McMichael, C. M., Bednarek, S. Y., and Staehelin, L. A. (2013). Cis-golgi cisternal assembly and biosynthetic activation occur sequentially in plants and algae. *Traffic (Copenhagen, Denmark),14*(5), 551-567.

Donovan, K. W., and Bretscher, A. (2015). Tracking individual secretory vesicles during exocytosis reveals an ordered and regulated process. *The Journal of Cell Biology, 210*(2), 181-189.

Drakakaki, G., and Dandekar, A. (2013). Protein secretion: How many secretory routes does a plant cell have? *Plant Science,203–204*, 74-78.

Edwards, K., Johnstone, C., and Thompson, C. (1991). A simple and rapid method for the preparation of plant genomic DNA for PCR analysis. *Nucleic Acids Research, 19*(6), 1349.

Elrod-Erickson, M. J., and Kaiser, C. A. (1996). Genes that control the fidelity of endoplasmic reticulum to golgi transport identified as suppressors of vesicle budding mutations. *Molecular Biology of the Cell, 7*(7), 1043-1058.

Emery, G., Parton, R. G., Rojo, M., and Gruenberg, J. (2003). The trans-membrane protein p25 forms highly specialized domains that regulate membrane composition and dynamics. *Journal of Cell Science, 116*(23), 4821-4832.

REFERENCES

Emery, G., Rojo, M., and Gruenberg, J. (2000). Coupled transport of p24 family members. *Journal of Cell Science, 113*(13), 2507-2516.

Ericson, M. C., Gafford, J. T., and Elbein, A. D. (1977). Tunicamycin inhibits GlcNAc-lipid formation in plants. *Journal of Biological Chemistry, 252*(21), 7431-7433.

Fatal, N., Karhinen, L., Jokitalo, E., and Makarow, M. (2004). Active and specific recruitment of a soluble cargo protein for endoplasmic reticulum exit in the absence of functional COPII component Sec24p. *Journal of Cell Science, 117*(9), 1665-1673.

Foresti, O., daSilva, L. L. P., and Denecke, J. (2006). Overexpression of the arabidopsis syntaxin PEP12/SYP21 inhibits transport from the prevacuolar compartment to the lytic vacuole in vivo. *The Plant Cell, 18*(9), 2275-2293.

Fox, R. M., Hanlon, C. D., and Andrew, D. J. (2010). The CrebA/Creb3-like transcription factors are major and direct regulators of secretory capacity. *The Journal of Cell Biology, 191*(3), 479-492.

Fujita, M., Watanabe, R., Jaensch, N., Romanova-Michaelides, M., Satoh, T., Kato, M., Riezman, H., Yamaguchi, Y., Maeda, Y. and Kinoshita, T. (2011). Sorting of GPI-anchored proteins into ER exit sites by p24 proteins is dependent on remodeled GPI. *The Journal of Cell Biology, 194*(1), 61-75.

Füllekrug, J., Suganuma, T., Tang, B. L., Hong, W., Storrie, B., and Nilsson, T. (1999). Localization and recycling of gp27 (hp24γ3): Complex formation with other p24 family members. *Molecular Biology of the Cell, 10*(6), 1939-1955.

Gao, C., Yu, C. K. Y., Qu, S., San, M. W. Y., Li, K. Y., Lo, S. W., and Jiang, L. (2012). The golgi-localized arabidopsis endomembrane Protein12 contains both endoplasmic reticulum export and golgi retention signals at its C terminus. *The Plant Cell,24*(5), 2086-2104. doi:10.1105/tpc.112.096057

Gao, C., Cai, Y., Wang, Y., Kang, B., Aniento, F., Robinson, D. G., and Jiang, L. (2014). Retention mechanisms for ER and golgi membrane proteins. *Trends in Plant Science, 19*(8), 508.

Gimeno-Ferrer, F., Pastor-Cantizano, N., Bernat-Silvestre, C., Selvi-Martinez, P., Vera-Sirera, F., Gao, C., Pérez-Amador, M. A., Jiang, L., Aniento, F., and Marcote, M. J. α2-COP is involved in early secretory traffic in Arabidopsis and is required for plant growth. *Journal of Experimental Botany*. Accepted manuscript.

Gommel, D., Orci, L., Emig, E. m., Hannah, M. j., Ravazzola, M., Nickel, W., Helms, J.B., Wieland, F.T. and Sohn, K. (1999). p24 and p23, the major transmembrane proteins of COPI-coated transport vesicles, form hetero-oligomeric complexes and cycle between the organelles of the early secretory pathway. *FEBS Letters, 447*(2-3), 179-185.

Gong, P., Roseman, J., Fernandez, C. G., Vetrivel, K. S., Bindokas, V. P., Zitzow, L. A., Kar, S., Parent, A.T. and Thinakaran, G. (2011). Transgenic neuronal overexpression reveals that stringently regulated p23 expression is critical for coordinated movement in mice.*Molecular Neurodegeneration, 6*, 87.

Hanton, S. L., Bortolotti, L. E., Renna, L., Stefano, G., and Brandizzi, F. (2005). Crossing the divide – transport between the endoplasmic reticulum and golgi apparatus in plants. *Traffic, 6*(4), 267-277.

Hanton, S. L., Chatre, L., Renna, L., Matheson, L. A., and Brandizzi, F. (2007). De novo formation of plant endoplasmic reticulum export sites is membrane cargo induced and signal mediated. *Plant Physiology, 143*(4), 1640-1650.

Hartley, T., Siva, M., Lai, E., Teodoro, T., Zhang, L., and Volchuk, A. (2010). Endoplasmic reticulum stress response in an INS-1 pancreatic β-cell line with inducible expression of a folding-deficient proinsulin. *BMC Cell Biology, 11*, 59.

Hasegawa, H., Liu, L., and Nishimura, M. (2010). Dilysine retrieval signal-containing p24 proteins collaborate in inhibiting γ-cleavage of amyloid precursor protein. *Journal of Neurochemistry, 115*(3), 771-781.

Häweker, H., Rips, S., Koiwa, H., Salomon, S., Saijo, Y., Chinchilla, D., ROBATZEK, S. and von Schaewen, A. (2010). Pattern recognition receptors require N-glycosylation to mediate plant immunity. *The Journal of Biological Chemistry, 285*(7), 4629-4636.

Hawes, C., Osterrieder, A., Hummel, E., and Sparkes, I. (2008). The plant ER–Golgi interface. *Traffic, 9*(10), 1571-1580.

Hebert, D. N., Lamriben, L., Powers, E. T., and Kelly, J. W. (2014). The intrinsic and extrinsic effects of N-linked glycans on glycoproteostasis. *Nature Chemical Biology, 10*(11), 902-910.

Hetz, C. (2012). The unfolded protein response: Controlling cell fate decisions under ER stress and beyond. *Nature Reviews Molecular Cell Biology, 13*(2), 89-102.

REFERENCES

Hirata, R., Nihei, C., and Nakano, A. (2013). Isoform-selective oligomer formation of saccharomyces cerevisiae p24 family proteins. *The Journal of Biological Chemistry, 288*(52), 37057-37070.

Ho, H. H., Gilbert, M. T., Nussenzveig, D. R., and Gershengorn, M. C. (1999). Glycosylation is important for binding to human calcitonin receptors. *Biochemistry, 38*(6), 1866-1872.

Hosaka, M., Watanabe, T., Yamauchi, Y., Sakai, Y., Suda, M., Mizutani, S., Takeuchi, T., Isobe, T., and Izumi, T. (2007). A subset of p23 localized on secretory granules in pancreatic β-cells. *Journal of Histochemistry and Cytochemistry, 55*(3), 235-245.

Huang, C., and Tai, H. H. (1998). Prostaglandin E2 receptor EP3alpha subtype: The role of N-glycosylation in ligand binding as revealed by site-directed mutagenesis. *Prostaglandins, Leukotrienes, and Essential Fatty Acids, 59*(4), 265-271.

Hughes, H., Budnik, A., Schmidt, K., Palmer, K. J., Mantell, J., Noakes, C., Johnson, A., Carter, D.A., Verkade, P., Watson, P., and Stephens, D. J. (2009). Organisation of human ER-exit sites: Requirements for the localisation of Sec16 to transitional ER. *Journal of Cell Science, 122*(16), 2924-2934.

Hwang, I., and Robinson, D. G. (2009). Transport vesicle formation in plant cells. *Current Opinion in Plant Biology, 12*(6), 660-669.

Ito, Y., Uemura, T., and Nakano, A. (2014). Formation and maintenance of the golgi apparatus in plant cells. *International Review of Cell and Molecular Biology, 310*, 221.

Ito, Y., Uemura, T., Shoda, K., Fujimoto, M., Ueda, T., and Nakano, A. (2012). Cis-golgi proteins accumulate near the ER exit sites and act as the scaffold for golgi regeneration after brefeldin A treatment in tobacco BY-2 cells. *Molecular Biology of the Cell, 23*(16), 3203-3214.

Iwata, Y., Fedoroff, N. V., and Koizumi, N. (2008). Arabidopsis bZIP60 is a proteolysis-activated transcription factor involved in the endoplasmic reticulum stress response. *The Plant Cell, 20*(11), 3107-3121.

Iwata, Y., and Koizumi, N. (2005). An arabidopsis transcription factor, AtbZIP60, regulates the endoplasmic reticulum stress response in a manner unique to plants. *Proceedings of the National Academy of Sciences of the United States of America, 102*(14), 5280-5285.

Jackson, L. P. (2014). Structure and mechanism of COPI vesicle biogenesis. *Current Opinion in Cell Biology, 29*, 67-73.

Jancowski, S., Catching, A., Pighin, J., Kudo, T., Foissner, I., and Wasteneys, G. O. (2014). Trafficking of the myrosinase-associated protein GLL23 requires NUC/MVP1/GOLD36/ERMO3 and the p24 protein CYB. *The Plant Journal, 77*(4), 497-510.

Jenne, N., Frey, K., Brügger, B., and Wieland, F. T. (2002). Oligomeric state and stoichiometry of p24 proteins in the early secretory pathway , *Journal of Biological Chemistry, 277*(48), 46504-46511.

Jerome-Majewska, L. A., Achkar, T., Luo, L., Lupu, F., and Lacy, E. (2010). The trafficking protein Tmed2/p24β1 is required for morphogenesis of the mouse embryo and placenta. *Developmental Biology, 341*(1), 154-166.

Joosten, M. A. J. (2012). Isolation of apoplastic fluid from leaf tissue by the vacuum infiltration-centrifugation technique. In M. D. Bolton, and Thomma, Bart P H J (Eds.), *Plant fungal pathogens* (pp. 603-610) Humana Press.

Jürgens, G. (2004). Membrane trafficking in plants. *Annual Review of Cell and Developmental Biology, 20*(1), 481-504.

Kamauchi, S., Nakatani, H., Nakano, C., and Urade, R. (2005). Gene expression in response to endoplasmic reticulum stress in arabidopsis thaliana. *FEBS Journal, 272*(13), 3461-3476.

Kamitani, S., and Sakata, T. (2001). Glycosylation of human CRLR at Asn123 is required for ligand binding and signaling.*Biochimica Et Biophysica Acta (BBA) - Molecular Cell Research, 1539*(1–2), 131-139.

Kang, B., and Staehelin, L. A. (2008). ER-to-golgi transport by COPII vesicles in arabidopsis involves a ribosome-excluding scaffold that is transferred with the vesicles to the golgi matrix. *Protoplasma, 234*(1), 51-64.

Kaushal, S., and Khorana, H. G. (1994). Structure and function in rhodopsin. 7. point mutations associated with autosomal dominant retinitis pigmentosa. *Biochemistry, 33*(20), 6121-6128.

Kim, S., and Brandizzi, F. (2012). News and views into the SNARE complexity in arabidopsis. *Frontiers in Plant Science, 3*, 28.

REFERENCES

Klann, M., Koeppl, H., and Reuss, M. (2012). Spatial modeling of vesicle transport and the cytoskeleton: The challenge of hitting the right road. *PloS One, 7*(1), e29645.

Kleinboelting, N., Huep, G., Kloetgen, A., Viehoever, P., and Weisshaar, B. (2012). GABI-kat SimpleSearch: New features of the arabidopsis thaliana T-DNA mutant database. *Nucleic Acids Research, 40*(D1), D1215.

Koegler, E., Bonnon, C., Waldmeier, L., Mitrovic, S., Halbeisen, R., and Hauri, H. (2010). p28, a novel ERGIC/cis golgi protein, required for golgi ribbon formation. *Traffic (Copenhagen, Denmark), 11*(1), 70-89.

Koizumi, N., Martinez, I. M., Kimata, Y., Kohno, K., Sano, H., and Chrispeels, M. J. (2001). Molecular characterization of two arabidopsis Ire1 homologs, endoplasmic reticulum-located transmembrane protein kinases. *Plant Physiology, 127*(3), 949-962.

Koncz, C., and Schell, J.(1986). The promoter of TL-DNA gene 5 controls the tissue-specific expression of chimaeric genes carried by a novel type of agrobacterium binary vector. Molecular and General Genetics MGG, 204(3), 383-396.

Krause, C., Richter, S., Knöll, C., and Jürgens, G. (2013). Plant secretome — from cellular process to biological activity.*Biochimica Et Biophysica Acta (BBA) - Proteins and Proteomics, 1834*(11), 2429-2441.

Kuiper, R. P., Waterham, H. R., Rötter, J., Bouw, G., and Martens, G. J. M. (2000). Differential induction of two p24δ putative cargo receptors upon activation of a prohormoneproducing cell. *Molecular Biology of the Cell, 11*(1), 131-140.

Laemmli, U. K. (1970). Cleavage of structural proteins during the assembly of the head of bacteriophage T4. *Nature,227*(5259), 680-685.

Lai, Y., Stefano, G., and Brandizzi, F. (2014). ER stress signaling requires RHD3, a functionally conserved ER-shaping GTPase.*Journal of Cell Science, 127*(15), 3227-3232.

Langhans, M., Meckel, T., Kress, A., Lerich, A., and Robinson, D. G. (2012). ERES (ER exit sites) and the "Secretory unit concept".*Journal of Microscopy, 247*(1), 48-59.

Langhans, M., Marcote, M. J., Pimpl, P., Virgili-López, G., Robinson, D. G., and Aniento, F. (2008). In vivo trafficking and localization of p24 proteins in plant cells. *Traffic, 9*(5), 770-785.

Latijnhouwers, M., Gillespie, T., Boevink, P., Kriechbaumer, V., Hawes, C., and Carvalho, C. M. (2007). Localization and domain characterization of arabidopsis golgin candidates. *Journal of Experimental Botany, 58*(15-16), 4373-4386.

Lavoie, C., Paiement, J., Dominguez, M., Roy, L., Dahan, S., Gushue, J. N., and Bergeron, J. J. M. (1999). Roles for α2P24 and copi in endoplasmic reticulum cargo exit site formation. *The Journal of Cell Biology, 146*(2), 285-300.

Lerich, A., Hillmer, S., Langhans, M., Scheuring, D., van Bentum, P., and Robinson, D. G. (2012). ER import sites and their relationship to ER exit sites: A new model for bidirectional ER-golgi transport in higher plants. *Frontiers in Plant Science,* 3, 143.

Leucci, M. R., Sansebastiano, G. D., Gigante, M., Dalessandro, G., and Piro, G. (2007). Secretion marker proteins and cell-wall polysaccharides move through different secretory pathways. *Planta, 225*(4), 1001-1017.

Lewis, M. J., and Pelham, H. R. B. (1992). Ligand-induced redistribution of a human KDEL receptor from the golgi complex to the endoplasmic reticulum. *Cell, 68*(2), 353-364.

Lewis, M. J., Sweet, D. J., and Pelham, H. R. B. (1990). The ERD2 gene determines the specificity of the luminal ER protein retention system. *Cell, 61*(7), 1359-1363.

Li, X., Wu, Y., Shen, C., Belenkaya, T. Y., Ray, L., and Lin, X. (2015). Drosophila p24 and Sec22 regulate wingless trafficking in the early secretory pathway. Biochemical and Biophysical Research Communications, 463(4), 483-489.

Li, J., Zhao-Hui, C., Batoux, M., Nekrasov, V., Roux, M., Chinchilla, D., Zipfel, C., and Jones, J. D. G. (2009). Specific ER quality control components required for biogenesis of the plant innate immune receptor EFR. *Proceedings of the National Academy of Sciences, 106*(37), 15973-15978.

Liaunardy-Jopeace, A., Bryant, C. E., and Gay, N. J. (2014). The COPII adaptor protein TMED7 is required to initiate and mediate the anterograde trafficking of toll-like receptor 4 to the plasma membrane. *Science Signaling, 7*(336), ra70.

Liaunardy-Jopeace, A., and Gay, N. J. (2014). Molecular and cellular regulation of toll-like receptor-4 activity induced by lipopolysaccharide ligands. *Frontiers in Immunology, 5*, 473.

Liu, J., and Howell, S. H. (2010). bZIP28 and NF-Y transcription factors are activated by ER stress and assemble into a transcriptional complex to regulate stress response genes in arabidopsis. *The Plant Cell, 22*(3), 782-796.

Liu, J., Srivastava, R., Che, P., and Howell, S. H. (2007a). An endoplasmic reticulum stress response in arabidopsis is mediated by proteolytic processing and nuclear relocation of a membrane-associated transcription factor, bZIP28. *The Plant Cell,19*(12), 4111-4119.

Liu, J., Srivastava, R., Che, P., and Howell, S. H. (2007b). Salt stress responses in arabidopsis utilize a signal transduction pathway related to endoplasmic reticulum stress signaling. *The Plant Journal, 51*(5), 897-909.

Liu, L., Fujino, K., and Nishimura, M. (2015). Pre-synaptic localization of the γ-secretase-inhibiting protein p24α2 in the mammalian brain. *Journal of Neurochemistry, 133*(3), 422-431.

Liu, S., Zhang, S., Bromley-Brits, K., Cai, F., Zhou, W., Xia, K., Mittelholtz, J. and Song, W. (2011). Transcriptional regulation of TMP21 by NFAT.*Molecular Neurodegeneration, 6*, 21.

Liu, Y., and Li, J. (2014). Endoplasmic reticulum-mediated protein quality control in arabidopsis. *Plant Cell Biology, 5*, 162.

Liu, Y., Burgos, J. S., Deng, Y., Srivastava, R., Howell, S. H., and Bassham, D. C. (2012). Degradation of the endoplasmic reticulum by autophagy during endoplasmic reticulum stress in arabidopsis. *The Plant Cell, 24*(11), 4635-4651.

Lu, D., and Christopher, D. A. (2008). Endoplasmic reticulum stress activates the expression of a sub-group of protein disulfide isomerase genes and AtbZIP60 modulates the response in arabidopsis thaliana. *Molecular Genetics and Genomics,280*(3), 199-210.

Luo, W., Wang, Y., and Reiser, G. (2007). p24A, a type I transmembrane protein, controls ARF1-dependent resensitization of protease-activated receptor-2 by influence on receptor trafficking. *Journal of Biological Chemistry, 282*(41), 30246-30255.

Luo, W., Wang, Y., and Reiser, G. (2011). Proteinase-activated receptors, nucleotide P2Y receptors, and μ-opioid receptor-1B are under the control of the type I transmembrane proteins p23 and p24A in post-golgi trafficking. *Journal of Neurochemistry, 117*(1), 71-81.

Majoul, I., Sohn, K., Wieland, F. T., Pepperkok, R., Pizza, M., Hillemann, J., and Söling, H. (1998). KDEL receptor (Erd2p)-mediated retrograde transport of the cholera toxin A subunit from the golgi involves COPI, p23, and the COOH terminus of Erd2p.*The Journal of Cell Biology, 143*(3), 601-612.

Majoul, I., Straub, M., Hell, S. W., Duden, R., and Soeling, H. (2001). KDEL-cargo regulates interactions between proteins involved in COPI vesicle traffic: Measurements in living cells using FRET. *Developmental Cell, 1*(1), 139-153.

Maley, F., Trimble, R. B., Tarentino, A. L., and Plummer, T. H. (1989). Characterization of glycoproteins and their associated oligosaccharides through the use of endoglycosidases. *Analytical Biochemistry, 180*(2), 195-204.

Mancias, J. D., and Goldberg, J. (2008). Structural basis of cargo membrane protein discrimination by the human COPII coat machinery. *The EMBO Journal, 27*(21), 2918-2928.

Manzano-Lopez, J., Perez-Linero, A., Aguilera-Romero, A., Martin, M., Okano, T., Silva, D., Seeberger, P., Riezman, H., Funato, K., Goder, V., Wellinger, R., and. Muñiz, M. (2015). COPII coat composition is actively regulated by luminal cargo maturation. *Current Biology, 25*(2), 152-162.

Marelli, M., Smith, J. J., Jung, S., Yi, E., Nesvizhskii, A. I., Christmas, R. H., Saleem, R.A., Tam, Y.Y.C., Fagarasanu, A., Goodlett, D.R., Aebersold, R., Rachubinski, R.A., and Aitchison, J. D. (2004). Quantitative mass spectrometry reveals a role for the GTPase Rho1p in actin organization on the peroxisome membrane. *The Journal of Cell Biology, 167*(6), 1099-1112.

Marsh, M., and McMahon, H. T. (1999). The structural era of endocytosis. *Science, 285*(5425), 215-220.

Marti, L., Fornaciari, S., Renna, L., Stefano, G., and Brandizzi, F. (2010). COPII-mediated traffic in plants. *Trends in Plant Science,15*(1), 522-528.

Marzioch, M., Henthorn, D. C., Herrmann, J. M., Wilson, R., Thomas, D. Y., Bergeron, J. J., SOLARI, R.C., and Rowley, A. (1999). Erp1p and Erp2p, partners for Emp24p and Erv25p in a yeast p24 complex. *Molecular Biology of the Cell, 10*(6), 1923-1938.

Miller, E. A., and Barlowe, C. (2010). Regulation of coat assembly- sorting things out at the ER. *Current Opinion in Cell Biology,22*(4), 447-453.

Miller, E. A., Beilharz, T. H., Malkus, P. N., Lee, M. C. S., Hamamoto, S., Orci, L., and Schekman, R. (2003). Multiple cargo binding sites on the COPII subunit Sec24p ensure capture of diverse membrane proteins into transport vesicles. *Cell, 114*(4), 497-509.

Mironov, A. A. (2014). ER-golgi transport could occur in the absence of COPII vesicles. *Nature Reviews. Molecular Cell Biology, 15*(3), 1.

Mishiba, K., Nagashima, Y., Suzuki, E., Hayashi, N., Ogata, Y., Shimada, Y., and Koizumi, N. (2013). Defects in IRE1 enhance cell death and fail to degrade mRNAs encoding secretory pathway proteins in the arabidopsis unfolded protein response.*Proceedings of the National Academy of Sciences, 110*(14), 5713-5718.

Mitrovic, S., Ben-Tekaya, H., Koegler, E., Gruenberg, J., and Hauri, H. (2008). The cargo receptors Surf4, endoplasmic reticulum-golgi intermediate compartment (ERGIC)-53, and p25 are required to maintain the architecture of ERGIC and golgi.*Molecular Biology of the Cell, 19*(5), 1976-1990.

Montesinos, J. C., Langhans, M., Sturm, S., Hillmer, S., Aniento, F., Robinson, D. G., and Marcote, M. J. (2013). Putative p24 complexes in arabidopsis contain members of the delta and beta subfamilies and cycle in the early secretory pathway.*Journal of Experimental Botany, 64*(11), 3147-3167.

Montesinos, J. C., Pastor-Cantizano, N., Robinson, D. G., Marcote, M. J., and Aniento, F. (2014). Arabidopsis p24δ5 and p24δ9 facilitate coat protein I-dependent transport of the K/HDEL receptor ERD2 from the golgi to the endoplasmic reticulum.*The Plant Journal, 80*(6), 1014-1030.

Montesinos, J. C., Sturm, S., Langhans, M., Hillmer, S., Marcote, M. J., Robinson, D. G., and Aniento, F. (2012). Coupled transport of arabidopsis p24 proteins at the ER–Golgi interface. *Journal of Experimental Botany, 63*(11), 4243-4261.

Moremen, K. W., Tiemeyer, M., and Nairn, A. V. (2012). Vertebrate protein glycosylation: Diversity, synthesis and function. *Nature Reviews. Molecular Cell Biology, 13*(7), 448-462.

Mossessova, E., Bickford, L. C., and Goldberg, J. (2003). SNARE selectivity of the COPII coat. *Cell, 114*(4), 483-495.

Muñiz, M., Nuoffer, C., Hauri, H. P., and Riezman, H. (2000). The Emp24 complex recruits a specific cargo molecule into endoplasmic reticulum-derived vesicles. *The Journal of Cell Biology, 148*(5), 925-930.

Munro, S., and Pelham, H. R. B. (1987). A C-terminal signal prevents secretion of luminal ER proteins. *Cell, 48*(5), 899-907.

Nagae, M., Hirata, T., Morita-Matsumoto, K., Theiler, R., Fujita, M., Kinoshita, T., and Yamaguchi, Y. (2016). 3D structure and interaction of p24β and p24δ golgi dynamics domains: Implication for p24 complex formation and cargo transport.*Journal of Molecular Biology, 428*(20), 4087-4099.

Nagashima, Y., Mishiba, K., Suzuki, E., Shimada, Y., Iwata, Y., and Koizumi, N. (2011). Arabidopsis IRE1 catalyses unconventional splicing of bZIP60 mRNA to produce the active transcription factor. *Scientific Reports, 1,* 29.

Nanjo, Y., Oka, H., Ikarashi, N., Kaneko, K., Kitajima, A., Mitsui, T., Muñoz, F.J., Rodríguez-López, M., Baroja-Fernández, E. and Pozueta-Romero, J. (2006). Rice plastidial N-glycosylated nucleotide pyrophosphatase/phosphodiesterase is transported from the ER-golgi to the chloroplast through the secretory pathway. *The Plant Cell, 18*(10), 2582-2592.

Nebenführ, A., Frohlick, J. A., and Staehelin, L. A. (2000). Redistribution of golgi stacks and other organelles during mitosis and cytokinesis in plant cells. *Plant Physiology, 124*(1), 135-152.

Nebenführ, A., Gallagher, L. A., Dunahay, T. G., Frohlick, J. A., Mazurkiewicz, A. M., Meehl, J. B., and Staehelin, L. A. (1999). Stop-and-go movements of plant golgi stacks are mediated by the acto-myosin system. *Plant Physiology, 121*(4), 1127-1141.

Nickel, W., Sohn, K., Bünning, C., and Wieland, F. T. (1997). p23, a major COPI-vesicle membrane protein, constitutively cycles through the early secretory pathway. *Proceedings of the National Academy of Sciences of the United States of America,94*(21), 11393-11398.

Niemes, S., Labs, M., Scheuring, D., Krueger, F., Langhans, M., Jesenofsky, B., Robinson, D.G., and Pimpl, P. (2010). Sorting of plant vacuolar proteins is initiated in the ER. *The Plant Journal, 62*(4), 601-614.

Niemes, S., Langhans, M., Viotti, C., Scheuring, D., San Wan Yan, M., Jiang, L., Hillmer, S., Robinson, D.G. and Pimpl, P. (2010). Retromer recycles vacuolar sorting receptors from the trans-golgi network. *The Plant Journal, 61*(1), 107-121.

Noh, S., Kwon, C. S., and Chung, W. (2002). Characterization of two homologs of Ire1p, a kinase/endoribonuclease in yeast, in arabidopsis thaliana. *Biochimica Et Biophysica Acta (BBA) - Gene Structure and Expression, 1575*(1–3), 130-134.

REFERENCES

Osiecka-Iwan, A., Niderla-Bielinska, J., Hyc, A., and Moskalewski, S. (2014). Rat chondrocyte-associated antigen identified as sialylated transmembrane protein Tmp21 belonging to the p24 protein family. *Calcified Tissue International, 94*(3), 348-352.

Pang, R. T., Ng, S. S., Cheng, C. H., Holtmann, M. H., Miller, L. J., and Chow, B. H. (1999). Role of N-linked glycosylation on the function and expression of the human secretin receptor. *Endocrinology, 140*(11), 5102-5111.

Park, M., and Jürgens, G. (2012). Membrane traffic and fusion at post-golgi compartments. *Frontiers in Plant Science, 2*, 111.

Pastor-Cantizano, N., Montesinos, J. C., Bernat-Silvestre, C., Marcote, M. J., and Aniento, F. (2016). P24 family proteins: Key players in the regulation of trafficking along the secretory pathway. *Protoplasma, 253*(4), 967-985.

Paul, M. J., and Frigerio, L. (2007). Coated vesicles in plant cells. *Seminars in Cell and Developmental Biology, 18*(4), 471-478.

Pelham, H. R. B. (2001). SNAREs and the specificity of membrane fusion. *Trends in Cell Biology, 11*(3), 99-101.

Pfeffer, S. R. (2001). *Rab GTPases: Specifying and deciphering organelle identity and function*. England: Elsevier Ltd.

Pfeffer, S. R. (2013). A prize for membrane magic. *Cell, 155*(6), 1203-1206.

Phillipson, B. A., Pimpl, P., daSilva, L. L. P., Crofts, A. J., Taylor, J. P., Movafeghi, A., Robinson, D.G., and Denecke, J. (2001). Secretory bulk flow of soluble proteins is efficient and COPII dependent. *The Plant Cell, 13*(9), 2005-2020.

Pinedo, M., Regente, M., Elizalde, M., Quiroga, I. Y., Pagnussat, L. A., Jorrin-Novo, J., Maldonado, A. and de la Canal, L. (2012). Extracellular sunflower proteins: Evidence on non-classical secretion of a jacalin-related lectin. *Protein and Peptide Letters, 19*(3), 270-276.

Pfaffl MW. (2004). Quantification strategies in real-time PCR. In: Bustin SA, ed. A-Z of quantitative PCR. La Jolla, CA, USA: International University Line (IUL), 87 – 112.

Popoff, V., Adolf, F., Brügger, B., and Wieland, F. (2011). COPI budding within the golgi stack. *Cold Spring Harbor Perspectives in Biology, 3*(11), a005231.

Port, F., Hausmann, G., and Basler, K. (2011). A genome-wide RNA interference screen uncovers two p24 proteins as regulators of wingless secretion. *EMBO Reports, 12*(11), 1144-1152.

Richter, S., Voß, U., and Jürgens, G. (2009). Post-Golgi traffic in plants. *Traffic, 10*(7), 819-828.

Robinson, D. G., Brandizzi, F., Hawes, C., and Nakano, A. (2015). Vesicles versus tubes: Is endoplasmic reticulum-golgi transport in plants fundamentally different from other eukaryotes?1. *Plant Physiology, 168*(2), 393-406.

Robinson, D. G., Ding, Y., and Jiang, L. (2016). Unconventional protein secretion in plants: A critical assessment. *Protoplasma,253*(1), 31-43.

Robinson, D. G., Herranz, M., Bubeck, J., Pepperkok, R., and Ritzenthaler, C. (2007). Membrane dynamics in the early secretory pathway. *Critical Reviews in Plant Sciences, 26*(4), 199-225.

Robinson, D. G., and Pimpl, P. (2014). Clathrin and post-golgi trafficking: A very complicated issue. *Trends in Plant Science,19*(3), 134-139.

Rojo, M., Emery, G., Marjomaki, V., McDowall, A. W., Parton, R. G., and Gruenberg, J. (2000). The transmembrane protein p23 contributes to the organization of the golgi apparatus. *Journal of Cell Science, 113*(6), 1043-1057.

Rojo, M., Pepperkok, R., Emery, G., Kellner, R., Stang, E., Parton, R. G., and Gruenberg, J. (1997). Involvement of the transmembrane protein p23 in biosynthetic protein transport. The Journal of Cell Biology, 139(5), 1119-1135.

Rothman, J. E., and Wieland, F. T. (1996). Protein sorting by transport vesicles. *Science, 272*(5259), 227-234.

Rötter, J., Kuiper, R. P., Bouw, G., and Martens, G. J. M. (2002). Cell-type-specific and selectively induced expression of members of the p24 family of putative cargo receptors. *Journal of Cell Science, 115*(5), 1049.

Ruberti, C., and Brandizzi, F. (2014). Conserved and plant-unique strategies for overcoming endoplasmic reticulum stress.*Frontiers in Plant Science, 5*, 69.

Scheel, A. A., and Pelham, H. R. B. (1996). Purification and characterization of the human KDEL receptor. *Biochemistry, 35*(31), 10203-10209.

REFERENCES

Scheuring, D., Viotti, C., Krüger, F., Künzl, F., Sturm, S., Bubeck, J., Hillmer, S., Frigerio, L., Robinson, D.G. and Pimpl, P. (2011). Multivesicular bodies mature from the trans-golgi network/early endosome in arabidopsis. *The Plant Cell, 23*(9), 3463-3481.

Schimmöller, F., Singer-Krüger, B., Schröder, S., Krüger, U., Barlowe, C., and Riezman, H. (1995). The absence of Emp24p, a component of ER-derived COPII-coated vesicles, causes a defect in transport of selected proteins to the golgi. *The EMBO Journal, 14*(7), 1329-1339.

Schröter, S., Beckmann, S., and Schmitt, H. D. (2016). ER arrival sites for COPI vesicles localize to hotspots of membrane trafficking. *The EMBO Journal, 35*(17), 1935-1955.

Schuiki, I., and Volchuk, A. (2012). Diverse roles for the p24 family of proteins in eukaryotic cells. *BioMolecular Concepts, 3*(6), 561-570.

Semenza, J. C., Hardwick, K. G., Dean, N., and Pelham, H. R. B. (1990). ERD2, a yeast gene required for the receptor-mediated retrieval of luminal ER proteins from the secretory pathway. *Cell, 61*(7), 1349-1357.

Semenzin, T.R. (2014). Studies on *Arabidopsis* p24delta proteins: characterization of a p24delta9 mutant and overexpression of p24delta5. Tesi di laurea. Università degli studi di Milano.

Sessions, A., Burke, E., Presting, G., Aux, G., McElver, J., Patton, D., Dietrich, B., Ho, P., Bacwaden, J., Ko, C., Clarke, J.D., Cotton, D., Bullis, D., Snell, J., Miguel, T., Hutchison, D., Kimmerly, B., Mitzel, T., Katagiri, F., Glazebrook, J., Law, M. and Goff, S. A. (2002). A high-throughput arabidopsis reverse genetics system. *The Plant Cell, 14*(12), 2985-2994.

Shen, J., Ding, Y., Gao, C., Rojo, E., and Jiang, L. (2014). N-linked glycosylation of AtVSR1 is important for vacuolar protein sorting in arabidopsis. *The Plant Journal, 80*(6), 977-992.

Singer-Krüger, B., Frank, R., Crausaz, F., and Riezman, H. (1993). Partial purification and characterization of early and late endosomes from yeast. identification of four novel proteins. *Journal of Biological Chemistry, 268*(19), 14376-14386.

Sohn, K., Orci, L., Ravazzola, M., Amherdt, M., Bremser, M., Lottspeich, F., Fiedler, K., Helms, J.B. and Wieland, F. T. (1996). A major transmembrane protein of golgi-derived COPI-coated vesicles involved in coatomer binding. *The Journal of Cell Biology, 135*(5), 1239-1248.

Song, Z., Sun, L., Lu, S., Tian, Y., Ding, Y., and Liu, J. (2015). Transcription factor interaction with COMPASS-like complex regulates histone H3K4 trimethylation for specific gene expression in plants. *Proceedings of the National Academy of Sciences, 112*(9), 2900-2905.

Springer, S., Chen, E., Duden, R., Marzioch, M., Rowley, A., Hamamoto, S., Merchant, S., and Schekman, R. (2000). The p24 proteins are not essential for vesicular transport in saccharomyces cerevisiae. *Proceedings of the National Academy of Sciences of the United States of America, 97*(8), 4034-4039.

Srivastava, R., Chen, Y., Deng, Y., Brandizzi, F., and Howell, S. H. (2012). Elements proximal to and within the transmembrane domain mediate the organelle-to-organelle movement of bZIP28 under ER stress conditions. *The Plant Journal, 70*(6), 1033-1042.

Srivastava, R., Deng, Y., and Howell, S. H. (2014). Stress sensing in plants by an ER stress sensor/transducer, bZIP28. *Plant Cell Biology, 5*, 59.

Srivastava, R., Deng, Y., Shah, S., Rao, A. G., and Howell, S. H. (2013). BINDING PROTEIN is a master regulator of the endoplasmic reticulum stress sensor/transducer bZIP28 in arabidopsis. *The Plant Cell, 25*(4), 1416-1429.

Stamnes, M. A., Craighead, M. W., Hoe, M. H., Lampen, N., Geromanos, S., Tempst, P., and Rothman, J. E. (1995). An integral membrane component of coatomer-coated transport vesicles defines a family of proteins involved in budding. *Proceedings of the National Academy of Sciences of the United States of America, 92*(17), 8011-8015.

Stefano, G., Renna, L., Chatre, L., Hanton, S. L., Moreau, P., Hawes, C., and Brandizzi, F. (2006). In tobacco leaf epidermal cells, the integrity of protein export from the endoplasmic reticulum and of ER export sites depends on active COPI machinery. *The Plant Journal, 46*(1), 95-110.

Stephens, D. J., and Pepperkok, R. (2001). Illuminating the secretory pathway: When do we need vesicles? *Journal of Cell Science, 114*(6), 1053.

Strasser, R. (2016). Plant protein glycosylation. *Glycobiology, 26*(9), 926-939.

REFERENCES

Strating, J R P M, and Martens, G. J. M. (2009). The p24 family and selective transport processes at the ER-golgi interface.*Biology of the Cell, 101*(9), 495-509.

Strating, Jeroen R P M, Bakel, Nick H M van, Leunissen, J. A. M., and Martens, G. J. M. (2009). A comprehensive overview of the vertebrate p24 family: Identification of a novel tissue-specifically expressed member. *Molecular Biology and Evolution,26*(8), 1707-1714.

Sztul, E., and Lupashin, V. (2009). Role of vesicle tethering factors in the ER–Golgi membrane traffic. *FEBS Letters, 583*(23), 3770-3783.

Szul, T., and Sztul, E. (2011). COPII and COPI traffic at the ER-golgi interface. *Physiology, 26*(5), 348-364.

Takagi, J., Renna, L., Takahashi, H., Koumoto, Y., Tamura, K., Stefano, G., Fukao, Y., Kondo, M., Nishimura, M., Shimada, T., Brandizzi, F., and Hara-Nishimura, I. (2013). MAIGO5 functions in protein export from golgi-associated endoplasmic reticulum exit sites in arabidopsis. *The Plant Cell, 25*(11), 4658-4675.

Takida, S., Maeda, Y., and Kinoshita, T. (2008). Mammalian GPI-anchored proteins require p24 proteins for their efficient transport from the ER to the plasma membrane. *The Biochemical Journal, 409*(2), 555-562.

Theiler, R., Fujita, M., Nagae, M., Yamaguchi, Y., Maeda, Y., and Kinoshita, T. (2014). The α-helical region in p24γ2 subunit of p24 protein cargo receptor is pivotal for the recognition and transport of glycosylphosphatidylinositol-anchored proteins.*The Journal of Biological Chemistry, 289*(24), 16835-16843.

Tissier, A. F., Marillonnet, S., Klimyuk, V., Patel, K., Torres, M. A., Murphy, G., and Jones, J. D. (1999). Multiple independent defective suppressor-mutator transposon insertions in arabidopsis: A tool for functional genomics. *The Plant Cell,11*(10), 1841-1852.

Titorenko, V. I., and Mullen, R. T. (2006). Peroxisome biogenesis: The peroxisomal endomembrane system and the role of the ER. *The Journal of Cell Biology, 174*(1), 11-17.

Townsley, F. M., Wilson, D. W., and Pelham, H. R. (1993). Mutational analysis of the human KDEL receptor: Distinct structural requirements for golgi retention, ligand binding and retrograde transport. *The EMBO Journal, 12*(7), 2821-2829.

Travers, K. J., Patil, C. K., Wodicka, L., Lockhart, D. J., Weissman, J. S., and Walter, P. (2000). Functional and genomic analyses reveal an essential coordination between the unfolded protein response and ER-associated degradation. *Cell, 101*(3), 249-258.

Tse, Y. C., Mo, B., Hillmer, S., Zhao, M., Lo, S. W., Robinson, D. G., and Jiang, L. (2004). Identification of multivesicular bodies as prevacuolar compartments in nicotiana tabacum BY-2 cells. *The Plant Cell, 16*(3), 672-693.

Uemura, T., and Ueda, T. (2014). Plant vacuolar trafficking driven by RAB and SNARE proteins. *Current Opinion in Plant Biology,22*, 116-121.

Valencia, J. P., Goodman, K., and Otegui, M. S. (2016). Endocytosis and endosomal trafficking in plants. *Annual Review of Plant Biology, 67*(1), 309-335.

van der Hoorn, Renier A L, Wulff, B. B. H., Rivas, S., Durrant, M. C., van der Ploeg, A., de Wit, Pierre J G M, and Jones, J. D. G. (2005). Structure–Function analysis of cf-9, a receptor-like protein with extracytoplasmic leucine-rich repeats. *The Plant Cell, 17*(3), 1000-1015.

van Noorden, R., and Ledford, H. (2016). Medicine nobel for research on how cells 'eat themselves'. *Nature News, 538*(7623), 18.

Vetrivel, K. S., Gong, P., Bowen, J. W., Cheng, H., Chen, Y., Carter, M., Nguyen, P.D., Placanica, L., Wieland, F.T., Li, Y., Kounnas, M.Z. and Thinakaran, G. (2007). Dual roles of the transmembrane protein p23/TMP21 in the modulation of amyloid precursor protein metabolism. *Molecular Neurodegeneration, 2*, 4.

Vetrivel, K. S., Kodam, A., Gong, P., Chen, Y., Parent, A. T., Kar, S., and Thinakaran, G. (2008). Localization and regional distribution of p23/TMP21 in the brain. *Neurobiology of Disease, 32*(1), 37-49.

Viotti, C. (2014). ER and vacuoles: Never been closer. *Frontiers in Plant Science, 5*, 20.

Viotti, C., Bubeck, J., Stierhof, Y., Krebs, M., Langhans, M., van den Berg, W., van Dongen, W., Richter, S., Geldner, N., Takano, J., Jürgens, G., De Vries, S.C., Robinson, D.G. and Schumacher, K. (2010). Endocytic and secretory traffic in arabidopsis merge in the trans-golgi network/early endosome, an independent and highly dynamic organelle. *The Plant Cell, 22*(4), 1344-1357.

Vukašinović, N., and Žárský, V. (2016). Tethering complexes in the arabidopsis endomembrane system. *Frontiers in Cell and Developmental Biology, 4*, 46.

REFERENCES

Wada, I., Rindress, D., Cameron, P. H., Ou, W. J., Doherty, J. J., Louvard, D., Bell, A.W., Dignard, D., Thomas, D.Y., and Bergeron, J. J. (1991). SSR alpha and associated calnexin are major calcium binding proteins of the endoplasmic reticulum membrane. Journal of Biological Chemistry, 266(29), 19599-19610.

Walter, P., and Ron, D. (2011). The unfolded protein response: From stress pathway to homeostatic regulation. *Science,334*(6059), 1081-1086.

Wan, S., and Jiang, L. (2016). Endoplasmic reticulum (ER) stress and the unfolded protein response (UPR) in plants.*Protoplasma, 253*(3), 753-764.

Wang, J., Ding, Y., Wang, J., Hillmer, S., Miao, Y., Lo, S. W., Wang, X., Robinson, D.G. and Jiang, L. (2010). EXPO, an exocyst-positive organelle distinct from multivesicular endosomes and autophagosomes, mediates cytosol to cell wall exocytosis in arabidopsis and tobacco cells. *The Plant Cell, 22*(12), 4009-4030.

Wang, S., Narendra, S., and Fedoroff, N. (2007). Heterotrimeric G protein signaling in the arabidopsis unfolded protein response.*Proceedings of the National Academy of Sciences, 104*(10), 3817-3822.

Wang, X., Yang, R., Jadhao, S. B., Yu, D., Hu, H., Glynn-Cunningham, N., Sztalryd, C., Silver, K.D. and Gong, D. (2012). Transmembrane Emp24 protein transport domain 6 is selectively expressed in pancreatic islets and implicated in insulin secretion and diabetes.*Pancreas, 41*(1)

Wang, X., Sun, P., O'Gorman, M., Tai, T., and Paller, A. S. (2001). Epidermal growth factor receptor glycosylation is required for ganglioside GM3 binding and GM3-mediated suppresion of activation. *Glycobiology, 11*(7), 515-522.

Weigel, D., and Glazebrook, J. (2002). Arabidopsis. *A Laboratory Manual, 165*

Wen, C., and Greenwald, I. (1999). p24 proteins and quality control of LIN-12 and GLP-1 trafficking in caenorhabditis elegans.*The Journal of Cell Biology, 145*(6), 1165-1175.

Whitehead, T. P., Kricka, L. J., Carter, T. J., and Thorpe, G. H. (1979). Analytical luminescence: Its potential in the clinical laboratory. *Clinical Chemistry, 25*(9), 1531.

Wilson, D. W., Lewis, M. J., and Pelham, H. R. (1993). pH-dependent binding of KDEL to its receptor in vitro. *Journal of Biological Chemistry, 268*(10), 7465-7468.

Woody, S. T., Austin-Phillips, S., Amasino, R. M., and Krysan, P. J. (2007). The WiscDsLox T-DNA collection: An arabidopsis community resource generated by using an improved high-throughput T-DNA sequencing pipeline. *Journal of Plant Research, 120*(1), 157-165.

Woollard, A. A., and Moore, I. (2008). The functions of rab GTPases in plant membrane traffic. *Current Opinion in Plant Biology,11*(6), 610-619.

Wu, F., Shen, S., Lee, L., Lee, S., Chan, M., and Lin, C. (2009). Tape-arabidopsis sandwich - a simpler arabidopsis protoplast isolation method. *Plant Methods, 5*(1), 16.

Xiang, Y., Zhang, X., Nix, D. B., Katoh, T., Aoki, K., Tiemeyer, M., and Wang, Y. (2013). Regulation of protein glycosylation and sorting by the golgi matrix proteins GRASP55/65. *Nature Communications, 4*, 1659.

Xie, J., Yang, Y., Li, J., Hou, J., Xia, K., Song, W., and Liu, S. (2014). Expression of tmp21 in normal adult human tissues.*International Journal of Clinical and Experimental Medicine, 7*(9), 2976-2983.

Xu, G., Li, S., Xie, K., Zhang, Q., Wang, Y., Tang, Y., Liu, D., Hong, Y., He, C. and Liu, Y. (2012). Plant ERD2-like proteins function as endoplasmic reticulum luminal protein receptors and participate in programmed cell death during innate immunity. *The Plant Journal,72*(1), 57-69.

Xu, G., and Liu, Y. (2012). Plant ERD2s self-interact and interact with GTPase-activating proteins and ADP-ribosylation factor 1. Plant Signaling & Behavior, 7(9), 1092-1094.

Yamamoto, K., Fujii, R., Toyofuku, Y., Saito, T., Koseki, H., Hsu, V. W., and Aoe, T. (2001). The KDEL receptor mediates a retrieval mechanism that contributes to quality control at the endoplasmic reticulum. *The EMBO Journal, 20*(12), 3082-3091.

Yamamoto, M., Maruyama, D., Endo, T., and Nishikawa, S. (2008). Arabidopsis thaliana has a set of J proteins in the endoplasmic reticulum that are conserved from yeast to animals and plants. *Plant and Cell Physiology, 49*(10), 1547-1562.

Yang, B., Hoe, M. H., Black, P., and Hunt, R. C. (1993). Role of oligosaccharides in the processing and function of human transferrin receptors. effect of the loss of the three N-glycosyl oligosaccharides individually or together. *Journal of Biological Chemistry, 268*(10), 7435-7441.

REFERENCES

Yang, Y., Elamawi, R., Bubeck, J., Pepperkok, R., Ritzenthaler, C., and Robinson, D. G. (2005). Dynamics of COPII vesicles and the golgi apparatus in cultured nicotiana tabacum BY-2 cells provides evidence for transient association of golgi stacks with endoplasmic reticulum exit sites. *The Plant Cell, 17*(5), 1513-1531.

Yoo, S., Cho, Y., and Sheen, J. (2007). Arabidopsis mesophyll protoplasts: A versatile cell system for transient gene expression analysis. *Nature Protocols, 2*(7), 1565-1572.

Zelazny, E., Santambrogio, M., Pourcher, M., Chambrier, P., Berne-Dedieu, A., Fobis-Loisy, I., MiègE, C., Jaillais, Y. and Gaude, T. (2013). Mechanisms governing the endosomal membrane recruitment of the core retromer in arabidopsis. *The Journal of Biological Chemistry, 288*(13), 8815-8825.

Zhang, L., and Volchuk, A. (2010). P24 family type 1 transmembrane proteins are required for insulin biosynthesis and secretion in pancreatic β-cells. *FEBS Letters, 584*(11), 2298-2304.

Zhang, L., Chen, H., Brandizzi, F., Verchot, J., and Wang, A. (2015). The UPR branch IRE1- bZIP60 in plants plays an essential role in viral infection and is complementary to the only UPR pathway in yeast. *PLOS Genet, 11*(4), e1005164.

Zhang, Z., Austin, S. C., and Smyth, E. M. (2001). Glycosylation of the human prostacyclin receptor: Role in ligand binding and signal transduction. *Molecular Pharmacology, 60*(3), 480-487.

Zimmermann, P., Hirsch-Hoffmann, M., Hennig, L., and Gruissem, W. (2004). GENEVESTIGATOR. arabidopsis microarray database and analysis toolbox. *Plant Physiology, 136*(1), 2621-2632.

APPENDIX

APPENDIX 1. Primers used for PCR reactions

Table A1. List of primers used in this thesis for genotyping and RT-sqPCR analysis.

Name	Gene	Sequence (5'→ 3')	Tm (ºC)
p24 genes			
LPδ3	*p24δ3*	TATACTGTACCAAGCCACCCG	56.6
RPδ3	*p24δ3*	CCGTCAAGGTAAGTGTCTTCG	56.6
RTRPδ3	*p24δ3*	GATGACTGCTAAGATGCGCCGTG	63.8
δ45	*p24δ4*	GGATCCACTTAGATCTCCTCAAAATTC	57.9
δ43c	*p24δ4*	CACGGTGCCATAAGGTGCTGT	62.4
LP24M11	*p24δ5*	GAAGACCATCGTTGTTCTCCGATGGC	66.7
RP241	*p24δ5*	TTGGTGATGAAGATTGTTCCC	54.8
LPGδ6	*p24δ6*	TAAACATACGCGTTACGTCCC	56.5
RPGδ6	*p24δ6*	TCTCCATATGGGAAGGAACTG	54.2
RTδ63	*p24δ6*	GGATCCACGACAATAGCTACTCCTA	57.7
RTδ75	*p24δ7*	GATTTCTCTCTATATCGGAGCCGTC	57.9
RTδ73	*p24δ7*	CAATCTCTGCCCTCAGGAGATGG	61.7
LPδ8	*p24δ8*	GATCATTGCGTTGTTATCTCC	52.2
δ83'utr	*p24δ8*	GGATCCGTGTGCATGTCTACTAC	56.6
RTsδ83	*p24δ8*	GGATCCGAATTGTAGACCAGCC	59.7
LPwδ9	*p24δ9*	TGTCTGAGATTGTCATGTGGG	54.4
RPwδ9	*p24δ9*	CCAAGGTTATGGAGTCGTGAG	55.9
δ9-5	*p24δ9*	GGATCCGATCACTCAATCTCTGTACA	59.0
δ9-3	*p24δ9*	GGATCCAGATTCTGCATCTCTTCTTCC	62.0
LPδ10	*p24δ10*	ACGAAGTACCCAAGGTTCCAC	57.6
RP10	*p24δ10*	CCGGTAACAATTACCATCACG	56.3
δ105	*p24δ10*	ACAAAGTGTATCGCCGAAGACATC	59.6
δ103	*p24δ10*	GCATCCCTGCAACTCCTATGCAGA	64.0
LP243	*p24δ11*	ACCGTTGGGACTTATTCCATC	56.2
RP24M33	*p24δ11*	CTTGATCAGAGGAGCTTCTTC	51.6
At5g22130			
LPGM	*At5g22130*	AAATTTGGGTGAATGTTTGGG	57.1
RPGM	At5g22130	ACCGTTGCATTTGTCACTTTC	56.7

Name	Gene	Sequence (5'→ 3')	Tm (ºC)
COPI genes			
LPα1	*α1-COP*	AGAATTACCTTGGCGAAGAGC	56.5
NRPα1	*α1-COP*	GGATCCGTGCCATTATCGTTGAGAGATT	69.0
LPNGα2	*α2-COP*	GGATCCCATAATCATTCTGACTTGT	71.0
RPGα2	*α2-COP*	GCGTACCAGCAGACAAAGAAC	59.8
RPβ2	β*2-COP*	AGATATGGTTGGAATCCTGCC	55.7
β1RT5	β*1-COP*	GGATCCTCACCTGACGAATCCACCACC	67.0
β1RT3	β*1-COP*	GGATCCAATCCTCTCATACGAATCAT	57.6
RT5β1'	β*1'-COP*	CGATGGCGTGAATTCGAGTG	56.3
RPβ1'	β*1'-COP*	TGTAACCAATTGCCCAGACTC	56.1
RT5β2'utr	β*2'-COP*	TTTCTCCGATCGCCGGTTAG	57.0
LPβ3'	β*3'-COP*	CTTCACTCTTCACCAACCCTA	53.5
RPβ3'	β*3'-COP*	ATGCAGATGGAATGATGAAGC	54.6
utrγ5	*γ-COP*	GCGCGAGATCTGAGTGACGGAG	60.8
Utr2γ3	*γ-COP*	ATAGATGACATTCTCTGATACTG	42.2
NLPdelta	*δ-COP*	ATCCTAGCAAAATCCGAGAAAA	52.2
RPdelta	*δ-COP*	CGTACCACTTCCTGCTCTGA	56.4
Z1-5	*ζ-COP*	CTGCCAAAGTCCAAAGGAGAGT	57.2
Z1-3	*ζ-COP*	AAGAACGGTAACTATCTCCCAAGTGC	58.4
Z2-5	*ζ-COP*	ACACTGAAACAGCGAAAGGAG	55.4
Z2-3	*ζ-COP*	CATTCATGCATTGCACAAAGC	53.8
Z3-5	*ζ-COP*	GCAAGCTCTCATCTTCTTCAG	53.4
Z3-3	*ζ-COP*	GGGGTTGATTTCTAGTGAACGGGTAA	58.5
Housekeeping genes			
Act25	*ACT-2*	GTTGGGATGAACCAGAAGGA	57.3
Act23	*ACT-2*	GAACCACCGATCCAGACACT	59.4
A5	*ACT-7*	GGAAAACTCACCACCACGAACCAG	64.4
A3	*ACT-7*	GGATCCAAATGGCCGATGGTGAGG	66.1
INSERTION			
LBb1	T-DNA	GGATCCGCGTGGACCGCTTGCTGCAACT	77.7
LBG	T-DNA	ATATTGACCATCATACTCATTGC	50.5
L4	T-DNA	TGATCCATGTAGATTTCCCGGACATGAAG	65.4
Spm32	dSpm	TACGAATAAGAGCGTCCATTTTAGAGTGA	60.8

APPENDIX 2. Primers used for RT-qPCR

Table A2. List of primers used in this thesis for RT-qPCR analysis.

Name	Gene	Sequence (5'→ 3')	Tm (ºC)
p24 genes			
qPCRd35F	*p24δ3*	GACTGCTAAGATGCGCCGTGAA	59
qPCRd35R	*p24δ3*	ATACAGCCTCACCGACCGGAAT	59
qPCRd45F	*p24δ4*	ATTCCGACGACGATCTTACTCTCAG	58
qPCRd45R	*p24δ4*	CGGTGTGAGGTACAGTAAGCCA	58
qPCRd5utrF	*p24δ5*	CGTTGTGGTTGTGGGTTCACAG	58
qPCRd5utrR	*p24δ5*	GTAAGAGTATCCTTCAGGCCAAGTTTC	57
qPCRd6F	*p24δ6*	ACGCAAGTGCTATTAGGGCCAACATAC	60
qPCRd6R	*p24δ6*	GACCCTCGTGTTTGTCTTCTCGTT	59
qPCRd7F	*p24δ7*	GGTCGCAGGTCTTCAGTTTTGGCA	61
qPCRd7R	*p24δ7*	GCCCTCAGGAGATGGTAATGGTTTTC	59
qPCRd8F	*p24δ8*	GGCTGGTCTACAATTCTGGC	59
qPCRd8R	*p24δ8*	GTGTGTGCATGTCTACTACTTAGATGAG	59
qPCRd9F	*p24δ9*	TCTTTTCCCAACTCAAAGGAGTCTTC	57
qPCRd9R	*p24δ9*	TTCCAGTTCCGAGAGTACATACTCAA	57
qPCRd10F	*p24δ10*	CTGAAACTCTCTACTACGGGGTTGGT	59
qPCRd10R	*p24δ10*	AGCCATTGATCTAATGTACAACACCC	57
qPCRd11F	*p24δ11*	GCAGCTCTCAGTTTACTGTCGTTCGTG	61
qPCRd11R	*p24δ11*	CCAAGAATGACTTGAGGTGCCGTAGTT	60
COPI genes			
5-gamma	*γ-COP*	GCTGACAGTTAGAGCTGAAGACGTT	58.7
3-gamma	*γ-COP*	AAGAGGTTTTAGCCGCTGGCAA	59.6
COPII genes			
Sec31AIF	*SEC31A*	AACGTGATTTTGGTGCAGCGTTA	57.9
Sec31AR	*SEC31A*	TGGAAGCCAAGAACTGCACTCATC	59.5
Sec31BF	*SEC31B*	CAGCAGCTGGACCCATAGGATTTAC	53.9
Sec31BR	*SEC31B*	GCTGTGTTGGAGGACTTGCTGGTTG	62.2

Name	Gene	Sequence (5'→ 3')	Tm (ºC)
UPR genes			
qPCRBIP12F	*BiP1/2*	CCACCGGCCCCAAGAG	59.1
qPCRBIP12R	*BiP1/2*	GGCGTCCACTTCGAATGTG	56.5
qPCRBIP3F	*BiP3*	AACCGCGAGCTTGGAAAAT	55.5
qPCRBIP3R	*BiP3*	TCCCCTGGGTGCAGGAA	59.2
qPCRERDJ3AF	*ERDJ3A*	TCAAGTGGTGGTGGTTTCAACT	56.9
qPCRERDJ3AR	*ERDJ3A*	CCCACCGCCCATATTTTG	54.1
qPCRERDJ3BF	*ERDJ3B*	GAGGAGGCGGCATGAATATG	55.8
qPCRERDJ3BR	*ERDJ3B*	CCATCGAACCTCCACCAAAA	55.3
qPCRCRT1F	*CRT1*	GATCAAGAAGGAGGTCCCATGT	56.4
qPCRCRT1R	*CRT1*	GACGGAGGACGAAGGTGTACA	58.5
qPCRPDI6F	*PDI6*	CGAAGTGGCTTTGTCATTCCA	55.7
qPCRPDI6R	*PDI6*	GCGGTTGCGTCCAATTTT	54.6
qPCRbZIPF	*bZIP60s*	GGAGACGATGATGCTGTGGCT	59.6
qPCRbZIPR	*bZIP60s*	CAGGGAACCCAACAGCAGACT	59.5
Housekeeping genes			
qPCRUBIQF	*UBIQ10*	GGCCTTGATTAATCCCTGATGAATAAG	55.7
qPCRUBIQR	*UBIQ10*	AAAGAGATAACAGGAACGGAAACATAGT	56.1

APPENDIX 3. Identification of a T-DNA insertion mutant of *p24δ3*

Table A3. Segregation analysis (sulfadiazine resistance) of *p24δ3E10* lines.

Plant	Number of seeds analyzed	Resistance to Sulfadiazine + (R)	Resistance to Sulfadiazine - (S)	Segregation R:S
E10.1	40	26	14	3:1
E10.2	40	29	11	3:1
E10.3	40	29	11	3:1
E10.4	40	40	0	40:0
E10.5	40	40	0	40:0
E10.6	40	40	0	40:0
E10.7	40	40	0	40:0
E10.8	40	30	10	3:1
E10.9	40	29	11	3:1
E10.10	40	28	12	3:1

R, resistant; S, sensitive.

Segregation of *p24δ3E10.01, p24δ3E10.02, p24δ3E10.03, p24δ3E10.08, p24δ3E10.09* and *p24δ3E10.10* lines correlated with a heterozygous line for the T-DNA insertion. In contrast, *p24δ3E10.04, p24δ3E10.05, p24δ3E10.06, p24δ3E10.07* segregation ratio corresponded to a homozygous line.

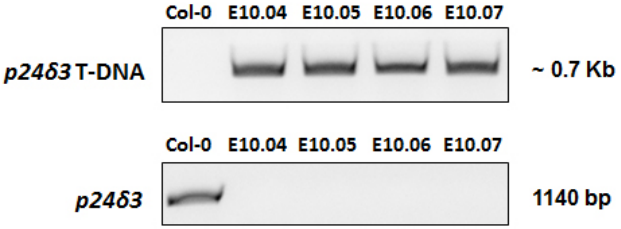

Figure A3.1. Identification of *p24δ3E10* homozygous plants for the T-DNA insertion in the *p24δ3* gene. Genomic DNA extraction from 13-days- old seedlings of the lines that showed to be resistant to sulfadiazine (see Table A3) and wild-type, and PCR were performed as described in sections 4.1.2. and 4.2.3. of Materials and methods. Upper panel: the presence of the T-DNA insertion was checked by a first PCR using the primers RPδ3 (specific of *p24δ3*) and LBG (specific of T-DNA). Lowe panel: homozygous lines were confirmed by a second PCR using p24δ3 specific primers (RPδ3/LPδ3) which are located at both sides of the insertion. The PCRs consisted of 26 cycles. Col-0., wild-type plant.

APPENDIX 4. Identification of a T-DNA insertion mutant of *p24δ6*

Table A4. Segregation analysis (sulfadiazine resistance) of *p24δ6* lines.

Plant	Number of seeds analyzed	Resistance to Sulfadiazine + (R)	Resistance to Sulfadiazine - (S)	Segregation R:S
p24δ6.38	40	17	23	1:1
p24δ6.39	40	30	10	3:1
p24δ6.40	40	34	6	3:1
p24δ6.41	40	35	5	3:1
p24δ6.42	40	23	17	1:1
p24δ6.43	40	25	15	1:1
p24δ6.44	40	36	4	1:1
p24δ6.45	40	40	0	40:0
p24δ6.46	40	38	2	15:1
p24δ6.47	40	21	19	1:1
p24δ6.48	40	40	0	40:0
p24δ6.49	40	36	4	3:1

R, resistant; S, sensitive.

Segregation of *p24δ6.38*, *p24δ6.42*¸ *p24δ6.43*, *p24δ6.44*, *p24δ6.46* and *p24δ6.47* lines did not adjust to any expected segregation (section 2.4. of Materials and methods). Segregation of *p24δ6.39*, *p24δ6.40*, *p24δ6.41* and *p24δ6.49* fitted the 3:1 (resistant:sensitive) segregation ratio, which correlated with a heterozygous line. Only segregation of *p24δ6.45* and *p24δ6.48* fitted the 40:0 (resistant:sensitives) segregation ratio, which correlated with a homozygous line.

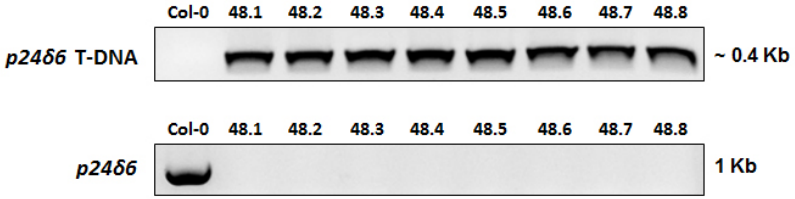

Figure A4.1. Identification of *p24δ6.48* homozygous plants for the T-DNA insertion in the *p24δ6* gene. Genomic DNA extraction from 30-days-old *p24δ6.48* (resistant to sulfadiazine, see Table A4) and wild-type plants, and PCR were performed as described in sections 4.1.2. and 4.2.3. of Materials and methods. Upper panel: the presence of the T-DNA insertion was checked by a first PCR using the primers RPGδ6 (specific of *p24δ6*) and LBG (specific of T-DNA). Lower panel: homozygous lines were confirmed by a second PCR using p24δ6 specific primers (RPGδ6/LPGδ6) which are located at both sides of the insertion. The PCRs consisted of 36 cycles. Col-0., wild-type plant.

APPENDIX 5. Identification of a T-DNA insertion mutant of *p24δ7*

Table A5. Segregation analysis (sulfadiazine resistance) of GK_503A10 lines.

Plant	Number of seeds analyzed	Resistance to Sulfadiazine + (R)	Resistance to Sulfadiazine - (S)	Segregation R:S
p24δ7-1	40	39	1	39:1
p24δ7-2	37	30	7	3:1
p24δ7-3	39	38	1	38:1
p24δ7-4	37	36	1	36:1
p24δ7-5	37	36	1	36:1

R, resistant; S, sensitive.

All lines tested, except *p24δ7-2,* showed a sulfadiazine resistance segregation that corresponds to two T-DNA insertions. Segregation of *p24δ7-2* corresponds to a heterozygous line for one T-DNA insertion. Seedlings of *p24δ7-1*, *p24δ7-2* and *p24δ7-5* lines were transferred to soil.

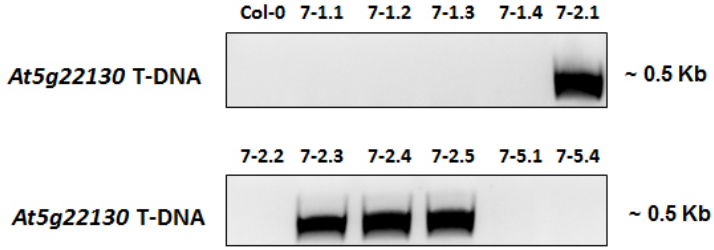

Figure A5.1. Identification of GK_503A10 lines with a T-DNA insertion in the *At5g22130* gene. Genomic DNA extraction from 7-days-old seedlings of *p24δ7*-1, *p24δ7-2* and *p24δ7-5* lines and wild-type, and PCR was performed as described in sections 4.1.2. and 4.2.3 of Materials and methods. The presence of the T-DNA insertion was checked by a first PCR using the LGB primer (specific for T-DNA) and the RPG primer (At5g22130 specific). The PCRs consisted of 36 cycles. Col-0, wild-type plant. A T-DNA insertion in the At5g22130 gene is detected in plants from the *p24δ7-2* line.

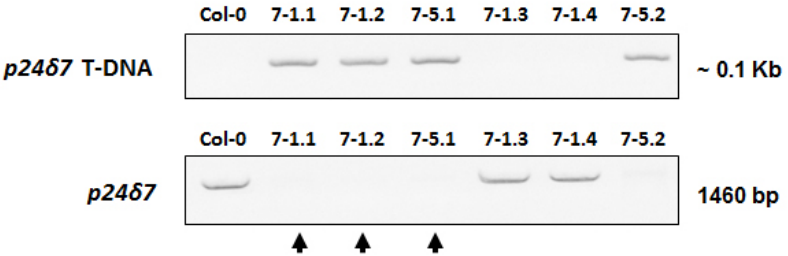

Figure A5.2. Identification of GK_503A10 7 homozygous plants for the T-DNA insertion in the *p24δ7* gene. Genomic DNA extraction from 7-day-old seedlings of *p24δ7*-1 and *p24δ7-5* lines (lines that do not have a T-DNA insertion in the At5g22130 gene, Figure A5.1.) and PCR was performed as described in sections 4.1.2. and 4.2.3. of Materials and methods. Upper panel: The presence of the T-DNA insertion was checked by a first PCR using the LGB primer (specific for T-DNA) and the RTδ73 primer (*p24δ7* specific). Lower panel: homozygous plants were confirmed by a second PCR using RTδ75 and RTδ73 primers, which are specific primers located at both sides of the insertion. The PCRs consisted of 36 cycles. Arrows indicate the plants identified as homozygous for the T-DNA insertion in *p24δ7* that were chosen to verify the absence of *p24δ7* mRNA. Col-0, wild-type plant.

APPENDIX 6. Identification of a T-DNA insertion mutant of *p24δ8*

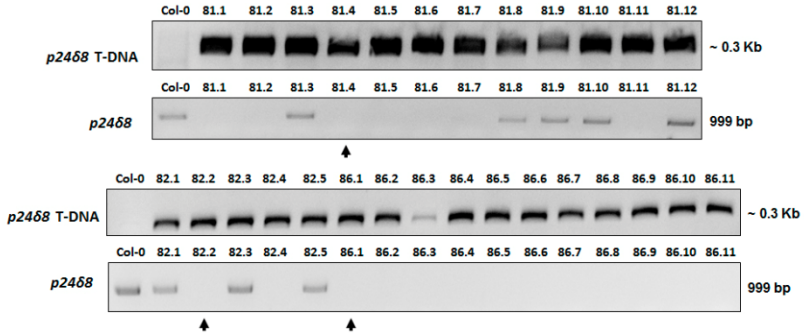

Figure A6.1. Identification of *p24δ8.81*, *p24δ8.82* and *p24δ8.86* homozygous plants for the dSpm transposon insertion in the *p24δ8* gene. Genomic DNA extraction from 30-day-old plants and PCR was performed as described in sections 4.1.2. and 4.2.3. of Materials and methods. Upper panels: the presence of the transposon insertion was checked by a first PCR using the Spm32 primer (specific for SM transposon) and the RTsδ83 primer (p24δ8 specific). Lower panels: homozygous plants were selected by a second PCR reaction using LPδ8 and δ83'utr primers, which are p24δ8 specific and are located at both sides of the insertion. The PCRs consisted of 36 cycles. Arrows indicate the plants identified as homozygous for the T-DNA insertion in p24δ8 that were chosen to verify the absence of p24δ8 mRNA. Col-0, wild-type plant.

81.1-12, 82.1-5, and 86.1-11 plants were from the *p24δ8.81 p24δ8.82* and *p24δ8.86* lines, respectively.

APPENDIX 7. Generation of the quadruple *p24δ3δ4δ5δ6* mutant

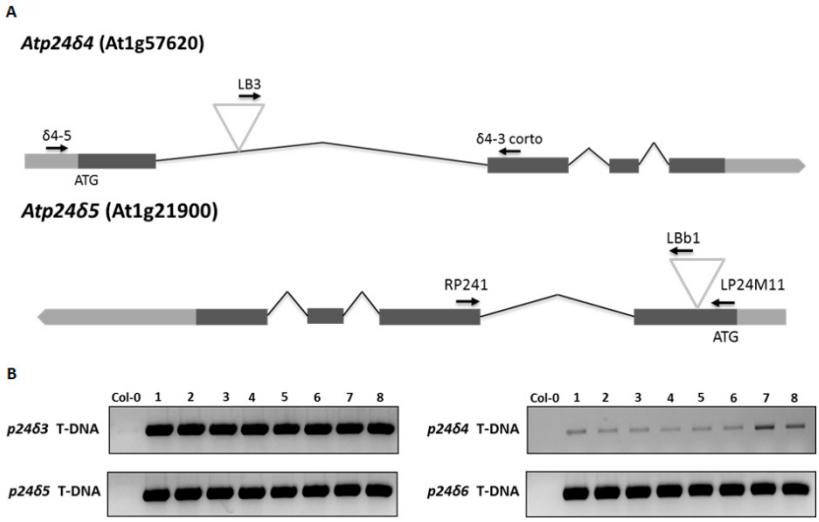

Figure A7.1. Identification by PCR of F1 plants from crosses of *p24δ3δ4δ5* with *p24δ4δ5δ6*. A) Diagrams of the *p24δ4* and *24δ5* genes and localization of the T-DNA insertion (triangle) in the *p24δ4* (SAIL_664_A06) and p24*δ5* (SALK_016402) mutants, respectively. Black boxes represent coding regions and grey boxes represent 5'-UTR and 3'-UTR regions. The primers used to identify the homozygous mutant plants are shown. The diagrams of the *p24δ3* and *24δ6* genes are in Figures 20 and 22. B) PCR Identification of 8 F1 plants with the T-DNA insertions in p24δ3, p24δ4, p24δ5 and p24δ6 genes from crosses of p*24δ3δ4δ5* (♀) with *p24δ4δ5δ6* (♂) (P1-4) and the reciprocal crosses (P5-8). For the PCRs, genomic DNA from rosette leaves of individual plants grown 4 weeks was used. The primers used for the identification of the corresponding insertions are in Table 8. The PCRs consisted of 36 cycles (see section 4.2.3. Materials and Methods). Col-0, wild-type plant. All F1 plants (plants 1-8) contain T-DNA insertions in the *p24δ3*, *p24δ4*, *p24δ5* and *p24δ6* genes. The DNA fragments amplified have the expected molecular weight (Table 8). Plant 1 was selected and F2 seeds collected to obtain the homozygous F2 plants for T-DNA insertions in the p24δ3, p24δ4, p24δ5 and p24δ6 genes.

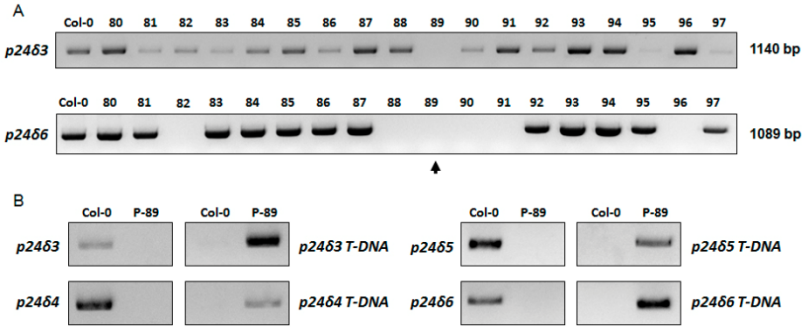

Figure A7.2. Identification by PCR of homozygous *p24δ3δ4δ5δ6* F2 plants for T-DNA insertions in *p24δ3, p24δ4,* p24δ5 and p24δ6 genes. 120 F2 seeds of F1 P1 (see Figure A7.1.) were sown in MS medium. All seeds germinated and after 8 days, 110 F2 plants were transferred to soil. A) PCRs of genomic DNA from (80-97) individual F2 30 days-old- plants were performed using the primers for the identification of the wild-type alleles for *p24δ3* (upper panel) and *p24δ6* (lower panel). The arrow indicates no amplification in both PCRs when using the genomic DNA of plant 89 that confirmed the absence of the wild-type allele of *p24δ3* and *p24δ6***.** B) PCRs of genomic DNA from *p24δ3δ4δ5δ6-89* plant that confirms that is homozygous for the T-DNA insertion in the *p24δ3, p24δ4, p24δ5* and *p24δ6* genes. PCRs for the identification of the corresponding insertions are in the right panels and for the identification of the wild-type allele in left panels. The primers used are in Table 8. The PCRs consisted of 36 cycles (see section 4.2.3. of Materials and Methods). The DNA fragments amplified have the expected molecular weight (Table 8). Col-0, wild-type plant.

APPENDIX 8. Generation of the quadruple *p24δ7δ8δ9δ10* mutant

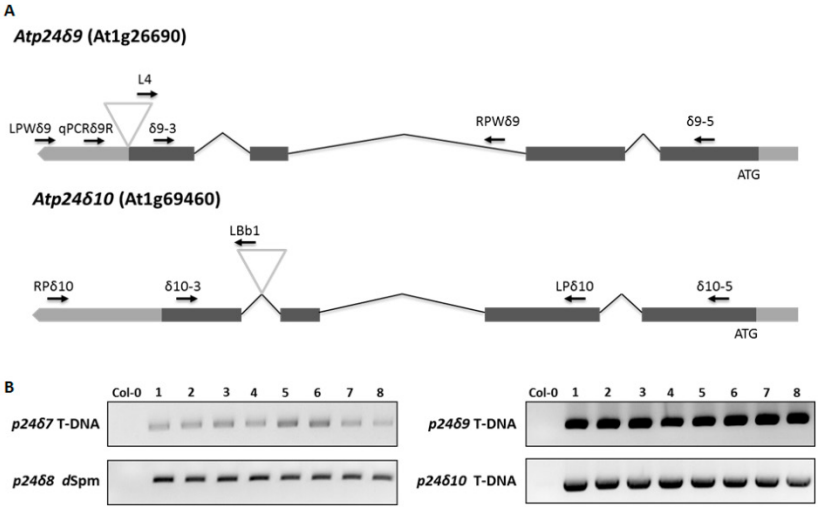

Figure A8.1. Identification by PCR of F1 plants from crosses of *p24δ7δ9δ10* with *p24δ8δ9δ10*. Diagrams of the *p24δ94* and p*24δ10* genes and localization of the T-DNA insertion (triangle) in the *p24δ9* (WiscDSLosHs161_04H) and *p24δ10* (SALK_144586) mutants, respectively. Black boxes represent coding regions and grey boxes represent 5'-UTR and 3'-UTR regions. The primers used to identify the homozygous mutant plants are shown. The diagrams of the *p24δ7* and *p24δ8* genes are in Figures 24 and 26. B) PCR Identification of 8 F1 plants with the insertions in p24δ7, p24δ8, p24δ9 and p24δ10 genes from crosses of *p24δ7δ9δ10* (♀) with *p24δ8δ9δ10* (♂) (P1-4) and the reciprocal crosses (P5-8). For the PCRs, genomic DNA from rosette leaves of individual plants grown 4 weeks was used. The primers used for the identification of the corresponding insertions are in Table 9. The PCRs consisted of 36 cycles (see section 4.2.3. of Materials and Methods). Col-0, wild-type plant. All F1 plants (plants 1-8) contain insertions in the *p24δ7*, *p24δ8*, *p24δ9* and *p24δ10* genes. The DNA fragments amplified have the expected molecular weight (Table 9). Plant 1 was selected and F2 seeds collected to obtain the homozygous F2 plants for T-DNA insertions in the p24δ7, p24δ8, p24δ9 and p24δ10 genes.

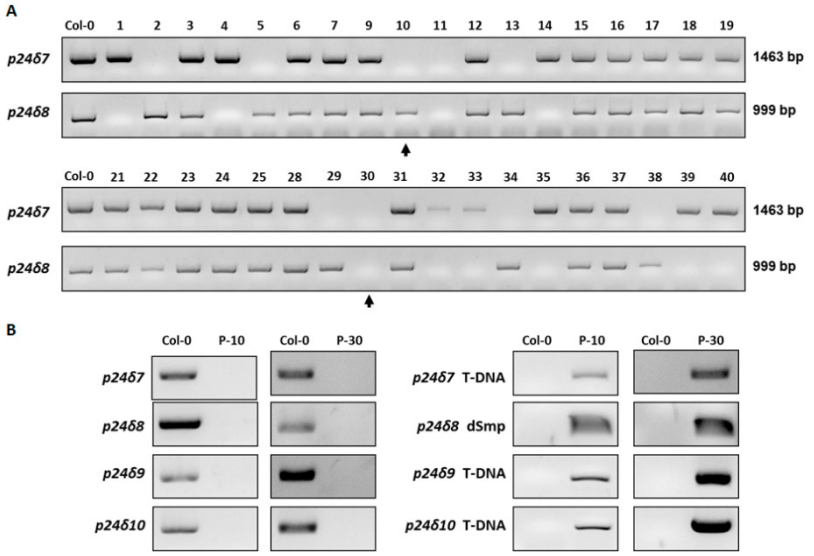

Figure A8.2. Identification by PCR of homozygous *p24δ7δ8δ9δ10* F2 plants from p24δ7δ9δ10 with 24δ8δ9δ10 for T-DNA insertions in *p24δ7, p24δ8,* p24δ9 and p24δ10 genes. 120 F2 seeds of F1 P1 (see Figure 1) were sown in MS medium. All seeds germinated and after 8 days, 100 F2 plants were transferred to soil. A) PCRs of genomic DNA from individual F2 30 days-old- plants were performed using the primers for the identification of the wild-type alleles for *p24δ7* (upper panel) and *p24δ8* (lower panel). The arrows indicate no amplification in both PCRs when using the genomic DNA of plants P10 and P30 that confirmed the absence of the wild-type allele of *p24δ7* and *p24δ8* in both plants**.** B) PCRs of genomic DNA from *p24δ7δ8δ9δ10-10 and p24δ7δ8δ9δ10-30* plants that confirms that are homozygous for the T-DNA insertion in the *p24δ7, p24δ8, p24δ9* and *p24δ10* genes. PCRs for the identification of the corresponding insertions are in the right panels and for the identification of the wild-type allele in left panels. The primers used are in Table 9. The PCRs consisted of 36 cycles (see section 4.2.3. of Materials and Methods). The DNA fragments amplified have the expected molecular weight (Table 9). Col-0, wild-type plant.

APPENDIX 9. Overexpression of ERD2a-YFP in *p24δ3δ4δ5δ6* and *p24δ7δ8δ9δ10* mutants

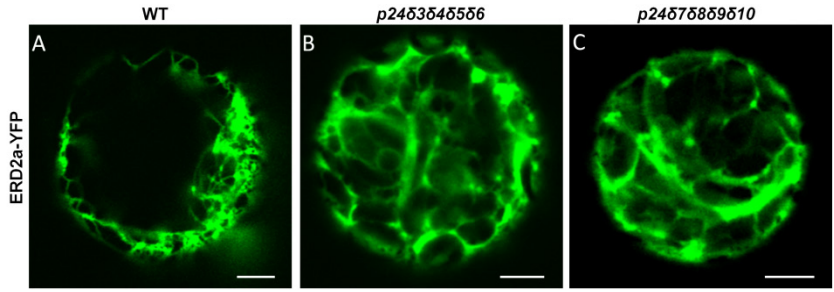

Figure A9. Overexpression of ERD2a-YFP in *p24δ3δ4δ5δ6* and *p24δ7δ8δ9δ10*. Transient gene expression in *Arabidopsis* protoplasts obtained from wild-type (Col-0), *p24δ3δ4δ5δ6* or *p24δ7δ8δ9δ10* plants grown 4 weeks in soil. ERD2a-YFP was partially localized in the ER in protoplasts obtained from wild-type, *p24δ3δ4δ5δ6* or *p24δ7δ8δ9δ10* plants. WT, wild-type (col-0). Scale bars = 5 µm.

APPENDIX 10. Germination of *p24δ3δ4δ5δ6* and *p24δ7δ8δ9δ10* seeds under ER stress conditions

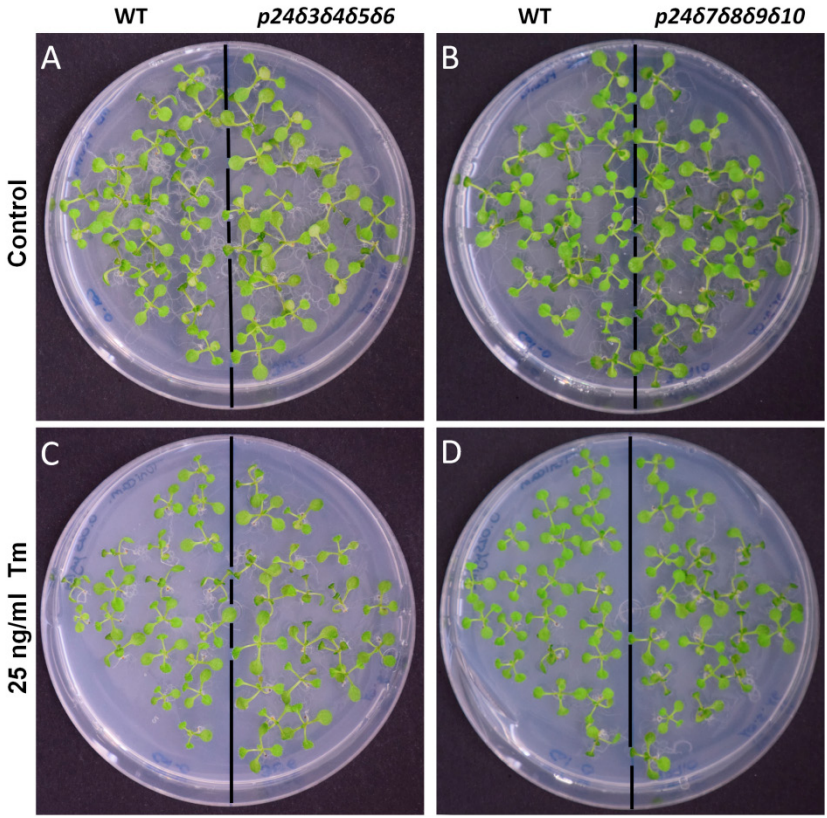

Figure A10.1. Germination of *p24δ3δ4δ5δ6* and *p24δ7δ8δ9δ10* seeds under ER stress conditions. Wild-type, *p24δ3δ4δ5δ6* and *p24δ7δ8δ9δ10* were germinated on MS medium supplemented or not with 25 ng/ml Tm for 10 days. Col-O, wild-type plant.

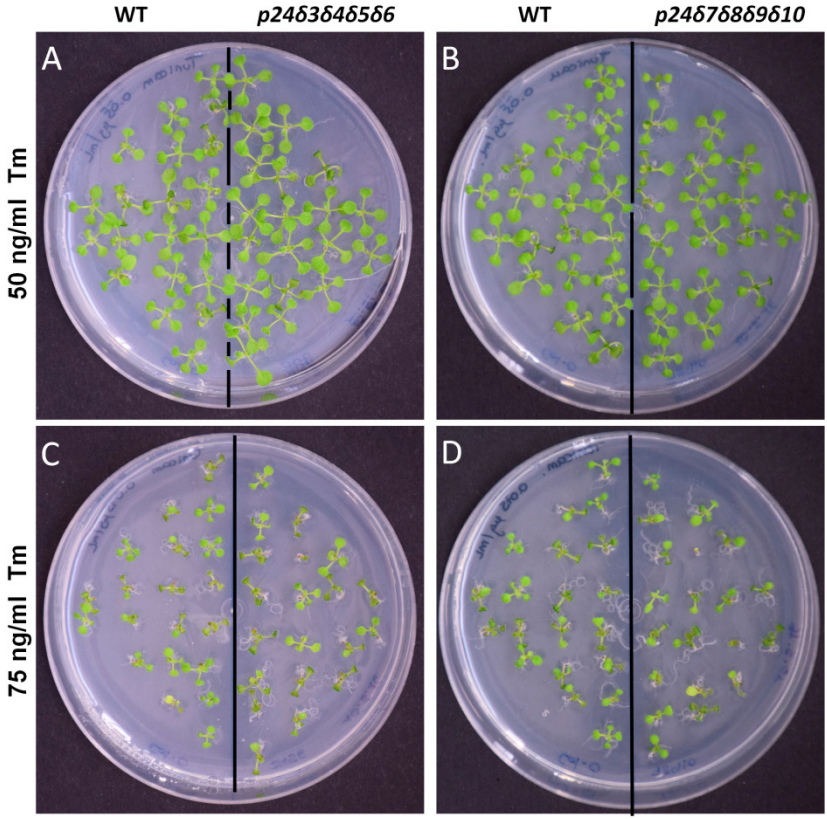

Figure A10.2. Germination of *p24δ3δ4δ5δ6* and *p24δ7δ8δ9δ10* seeds under ER stress conditions. Wild-type, *p24δ3δ4δ5δ6* and *p24δ7δ8δ9δ10* were germinated on MS medium containing 75 or 100 ng/ml Tm for 10 days. Col-0, wild-type plant.

APPENDIX 11. Analysis of COPI genes in *p24δ3δ4δ5δ6* and p*24δ7δ8δ9δ10* mutants

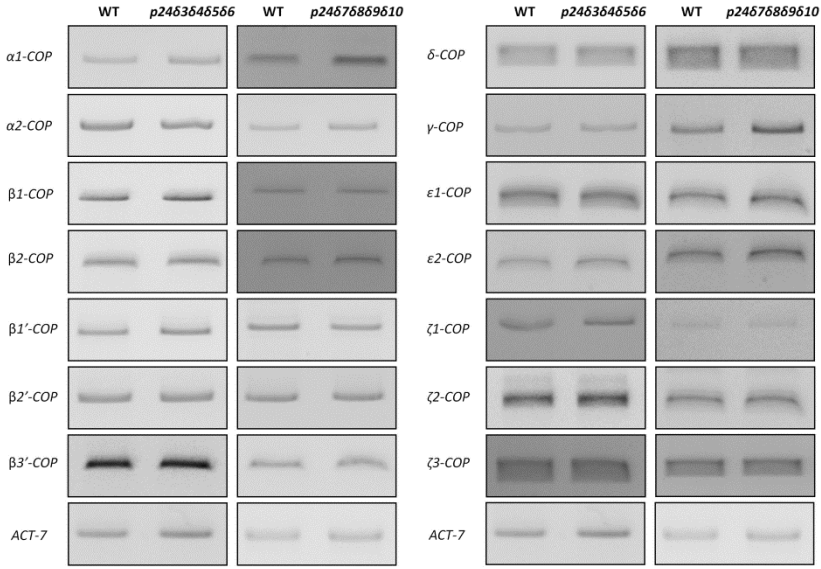

Figure A11. RT-sqPCR analysis of COPI genes in *p24δ3δ4δ5δ6* and *p24δ7δ8δ9δ10* mutants. Total RNA from *p24δ3δ4δ5δ6, p24δ7δ8δ9δ10* and wild-type (Col-0) 7-days-old seedlings were used for the RT-PCR. In the PCRs, specific primers for COPI genes were used (Appendix 1, Table A1). *Actin-7* (*ACT7*) was used as a control. The PCRs were performed as described in section 4.2.3. of Materials and methods and PCR samples were collected at cycle 22 for *ACT7,* at cycle 23 for *α2*- and β3'-COP, at cycle 24 for *δ*- and *ζ3-COP,* at cycle 25 for *α1-*, *γ*- and *ε2-COP,* at cycle 27 for β2'-*COP,* at cycle 28 for β2- and *ζ2-COP*, at cycle 29 for β1-*COP*, at cycle 30 for *ε1-COP*, at cycle 32 for β1'-*COP*, and at cycle 34 for *ζ1-CO*. Col-0, wild-type plant (ecotype Columbia). It was observed that the expected molecular weight cDNA fragments were amplified.

APPENDIX 12. Alternative patterns obtained for ERD2a-YFP upon co-expression with RFP-p24δ5N86Q

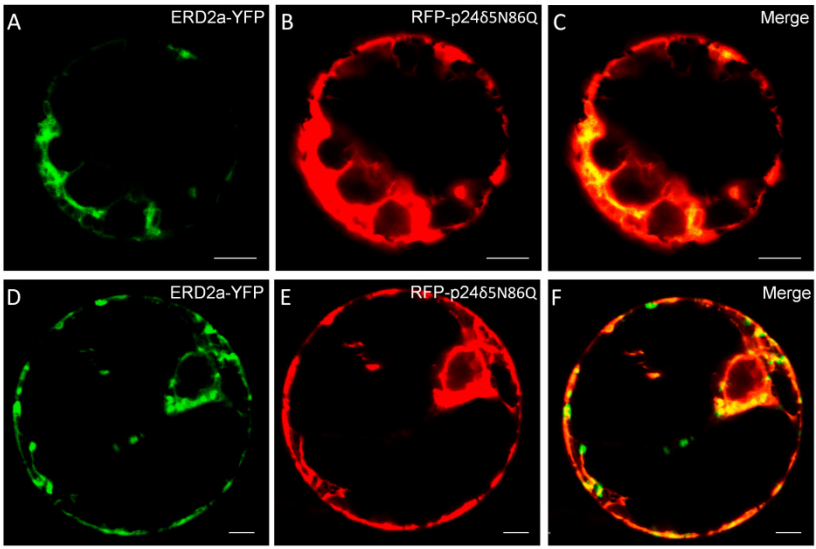

Figure A12. Alternative patterns obtained for ERD2a-YFP upon co-expression with RFP-p24δ5N86Q. A-C) ER pattern. D-F) Golgi and ER pattern.